Synaptotagmins and Weibel-Palade Body Exocytosis in Human Endothelial Cells

Jennifer Frampton

A thesis submitted in partial fulfillment of the requirements of University College London for the degree of Doctor of Philosophy

Division of Physical Biochemistry

National Institute for Medical Research

Mill Hill, London

2013

Declaration

I, Jennifer Frampton, confirm that the work presented in this thesis is my own. Where information has been derived from other sources I confirm that this has been appropriately indicated and referenced.

Jennifer Frampton Date

Acknowledgments

First and foremost I would like to thank my supervisor, Dr. Tom Carter, for the years of guidance and for creating a relaxed yet stimulating environment in which to work. I am grateful for his constant patience, support, and encouragement and for always having an open-door policy. I thank the Medical Research Council for funding the Carter lab and for giving me the opportunity to work towards this PhD.

I would also like to thank the members of the Carter lab, past and present, for the help and support they have given me over the last four years. In particular, I am indebted to Nicola Hellen, Emma Cookson, and Laura Knipe for teaching me the basics and for always offering a helping hand or sympathetic ear when experiments were not going according to plan.

I am grateful for the support of my thesis committee, Drs Justin Molloy, Jean Langhorne, Peter Rosenthal, and Talvinder Sihra for regularly meeting with me to discuss my progress and for providing expert guidance wherever possible. Their valuable insights helped to focus my work and gave me confidence in my abilities.

I thank my wonderful fiancé Michael for putting up with the late nights, early mornings, and constant commandeering of his car. Lastly, I am eternally grateful to my parents, Steve and Pauline, who have encouraged and supported me throughout my life and to whom I dedicate this work.

Abstract

Weibel-Palade bodies (WPBs) are large rod-shaped secretory organelles found exclusively in endothelial cells. In response to the activation of the endothelium by chemical or mechanical stimulation they undergo regulated exocytosis and release their contents into the bloodstream. Their primary cargo proteins are the large pro-thrombotic glycoprotein von Willebrand Factor (VWF) and the leukocyte adhesion receptor P-selectin. Hence, the principal function of WPBs is to act as a storage compartment for molecular mediators of thrombosis and inflammation. It is known that the exocytosis of WPBs is induced by increasing levels of free Ca^{2+} ions in the cytosol. However, the molecular machinery which drives exocytosis is currently unclear. The aim of my PhD was to determine the identity of the Ca^{2+} sensor responsible for the regulation of WPB secretion and it is my hypothesis that this process is driven by one or more members of the synaptotagmin (SYT) family. SYTs are the most well-characterized family of calcium sensors and have established roles in mediating the Ca^{2+}-driven exocytosis of large secretory organelles from a range of cell types. However the expression, subcellular distribution, and function of SYTs in endothelial cells remains largely unknown. Here, I show by RT-PCR and Western blotting that SYTs I, III, V, VI, VII, VIII, XI, and XVII are expressed in Human Umbilical Vein Endothelial Cells (HUVECs). Additionally, I constructed fluorescent fusion proteins of these endothelial-expressed SYTs and have demonstrated by over-expression that SYTs V, VII, VIII, and XVII are trafficked to the WPBs in HUVECs. The use of a novel dose-response assay has revealed that the up-regulation of SYT VII modulates the calcium sensitivity of WPB exocytosis and thus this raises the intriging possibility that SYT VII may be a principle component of the Ca^{2+}-sensing complex on the organelle membrane.

Table of Contents

List of Figures

List of Tables

Abbreviations

ADP – Adenosine Diphosphate

AP – Adaptor Protein

ATP – Adenosine Triphosphate

BOEC – Blood Outgrowth Endothelial Cell

BSA – Bovine Serum Albumin

cAMP – cyclic Adenosine Monophosphate

dH_20 – Distilled H_20

dAMP – Deoxyadenosine Monophosphate

dATP – Deoxyadenosine Triphosphate

dTMP – Deoxythymidine Monophosphate

DTT – Dithiothreitol

dTTP – Deoxythymidine Triphosphate

DSHB – Developmental Studies Hybridoma Bank

ECGS – Endothelial Cell Growth Supplement

EDHF – Endothelium-derived Hyperpolarizing Factor

EDTA – Ethylenediaminetetraacetic Acid

EEA-1 – Early Endosome Antigen-1

EGFP – Enhanced Green Fluorescent Protein

EYFP – Enhanced Yellow Fluorescent Protein

ELISA – Enzyme-Linked Immunosorbent Assay

ER – Endoplasmic Reticulum

ET-1 – Endothelin-1

GFP – Green Fluorescent Protein

GTP – Guanosine Triphosphate

HAEC – Human Aortic Endothelial Cell

HEK (Cell) – Human Embryonic Kidney (Cell)

HGM – HUVEC Growth Media

HRP – Horseradish Peroxidase

HUVEC – Human Umbilical Vein Endothelial Cell

ICAM – Intercellular Adhesion Molecule

ICC – Immunocytochemistry

IL – Interleukin

IP_3 – Inositol 1,4,5-triphosphate

IP_3R – IP_3 Receptor

IP_4 – Inositol 1,3,4,5-tetrakisphosphate

IFN – Interferon

kDa – kiloDaltons

KLF2 – Krüppel-like factor 2

LAMP1– Lysosome-Associated Membrane Glycoprotein 1

LDCV – Large Dense-Core Vesicle

LIC – Ligation-Independent Cloning

LPG – Lipophosphoglycan

LPS – Lipopolysaccharide

LRO – Lysosome-Related Organelle

MCTP – Multiple C2 and Transmembrane Domain-containing Protein

MEM – Minimal Essential Medium

MHC – Major Histocompatibility Complex

MyRIP – Myosin and Rab27a Interacting Protein

NEB – New England Biolabs

NO – Nitric Oxide

NRK (Cell) – Normal Rat Kidney Epithelial (Cell)

NSF – N-ethylmaleimide Sensitive Factor

OPD – 1,2-phenyldiamine Dihydrochloride

PAF – Platelet Activating Factor

PAI-I – Plasminogen Activator Inhibitor

PAR – Protease-Activated Receptor

PBS – Phosphate Buffered Saline

PC12 (Cell) – Pheochromocytoma 12 (Cell)

PCR – Polymerase Chain Reaction

PDI – Protein Disulphide Isomerase

PECAM – Platelet Endothelial Cell Adhesion Molecule

PFA – Paraformaldehyde

PGI_2 – Prostacyclin

PIP_2 – Phopsphatidylinositol-4,5-bisphosphate

PKA – Protein Kinase A

PKC – Protein Kinase C

PSGL – P-selectin Glycoprotein Ligand

Q-PCR – Quantitative-PCR

RCF – Relative Centrifugal Force

RPM – Rotations per Minute

RRP- Readily-Releasable Pool

RT-PCR – Reverse-Transcription Polymerase Chain Reaction

SDS – Sodium Dodecyl Sulphate

siRNA – small interfering RNA

Slp – Synaptotagmin-like Protein

SM (Protein) – Sec1/munc18-like (Protein)

SNAP-25 - Synaptosomal-associated Protein of Relative Molecular Mass 25 kDa

SNARE – Soluble N-ethylmaleimide Sensitive Factor Attachment Protein Receptor

SUMO (Proteins) – Small Ubiquitin-like Modifier (Proteins)

SYT – Synaptotagmin

TFPI - Tissue Factor Pathway Inhibitor

TGN – *trans* Golgi Network

TMD – Transmembrane Domain

tPA – tissue Plasminogen Activator

TNF – Tumour Necrosis Factor

t-SNARE – target SNARE

tfR – Transferrin Receptor

TX – Triton

uPA – Urokinse-type Plasminogen Activator

VAMP – Vesicle-Associated Membrane Protein

VCAM – Vascular Cell Adhesion Molecule

v-SNARE – vesicle SNARE

VVO – Vesiculo-Vacuolar Organelle

VWD – von Willebrand Disease

VWF – von Willebrand Factor

WPB – Weibel-Palade Body

w/v – weight/volume

YFP – Yellow Fluorescent Protein

Chapter One
Introduction

1.1 The Endothelial Cell: A Brief Introduction

1.1.1 Endothelial Cells are Heterogeneous Secretory Systems:

Endothelial cells line the vasculature and the lymphatic system and are essentially the gatekeepers between tissue and blood. These cells are highly-metabolically active secretory systems which play a pivotal role in the maintenance of healthy blood vessels. Under unstimulated, resting conditions endothelial cells promote vasodilatation and inhibit coagulation through the secretion of a wide range of vasoregulatory factors. However, once activated by injury or infection they become pro-thrombotic and promote vasoconstriction and inflammation. The dysregulation of the equilibrium between pro- and anti-thrombotic states contributes to the pathogenesis of many diseases which affect the vasculature including atherosclerosis, diabetes, and malaria (reviewed in Cines *et al.* 1998).

Endothelial cells originate in the splanchnopleuric mesoderm from hemangioblasts which are also the precursors of hematopoietic cells (Choi *et al.* 1998). They constitute a highly heterogeneous population of cells which can be differentiated by their size, shape, secretory repertoire, solute permeability, and glycocalyx thickness (reviewed in Aird, 2007). The final phenotype of an endothelial cell is influenced by a number of factors such as its exposure to growth factors, cytokines, hormones, antibodies, microbes and is also modulated by local blood flow dynamics, interactions with surrounding smooth muscle cells, and the composition of the extracellular matrix (van Hinsbergh, 2012). Indeed, it is difficult to provide a precise definition of an endothelial cell as there are few phenotypic properties which are shared across the vasculature tree and which are unique to this cell type. Features which are generally considered to be universal such as the presence of the secretory organelles Weibel-Palade bodies are not common to all endothelial cells (Turner *et al.* 1985, Kumar *et al.* 1987). Additionally, the plasma membrane protein PECAM-1 is a commonly-used endothelial marker but this molecule is not expressed by sinusoidal intrahepatic endothelial cells (Morin *et al.* 1984).

The most obvious and fundamental function of endothelial cells is to provide a selectively-permeable barrier between the blood and underlying tissue. Therefore it is

essential that these cells engage in both regulated exocytosis and endocytosis to allow the controlled uptake and release of material from both sides of the vasculature. Endothelial cells engage in the process of transcytosis whereby material is removed from the bloodstream by endocytosis and expelled into the basal lamina from the opposite pole of the cell through the process of regulated exocytosis (Simionescu *et al*. 2002). These transcytotic events occur through the formation of caveolae and vesiculo-vacuolar organelles (VVOs), two structures which are commonly seen features of endothelial cells but which are rare in most other cell types. Indeed, caveolae are more common than clathrin-coated pits in endothelial cells (Gratton *et al.* 2004). VVOs are aggregations of intracellular vesicles which are thought to result from fusion events between caveolae and which have been linked with the vascular leakage associated with tumour angiogenesis and allergic reactions (Pober and Sessa, 2007). In the skin venules, where endothelial cells are unusually long, VVOs consisting of over 100 individual vesicles occupying 20% of the cytoplasm have been reported (Dvorak *et al.* 2001). Clearly, endothelial cells do not constitute an inert, metabolically inactive barrier but rather are specialized secretory cells responsible for regulating the constant movement of material between the bloodstream and tissues whilst maintaining the integrity of the vessel wall.

1.1.2 The Primary Functions of Endothelial Cells:

1.1.2.1 The Resting State: Vasodilation and Fibrinolysis

Endothelial cells are responsible for the maintenance of healthy, non-thrombogenic blood vessels through the secretion of a range of molecular mediators which act on platelets, leukocytes, and surrounding smooth muscle cells (reviewed in Cines *et al.* 1998). Firstly, when in the unperturbed resting state endothelial cells promote the dilation of blood vessels through the secretion of the eicosanoid prostacyclin (PGI_2) (Egan and FitzGerald, 2006) and the gas nitric oxide (NO) (Moncada and Higgs, 2006), both of which act on smooth muscle cells to dilate the vessel. PGI_2 and NO are released by endothelial cells following their exposure to agonists including ADP and thrombin or in response to physical stimulation such as exposure to shear stress (Pober and Sessa, 2007). NO inhibits platelet aggregation, adhesion, activation, and secretion and also inhibits leukocyte adhesion to the endothelium (Moncada and Higgs, 2006). The secretion of endothelium-derived hyperpolarizing factor (EDHF) results in smooth muscle relaxation and is released by endothelial cells in response to muscarinic agonists (Garland *et al.* 1995).

In addition to promoting vasodilation, endothelial cells are responsible for the maintenance of an anti-thrombotic environment which is essential for the prevention of potentially-fatal blood clots. The two most common fribrinolytic agents secreted by endothelial cells are tissue plasminogen activator (tPA) and urokinse-type plasminogen activator (uPa). The serine protease tPA is primarily expressed by microvascular endothelial cells and promotes the breakdown of blood clots by converting plasminogen to plasmin (Medcalf, 2007). Endothelial cells also secrete the t-PA inhibitor PAI-I (plasminogen activator inhibitor), thus providing a negative-feedback mechanism which prevents excessive fibrinolysis (van Hinsbergh, 2012). uPA is expressed by endothelial cells which are involved in tissue repair following injury and aids the breakdown of plasminogen (Bacharach *et al.* 1992). The uPA knock-out mouse develops inflammation-induced thrombi and when exposed to LPS suffers thrombosis and tissue damage due to unchecked coagulation and inflammation (Carmeliet *et al.* 1994, Yamamoto *et al*. 1996).

Endothelial cells secrete thrombomodulin which binds to thrombin, resulting in the activation of the anti-coagulant protein C (Pober and Sessa, 2007). The thrombin:thrombomodulin complex is then internalized and destroyed (Esmon *et al.* 1993). Cytokine exposure decreases the expression of thrombomodulin and encourages its internalization, thus converting endothelial cells from the resting, anti-thrombotic state to an activated pro-thrombotic one (Mantovani *et al*. 1997). Lastly, in response to heparin stimulation endothelial cells secrete tissue factor pathway inhibitor (TFPI) which binds to factor Xa and thereby inhibits coagulation (van Hinsbergh, 2001). Thus, in order to maintain an anti-thrombotic, anti-inflammatory environment endothelial cells secrete a range of molecules including those which directly degrade and remove fibrin clots (thrombomodulin, tPA, uPA, TFPI), those which relax smooth muscle cells (PGI_2, EDHF, NO), and those which act on platelets and leukocytes to prevent their activation (NO). The actions of these substances are summarized in Figure 1.1.

1.1.2.2 The Activated State: Vasoconstriction and Coagulation

Following their activation by injury or inflammation endothelial cells alter their secretory repertoire to promote vasoconstriction and coagulation at the expense of vasodilation and fibrinolysis. Firstly, vasoconstriction is achieved by the release of the 21-residue protein endothelin-1 (ET-1) following endothelial activation by molecular mediators such as thrombin, histamine, and adrenaline (Levin, 1996). ET-1 binds to ET-A receptors on

smooth muscle cells, resulting in a signalling cascade which ultimately raises cytosolic Ca^{2+} levels and induces vessel constriction (Simonson and Dunn, 1990). The consequences of ET-A activation are long-lasting and Ca^{2+} levels only return to baseline following smooth muscle cell exposure to counteracting signals such as NO and PGI_2 secreted by surrounding endothelial cells. Therefore, a delicate balance exists between vasodilatation and vasoconstriction and the dysregulation of this equilibrium has clinical implications. For example, in patients suffering from atherosclerosis the level of secreted NO is lower than normal whereas ET-1 levels are abnormally high (Hansson and Libby, 2006). This suggests that the regulation of vascular tonicity is disrupted in these patients, resulting in smooth muscle proliferation and contraction which ultimately contribute to the development of atherosclerotic plaques.

Endothelial cells secrete the vasoregulatory agent platelet activating factor (PAF) following thrombin or histamine exposure (Whatley and Zimmerman, 1996). PAF is a cell-surface endothelial phospholipid which acts by binding to G-protein-linked receptors on leukocytes, resulting in juxtacrine signalling between the two cell types which ultimately induces leukocyte extravasation to underlying tissue (Lorant *et al.* 1991). Like ET-1, PAF is not stored within resting endothelial cells but instead is synthesized following their activation. PAF can also induce vasodilation and the exact consequences of its synthesis depend on its concentration in the endothelial cell membrane (Campbell *et al.* 1996).

In addition to inducing vasoconstriction endothelial cells protect against injury by driving thrombosis. The expression of Tissue Factor following endothelial activation by, for example, thrombin, cytokines, endotoxin, or hypoxic conditions is fundamental in bringing about the pro-thrombotic state (Pober and Sessa, 2007). Tissue Factor induces the activation of factors X and IX through an interaction with Factor VIIa (Drake *et al.* 1989) and its importance is demonstrated by mice lacking this protein which show increased ferric chloride-induced arterial thrombosis (White *et al.* 2010). Additionally, the up-regulation of Tissue Factor has clinical importance as its expression is seen in endothelial cells lining atherosclerotic plaques and in blood vessels surrounding tumors (van Hinsbergh, 2012).

As well as being involved in vasoregulation PAF also acts as a pro-coagulant molecule by inducing both platelet adhesion to the vessel wall and the formation of fibrin clots. The mechanism behind PAF's action is complex and poorly understood but ultimately it induces the expression of platelet-binding adhesion molecules on the endothelium, the increased secretion of Tissue Factor, and the release of the pro-thrombotic protein von Willebrand Factor (VWF) from Weibel-Palade bodies (reviewed in Cines *et al*. 1998).

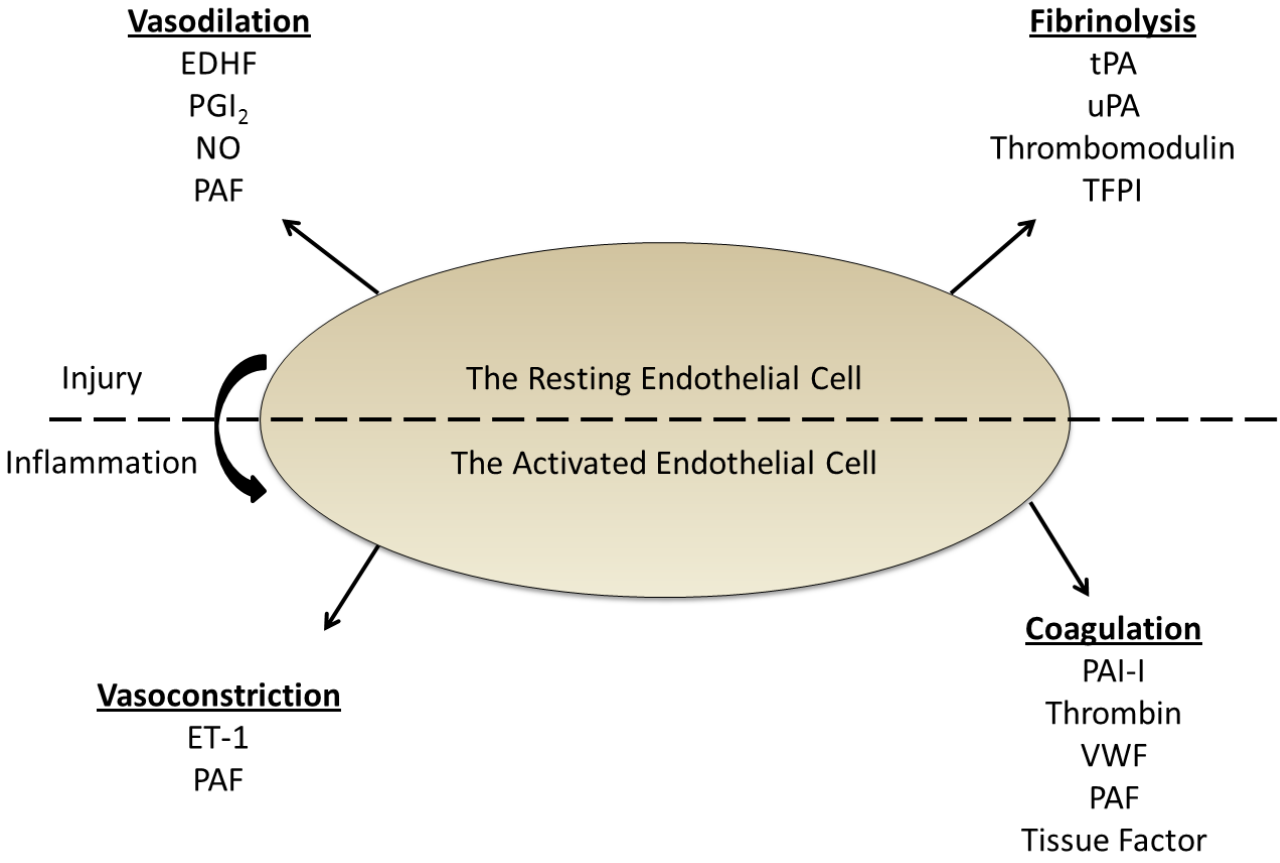

Figure 1.1 Endothelial cells secrete a range of molecular mediators.

Endothelial cells in the resting state induce vasodilation and fibrinolysis. Once activated by injury or infection they induce vasoconstriction and coagulation. The ability of an endothelial cell to influence vascular tonicity and the coagulatory state depends on the regulated secretion of a range of molecular mediators, as shown. Note that this is by no means an exhaustive list of the molecules secreted by endothelial cells.

Lastly, endothelial cells secrete the highly-thrombogenic serine protease thrombin which results in the activation of platelets and the coagulation cascade. Thrombin binds to the well-characterized G-protein-linked PAR (Protease-Activated Receptor) proteins on platelets and endothelial cells (Woolkanis *et al.* 1995). Following thrombin binding, an N-terminal fragment of the receptor is cleaved resulting in the generation of signalling pathways which ultimately induce the expression of intercellular adhesion proteins and Tissue Factor (Kanthou and Benzakour, 1995). Thus, following their activation by inflammation or injury endothelial cells adopt a strongly pro-thrombotic and vasoconstrictive state. The molecules which drive these processes are summarized in Figure 1.1.

1.1.3 The Role of Endothelial Cells in Inflammation and Disease:

Following the activation of the immune system by injury or invasion endothelial cells contribute to the inflammatory state through interactions with circulating leukocytes. Firstly, in response to cytokine or LPS exposure endothelial cells express a variety of adhesion molecules which bind to complementary proteins on circulating leukocytes to induce their migration to underlying tissue through the process of extravasation (reviewed in Cines *et al.* 1998, Wagner and Frenette, 2008). Extravasation can be considered as a series of steps which are illustrated in Figure 1.2. Initially, a reversible attachment is formed between the leukocyte and the endothelium, mediated in part by the endothelial protein P-selectin which binds to Glycoprotein Ligand 1 (PSGL-1) on leukocytes. This initial interaction is weak and so the surrounding blood flow drives the rolling of the leukocyte along the vessel wall. As the inflammatory state increases, both endothelial cells and leukocytes become activated and this is assisted by the secretion of PAF which induces the up-regulation of the β2 integrins LFA (Leukocyte Function-associated Antigen-1) and MAC-1 (Macrophage-1) on leukocytes (Huo *et al.* 2000). Activation also induces the expression of VCAMs (Vascular Cell Adhesion Molecules), ICAMs (Intercellular Adhesion Molecules) and E-selectin on endothelial cells which bind with high-affinity to their complementary partners on leukocytes (Sumpio *et al.* 2002). This strong interaction causes the firm attachment of the leukocyte to the vessel wall and allows its ultimate extravasation. The precise molecular mechanisms controlling leukocyte extravasation to underlying tissues are poorly understood but are thought to depend on a chemokine gradient, β_2 integrin and myosin light chain kinase activation, and the activity of the transmembrane proteins PECAM-1, CD99, and Junctional Adhesion Molecule (JAM)-A (Schenkel *et al.* 2002, Aird, 2012, Dejana, 2004).

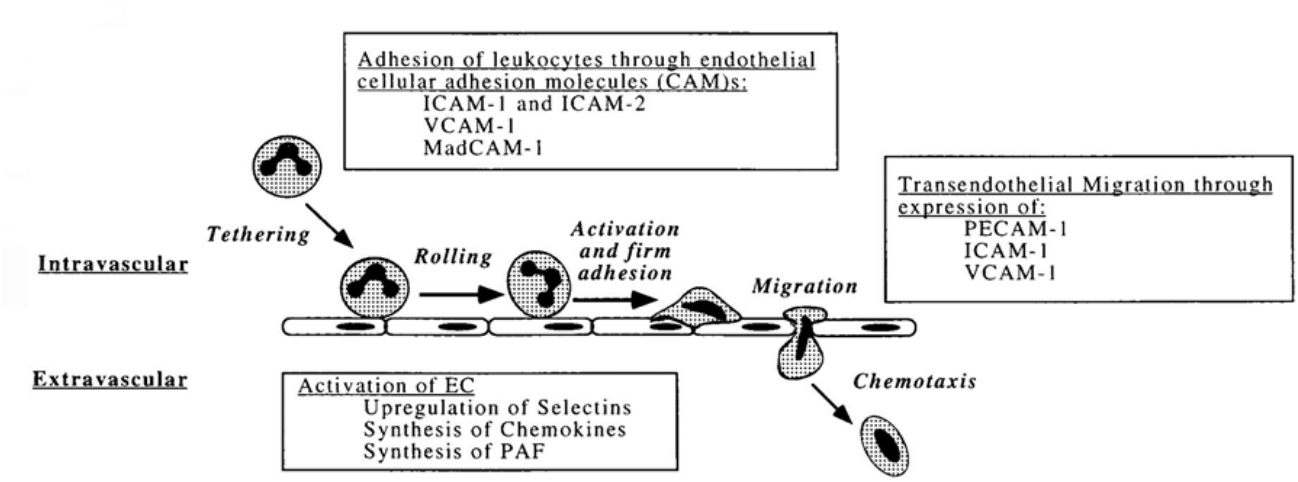

Figure 1.2. Endothelial cells mediate leukocyte extravasation.

Endothelial cells regulate the migration of leukocytes from the bloodstream to underlying tissues (extravasation) through the expression of a range of adhesion proteins which bind to complementary ligands on leukocytes. Extravasation can be considered as a series of steps requiring the tethering, rolling, activation, adhesion, and migration of leukocytes. Each step is regulated by the expression of a unique set of adhesion molecules on both the endothelial cells and leukocytes.

Figure taken from Cines *et al.* 1998 with permission from *Blood* journal.

Endothelial cells are immunocompetent in that they express MHC markers and present antigens to T-cells in peripheral tissues (Pober *et al.* 1996). Most endothelial cells, including those grown in culture, express MHC class I molecules and IFN-γ exposure induces the expression of MHC class II molecules (Shiao *et al* 2005). Thus, endothelial cells play a direct role in cell-mediated immunity. Additionally, T-cells express CD40 ligand which binds to CD40 on endothelial cells, inducing the expression and secretion of mediators of vasoconstriction, chemokines, and adhesion proteins (van Hinsbergh, 2012).

Endothelial cells which are exposed to cytokines for an extended period of time drastically alter their phenotype and can in some circumstances suffer adverse effects. Within a few hours of continuous cytokine exposure, the intercellular junctions between neighbouring endothelial cells disassemble to induce maximum lymphocyte extravasation (Frangogiannis, 2006). Ultimately very long-term exposure to inflammatory stimuli as is experienced during chronic disease results in the induction of endothelial cell proliferation and angiogenesis (Pober and Sessa, 2007). These processes occur over a period of months

and, in some cases, years. Organ transplantation, atherosclerosis, and cancer are examples of conditions which can lead to serious damage of the endothelium as over-stimulated T-cells attack and destroy endothelial cells (Cines *et al.* 1998, Jutte *et al.* 1996, Taflin *et al.* 2011). Indeed LAK (Lymphokine-Activated Killer) cells may be responsible for vascular leak syndrome which is often seen in cancer patients undergoing IL-2 and LAK therapy (Damle *et al.* 1987).

A detailed discussion of the relationship between the endothelium and disease progression is beyond the scope of this thesis. However, it is clear that endothelial cells play a fundamental role in the maintenance of the healthy vasculature and are heavily involved in tissue repair, coagulation, and the inflammatory response. It is therefore essential that we develop a complete understanding of their biology as the dysregulation of endothelial activity contributes to the pathology of a number of diseases including diabetes, sickle-cell anemia, atherosclerosis, malaria, and the thrombotic disorders Thrombotic Thrombocytopenic Purpura (TTP) and Hemolytic Uremmic Syndrome (HUS) (reviewed in Cines *et al.* 1998). Endothelial cells also play a key role in the biology of transplant rejection and tumor-induced angiogenesis (van Hinsbergh, 2012, Taflin *et al.* 2011).

1.1.4 Endothelial Cells in Culture:

Endothelial cells were first successfully grown in culture in the 1970s and have a characteristic ‘cobblestone’ morphology when viewed through a light microscope (Gimbrone *et al.* 1974). They are typically grown in confluent monolayers although they can form vessel-like tubes when cultured in fibrin or collagen gels in the presence of the appropriate growth hormones (Mueller-Klieser, 1997). Additionally, when cultured cells are exposed to perfusion systems aiming to mimic the bloodstream they adopt an elongated shape orientated in the direction of flow (Bachetti and Morbidelli, 2000, Wagner and Frenette, 2008). Hence, although endothelial cells are typically grown in single inert monolayers it is possible to create vessel-like environments with the aim to approximate the conditions experienced by endothelial cells *in vivo*.

Human Umbilical Vein Endothelial Cells (HUVECs) are considered to be model endothelial cells because they show features common to most of the vasculature and are readily available. As their name suggests, HUVECs are derived from the human umbilical vein by collagenase treatment which isolates individual cells from the basal lamina (Gimbrone *et al.* 1974). This approach is efficient and results in little contamination from

non-endothelial cells. Other possible isolation methods include vessel mincing and enzymatic digestion or physically disrupting cells by scraping from the vessel wall (Gospodarowicz *et al.* 1976, Schelling *et al.* 1988). In both cases endothelial cells must be purified by cell sorting with endothelial-specific antibodies and the yield is generally lower than that achieved following collagenase digestion (Bachetti and Morbidelli, 2000).

The major difficulty with using cultured cells as a model for the endothelium is that endothelial cells *in vivo* replicate at a rate of 0.1% per day whereas in culture this increases to 1-10% per day (Bachetti and Morbidelli, 2000). Although this might be considered a hindrance when studying the function of healthy cells it is beneficial when examining the mechanisms of wound healing and cancer development as this rapid rate of division mimics the phenotype shown by endothelial cells mediating tissue repair and angiogenesis. An additional consideration when culturing endothelial cells is that functions specific to certain parts of the vasculature will be lost over time (Aird 2012, Burridge and Friedman 2010) and for this reason cultured cells are generally derived from primary sources and rarely used above passage 6 or 7. Finally, endothelial cells are a highly heterogeneous population and therefore observations made from cells derived from one source cannot be assumed to be valid for all endothelial cell types. Although it is necessary to be aware of the inherent limitations with using cultured endothelial cells as a model system, the ability to grow cells *in vitro* has proved invaluable to our understanding of endothelial cell biology.

1.2 Regulated Exocytosis and the Molecular Mediators of Secretion:

1.2.1 An Overview of Regulated Exocytosis:

Proteins destined for secretion to the extracellular milieu are first synthesized in the endoplasmic reticulum and then transported to the Golgi apparatus where they are modified by glycosylation and sulfation. In the trans Golgi network (TGN), secretory proteins are packaged into vesicles which are then directed to either the constitutive or regulated secretory pathway. The constitutive pathway mediates the stimulus-independent release of material whereas vesicles secreted by the regulated pathway are held at the plasma membrane until an appropriate signal induces their temporally-controlled and highly-ordered release. In both cases, once vesicles have undergone exocytosis their membranes are internalized by endocytosis in order to maintain a constant cell surface area and allow the recycling of membrane proteins.

Regulated exocytosis is a tightly-controlled process which can be considered as a series of steps (reviewed in Gerber and Sudhof, 2002). Firstly, secretory vesicles are recruited to and tethered at the plasma membrane. These vesicles are then primed for fusion, thus creating what is called the 'readily-releasable pool' (RRP). Lastly, fusion is induced by a specific stimulus which is usually the influx of Ca^{2+} ions into the cytosol and the contents of the granules are expelled by exocytosis.

1.2.2 The Fusion Pore:

The defining step in the initiation of fusion between two membranes is the formation of the fusion pore. This structure is a narrow fluid-filled channel formed by the mixing of the two outer leaflets of opposing membranes (reviewed in Jackson and Chapman, 2008). It functions to provide a physical connection between two structures which are on the cusp of undergoing fusion such as a secretory vesicle and the plasma membrane and its formation represents the final crucial step in the pathway of regulated exocytosis. Although the exact structure of the fusion pore is currently unclear it is most likely formed following the Ca^{2+}-induced oligomerization of proteins which mediate the final stage of exocytosis (the fusion apparatus, see 1.2.3 The Molecular Mediators of Regulated Exocytosis). Indeed, in PC12 cells mutations which introduce bulky tryptophan residues into the transmembrane α-helix of the t-SNARE syntaxin result in reduced pore sizes (Han *et al.* 2004). Based on this study it has been predicted that between five and eight syntaxin transmembrane domains line the wall of the fusion pore and determine its physical structure.

The formation of the fusion pore (also called hemifusion) is a reversible process. A fusing granule can undergo full fusion and release its contents into the opposing lumen or alternatively the fusion pore can collapse and the membranes re-seal. This process is now referred to as 'kiss-and-run' and was first described following capacitance measurements of degranulating rat peritoneal mast cells (Fernandez *et al.* 1984). Kiss-and-run events result in the secretory vesicle remaining intact with larger proteins sequestered inside but during the time when the pore is open smaller molecules can escape and hence a degree of exocytosis does occur through a size-exclusion mechanism (Fulop *et al.* 2005). Additionally, kiss-and-run events at the synapse may regulate the kinetics and amplitude of the synaptic current and hence function to fine-tune synaptic transmission (He *et al.* 2006).

1.2.3 The Molecular Mediators of Regulated Exocytosis:

1.2.3.1 SNAREs:

The SNARE (soluble N-ethylmaleimide-sensitive factor attachment protein receptor) proteins constitute a family of 36 members in mammals and are defined by a 60-70 residue coiled-coil SNARE motif (reviewed in Jahn and Scheller, 2006, Sudhof and Rothman, 2009, Kreyet and Sollner, 2008, Jahn and Fasshauer, 2012). SNAREs function to physically tether vesicles together as their coiled-coil motifs spontaneously form an extremely stable four-helix structure called the SNAREpin or *trans*-SNARE complex. The formation of this SNAREpin likely provides the energy needed to force opposing membranes together and thereby promotes fusion pore formation.

For fusion events which occur at the plasma membrane the SNAREpin is made up of two plasma-membrane SNAREs (t-SNAREs) and one vesicular SNARE (v-SNARE). There are two classes of t-SNAREs: the syntaxins and SNAP-25 (synaptosomal-associated protein of relative molecular mass 25 kDa). Syntaxins contain a C-terminal SNARE motif, a transmembrane domain, and an N-terminal sequence which folds to form a three-helix structure known as the Habc domain (Fernandez *et al.* 1998). This domain is inhibitory and when not in a complex with SNAP-25 folds back onto syntaxin and blocks the SNARE motif (Nicholson *et al.* 1998). Hence, syntaxin can exist in either an open or closed conformation depending on the position of the Habc domain. SNAP-25 is not a transmembrane protein but instead is tethered to the membrane by multiple palmitoylated cysteine residues (Oyler *et al.* 1989). This protein contains two SNARE motifs connected by a linker region and hence contributes two coiled-coils to the SNAREpin. It is thought that, in the plasma membrane, syntaxin and SNAP-25 form a complex which functions as the receptor for the v-SNARE of which there is only one class, the VAMPs (vesicle-associated membrane proteins, also called synaptobrevins) (Sutton *et al.* 1998).

The accepted model of SNARE function states that when opposing SNAREs are in close proximity they form the SNAREpin complex which consists of two SNARE motifs from a SNAP-25 molecule and one each from syntaxin and VAMP. The spontaneous formation of this complex forces the membranes together and provides the activation energy necessary for membrane fusion. Additionally, as has been discussed (see 1.2.2 The Fusion Pore**)** the syntaxins may be essential for the formation of the fusion pore. However, other proteins are required for fast secretory events, and it is likely that SNAREs and members of the synaptotagmin family (see below) function cooperatively to induce membrane merging during fusion.

Lastly, NSF (N-ethylmaleimide-sensitive factor) is a highly-conserved hexameric ATPase which binds to SNARE complexes post-fusion via the adaptor protein SNAP (no relation to SNAP-25) (Sollner *et al.* 1993). This protein is an essential component of the fusion apparatus and functions to recycle SNAREs following membrane fusion by dismantling the *cis*-SNARE (post-fusion) complex through repeated cycles of ATP hydrolysis (Jahn and Scheller, 2006).

1.2.3.2 Sec1/munc18-like Proteins:

Sec1/munc18-like (SM) proteins are small (60-70 kDa) arch-shaped cytosolic proteins which interact with SNARE proteins and have been shown to have a fundamental and increasingly diverse role in the regulation of exocytosis (Jahn and Scheller, 2006, Kreye and Sollner, 2008). There are 7 members of the SM protein family in humans and the most well-characterized member to-date is Munc18-1 (Kreye and Sollner, 2008). It was originally believed that Munc18-1 acts as an inhibitor of exocytosis by binding to the N-terminal Habc domain of syntaxin and stabilizing its 'closed' conformation (Misura *et al.* 2000). Although this mechanism of action of Munc18-1 is still largely accepted it is now known that SM proteins also bind to the *trans*-SNARE complex, again via the N-terminal region of syntaxin, and are likely to be involved in SNARE priming prior to fusion (Dulubova *et al* 2002, Shen *et al.* 2007). Indeed, SM proteins are absolutely required for fusion to proceed as the ablation of Munc18-1 completely blocks synaptic exocytosis (Verhage *et al.* 2000). Thus SM proteins have been proposed to act as catalysts for SNAREs by stabilizing the *trans*-SNARE complex and may be involved in determining the spatial and temporal organization of fusion (Sudhof and Rothman, 2009, Jahn and Fasshauer, 2012).

In addition to their roles as both inhibitors and activators of fusion, SM proteins have been shown to have a number of accessory functions essential for vesicle exocytosis. Firstly, SM proteins mediate the specificity of SNARE pairings as their inclusion in liposome fusion assays decreases the extent of promiscuity among SNARE binding partners (Shen *et al.* 2007). SM proteins also act as chaperones for syntaxin as it traverses through the secretory pathway by protecting it from degradation (Braun and Jentsch, 2007) and inhibiting the formation of inappropriate SNARE complexes (Bryant and James, 2001). Lastly, SM proteins are likely to be involved in vesicle docking, as shown by the observation that mouse chromaffin cells deficient in Munc18-1 show an increased number of undocked vesicles (Voets *et al.* 2001). This function of SM proteins may be achieved through their ability to

interact directly with Rab tethering complexes (see later) at the plasma membrane (van Weering *et al.* 2007).

Munc13 is not strictly an SM protein but instead belongs to the CATCHR protein family (Jahn and Fasshauer, 2012). However, this protein acts synergistically with Munc18-1 by displacing it from syntaxin, thus allowing the t-SNARE to adopt the 'open' conformation and the initiation of fusion (Richmond *et al.* 2001, Ma *et al.* 2011). The Munc13-deficient mouse shows impaired spontaneous and evoked fusion with a notable reduction in the size of the RRP (Augustin et al. 1999, Varoqueaux et al. 2002). Lastly, the CAPS (Ca^{2+}-dependent activator protein for secretion) family shows sequence homology to Munc13 proteins (Walent *et al.* 1992). These molecules are thought to be involved in vesicle priming and convert syntaxin to its open conformation via an interaction with PIP_2 and Ca^{2+} ions (Grishanin *et al.* 2004).

1.2.3.3 Complexins:

Complexins are small 15-kDa helical proteins which associate with partially-assembled SNARE complexes (Jahn and Scheller, 2006, Chen *et al.* 2002). Their primary function is to act as a 'fusion-clamp' through the insertion of a central α-helix into the *trans*-SNARE complex, an interaction which impairs full SNAREpin formation (Giraudo *et al.* 2009, Chen *et al.* 2002). Indeed, complexin-deficient synapses show increased spontaneous synaptic fusion events (Maximov *et al.* 2009). The activity of complexin results in the generation of a pool of vesicles which are docked, primed, and on the verge of undergoing full fusion. Increasing Ca^{2+} levels in the cytosol results in the displacement of complexin from the *trans*-SNARE complex by the pro-fusogenic protein synaptotagmin (see below) and the initiation of exocytosis (Fernandez-Chacon *et al.* 2001, Sudhof and Rothman, 2009). Interestingly, complexin may be involved in priming the *trans*-SNARE complex in addition to its role as an inhibitor of fusion as complexin-deficient neurons show a loss of Ca^{2+}-mediated synchronous exocytosis (Reim *et al.* 2001). Thus, these proteins are likely to have dual functions as both activators and inhibitors of regulated exocytosis.

1.2.3.4 The Rab Family:

Rab proteins are monomeric GTPases of the Ras superfamily which play an essential role in all aspects of regulated exocytosis including vesicle budding, trafficking, docking,

priming, and fusion (reviewed in Fukuda, 2008). They are GTP-binding proteins which cycle between an active GTP-bound state and an inactive GDP-bound state. In mammalian cells, Rab proteins constitute a family of more than 60 members (Bock *et al.* 2001). However, the role of individual Rabs is relatively specific and most show a limited subcellular distribution. For example, Rabs 5 and 21 are endosomal proteins whereas Rabs 1 and 2 can be found as components of the Golgi apparatus (Fukuda, 2008). The Rab27 family consists of Rab27a and Rab27b and these two isoforms have particular importance in regulated exocytosis as they play general roles in mediating the fusion of secretory vesicles (Tolmachova *et al.* 2007, Mizuno *et al.* 2007, Munafo *et al.* 2007). These proteins are found on a range of secretory granules and Rab27 $^{-/-}$ animals show a variety of secretory defects (Menasche *et al*. 2000, Wilson *et al.* 2000). It is now known that the primary purpose of Rab27 proteins is to regulate the docking of secretory vesicles at the plasma membrane (Tsuboi and Fukuda, 2006). They may also function to regulate the size and shape of vesicles as the number of dense granules in platelets derived from Rab27b $^{-/-}$ mice is diminished compared with those from wild-type mice (Tolmachova *et al.* 2007).

Rab proteins regulate vesicle trafficking and fusion via a large family of effector proteins which are characterized by the presence of a Rab-binding domain (RBD) at their N-terminus (Fukuda, 2008). Effector proteins generally function to provide a physical link between vesicle-associated Rabs and molecules found on target structures such as SNAREs, phospholipids, and components of the cytoskeleton. Examples of Rab effectors include the synaptotagmin-like proteins 1-5 (Slps 1-5), rabphilin, Noc2, Munc13-4, and Rim (Fukuda, 2008) and indeed the effector proteins for Rab27 (Slp2-a, Slp4-a/granuphilin-a, and rabphilin) are known to mediate the tethering of secretory vesicles to the plasma membrane in neuroendocrine and gastric surface mucous cells (Gomi *et al.* 2005, Saegusa *et al*. 2006). In some cases, additional tethering proteins consisting of large complexes or coiled-coil structures connect Rab effectors with components of the SNARE apparatus, and the classic example of this is the yeast exocyst complex (Whyte and Munro, 2001). Lastly, the activation state of the Rabs is governed by a further set of proteins, the GEFs (guanine nucleotide exchange factor) and GAPs (GTPase activating protein), although little is known concerning the tissue distribution and activity of these enzymes (Fukuda, 2008).

1.2.3.5 The Core Complex in the Regulation of Exocytosis:

The process of regulated exocytosis is orchestrated by the coordinated action of a number of protein families including the SNAREs, SM proteins, complexins, and Rabs. Indeed, the precise repertoire of these proteins which are expressed by a cell determines its specific secretory properties. The 'core' complex required for the final stage of vesicle fusion at the plasma membrane is thought to consist of v- and t-SNAREs, complexins, and SM proteins. The Rabs generally play a pre-fusion role in either vesicle trafficking or docking. A model depicting how the components of the core complex interact to mediate the final stages of regulated exocytosis is shown in Figure 1.3. Note that, in addition to the proteins described thus far, Ca^{2+}-mediated exocytosis also requires a calcium sensor which is generally a member of the SYT family.

1.2.3.6 Molecular Mediators of Regulated Exocytosis in Endothelial Cells:

SNARE proteins and their binding partners will undoubtedly play a fundamental role in mediating vesicle trafficking and regulated exocytosis in endothelial cells as they do in all other eukaryotic cell types. However, the identity of the SNAREs, SM proteins, complexins, and Rabs which are expressed in endothelial cells is currently unclear. It is known that the Golgi/endosomal t-SNARE syntaxin-6 plays a crucial role in endothelial cell biology as its inhibition disrupts both cell migration and angiogenesis through the impaired trafficking of two essential signaling molecules, integrin $\alpha_5\beta_1$ and vascular endothelial growth factor receptor 2 (VEGF2) (Tiwani *et al.* 2011, Manickan *et al.* 2011). Equally, it has been shown that the process of caveolae formation is regulated by the v-SNARE VAMP2 (McIntosh and Schnitzer, 1999) and caveolae fusion with the basolateral membrane is regulated by the t-SNAREs syntaxin-4 and SNAP-23 (Preduscu *et al*. 2005). Lastly, the exocytosis of lysosomes following death receptor activation in aortic endothelial cells is regulated by syntaxin-4 and VAMP2 (Han *et al*. 2011), whereas the process of WPB exocytosis is mediated by a complex consisting of syntaxin-4, VAMP3, and SNAP-23 (Pulido *et al.* 2011).

Although our knowledge concerning the roles of individual SNAREs in the endothelium is becoming more detailed there is still very little known regarding the expression and function of the SNARE-binding partners, SM proteins and complexins, in endothelial cells. Thus far, it has been reported that Munc18c is expressed in human lung microvascular endothelial cells (Fu *et al.* 2005) and Munc13-4 is expressed in HUVECs (Zografou *et al.* 2012). Both proteins are known to play an as-yet unclear role in the

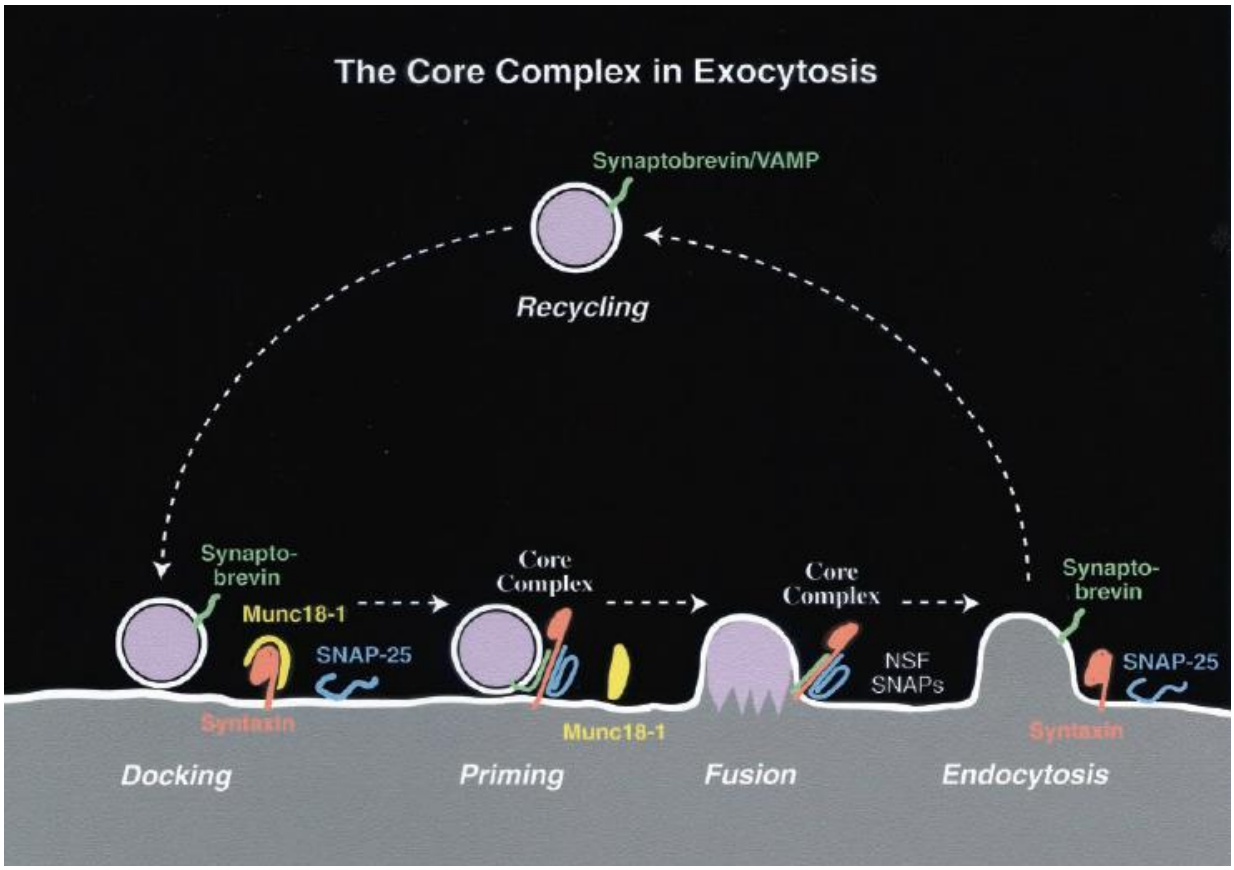

Figure 1.3. A core complex of proteins regulates exocytosis

A likely model explaining the action of the core complex in regulated exocytosis at the plasma membrane is shown. In resting cells, the plasma membrane-associated SNARE syntaxin is found in a 'closed' complex with Munc18-1. Following cell stimulation, Munc18-1 dissociates from syntaxin, allowing it to adopt the 'open' state and bind to SNAP-25. Following the docking of VAMP-containing vesicles at the plasma membrane a SNAREpin is formed by the binding of the syntaxin:SNAP-25 complex to the v-SNARE VAMP (synaptobrevin). This is thought to pull the opposing membranes together and may provide the activation energy required to drive fusion pore formation. Following fusion, NSF and its adaptor protein SNAP dissociate the *cis*-SNARE complex, allowing all components to be recycled for future events.

Taken from Gerber and Sudhof, 2002.

regulation of WPB exocytosis (see 1.5.3.3 The Fusion Apparatus Mediating WPB Exocytosis).

Considering the central importance of the Rab family in eukaryotic cell biology as well as its size and diversity it stands to reason that these proteins are widely expressed in the endothelium. As expected, endothelial cells express a range of Rab family members and indeed the plasma membrane/early endosome protein Rab5b was initially identified and characterized in HUVECs (Wilson and Wilson, 1992). An early study determined that Rabs 2, 4b, 7, 9, 15, and 30 are expressed in HUVECs (de Leeuw *et al.* 1998) and functions have slowly been assigned to each of these endothelial-expressed Rabs. It is known that Rab5a and Rab7a function synergistically to mediate VEGFR2 trafficking and degradation (Jopling *et al*. 2009). Additionally, Rab5a and Rab11 have been shown to play a role in the internalization and trafficking of Factor VIII in HUVECs (Nayak *et al*. 2013). Lastly, a recent study has shown that Rabs 3, 27, 15, 30, and 37 associate with WPBs in HUVECs, and the central role of Rab27a in mediating WPB trafficking is well-established (Bierings *et al.* 2012, Pulido *et al*. 2011, Nightingale *et al.* 2009).

1.3 The Synaptotagmins:

1.3.1 An Overview of the SYTs:

In order for regulated exocytosis to proceed in response to increasing Ca^{2+} levels there must be a molecule associated with the core complex which can in some way 'sense' and respond to cytosolic Ca^{2+} ions. The synaptotagmin (SYT) family is the most well-characterized family of calcium-sensing proteins and these molecules are thought to mediate secretory events by providing the physical link between rising Ca^{2+} concentrations in the cytosol and the fusion apparatus (for reviews see Yoshihara and Montana 2004, Tucker and Chapman 2002, and Sudhof, 2002).

There are currently 17 reported mammalian SYT family members. They are all type I integral membrane proteins which share a common basic structure consisting of a short, highly-variable N-terminal region, a transmembrane domain, a linker region, and two C-terminal C2 domains (Perin *et al.* 1991). The structure of a typical SYT is shown in Figure 1.4. Although SYTs are defined by the presence of these five domains they do show significant diversity within the family. For example, the length of the transmembrane domain varies considerably between SYTs, ranging from 43 residues for SYT VIII to 417 residues

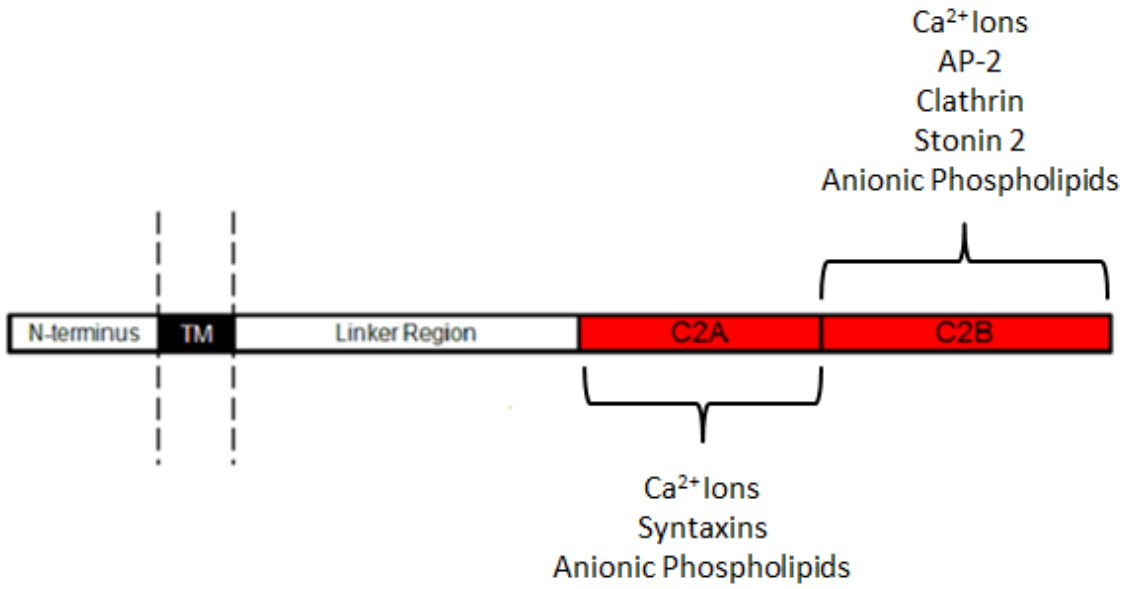

Figure 1.4. **SYTs share a common structure consisting of five domains.**
A simple schematic describing the general structure of the SYT proteins is shown. All isoforms are type I integral membrane proteins containing five distinct domains: the N-terminus, the transmembrane domain (shown in black), the linker region, and two C2 domains (shown in red). Note that the size of the transmembrane domain and the linker region can vary considerably depending on the SYT isoform. The C2 domains have a number of binding partners which are essential for the function of the SYTs, as indicated.

for the longest variant of SYT VII (Sudhof, 2002). The linker region is an additional source of variability and is also the target for extensive gene splicing, leading to the generation of multiple isoforms of the same SYT family members (Gauthier *et al.* 2007, Fukuda and Mikoshiba, 1999). Indeed, the majority of the SYTs exist as multiple splice variants which can have their own unique properties and subcellular distributions. It is currently unclear how many variants exist for each SYT and in which cell types they are specifically expressed.

The crucial Ca^{2+}-binding regions of the SYTs are the two C2 domains, so called because they are highly homologous to the second constant sequence of protein kinase C (Perin *et al.* 1990). The C2 domains consist of an eight-stranded β-sandwich surrounding a conserved 60-residue four-stranded motif known as the C_2 key (Sutton *et al.* 1995). A polybasic region comprising four lysine residues is found in a hairpin loop connecting β-strands 3 and 4, and this region is most likely involved in mediating interactions with anionic phospholipids and protein binding partners (Sutton *et al.* 1995).

The C2A domain of SYT I binds three Ca^{2+} ions while the C2B domain binds two although variations do exist within the family (Sutton *et al.* 1995, Fernandez *et al.* 2001). The crystal structure of the SYT I C2A domain has revealed that the Ca^{2+} binding pocket is found in a cluster spanning 6Å at the tips of flexible loops protruding from the β-sandwich (Ubach *et al.* 1998). Binding requires one serine residue, five aspartate residues, and three backbone carbonyl groups. The conformation of the domain is stabilized by Ca^{2+}-binding. The structure of the C2B domain is similar to the C2A domain although two additional α-helixes are present, one between the 7^{th} and 8^{th} β-strands (helix A) and the other in the C-terminal region (helix B) (Fernandez *et al.* 2001). The physiological implications of these motifs are currently unknown although they may be related to the specific role of the C2B domain in mediating endocytosis by binding to AP2 and clathrin (see Figure 1.4 and Section 1.3.3.2). Ca^{2+} coordination by the C2B domain is achieved by five aspartate residues and two carbonyl groups (Fernandez *et al.* 2001). Interestingly, the C2A and C2B domains function cooperatively in that the physical presence but not necessarily the functional activity of the C2A domain is required for the activation of the Ca^{2+}-binding site of the C2B domain (Bai *et al.* 2002).

Importantly, the SYT family can form hetero- and homo-oligomers and normally function in an oligomeric state (Fukuda *et al.* 2000). Oligomerization can be both Ca^{2+}-dependent and Ca^{2+}-independent, with Ca^{2+}-dependent oligomers forming as a result of interactions between the cytoplasmic domains and Ca^{2+}-independent oligomers resulting from the aggregation of the N-terminal domains. Mutations which abolish the ability of SYTs to undergo oligomerization often render them non-functional (Fukuda *et al.* 2000).

1.3.2 The Classification of the SYT Family Members:

SYTs are generally classified based on their Ca^{2+}-dependency as approximately half of the family (SYTs IV, VIII, and XI – XVII) does not bind Ca^{2+} ions due to an evolutionary-conserved mutation whereby serine is found in place of one of the crucial Ca^{2+}-coordinating aspartate residues in the C2A domain (von Poser *et al.* 1997). Therefore these SYTs are considered to be 'Ca^{2+}-independent.' Indeed, it has been shown that mutating this serine back to aspartate restores the Ca^{2+}-dependency of SYTs IV and XI (von Poser *et al.* 1997). Clearly some SYT family members have Ca^{2+}-independent functions which are more valued than the conventional SYT Ca^{2+}-dependent activities. It is likely that the Ca^{2+}-independent SYTs function to modulate secretion by competing with Ca^{2+}-dependent SYTs for oligomer

SYT	$[Ca^{2+}]_{50}$	Group
I	10	Fast
II	20	Fast
III	2	Medium/Fast
V	2.5	Medium
VI	N/A	Medium
VII	1.5	Slow
IX	N/A	Medium
X	8	Medium

Table 1.1 SYTs can be classified according to their Ca^{2+} binding kinetics.

The estimated Ca^{2+} concentrations which induce half-maximal binding ($[Ca^{2+}]_{50}$) are listed for the C2A domains of each Ca^{2+}-dependent SYT along with the kinetic group to which they belong.

formation and therefore the ratio of expression of Ca^{2+}-dependent and -independent SYTs may provide a mechanism for fine-tuning the calcium sensitivity of secretory events.

The Ca^{2+}-dependent SYTs can be further classified into three distinct kinetic groups based on their Ca^{2+} binding properties. The Ca^{2+} affinity of the SYTs is determined from *in vitro* assays which measure the disassembly kinetics of the cytoplasmic domains following liposome binding (Sugita *et al.* 2002, Hui *et al.* 2005). From this, SYTs I, II, and III have been found to comprise the 'fast' group, SYTs V, VI, IX, and X constitute a group with medium binding kinetics, and finally SYT VII is considered to be the 'slowest' SYT family member (Hui *et al*. 2005). The precise Ca^{2+} binding affinities of the C2A domains of the SYTs are shown in Table 1.1 (information derived from Sugita *et al*. 2002). However, it should be noted that these figures, although a good estimate of the relative Ca^{2+} affinities of the SYT family members, are unlikely to represent the true values seen *in vivo* because the phospholipid composition of target membranes is known to affect the Ca^{2+} binding abilities of the SYTs and full-length molecules most likely have a higher Ca^{2+} affinity than individual C2 domains (Sugita *et al.* 2002).

A further criteria which is often used to classify the SYT family members is whether or not they bind to inositol 1,3,4,5-tetrakisphosphate (IP_4). The putative IP_4 binding site consists of a series of lysine residues found in the C2B domain which are not present in the C2A domain (Ibata *et al.* 1998). SYTs III, V, VI, and X show no significant IP_4 binding ability although they contain putative IP_4 binding sequences whereas SYTs I, II, IV, VII, VIII, IX, and XI show strong IP_4 binding activity (Ibata *et al.* 1998). The deletion of the C-terminus restores the ability of SYTs III, V, VI, and X to bind IP_4, indicating that this region

masks the binding site. The functional significance of IP_4 binding to the SYT family members is currently unclear although it may act to inhibit secretion as inositol polyphosphates are known to prevent neurotransmitter release (Llinas *et al.* 1994).

Lastly, the SYTs show considerable variability in certain aspects of their structure which can be used to differentiate between family members. For example, the N-terminals are highly variable with only SYTs I and II displaying N-linked glycosylation in this region and only SYTs III, V, VI, and X having the ability to undergo disulphide bonding (Sudhof, 2002). Additionally, there is little similarity between the transmembrane domains (TMDs) although all except SYT XII contain a series of cysteine residues in the cytoplasmic region directly adjacent to the TMD. This region is palmitoylated in SYTs I and VII (Sudhof, 2002).

1.3.3 An Overview of the SYT Binding Partners:

As shown in Figure 1.4 the SYTs have a number of binding partners, many of which are components of the exocytic machinery. The interactions between SYTs and these proteins are thought to be essential for mediating regulated secretion by providing a physical link between rising Ca^{2+} levels in the cytosol and the initiation of fusion pore formation following the activation of the exocytic core complex. Equally, as a consequence of their ability to interact with the endocytic proteins clathrin, AP-2, and stonin 2 SYTs most likely play a fundamental role in the regulation of endocytosis as well as exocytosis.

1.3.3.1 SNAREs:

SYTs bind to the C-terminal region of syntaxins in a Ca^{2+}-dependent manner. This ability is not disrupted by mutations which abolish the Ca^{2+}-dependency of SYT I suggesting that SNARE binding is an intrinsic property of all SYTs regardless of their Ca^{2+}-dependency (Chapman *et al.* 1995). The C2A domain of SYTs can also bind to an acidic region in the N-terminal Habc domain of syntaxin in a Ca^{2+}-dependent manner (Fernandez *et al*. 1998). The binding of SYT to syntaxin is now known to be dependent on the ability of Ca^{2+} ions to neutralize basic residues surrounding the Ca^{2+}-binding site in the SYT C2A domain, and hence calcium binding results in an electrostatic switch within the SYT molecule which allows syntaxin binding and possibly the initiation of vesicle fusion (Shao *et al.* 1997).

The affinity of the SYT:syntaxin interaction varies depending on the SYT family member under investigation. For example, SYTs I, II, and V bind syntaxins at Ca^{2+}

concentrations greater than 200 µM, whereas SYTs III and VII can bind syntaxins at concentrations less than 10 µM (Li *et al*. 1995). Interestingly, when SYTs and syntaxins are present at artificially high levels the binding between the two protein families is relatively non-specific as SYTs I, VI, and VII can bind to syntaxins I - IV in any combination. However, at physiological concentrations SYT I binds specifically to syntaxin I and so the SYT:syntaxin interaction *in vivo* is likely to be specific (Li *et al*. 1995).

In addition to its established ability to bind syntaxin in a Ca^{2+}-dependent manner SYT also binds to the second t-SNARE, SNAP-25 (Gerona *et al*. 2000). Indeed, this interaction is thought to enhance the ability of SYT to bind to syntaxin and so possibly promotes the formation of syntaxin/SNAP25 heterodimers (Gerona *et al.* 2000). Chemical cross-linking experiments have demonstrated that SYT proteins bind to three aspartate residues found in the C-terminal helix of SNAP-25 in a Ca^{2+}-dependent manner (Zhang *et al.* 2002). If this region of SNAP-25 is mutated then the exocytosis of LDCVs from PC12 cells is severely inhibited, indicating that the binding of SYT to SNAP-25 plays an essential role in Ca^{2+}-mediated exocytosis, possibly through the stabilization of the SNAREpin.

1.3.3.2 AP2 and Other Components of the Endocytic Machinery:

Clathrin-mediated endocytosis is the primary pathway through which the cargo proteins of fused vesicles are removed from the plasma membrane and returned to intracellular organelles for recycling or degradation. The main constituents of this pathway are the coat protein clathrin, the adaptor complex AP2, and the fission-driving enzyme dynamin. The SYTs bind clathrin and AP2 via their C2B domains in a Ca^{2+}-independent manner and so are likely to play a role in the facilitation of endocytosis as well as exocytosis (Zhang *et al.* 1994, Li *et al.* 1995). Indeed, the expression of mutant SYTs I and VII lacking the C2B domain in HeLa cells inhibits the formation of cell surface clathrin-coated pits (von Poser *et al.* 2000). The interaction between SYT and AP2 is stimulated by the activity of phospholipase D and the presence of tyrosine-based endocytoic motifs similar to those found in cargo proteins (Haucke and De Camilli, 1999). Additionally, endocytosis is dependent on the oligomerization ability of SYTs as over-expressed proteins with truncated transmembrane domains containing mutated cysteine residues are unable to act as dominant-negative inhibitors of endocytosis unlike wild-type truncated proteins (von Poser *et al.* 2000).

SYTs can also interact with the ubiquitous endocytoic protein stonin 2 which facilitates the uncoating of vesicles following their budding from the plasma membrane.

Indeed stonin 2 competes with AP2 for the same binding site in the C2B domain of the SYT protein (Martina *et al.* 2001, Walther *et al.* 2001). Particularly, the mutation of two residues (W719 and K721) in the μ2 homology domain of stonin 2 impairs its ability to bind to SYT I. Therefore it is likely that stonin 2 functions to displace AP2 from SYTs following vesicle budding and thereby stimulates the disassembly of the clathrin coat.

Following exocytosis SYTs play a direct role in mediating endocytosis and therefore are required for granule recycling. Indeed, *C. elegans* with mutant SYT C2B domains show defective recycling of synaptic vesicles at their neuromuscular junctions, leading to reduced quantities of plasma membrane-associated vesicles and impaired neurotransmission (Jorgensen *et al.* 1995).

1.3.3.3 Additional SYT Binding Partners:

SYT I is known to associate with ω-conotoxin-sensitive calcium channels as both proteins co-precipitate in rat brain synaptic membrane preparations (Leveque *et al.* 1992). Additionally, the C-terminus of SYT I binds to the cytoplasmic domains of α- and β-neurexins in a Ca^{2+}-independent manner and this interaction inhibits the phosphorylation of SYT (Petrenko *et al.* 1991, Hata *et al.* 1993, Perin, 1994). Neurexins are brain-specific transmembrane adhesion proteins which were initially identified as the receptors for α-latrotoxin, a component of black widow spider venom. Hence, the interaction between the cytoplasmic portions of the synaptic vesicle protein SYT and a neuronal plasma membrane protein suggests that SYTs play a role in mediating synaptic vesicle tethering.

1.3.4 A Model for the Mechanism of Action of the SYTs:

It is currently unclear exactly how SYTs induce fusion pore formation and vesicle exocytosis following Ca^{2+} binding. However, as a result of the many investigations of recent years examining the mechanism of SYT binding to target membranes and components of the exocytic machinery, a generally-accepted model has been proposed (Tucker and Chapman, 2002). This is shown in Figure 1.5. It is thought that in resting cells vesicle-associated SYTs are in close contact with the plasma membrane syntaxin:SNAP-25 complex. Following cell stimulation SYTs bind Ca^{2+} ions in a coordination sphere which requires negatively-charged molecules contributed from both the SYT C2 domains and anionic phospholipids in the target membrane. Ca^{2+} binding does not cause a large conformational change in the SYT protein but

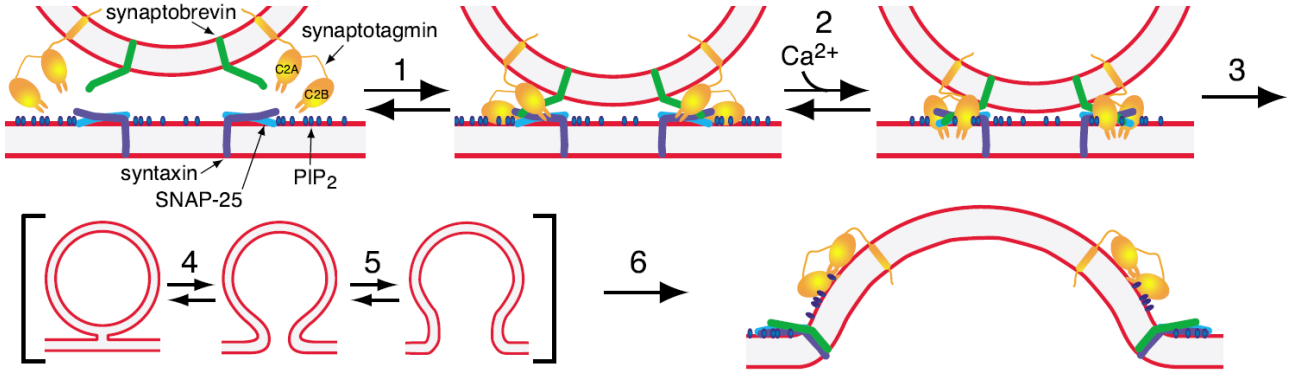

Figure 1.5. A Model Explaining the Mechanism of Action of the SYTs.

In resting cells (1), vesicle-associated SYTs are in close proximity to the target membrane and may form a weak interaction with t-SNAREs. Following Ca^{2+} binding (2), an electrostatic switch in the SYT proteins drives them into the target membrane (3), enhancing their binding affinity to the SNARE complex and physically disrupting the membrane. Hemifusion proceeds (4 and 5) assisted by the oligomerization of the SYTs and SNARE complex formation. Full fusion then occurs and the vesicle's cargo is expelled into the opposing lumen (6).

Figure taken from Tucker and Chapman, 2002

rather results in an electrostatic switch which neutralizes acidic residues and allows the insertion of the SYT into the target membrane. This is thought to disrupt the integrity of the membrane, decreasing the activation energy required for fusion pore formation (Sollner, 2003). At the same time, Ca^{2+}-binding allows SYTs to bind to SNAREs which assists in vesicle tethering and SNAREpin formation. This model was supported by the observation that following Ca^{2+} binding SYT I binds simultaneously to phospholipids in the target membrane and to the ternary SNARE complex with kinetics which are rapid enough to satisfy the requirements for synaptic transmission (Davis *et al.* 1999).

Crucially, it is now thought that the oligomerization of members of the SYT family into ring-like structures, possibly in combination with SNARE proteins, contributes to fusion pore formation by providing physical support for the wall of the aqueous stalk (Tucker and Chapman, 2002). Indeed, mutations which increase the length of the 9-residue linker region connecting the SYT C2A and C2B domains result in a progressive disruption of both the

syntaxin:SNAP-25 interaction and the stability of the fusion pore (Bai *et al.* 2004). Additionally, an elegant single-vesicle content-mixing assay has shown that SNARE proteins alone can drive membrane hemifusion but full pore formation and expansion requires the cooperative action of SYT I and Ca^{2+} (Lai *et al.* 2013).

Lastly, SYTs are likely to play a role in mediating vesicle docking and clustering at the plasma membrane as a consequence of their ability to bind to SNARE proteins. SYT I plays an essential role in the docking of LDCVs in adrenal chromaffin cells via a direct interaction with SNAP-25, as both SNAP-25- and SYT 1-deficient cells show a significantly reduced number of docked vesicles at the plasma membrane (de Wit *et al*. 2009). The over-expression of wild-type, but not a mutant variant of SYT I with impaired SNAP-25 binding ability, was able to rescue docking in SYT I-deficient chromaffin cells. Therefore it is likely that SYT I mediates vesicle docking through a physical interaction with the syntaxin:SNAP-25 acceptor complex in the plasma membrane. This hypothesis has been supported by more-recent studies which have shown that SYT I mediates the rapid docking of synaptic vesicles in a reconstituted membrane fusion system through a mechanism which requires the polybasic region of the SYT C2B domain and the presence of PIP_2 in the target membrane (Wang *et al.* 2011). Lastly, it has been shown that vesicle docking mediated by SYT I is a prerequisite for SNAREpin assembly which is in turn driven by munc18-1 (Parisotto *et al.* 2012). Munc18-1 in isolation cannot drive efficient vesicle docking, demonstrating that SYT is the major docking protein at the plasma membrane. Therefore, on the basis of these studies a model for vesicle docking has been proposed whereby the C2B domain of SYT I binds to SNAP-25 and PIP_2 in the target membrane. This step in the secretory pathway is an essential prerequisite for vesicle fusion.

Therefore, SYTs regulate Ca^{2+}-mediated exocytosis through a coordinated interaction with phospholipids and SNAREs in the target membrane. They are likely to be crucial for the formation of the fusion pore and for vesicle tethering prior to fusion. However the true mechanism of action of the SYT proteins is likely to be more complicated than the model shown in Figure 1.5. Indeed, evidence has been provided suggesting that in resting cells SYTs form a weak Ca^{2+}-independent interaction with SNAREs and phospholipids in the target membrane and this pre-fusion complex prevents spontaneous premature SNAREpin formation (Tucker and Chapman, 2002). It is possible that Ca^{2+} binding then forces the SYTs deeper into the target membrane, thus liberating the *trans*SNARE complex and allowing fusion to proceed.

1.4 Ca^{2+} Signalling and Regulated Exocytosis:

The first indication that regulated exocytosis is initiated by Ca^{2+} ions was provided in 1967 by the pivotal observation that extracellular Ca^{2+} ions are required for synaptic vesicle exocytosis (Katz and Miledi, 1967). It is now known that increasing Ca^{2+} levels in the cytosol act as the crucial trigger for a wide range of secretory events from the rapid release of small synaptic vesicles in neurons to the slower secretion of Large Dense-Core Vesicles (LDCVs) from endocrine cells. These Ca^{2+}-mediated secretory events differ in their kinetics and calcium sensitivity of exocytosis and are regulated by a diverse array of calcium sensors with varying Ca^{2+} affinities (reviewed in Pang and Sudhof, 2010).

In neurons, synaptic vesicles are tethered in the immediate vicinity of plasma membrane Ca^{2+}-channels and so Ca^{2+} influx into the cell from the extracellular medium following the generation of the action potential directly triggers synaptic transmission. However, in non-neuronal cells the Ca^{2+} ions which act as the initial trigger for exocytosis are generally derived from internal sources. In endothelial cells, the binding of a suitable agonist such as histamine or thrombin to cell-surface G-protein-linked receptors results in the activation of a GTP-binding protein which in turn activates phospholipase C-β-1. This enzyme hydrolyses phopsphatidylinositol-4,5-bisphosphate (PIP_2), generating the second messengers inositol 1,4,5-triphosphate (IP_3) and diacylglycerol (reviewed in Berridge, 2009). Mechanical stimulation also activates IP_3 production, providing a mechanism whereby wounding can activate endothelial cells and induce the secretion of pro-thrombotic and vasoconstrictive substances.

Once formed, IP_3 binds to IP_3 receptors (IP_3R) on the surface of the endoplasmic reticulum, leading to the activation and opening of IP_3R Ca^{2+} release channels (Streb *et al.* 1983). Ca^{2+} ions sequestered in the ER then flood the cytoplasm and eventually trigger regulated fusion events at the plasma membrane. In endothelial cells, the mitochondria also constitute a major source of free Ca^{2+} ions which are released following the stimulation of mitochondrial permeability transition pores (PTPs) in the inner membrane (Wood and Gillespie, 1998). Mitochondrial activation is critical for the formation of the Ca^{2+} oscillation patterns which are regularly seen following endothelial stimulation (Falcke *et al.* 1999).

Once internal supplies of Ca^{2+} have been depleted transplasmalemmal Ca^{2+} channels open, allowing the influx of Ca^{2+} ions into the cell from the extracellular medium (Schilling *et al.* 1992). Equally, stimulation of the cell results in the activation of phospholipase A_2 which generates arachidonic acid. This lipid induces Ca^{2+} entry into the cell across the

plasma membrane through a mechanism which is independent of store depletion (Shuttleworth, 1997). Hence, in endothelial cells most agonists trigger a biphasic rise in cytosolic Ca^{2+} whereby the first component is transient and mediated by the release of stored intracellular Ca^{2+} ions. The second component of the Ca^{2+} signalling pattern is larger and more sustained, resulting from the influx of Ca^{2+} across the plasma membrane. Lastly, it is noteworthy that certain endothelial agonists such as thrombin, serotonin, and ATP activate non-selective plasma membrane cation channels which allow the direct entry of Ca^{2+} ions into the cell and so are able to by-pass the requirement for phosphoinositols and internal Ca^{2+} supplies (Brauneis *et al.* 1992, Popp and Gogelein, 1992).

1.5 Weibel-Palade Bodies: A Model System for Regulated Exocytosis

1.5.1 An Introduction to WPBs:

The distinctive rod-shaped secretory organelles which are now referred to as Weibel-Palade bodies (WPBs) were first observed in 1958 by Hibbs and colleagues following an investigation examining the heterogeneity of the endothelium of human skin (Hibbs *et al.* 1958). These investigators reported the presence of 'groups of very dense, rod-shaped granules, varying from 0.1 to 0.3 μ in diameter and 0.3 to 0.6 μ in length,' but did not hazard to guess the function of these novel organelles. Subsequently, in 1964 Edward Weibel and George Palade described a 'hitherto unknown rod-shaped cytoplasmic component' during an electron micrographic study of rat vascular tissue (Weibel and Palade, 1964). They also observed that the bodies contained regularly-spaced fibrous tubules which were approximately 150 Å thick and embedded in a dense matrix. This paper was the first to characterize the structural features of these new organelles and as a result they became known as Weibel-Palade bodies.

In 1982, Wagner and colleagues determined by immunohistochemistry and electron microscopy that the tubular structures seen in WPBs are made up of von Willebrand Factor (VWF) (Wagner *et al.* 1982). VWF is a large multimeric glycoprotein which is synthesized exclusively in megakaryotcytes and endothelial cells and stimulates thrombosis upon its release. The leukocyte receptor P-selectin was subsequently identified as a WPB membrane protein (Bonfanti *et al.* 1989), providing evidence that these organelles are involved in the regulation of both inflammation and thrombosis. In later years, additional WPB cargo

proteins and the ability of these organelles to undergo regulated secretion following the stimulation of the endothelium by suitable agonists would be described.

In short, WPBs are large rod-shaped secretory organelles found exclusively within endothelial cells (for reviews see Valentijn *et al.* 2011, Rondaij *et al.* 2006, Michaux and Culter, 2004). Their primary function is to act as a storage compartment for VWF although they do contain a range of additional cargo proteins including many which regulate inflammation, angiogenesis, and vascular tonicity. A representative immunofluorescence image of a HUVEC teaming with these organelles is shown in Figure 1.6.

1.5.2 The Contents of WPBs:

WPBs contain a range of proteins which regulate diverse biological processes including haemostasis, inflammation, vascular tonicity, and angiogenesis. Table 1.2 provides a comprehensive list of the molecules which have been detected in WPBs thus far and their putative functions. The principal WPB cargo protein is the pro-thrombotic glycoprotein VWF and indeed this molecule and its cleaved peptide make up 95% of the protein content of WPBs (Ewenstein *et al*. 1987). Following the stimulation of the endothelium VWF is rapidly released into the bloodstream where it mediates platelet aggregation by forming long strings which adhere strongly to both the vessel wall and circulating platelets (Dong *et al*. 2002).

Monomeric unprocessed VWF (proVWF) is a large protein of 250 kDa which contains a 22-residue signal sequence and a pro-peptide of 741 residues (Bonthron *et al.* 1986). The pro-peptide is cleaved from the main protein in the TGN by an unknown protease and remains with the mature protein in a 1:1 stoichiometry until the point of WPB fusion at the plasma membrane (Ewenstein *et al.* 1987). Indeed, despite being physically separated from the mature protein the propeptide is essential for its correct multimerization and WPB formation (Journet *et al.* 1993, Leyte *et al.* 1991). From herein the pro-peptide will be referred to as ‘proregion’ and this terminology has relevance for the biochemical assays described at a later point (see 2.7.3 Proregion ELISAs).

VWF is instrumental in driving the formation of WPBs and is solely responsible for their distinctive rod-shaped morphology. The importance of VWF for WPB formation is demonstrated by studies which show that when VWF cDNA is expressed in non-endothelial cells such as the mouse pituitary cell line AtT-20 and the rat insulinoma cell line RIN5F VWF-containing rod-shaped storage granules are produced by these cells (Wagner *et al.*

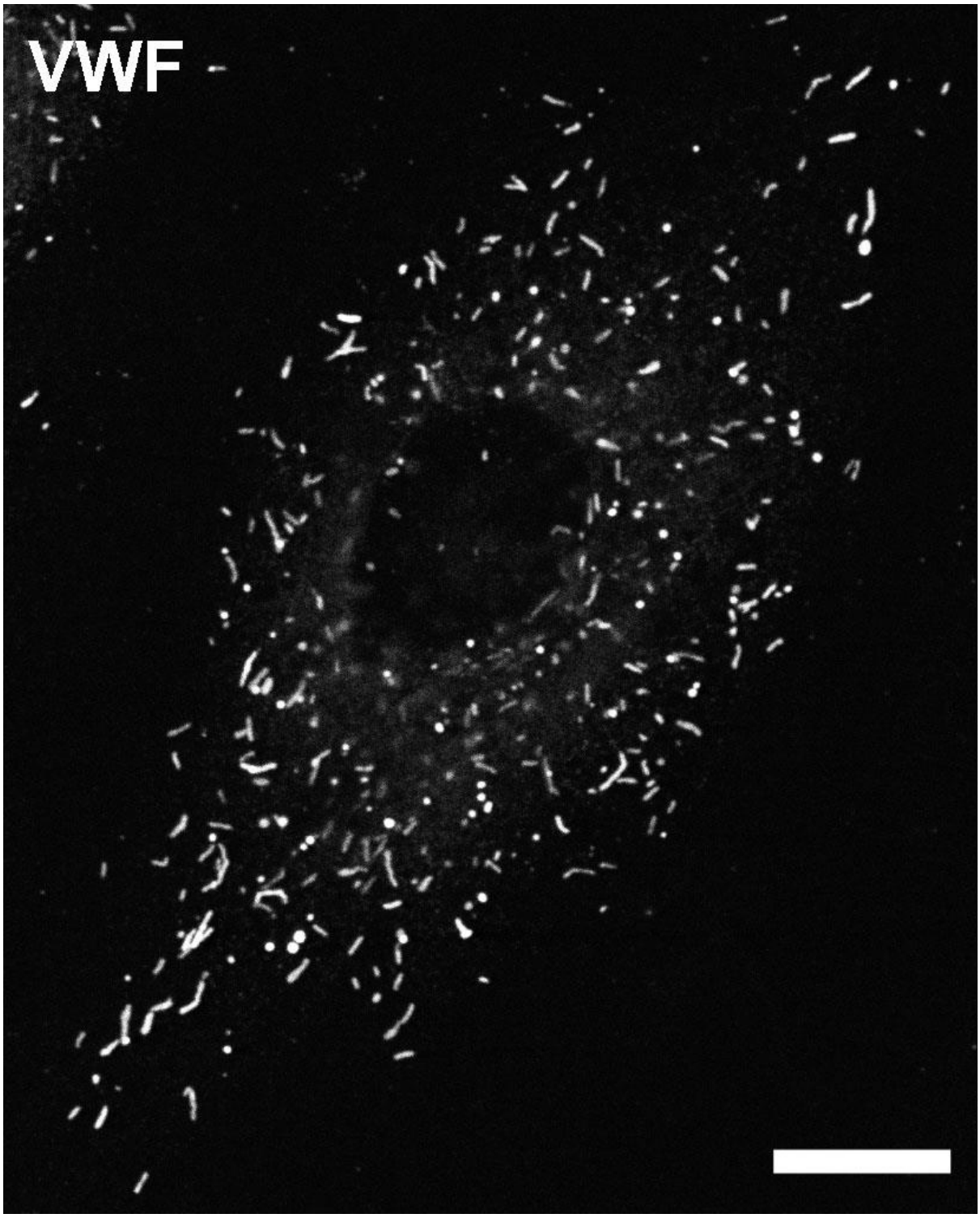

Figure 1.6. Weibel-Palade bodies are large rod-shaped secretory organelles.

A representative image of a HUVEC stained with an antibody specific for the major WPB cargo protein VWF. Numerous rod-shaped WPBs distributed throughout the cytoplasm of the cell have been identified. The scale bar is 20 µm.

Cargo	Function	Reference
VWF	Thrombosis	Wagner *et al*. 1982
P-selectin	Inflammation	Bonfanti *et al.* 1989; McEver *et al.* 1989
Factor XIIIa	Thrombosis	Schaumburg-Lever *et al*. 1994
tPA	Fibrinolysis	Rosnoblet *et al*. 1999
IL-8	Inflammation (neutrophil activation)	Utgaard *et al.* 1998
Exotaxin-3	Inflammation (eosinophil attraction)	Oynebraten *et al.* 2004
α–1,3-fucoysyltransferase VI	Glycosylation	Schnyder-Candrian *et al*. 2000
CD63	Adhesion / Membrane Organization	Vischer and Wagner 1992
Endothelin-1	Vasoconstriction	Ozaka *et al*. 1997, Russell *et al.* 1998a
Endothelin Converting Enzymes	Vasoconstriction	Russell *et al*. 1998a
Calcitonin-gene-related Peptide	Vasodilatation	Ozaka *et al.* 1997
Angiopoietin-2	Inflammation	Fielder *et al.* 2004
Osteoprotegerin	Bone Growth / Cell Survival	Zannettino *et al.* 2005
IL-6	Inflammation	Knipe *et al.* 2010
MCP-1	Inflammation	Knipe *et al*. 2010
Gro-α	Inflammation	Knipe *et al.* 2010
Factor VIII	Coagulation	Rosenberg *et al.* 1998
IGFBP7	Angiogenesis	van Breevoort *et al.* 2012

Table 1.2. WPBs store a wide range of molecules with diverse physiological functions.
A full list of the cargo proteins reported to be resident within WPBs is provided along with each molecule's primary function.

1991). These granules are morphologically identical to endogenous WPBs. Conversely, humans and animals which suffer from severe forms of von Willebrand disease (VWD) and therefore synthesize no functional VWF fail to produce WPBs (Castaman *et al.* 2010, Sadler, 1998). In addition to driving the formation of WPBs, VWF is responsible for the recruitment of a number of other cargo molecules to the forming vesicles such as P-selectin, osteoprotegrin, and IL-8 (Metcalf *et al.* 2008).

P-selectin is found exclusively in platelets, megakaryocytes, and endothelial cells and is the most well-characterized membrane protein found on WPBs. P-selectin is a highly-glycosylated adhesion molecule which binds to P-selectin Glycoprotein Ligand 1 (PSGL-1) on leukocytes, triggering their extravasation to underlying tissues. It is therefore involved in the inflammatory response and may also play a role in mediating thrombosis as it is thought to activate microparticle production (Cambien and Wagner, 2004). Mice which are deficient in P-selectin show a decreased efficiency of leukocyte adherence to the vessel wall following endothelial stimulation (Mayadas *et al.* 1993).

WPBs are heterogeneous organelles and their contents vary depending on the location of a particular endothelial cell within the vasculature and the prevailing environmental conditions. IL-8, for example, is only stored in WPBs following exposure to inflammatory mediators such as TNF-α and IL-1β (Utgaard *et al*. 1998). Exotaxin-3 likewise is only found

in WPBs following their exposure to IL-4 (Oynebraten *et al*. 2004). Interestingly, P-selectin and angiopoeitin-2 are never found within the same organelles, suggesting that the trafficking of these two proteins to WPBs is mutually exclusive although the mechanisms governing this are currently unclear (Fiedler *et al.* 2004). The ability to regulate the exocytosis of certain subsets of WPBs at a given time could impart endothelial cells with considerable flexibility when responding to different environmental stimuli.

Lastly, WPBs contain the tetraspanin CD63 on their limiting membranes which is a marker protein for late endosomes and lysosomes (Vischer and Wagner 1993). The role of CD63 on WPBs is currently unclear although it may function to organize proteins into specific domains within the membrane. Importantly, its presence on WPBs as well as the fact that they require the adaptor protein AP-3 for full maturation has led to the argument that WPBs should be classified as lysosome-related organelles (LROs) rather than simply secretory organelles (Hannah *et al*. 2002). LROs are storage granules which have features in common with lysosomes such as a low internal pH and access to proteins from the endocytic pathway, hence their requirement for AP-3 (Cutler 2002). These organelles include melanosomes, T-cell lytic granules, platelet α-granules, and the secretory granules found in basophils and azurophils. The idea that WBPs may be classified as LROs is important to consider when identifying potential candidate proteins for the regulation of their biogenesis and secretion.

1.5.3 The Biosynthesis, Trafficking, Docking, and Secretion of WPBs:

1.5.3.1 The Formation of WPBs at the TGN:

WPBs develop at the TGN through a process which requires the coat protein clathrin and the adaptor protein AP1. Indeed, both these molecules are seen to coat immature WPBs as they emerge from the TGN, and in some cases cover the entire organelle (Lui-Roberts *et al*. 2005). Disrupting the clathrin coat by over-expressing a dominant-negative version of AP180 inhibits WPB formation and increases the quantity of VWF which undergoes constitutive secretion from HUVECs. In place of wild-type rod-shaped WPBs, small punctate vesicles which do not undergo regulated secretion are formed. The same effect is seen following the knock-down of AP1. As VWF tubulation is responsible for the distinctive rod-shaped morphology of WPBs, it has been proposed that the AP1/clathrin coat provides a

physical scaffold on which VWF can begin folding into tubules. It may be that the coat proteins hold the membrane in an elongated shape allowing time for the VWF subunits to tubulate (Lui-Roberts *et al.* 2005). It is unusual for clathrin to be involved in the biosynthesis of a large secretory granule as this coat protein is generally required for the formation of small vesicles or for the recycling of material back to the TGN. It is probable that the distinctive shape of the WPB requires an unusual coat protein for its biosynthesis. Once the forming WPBs have budded from the TGN, clathrin is no longer necessary for the maintenance of their morphology as brefeldin-A treatment has no effect on the shape of the immature granules (Lui-Roberts *et al*. 2005). However, clathrin-coated buds are seen on newly-formed WPBs, and presumably these are involved in the recycling of unwanted cargo back to the TGN.

It is currently unclear which AP1-interacting proteins are involved in the formation of WPBs at the TGN. However, the inhibition of the AP1 effector proteins γ-synergin and aftiphilin disrupts the ability of mature WPBs to undergo regulated secretion (Lui-Roberts *et al*. 2008). Aftiphilin and γ-synergin are members of the AP1-interacting aftiphilin/γ-synergin/p200 complex which has been reported to be present on both forming WPBs at the TGN and on immature granules in the perinuclear area. The treatment of HUVECs with siRNA for either γ-synergin or aftiphilin results in the production of WPBs which are morphologically normal, have a high electron density, and are positive for Rab27A. However, siRNA-treated HUVECs show an increased quantity of constitutively-secreted VWF while the quantity of VWF which undergoes regulated secretion is only 20% of that seen from control cells. The multimeric state of the VWF released from treated HUVECs is equivalent to that released from control cells, suggesting that the knock-down of aftiphilin and γ-synergin allows the unregulated release of mature WPBs rather than increasing the quantity of VWF directed to the constitutive pathway. Therefore, it appears that aftiphilin and γ-synergin are essential for determining the regulated nature of WPB secretion, and indeed it is possible that these effector proteins function to recruit other components of the fusion apparatus to the forming vesicles (Lui-Roberts *et al*. 2008).

Recently, an AP1 interactor screen performed in *C. elegans* has implicated Rab10 and Rab8a as having key roles in the formation of WPBs (Michaux *et al*. 2010). Both Rab10 and Rab8a are found in the TGN of HUVECs although they are not seen to co-localize with VWF. However, the knock-down of either Rab10 or Rab8a inhibits the secretion of VWF following PMA stimulation by up to 40% (Michaux *et al*. 2010). Interestingly, this inhibition is specific for the immediate secretion of VWF following stimulation and so Rab10 and

Rab8a are most likely involved in the formation or secretion of the RRP. The WPBs in treated cells are morphologically normal and are positive for CD63 and MyRIP as expected, indicating that these two Rabs are involved in WPB formation at the TGN. An identical effect on VWF secretion is seen if Rab10 and Rab8a are knocked-down singularly or together suggesting that these two proteins play a functionally-equivalent role within the cell.

The mechanism by which cargo proteins are targeted to forming WPBs at the TGN is currently unclear. Both osteoprotegrin and IL-8 are retained within WPBs via a direct interaction with VWF. Indeed, if VWF-GFP is expressed in the non-WPB-containing endothelial cell line EC0RF24, IL-8 is recruited to the fluorescent WPBs (Romani de Wit *et al.* 2003). CD63 is recruited to WPBs after they have budded from the TGN via a mechanism which is dependent on AP3 and the tyrosine-based AP3-binding motif, GYEVM (Harrison-Lavoie *et al*. 2006). The mutation of this motif inhibits the recruitment of CD63 to WPBs. As a result of its absence on newly-formed WPBs, CD63 is considered to be one of the markers of mature granules.

The targeting of P-selectin to WPBs is more complicated because it is derived from two pools; newly synthesized protein and protein which has been recycled from the cell membrane. Like IL-8 and osteoprotegrin, P-selectin is able to bind directly to VWF, as shown by the observation that when VWF is over-expressed in epithelial cells P-selectin is found within the VWF-positive organelles formed (Hop *et al*. 2000). This interaction is dependent on the D'-D3 domains of VWF, as when truncated forms of VWF are expressed in HEK-293 cells P-selectin is able to bind only to variants which contain the D'-D3 domains (Michaux *et al.* 2006). These findings have functional consequences for VWD sufferers who have mutations in the D'-D3 domains of VWF and therefore are unable to recruit P-selectin to their WPBs. Newly-synthesized P-selectin arrives in WPBs at the TGN in an AP3-independent manner and efficient trafficking requires its luminal domain and a YGVF motif (Harrison-Lavoie *et al*. 2006). When the luminal domain of P-selectin is expressed in isolation, the peptide does enter WPBs as a result of its interaction with VWF. However, replacing the luminal domain with horseradish peroxidase does not prevent the recruitment of P-selectin to WPBs. Therefore it is likely that the mechanism whereby the cytoplasmic tail of P-selectin mediates its trafficking is indirect. If the luminal domain is deleted leaving only the cytoplasmic domain, recruitment does still occur but is very slow. The YGVF motif is involved in the trafficking of newly-synthesized P-selectin to forming WPBs, as following its deletion mutated P-selectin is trafficked to the lysosomes and endosomes but not to WPBs. It is likely that the loading of P-selectin into WPBs is AP1-dependent as when this protein is

knocked-down in HUVECs P-selectin is absent from the small spherical VWF-containing vesicles which are the by-product of AP1 deletion (Harrison-Lavoie *et al*. 2006). The recruitment of recycled P-selectin back to the WPBs is dependent on two cytoplasmic motifs and the adaptor protein AP3. The KCPL motif contains a key lysosine which mediates AP3 binding, and this regulates the movement of P-selectin from the early to late endosomes. The YGVF motif controls movement from the endosome to the TGN (Harrison-Lavoie *et al*. 2006).

It is currently unclear how the biosynthesis, content, morphology, and secretion of WPBs is regulated at the genomic level. However, the shear-stress induced transcription factor Krüppel-like factor 2 (KLF2) is known to influence the number, morphology, and content of WPBs by inducing an atheroprotective phenotype. When KLF2 is expressed in HUVECs, the result is a quiescent endothelial phenotype which shows anti-inflammatory properties, delayed wound healing, and stress-fibre formation (Dekker *et al.* 2006). Additionally, KLF-2 attenuates the thrombin-induced release of WPBs from HUVECs but does not affect secretion following stimulation by epinephrine. When KLF2 expression is induced in blood outgrowth endothelial cells (BOECs) the result is a 4.5-fold increase in the number of WPBs per cell and these organelles, although rod-shaped, are significantly shorter than those in mock-transfected cells (van Agtmaal *et al*. 2012). The increase in WPB number per cell is most likely a consequence of increased VWF synthesis, as it is known that KLF2 expression increases the quantity of VWF mRNA found within HUVECs (Dekker *et al.* 2006). KLF2 also influences the content of WPBs as granules in transfected BOECs do not contain angiopoietin-2 (ANG-2) and also show reduced levels of IL-8 storage after IL-1β treatment. Following stimulation, virtually no ANG-2 is released from KLF2-treated cells and the level of IL-8 secretion is significantly reduced. Hence, the exposure of the endothelium to shear stress results in an up-regulation of KLF2 which in turn induces WPBs to display an anti-inflammatory, atheroprotective phenotype. Sites of low shear stress such as arterial branch points may be prone to developing atherosclerotic plaques due to a lack of expression of KLF2.

1.5.3.2 The Trafficking of WPBs to the Plasma Membrane:

The first indication that Rab proteins may be involved in the regulation of WPB trafficking and exocytosis came from the observation that non-hydrolysable GTP analogues stimulate VWF exocytosis from endothelial cells (Fayos and Wattenberg, 1997). A number of

specific Rab proteins have since been implicated in regulating WPB secretion. Firstly, Rab27a is recruited to WPBs both in endothelial cells and in non-endothelial cells types where VWF expression has been induced (Hannah *et al.* 2003). This suggests that the recruitment of Rab27a to granules is due to either a direct or indirect association with VWF. Interestingly, Rab27a is not associated with newly-formed perinuclear WPBs but instead is found on peripheral WPBs which are several hours old. This population of peripheral WPBs makes up the RRP which is docked to the actin cortex. The majority of WPBs are associated with microtubules which are then transferred to the actin cortex to replenish the RRP. It is thought that Rab27a may function to transfer WPBs to the actin cortex, as in melanocytes Rab27a is essential for the transfer of melanosomes from the microtubules to the actin cortex prior to their exocytosis (Wu *et al.* 2001). Indeed, if Rab27a is over-expressed in HUVECs the result is an increased number of WPBs in the periphery (Hannah *et al*. 2003).

Immunofluorescence and PCR has revealed that the Rab27a effector protein MyRIP (myosin and Rab27a interacting protein) is localized to mature WPBs where it concentrates at one pole of the granule (Nightingale *et al.* 2009). The recruitment of MyRIP is temporally coupled to that of Rab27a. The knock-down of either Rab27a or MyRIP in HUVECs results in the loss of peripheral WPBs, a 2-fold increase in basal secretion, and a 3.5-fold increase in regulated secretion. The VWF released from transfected cells is less highly-multimerized than that released from mock-transfected HUVECs and following secretion generates VWF strings which are shorter and more numerous. This work suggests that the function of Rab27a and MyRIP is to anchor the WPBs in the actin cortex, allowing time for VWF to multimerize fully. It is noteworthy that patients suffering from Griscelli type II disease who lack a functional Rab27a protein and the naturally occurring Rab27a-negative ashen mouse both show a bleeding phenotype (Nightingale *et al.* 2009). The cause of this unregulated bleeding has not been investigated in any great detail although it is tempting to speculate that the lack of Rab27a may impair regulated WPB secretion and therefore thrombosis in these cases.

A recent paper has demonstrated that myosin Va is found on mature WPBs located in the periphery of the cell and forms a triple complex with Rab27a and MyRIP (Pulido *et al.* 2011). Myosin Va is a member of the myosin V family and HUVECs express both the exon-D-containing isoform and the exon-D-lacking isoform. If either isoform is knocked-down or inhibited by the expression of a dominant-negative variant the result is increased WPB clustering in the perinuclear area and the secretion of less highly-multimerized VWF (Pulido *et al.* 2011). These results suggest that myosin Va functions to inhibit the secretion of immature WPBs from endothelial cells.

A second Rab protein, Rab3D, is found on mature WPBs in the GTP-bound state following its over-expression and functions to regulate WPB formation (Knop *et al*. 2004). If a constitutively-active form of Rab3D is expressed in HUVECs the result is larger and rounder WPBs. In contrast, if a constitutively-inactive version of Rab3D is over-expressed no WPBs are formed. Therefore, Rab3D is essential for WPB formation and most likely functions to regulate the size and shape of mature granules. However, the over-expression of wild-type Rab3D, constitutively-active Rab3D, or constitutively-inactive Rab3D leads to reduced VWF secretion and so its precise role in WPB biogenesis is currently unclear.

Recent work has shown that Rab27 functions cooperatively with Rab15 through a mutual effector protein, Munc13-4, to regulate WPB exocytosis (Zografou *et al.* 2012). Endogenous Munc13-4 localizes to WPBs and its knock-down in HUVECs results in the inhibition of VWF secretion. Rab15 is commonly associated with the endosomal pathway and so many be involved in the recycling of components of the fusion apparatus to newly-synthesized WPBs following endothelial stimulation. The importance of Rab27a and its effectors in the regulation of WPB exocytosis was further demonstrated by the observation that the two Rab27a effectors MyRIP and Slp4-a/granuphilin function cooperatively to mediate the probability of WPB release, with MyRIP acting to inhibit secretion and Slp4-a acting to induce fusion (Bierings *et al.* 2012). It has been proposed that the interplay between these two proteins through Rab27a determines WPB tethering and fusion at the plasma membrane.

1.5.3.3 The Fusion Apparatus Mediating WPB Exocytosis:

It is currently unclear which proteins constitute the fusion apparatus of WPBs. It is known that human aortic endothelial cells express syntaxin-4, VAMP-3, syntaxin-2, and SNAP-23, and thus far evidence has been provided to suggest that syntaxin-4 is the t-SNARE controlling WPB exocytosis on the plasma membrane (Matsushita *et al.* 2003). Indeed, if syntaxin-4 is inhibited with α-syntaxin-4 antibodies WPB exocytosis is decreased by 75% compared with control cells. Recent evidence has shown that VAMP3 and VAMP8 are found on the WPB membrane although only VAMP3 participates in Ca^{2+}-dependent exocytosis (Pulido *et al*. 2010). Cytoplasmic fragments of VAMP3 but not VAMP8 are able to inhibit VWF secretion by approximately 30% compared with untreated cells. As VAMP8 is present on WPBs but does not regulate their fusion it is possible that this SNARE may be involved in the biogenesis of the organelle. VAMP3 can be precipitated from endothelial cells as a

complex with syntaxin-4 and SNAP-23, and so these three SNAREs are likely to be responsible for mediating WPB secretion through the formation of the SNAREpin. However, it is difficult to verify this hypothesis due to the high level of redundancy between SNAREs and the low level of protein needed to facilitate fusion. Indeed, siRNA studies generally fail to detect any significant effects following the knock-down of individual SNAREs.

The expression of Munc18c has been identified in human lung microvascular endothelial cells and following thrombin stimulation both syntaxin-4 and Munc18c are phosphorylated (Fu *et al.* 2005). This modification has been proposed to disrupt the Munc18c:syntaxin-4 interaction, allowing exocytosis to proceed. Hence, Munc18c may have an inhibitory effect on WPB exocytosis.

Finally, it is now known that the annexinA2/S100A10 complex is required for WPB secretion (Knop *et al.* 2004). This heterotetrameric complex is not found on WPBs but instead is localized to the plasma membrane and cytoplasm where it binds to phosphatidic acid in the membrane. The inhibition of annexin-A2 by the treatment of HUVECs with either siRNA or blocking peptides leads to reduced VWF secretion (Knop *et al.* 2004). The annexin A2/S100A10 complex has been implicated in forming actin-rich membrane domains in other cell types and so it may be involved in organising the plasma membrane to allow WPB fusion.

1.5.3.4 Signalling Mechanisms Governing WPB Exocytosis:

Mature WPBs are held at the plasma membrane and undergo regulated secretion in response to stimulation of the endothelium by a wide range of agonists, most of which are associated with tissue injury or inflammation. A number of WPB agonists are proteins associated with the coagulation cascade and include thrombin and fibrin (Levine *et al*. 1982, Ribes *et al.* 1987). Others are released from activated platelets such as ATP, serotonin, and sphingosine-1-phosphate (Vishcer and Wollheim 2000, Schluter and Bohnensack, 1999, Matsushita *et al.* 2004). Others still are associated with inflammation including IL-4 and the complement proteins (Inomata *et al.* 2009, Hattori *et al.* 1989). Indeed, WPB exocytosis can be initiated by the direct contact of endothelial cells with bacterial constituents such as LPS and lipoteichoic acid (Schorer *et al.* 1987, Into *et al.* 2007). Exocytosis can also be induced by environmental conditions such as exposure to hypoxic conditions and radiation (Pinsky *et al.* 1996, Sporn *et al.* 1984). The list of substances which induce WPB exocytosis is large and

growing. The most recent observation is that WPB secretion is stimulated by silica nanoparticles which are used extensively in medical procedures for drug delivery, cancer therapy, and are often added to cosmetics and paint (Bauer *et al.* 2011).

Stimulants which trigger WPB secretion do so either through Ca^{2+}- or cAMP-dependent signalling, with the pathway utilized determined by the particular agonist. Thrombin is currently the most well-characterized Ca^{2+}-dependent agonist and its application to endothelial cells causes a rapid localized increase in the intracellular free Ca^{2+} concentration (Vischer *et al.* 2000). The Ca^{2+} sensitivity of WPB exocytosis is currently unclear although a number of studies have reported that secretion requires the prolonged exposure of endothelial cells to high Ca^{2+} concentrations of between 10-20 µM (Birch *et al.* 1992, Carter *et al.* 1998, Zupancic *et al.* 2002). It is assumed that, as with classical models of regulated secretion, free Ca^{2+} ions bind to an as-yet unidentified calcium sensor which then drives the fusion of WPBs with the plasma membrane. Based on the estimated Ca^{2+} sensitivity of WPB exocytosis, it is likely that this protein is a low-affinity Ca^{2+} sensor. For example, the well-characterized calcium sensors SYTs I and II show Ca^{2+} binding kinetics which match the secretion profile of WPBs (see Table 1.1). However, it is important to consider that the true Ca^{2+} threshold required for WPB exocytosis following receptor stimulation *in vivo* is likely to differ from the estimates provided thus far as these studies do not account for the spatial control of Ca^{2+} increases within the cell. Additionally, the optimum Ca^{2+} levels required for WPB exocytosis vary depending on the stimulation technique employed. For example, flash photolysis of caged Ca^{2+} results in maximal WPB exocytosis at 20 µM Ca^{2+} whereas this occurs at 7.1 ± 1.5 µM Ca^{2+} following the direct stimulation of HUVECs with thrombin (Zupancic *et al.* 2002). Hence the true calcium sensitivity of WPB secretion is currently debatable and requires further investigation, ideally with the aim to mimic physiological conditions.

The mechanisms regulating cAMP signalling in endothelial cells are unclear although they are known to be blocked *in vitro* by the inhibition of PKA (Vischer *et al.* 1997). An interesting feature of cAMP-dependent secretion is that in response to increased levels of cAMP in the cell WPBs congregate in the perinuclear region in what is thought to be the centrosome (Rondaij *et al.* 2006). It is likely that this is a mechanism to limit the number of organelles secreted at once as only WPBs in the periphery of the cell undergo exocytosis. This clustering may also result in only a subset of WBPs being released, hence allowing a more tailored response to specific agonists.

The stimulation of endothelial cells by increasing levels of either Ca^{2+} or cAMP leads to cytoskeletal rearrangements which increase or decrease endothelial cell permeability and hence impact the vascular tonicity of blood vessels. The precise effect depends on the nature of the stimulant. For example, exposure to thrombin leads to RhoA activation and this results in the formation of stress fibres which in turn causes endothelial permeability to increase as tight junctions disassemble (van Nieuw Amerongen *et al*. 2000). Conversely, cAMP-induced signalling results in Rap1 activation and decreased permeability of the endothelium as adherens junctions are strengthened (Cullere *et al.* 2005). In both cases, WPBs are released but this is accompanied by opposing effects on endothelial permeability. Therefore, it is likely that different agonists result in varying degrees of inflammation as stimulation which increases levels of cAMP results in thrombosis but minimized leukocyte extravasation whereas stimulants which raise calcium levels lead to a more pronounced inflammatory response.

1.5.4 The Clinical Importance of WPBs:

As is apparent from Table 1.2, WPBs secrete a wide range of proteins which regulate diverse biological processes including thrombosis, vascular tonicity, angiogenesis, and inflammation. It is not surprising therefore that the errant secretion of WPBs from chronically-activated endothelial cells has been implicated in the pathogenesis of many human diseases. The most well-characterized example of this is the established link between WPB exocytosis and the development of atherosclerotic plaques. Indeed, $VWF^{-/-}$ mice show a reduced number and size of atherosclerotic plaques (Methia *et al*. 2001). Equally, pig models for VWD show a resistance to developing atherosclerosis (Fuster *et al*. 1978). It is thought that the excessive release of VWF in the vicinity of atherosclerotic lesions promotes thrombosis and exacerbates the condition.

A number of infectious diseases which attack the endothelium such as malaria, dengue fever, and sickle cell anaemia induce the release of WPBs. It is highly likely that this results in severe clinical consequences by contributing to the obstruction of small blood vessels which is often the cause of death in these conditions. Additionally, the increased level of VWF and proregion in the plasma of infected people can be used as a useful biomarker for disease progression. For example, numerous studies have demonstrated that the plasma levels of VWF and proregion are considerably elevated in children with malaria and correlate with

the level of plasma lactate, an established biomarker for disease severity (Hollestelle *et al.* 2006, Larkin *et al.* 2009, de Mast *et al.* 2009, Phiri *et al*. 2011). The levels of these proteins decrease as treatment commences and clinical symptoms improve. Additionally, a recent study has demonstrated that Indonesian children suffering from dengue haemorrhagic fever show increased plasma levels of highly-multimerized VWF, proregion, and osteoprotegrin compared with healthy controls (Djamiatun *et al.* 2012).

Recently, the release of WPBs has been linked to the development of the degenerative neurological condition multiple sclerosis and to the recruitment of stem cells. Firstly, mice models for multiple sclerosis which are deficient in VWF show an earlier onset of encephalomyelitis, a greater number of lesions, and a more severe disease phenotype characterized by increased demyelination and neutrophil infiltration into the brain (Noubade *et al*. 2008). Therefore VWF may protect against the development of multiple sclerosis although the rationale behind this is currently unclear as it was initially anticipated that the release of WPBs would exacerbate the condition by increasing the permeability of the blood-brain barrier and allowing the extravasation of leukocytes into the brain. WPBs have also been loosely linked to the process of stem cell recruitment as they are released following exposure to the stem cell mobilizing agent uric acid (Kuo *et al.* 2008). The WPB cargo protein angiopoeitin-2 also stimulates the rapid mobilization of hematopoietic stem cells, indicating that the release of WPBs may provide a positive-feedback mechanism ensuring the rapid recruitment and activation of stem cells following tissue injury.

Lastly, it has always been anticipated that the endothelium would play a role in the development of tumours and their metastasis as both processes require increased angiogenesis which is governed by endothelial cells. It is now known that VWF adheres directly to the murine melanoma cells B16-BL6 *in vitro* via its RGD domain (Terraube *et al*. 2006). Additionally, VWF $^{-/-}$ mice injected with B16-BL6 cells show a significantly greater occurrence of metastatic foci compared with wild-type mice due to the increased survival rate of tumour cells in the lungs of VWF-deficient animals. Hence VWF plays a protective role in metastasis by inducing the destruction of cancerous cells.

Therefore, in addition to providing a useful model for regulated exocytosis WPBs have considerable clinical importance in their own right. Our understanding of the control of WPB exocytosis at the molecular level is however lacking and therefore further studies attempting to identify the components of the signalling pathways and fusion apparatus which mediate the release of these organelles from endothelial cells are necessary. Information

derived from these investigations may aid in our understanding of how the errant release of WPBs contributes to the pathogenesis of human disease.

1.6 SYTs and WPB Exocytosis in Human Endothelial Cells: Thesis Aims

As has been discussed thus far, endothelial cells are metabolically active specialized secretory cells and their major defining feature is the presence of the large rod-shaped organelles WPBs. These granules are not only useful models for regulated secretion but they are also clinically important. Our knowledge concerning the physical structure, molecular composition, and synthesis of WPBs has become more detailed in recent years. However, the signalling pathways which govern their release and the molecules which make up the WPB fusion apparatus are currently unclear. Specifically, it is unknown which protein or group of proteins constitute the calcium sensor regulating WPB fusion with the plasma membrane. SYTs are the most well-characterized family of calcium sensors and have an established role in mediating the Ca^{2+}-dependent exocytosis of a large number of vesicles and organelles from a range of cell types. Therefore, it is my hypothesis that the Ca^{2+}-mediated release of WPBs from endothelial cells is regulated by one or more members of the SYT family. This thesis describes my efforts to test this hypothesis by determining which SYTs are expressed in HUVECs and attempting to assign functional roles to these endothelial-expressed SYTs.

Chapter Two
Materials and Methods

2.1 Reagents:

The SYTVII-YFP and SYTVII-YFP-D/N constructs were a kind gift from Professor Norma Andrews (University of Maryland). The CLB proregion-35 antibody was a kind gift from Professor M.J.A van Mourik (Sanquin Research, Amsterdam). The full details of all commercial antibodies used for Western blotting and ICC are listed in Table 2.1 (for α-SYT antibodies) and Table 2.2 (for all other antibodies).

2.2 Tissue Culture and Nucleofection™:

2.2.1 The Culture of HUVECs:

Passage 1 Human Umbilical Vein Endothelial Cells (HUVECs) were purchased from PromoCell GmbH (Heidelberg, Germany). Initially, passage 1 HUVECs were grown on a 14-cm dish and once confluent were expanded to 4 x 14-cm dishes. These cultures were grown to confluency prior to collection into vials (3 per dish) which were then frozen at -80°C. The vials (now passage 3) were used as stocks for individual experiments (e.g. for ELISAs each individual assay was performed with a separate vial of stock cells). HUVECs are primary human cells and as such are inherently heterogeneous. The passage 1 cells purchased from PromoCell are derived from a pool of umbilical cords and therefore are representative of a number of individuals, hence providing some degree of control over the natural variability of HUVECs. Additionally, prior to despatch from the manufacturer all HUVECs are screened for their morphology, adherence, viability, and expression of the endothelial marker proteins VWF and CD31. It is well-known in the Carter lab and has been reported by other groups that the rate and extent of WPB exocytosis from HUVECs varies due to the inherent heterogeneity of individual cultures and is also affected by passage number and confluency states (Nightingale *et al.* 2009, Howell *et al.* 2004). When repeating biochemical assays and ICC protocols this was controlled for by ensuring that HUVECs were plated at similar densities and used at the same passage number. Even so, I observed considerable variability in the secretory response of ionomycin-stimulated HUVECs. The

Antigen	Manufacturer	Catalogue Number	Host Species	Optimum Dilution for ICC	Optimum Dilution for Western Blotting
SYT I	Synaptic Systems	105 011	Mouse	1:200*	1:200
SYT III	abcam®	ab81538	Rabbit	N/D**	N/D
SYT III	Synaptic Systems	105 133	Rabbit	1:200	1:200
SYT V	abcam®	ab116452	Rabbit	N/D	1:200
SYT VI	abcam®	ab24250	Rabbit	1:200	1:200
SYT VII	Synaptic Systems	105 172	Rabbit	1:200	1:200
SYT VII	Santa Cruz	Sc-15418	Goat	N/D	N/D
SYT VIII	Acris Antibodies	AP54128PU-N	Rabbit	N/D	1:200
SYT XI	Santa Cruz	Sc-101299	Mouse	N/D	1:200
SYT XVII	abcam®	ab76274	Rabbit	N/D	1:500

Table 2.1. The details of the α-SYT antibodies.

* Unless otherwise stated, the optimum dilutions of the SYT antibodies for ICC were determined in HEK cells expressing fluorescent constructs of the SYT proteins.

** N/D = Not Determined. The antibody failed to recognize its antigen under any of the conditions tested.

Antigen	Manufacturer	Catalogue Number	Host Species	Optimum Dilution for ICC	Optimum Dilution for Western Blotting
VWF	DAKO	A0082	Rabbit	1:10000	N/A*
VWF	Serotec	AHP062	Sheep	1:10000	N/A
VWF	Serotec	MCA127	Mouse	1:100	N/A
Actin	Sigma-Aldrich	A5060	Rabbit	N/A	1:1000
Tubulin	Sigma-Aldrich	T9026	Mouse	N/A	1:5000
LAMP1	DSHB**	H4B4	Mouse	1:100	N/A
CD63	DSHB	H5C6	Mouse	1:200	N/A
EEA-1	BD Transduction Laboratories	610456/7	Mouse	1:100	N/A
TGN-46	Serotec	AHP500	Sheep	1:300	N/A
PDI	Stressgen	SPA-891	Mouse	1:100	N/A
tfR	Invitrogen	13-6800	Mouse	1:200	N/A
VAMP3	Synaptic Systems	104 102	Rabbit	1:200	N/A
GFP	Molecular Probes	A-11122	Rabbit	1:300	Variable
GFP	Biogenesis	4745-1051	Sheep	1:250	Variable
Rab27a	BD Transduction Laboratories	610595/6	Mouse	1:100	N/A
tPA	abcam®	ab28219	Rabbit	1:250	N/A
PECAM	DSHB	PSB1	Mouse	1:20	N/A

Table 2.2. The details of the non-SYT commercial antibodies.

* N/A = Not Applicable. Western blotting or ICC was not performed for this antigen.

** DSHB = Developmental Studies Hybridoma Bank

extent of the basal release of VWF from unstimulated cells ranged from 0.2 - 2.5% of the total VWF within the cells whereas the equivalent figure for proregion was generally around 1%. The extent of the stimulated secretion of VWF in response to 1 µM ionomycin exposure ranged from 8 – 30% of the total VWF within the cells and that of proregion ranged from 35 - 65%. When assaying HUVECs cultured in 24- rather than 6-well plates this value could be as high as 85% total secreted protein.

HUVECs were cultured in HUVEC growth media (HGM) consisting of medium 199 (Invitrogen, Paisly, UK) supplemented with 20% fetal calf serum (Biosera, Ringmer, UK), 50 µg/ml gentamicin (Invitrogen), 10 U/ml heparin (Invitrogen) and 30 µg/ml endothelial cell growth supplement (ECGS) (Upstate, Dundee, UK). Cells were grown at 37°C under 5% CO_2 on 14-cm dishes, 6-well plates, 24-well plates, or 9-mm ethanol-sterilized glass coverslips. All culture dishes were purchased from Thermo Scientific (Langenselbold, Germany) and were coated with 1% porcine gelatin (Sigma-Aldrich, St. Louis, USA) prior to use. For passaging, confluent HUVECs were washed once with Dulbecco's 1x sterile PBS (Invitrogen) followed by a short incubation with 2.5 mL of 0.25% trypsin-EDTA (Invitrogen). When the HUVECs had fully detached from the growth surface, the trypsin was inactivated by the addition of 9.5 mL of HGM. The required quantity of the cell suspension was added to fresh HGM which was then re-plated onto new gelatin-coated growth surfaces. For experiments, HUVECs were grown to confluency and used at either passage 4 or 5.

2.2.2 The Culture of HEK-293 Cells:

Human Embryonic Kidney-293 (HEK-293) cells were cultured in Minimal Essential Medium (MEM) Alpha Medium 1x (Invitrogen) supplemented with 10% fetal calf serum (Biosera, Ringmer, UK) and 50 µg/ml gentamycin (Invitrogen). Cells were grown at 37°C under 5% CO_2 on 14-cm dishes, 6-well plates, or 9-mm ethanol-sterilized glass coverslips. There was no need to pre-coat growth surfaces with gelatin. HEK cells were split using the same protocol as for HUVECs (2.2.1 The Culture of HUVECs) with the exception that MEM Alpha medium was used in place of HGM. HEK cells were maintained at approximately 80% confluency and were used up to passage 25.

2.2.3 The Nucleofection™ Protocol:

Nucleofection™ is a form of transfection which allows the direct transfer of DNA into cell nuclei and generally results in excellent transfection efficiency (between 40-70%) and cell viability (around 95%) (Hamm *et al.* 2002, Maasho *et al.* 2003). For the transfection of HUVECs with DNA constructs and siRNA, the Amaxa Nucleofection™ system was used according to the manufacturer's instructions (Lonza Biologics Plc, Slough, UK). Briefly, confluent HUVECs were washed once with Dulbecco's 1x sterile PBS, incubated with 2.5 mL of 0.25% trypsin-EDTA until they had fully detached from the growth surface, and 9.5 mL of HGM was added to the trypsinzed cells. The required quantity of cell suspension was then centrifuged for 3 minutes at 1000 RCF. The HGM was removed and the cell pellet was re-suspended in 100 µL of HUVEC OLD Nucleofector™ Solution containing 2-4 µg of target DNA. The solution was transferred to a supplied curvette and transfected using programme U-01 of the Nucleofector™ device. Immediately following transfection, the cell suspension was transferred to fresh HGM pre-warmed to 37°C and then plated onto gelatin-coated growth surfaces. Cells were used for experiments 8 – 48 hours following transfection depending on the expression properties of the transfected construct.

The Nucleofection™ procedure for HEK cells was identical to that for HUVECs with the exceptions that MEM Alpha medium was used in place of HGM, Cell Line Nucleofector™ Solution V was used in place of HUVEC OLD Nucleofector™ Solution, the cells were transfected with programme Q-01 rather than U-01, and growth surfaces were not pre-coated with gelatin.

2.2.4 The Knock-Down of SYT mRNA:

For the knock-down of SYT mRNA in HUVECs, ON-TARGET*plus* SMARTpool siRNA was purchased from Dharmacon (Thermo Scientific, St. Leon-Rot, Germany) and prepared in 5 x siRNA resuspension buffer (Dharmacon) according to the manufacturer's instructions. HUVECs were transfected with 200 – 400 pMol of SYT siRNA using the Amaxa Nucleofection™ system as detailed above (2.2.3 The Nucleofection™ Protocol). As a control, HUVECs were transfected with non-targeting siRNA (ON-TARGET*plus* Non-targeting Control Pool #D-001810, Dharmacon, Thermo Scientific, St. Leon-Rot, Germany). The extent of protein knock-down for each SYT was determined by Western blotting and quantified using ImageJ software (National Institutes of Health, Bethesda, Maryland, USA).

2.3 Reverse-Transcription PCR:

Reverse-transcription polymerase chain reaction (RT-PCR) was used to detect the expression of SYT mRNA transcripts in HUVECs and HEK cells. For each of the 17 members of the SYT family, two sets of unmodified DNA primers were purchased from eurofins (Ebersberg, Germany). These primers were designed to span two exons flanking an intron as shown in Figure 2.1 using the SYT gene sequences provided in the Ensembl database (http://www.ensembl.org/index.html). The purpose of this was to discriminate between coding mRNA and any contaminating genomic DNA as the sizes of amplified fragments would be considerably different. The sequences of the primers are shown in Table 2.3. Template RNA for RT-PCR was extracted from confluent HUVECs and HEK cells using the RNeasy® Mini Kit (Qiagen, Manchester, UK) according to the manufacturer's instructions. The quantity and purity of extracted RNA was determined by measuring its absorbance at 280 and 260 nm using a Nandrop-1000® device (Wilmington, DE, USA). Purified RNA was stored at -20°C and thawed on ice. RT-PCR was performed using a SuperScript™ One-Step kit (Invitrogen, Paisley, UK) according to the manufacturer's instructions. Briefly, 1 µg of RNA was added to the reaction mix and cDNA was synthesized using one cycle of heating to 55°C for 20 minutes following by an increase to 94°C for two minutes. Subsequent PCR amplification of HUVEC cDNA was achieved using 40 cycles of denaturation (94°C for 15 seconds), followed by annealing (55°C for 30 seconds) and extension (72°C for 1 minute). PCR was performed using a Mastercycler® machine (eppendorf, Stevenage).The products of PCR were run on a 1.5% agarose gel and visualized by ethidium-bromide staining. All bands of interest were sent for sequencing to confirm their identities (GATC Biotech, Cologne, Germany).

2.4 Western Blotting:

2.4.1 Lysate Extraction:

2.4.1.1 Conventional Lysate Extraction:

Lysates were extracted from confluent HUVECs and HEK cells grown on either 14-cm dishes or 6-well plates. For lysate extraction from 14-cm dishes, the cells were trypsinized as described (2.2.1 The Culture of HUVECs) and the cell suspension was centrifuged for three minutes at 1000 RCF. The cell pellet was re-suspended in PBS and centrifuged again for three minutes at 1000 RCF. The supernatant was removed, and 2 x Laemmli sample

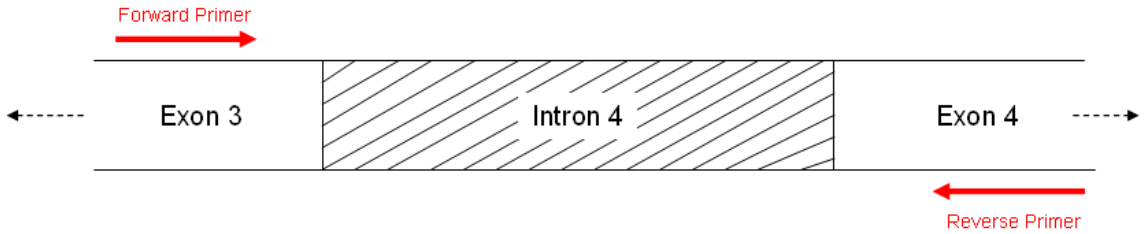

Figure 2.1. The strategy used to design the SYT primers.

Primers were selected to span two exons flanking an intron. During splicing, the intronic sequence is removed, allowing discrimination between coding mRNA and contaminating genomic DNA.

SYT	Primer Set One		Primer Set Two	
	Forward Primer	Reverse Primer	Forward Primer	Reverse Primer
I	GCCATAGTCGC AGTCCTTTT	ATCCTTGAGGGCC TGATCTT	ACAGTGGATTTTG GCCATGT	CCACCCACATCCA TCTTCTT
II	GAAGGGGAGG AGGAGAAAGA	TTCCGATGGACTTT GGTCTC	TCACTGTCTGCAT CCTGGAG	AATCTGCTCGAAG GGGATCT
III	GATCTACCTGC TGCCTGACC	CGAGAAGCGGTCA AAGTCAT	ATAATGAGGCGCT GGTGTTC	CACTAGCTGATGC CAGTGCT
IV	GGCCTTGCACT TCACAATTT	GTAACTCACCCCG TCCTGAA	TTCAGGACGGGGT GAGTTAC	TTTGGCATGGTAC AGGTTCA
V	CTCAGGCCTCC TCATCTTCA	TTCTGGCTGCACCT TGTCTA	CCCTATGAGCTCC GTGGAC	TTTTAGCCTCCAGG ACGATG
VI	TTGAGGCCTCT GACCTGTCT	GCCTTGAGGTTCC GACACT	TGAGGCCATCATC TTTGACA	TTACCTCCACCAA GGAGTGC
VII	GCGCAGTGAGA AGAAGGCTA	ATCTCGCTGGTGA GGGAGT	AGGTGTCCATCCC CCTTAAC	GATGTCCATGGCT TTGAGGT
VIII	GAAGAAGCCCA GGGACAAG	GCTTCCAAAGTCG AACTCCA	GCTTCTCTCTCCGG TACGTG	AGGAAGGTGAAGG CCTCATT
IX	ACTTAATCGGC CAAGTGGTG	CAGCCGTTGGAAG ATAGCAC	CCCGAGAACATTG ACCAAAT	GGCTTCCGAGGAT ATGACAA
X	TGACATGATTG GGGAAGTGA	AGCCGTCGGTAGG TAACAAA	ACATCCCTCCAGA GAACGTG	GCCAGTGCGTTAT TGGTTTT
XI	CAGCACAGGCA AGGTACAAC	ATCCATCTTCGGC AAGTGTC	GACACTTGCCGAA GATGGAT	GGTCAGTGGGGAT GTCGTAG
XII	CCGTTCCCCAA TTACGACTA	CCCCAGTTCACTG ATGCTCT	TCCTGCTCTCCCTC AGCTAC	CGGCTGTCTTCTTT TTGCTC
XIII	AAGAGGCAGGT CACAGAGGA	CAAACAATTCTGC CTTCTGACA	TCCTGGTGGTGCT GATTAAA	TGATCATCTCGTTC CACACG
XIV	CTTGGGAAACA AGGCAGAAA	ACAGATGGGGAGA ACCACTG	TTCAAGGGAAAAT GTCATTGC	GGCATTATAAAGC AGGCCAAT
XV	GTGCTCTTCCCC TTGAAGAA	ACAATGCCTCTGT CCTCCTG	GACCTCCAGTTCT GCCTCAG	GCCTTGAAGCTGA AGGTCTC
XVI	AGCAAAGAAGT GGCCTTCAA	TTTGGTTTCTGCTC CAATCC	GGACTCTGCCCAA AATTCAA	TGAAGGCCACTTC TTTGCTT
XVII	AGCGACGATGT GGACTCTCT	CTTCTGGTCTGGC AGGAGAC	GTCTCCTGCCAGA CCAGAAG	GTGGCGGGAGAAC TTATCAA

Table 2.3. The sequences of the primers used to identify SYT family members.

buffer (50% w/v glycerol, 15% SDS, 400mM Tris pH 6.8, 0.01% bromophenol blue) supplemented with 5% β-mercaptoethanol and a protease inhibitor cocktail (1:100 dilution, Sigma-Aldrich) was added to the pellet at a 1:10 weight/volume ratio followed by heating to 95°C for 5 minutes. Samples were frozen at -20°C if necessary. For lysate extraction from 6-well plates, the media was removed from each well followed by a brief PBS wash. 400 µL of 2 x Laemmli sample buffer supplemented with 5% β-mercaptoethanol and a cocktail of protease inhibitors was added to each well. Lysates were collected by scraping into 1.5 mL eppendorfs and transferred to a heat block set at 95°C for 5 minutes. The samples were homogenized by shearing with a 23G needle, centrifuged at 13,000 RPM for 1 minute, and frozen at -20°C if necessary.

2.4.1.2 TX-114 Lysate Partitioning:

TX-114 partitioning is a technique used to enrich a solubilized whole-cell sample with membrane proteins using the mild detergent TX-114. Following the heating of a lysate sample from 0°C, TX-114 separates into an aqueous phase containing hydrophilic proteins and a detergent phase which contains amphiphilic integral membrane proteins (Bordier, 1981). Here, cells were lysed in cold TX-114 lysis buffer (consisting of 1% TX-114 buffer (10% stock, Sigma-Aldrich), 1 mM EDTA, and 1:100 protease inhibitors) and the lysate was mixed by rotation at 4°C for 1 hour. The sample was then spun for 10 minutes at 13,000 RPM at 4°C. The supernatant was removed, heated to 37°C for 1 minute with mild agitation, and then centrifuged for 1 minute at 13,000 RPM. The pellet was washed with cold PBS, incubated on ice for 5 minutes, and heated to 37°C with mild agitation. The sample was then centrifuged for 1 minute at 13,000 RPM, the supernatant was removed, and 10 µL of 10 mg/ml bovine haemoglobin (Sigma-Aldrich) was added to the TX-114 layer which now contains the membrane proteins. 400 µL of methanol, 200 µL of chloroform, and 300 µL of dH_20 were added sequentially to the sample which was then spun for 3 minutes at 13,000 RPM. The top phase containing the extracted proteins was transferred to 300 µL of methanol. The mixture was then spun for 5 minutes at 13,000 RPM and the supernatant was removed. Finally, the pellet was incubated with 2 x Laemmli sample buffer, heated to 95°C for 5 minutes, and frozen at - 20°C if necessary.

2.4.2 Immunoblotting:

Lysates were diluted to a 1:1 ratio in 2 x Laemmli sample buffer, loaded onto home-made 10% acrylamide gels, and separated by running for 40 minutes at 200 volts on a Mini-Protean® II Cell electrophoresis device (Biorad, Hemel Hempstead, UK). The separated proteins were transferred to 0.2 µm nitrocellulose membranes (Whatman®, Maidstone, UK) at 12 volts for 1 hour. The extent of protein transfer was visualized by a brief incubation with 0.2% Ponceau S (Sigma-Aldrich), which was then removed by washing with PBS. The blots were blocked with 5% milk (Marvel, Premier Foods) for 30 minutes followed by 2 x PBS washes and 2 x dH_20 washes. For immunoblotting, blots were incubated with primary antibodies diluted in PBS/Tween (PBS supplemented with 0.3% Tween-20) for one hour. The optimized dilutions of the primary antibodies are shown in Tables 2.1 and 2.2. When initially optimizing an antibody for Western blotting it was necessary to use the Miniblotter-28® device (Immunetics, Cambridge, MA), which allows the simultaneous screening of multiple antibodies at various concentrations. The Miniblotter-28® was used according to the manufacturer's instructions and blots were rinsed extensively with PBS/Tween to prevent any over-spill between wells prior to their removal from the device. Following incubation with the primary antibodies, blots underwent 5 x 5 minute PBS washes and were then incubated in the dark for 25 minutes with dye-coupled secondary antibodies diluted in blocking buffer (PBS-Tween containing 5% milk) to 1:5000. All secondary antibodies for Western blotting were purchased from LI-COR Biosciences (Cambridge, United Kingdom). Blots then underwent 5 x 5 minute PBS/Tween washes in the dark followed by 2 x PBS washes and 2 x dH_20 washes. Finally, the blots were visualized using a LI-COR Odyssey Infrared Imaging System (LI-COR Biosciences, Cambridge, United Kingdom).

2.5 Immunocytochemistry:

2.5.1 Fixation Methods:

2.5.1.1 Methanol Fixation:

HUVECs or HEK cells were grown to confluency on 9-mm glass coverslips. The media was removed and the cells were fixed for 5 minutes at -20°C with ice-cold methanol. The coverslips were then washed once with PBS and incubated with permeabilisation solution (PGAS, 0.2% w/v gelatin, 0.02% w/v saponin, 0.02% w/v NaN_3, made up in PBS) for at least 5 minutes prior to staining.

2.5.1.2 PFA/Saponin Fixation:

HUVECs or HEK cells were grown to confluency on 9-mm glass coverslips. The media was removed and the cells were fixed with 3% paraformaldehyde (PFA) in PBS for 20 minutes. Cells were then permeabilised and quenched by incubation for 15 minutes with 50 mM NH_4CL and 0.2% saponin made up in PBS. Cells were incubated with PGAS for at least 5 minutes prior to staining.

2.5.1.3 TX-100 Fixation:

HUVECs or HEK cells were grown to confluency on 9-mm glass coverslips. The media was removed and the cells were fixed with 3% PFA in PBS for 20 minutes. Cells were then quenched by incubation for 15 minutes with 50 mM NH_4CL made up in PBS, followed by a 5 minute permabilisation with 0.03% TX-100 in PBS. Cells were incubated with PGAS for at least 5 minutes prior to staining.

2.5.2 Immunostaining:

Individual 9-mm glass coverslips were incubated cell-side down in a humidified chamber with 50 µL of a solution containing the primary antibodies diluted in PGAS. The optimum dilutions of the primary antibodies used for immunocytochemistry (ICC) are shown in Tables 2.1 and 2.2. Following the 1 hour primary incubation, the coverslips were removed and washed 3 times with PGAS. The coverslips were then incubated in the dark for 45 minutes with 50 µL of flurophore-conjugated secondary antibodies diluted in PGAS. Secondary antibodies were purchased from Jackson ImmunoResearch (West Grove PA, USA) and were used at dilutions of 1:200 (for Rhodamine Red™-X and Cy™-5) and 1:150 (for Cy™-2). The coverslips were then washed three times with PGAS and three times with PBS. They were dipped twice in dH_20 prior to mounting with Mowiol (Polysciences Inc., PA, USA) onto glass microscope slides (Thermo Scientific, Waltham, MA, USA). Mounted coverslips were viewed using a Leica SP2 Scanning Spectral Confocal Microscope (Milton Keynes, UK) equipped with a 100x/1.40 NA oil immersion objective lens. Images were prepared in Adobe Photoshop CS4 (San Jose, CA, USA).

2.6 Molecular Biology:

Fluorescent constructs containing DNA encoding the *Aequorea Victoria* green fluorescent protein (GFP) were constructed for each member of the SYT family which is known to be expressed in HUVECs and were used to determine the subcellular localization of the endothelial SYTs. GFP is a non-toxic, stable protein which does not affect the growth or function of transfected cells (Chalfie *et al.* 2004). Therefore, GFP fusion proteins are excellent tools for determining the subcellular localization of endogenous proteins when conventional techniques such as ICC fail.

2.6.1 Conventional Ligation-Dependent Cloning:

To generate the SYTI-EGFP construct, conventional cloning methods were used as illustrated in Figure 2.2. Initially, HUVEC mRNA was extracted from a confluent 14-cm dish using the RNeasy® Mini Kit (Qiagen, Manchester, UK) according to the manufacturer's instructions. HUVEC cDNA was synthesized from the purified mRNA using the Quanitect® Reverse-Transcription Kit (Qiagen, Manchester, UK) according to the manufacturer's instructions. Primers were designed which encompassed the cDNA sequence for SYT I and incorporated sites for the restriction enzymes HindIII and AgeI. The sequences of the primers were as follows: 5'-AGTTT**AAGCTT**ATGGTGAGCGA-3' (forward primer) and 5'-GCCGTCAAGAAGGG**ACCGGT**TTTA-3' (reverse primer), where the sequences in bold show the positions of the restriction sites for HindIII (forward) and AgeI (reverse). PCR was performed using the KOD Hot Start DNA Polymerase kit (Merck, Feltham, UK) according to the manufacturer's instructions. The cycling conditions were as follows: heating to 50°C for 30 minutes followed by an increase to 94°C for 2 minutes followed by 40 x [94°C for 15 seconds, 55°C for 30 minutes, and 70°C for 1 minute] followed by a final step of heating to 72°C for 5 minutes. The PCR product was run on a 1.5% agarose gel and purified using the GenElute™ Gel Extraction Kit (Sigma-Aldrich) according to the manufacturer's instructions. Both the purified PCR fragment and 2 µL of a Clontech pEGFP-N1 vector (BD Biosciences Clontech, Saint-Germain-en-Laye, France) were digested using the restriction enzymes HindIII (Roche, Welwyn Garden City, UK) and AgeI (New England Biolabs (NEB), Hitchin, UK) at 37°C for 3 hours in the presence of the appropriate NEB buffer and BSA. Digested products were run on a 1.5% agarose gel and purified using the GenElute™ Gel Extraction Kit (Sigma-Aldrich) according to the manufacturer's instructions. The vector and SYT I

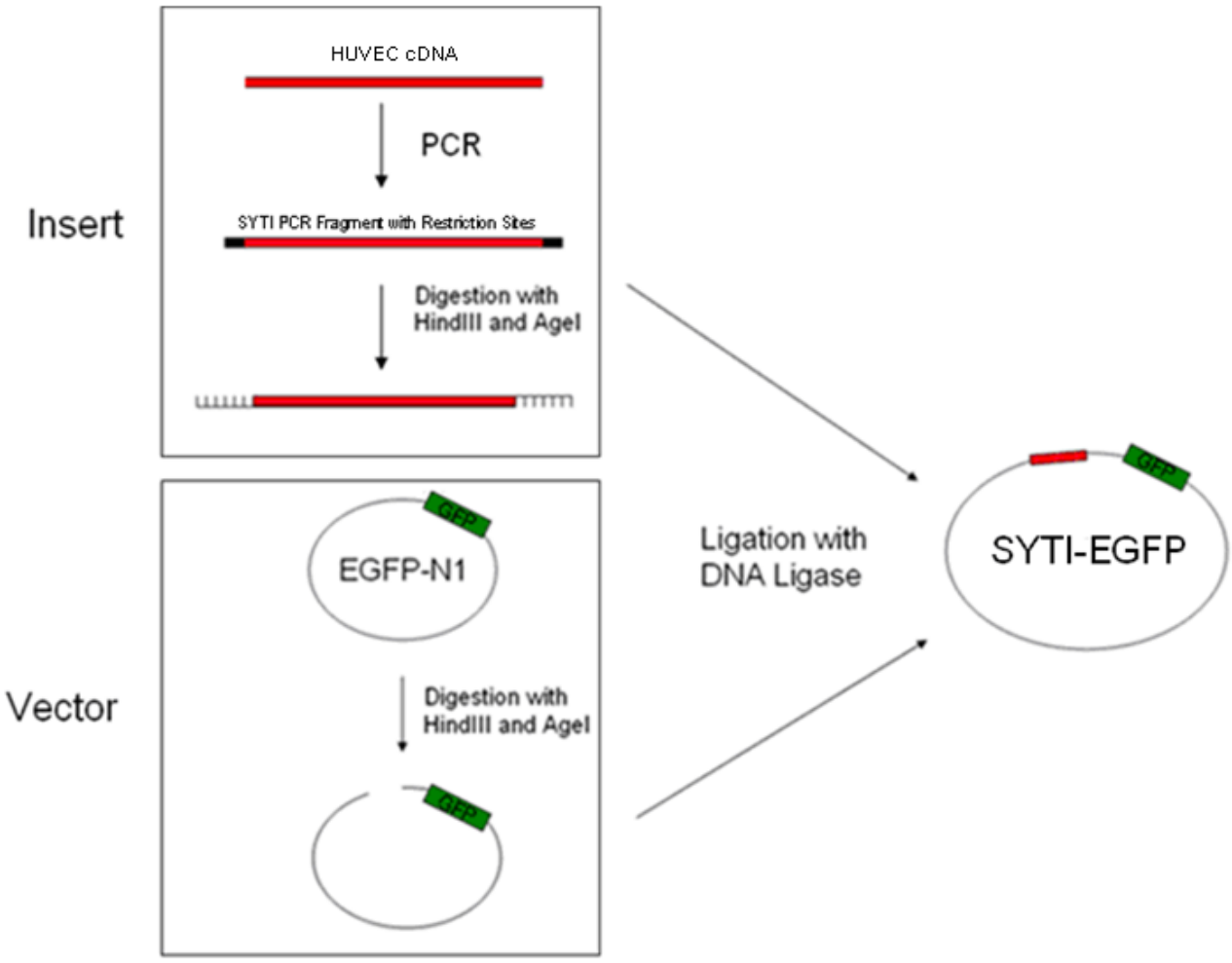

Figure 2.2. The strategy used to produce the SYTI-EGFP construct.
The cDNA sequence for SYT I was amplified from a pool of HUVEC cDNA using primers containing restriction sites for AgeI and HindIII and then digested using these same enzymes. Meanwhile, the EGFP-N1 vector was digested with HindIII and AgeI and both the insert and vector were combined by ligation to produce the SYTI-EGFP vector.

insert were then incubated together in a 1:1 ratio in the presence of 0.25 µL of T4 DNA ligase (New England Biolabs, Hitchin, UK) and 0.25 µL of its accompanying buffer at room temperature for 2 ½ hours. The ligated product was used to transform competent bacteria according to the protocol detailed below (2.6.4 The Transformation of Competent Bacteria). The purified construct was sequenced to confirm its identity. The SYTI-mCherry construct was produced using this same protocol with the exception that a pmCherry-N1 parent vector (BD Biosciences Clontech, Saint-Germain-en-Laye, France) was used in place of the pEGFP-N1 parent vector.

2.6.2 Ligation-Independent Cloning (LIC):

2.6.2.1 The Theory of the LIC Method:

Ligation-independent cloning (LIC) is a relatively novel technique for cloning PCR fragments which eliminates the need for restriction enzymes and DNA ligase (Aslanidis and Jong, 1990). For the LIC method, PCR primers are designed which contain a 12-nucleotide dTMP-free sequence at their 5'-ends and therefore yield products which do not contain dAMP at their 3'-ends. The final 12 nucleotides of the amplified product can be removed by digestion using the (3'- 5') exonuclease activity of T4 DNA polymerase in the presence of dATP. This leaves 5' single-stranded ends on the amplified PCR fragments. The LIC parent vector contains a specific TMP-lacking sequence which can also be digested with T4 DNA polymerase in the presence of dTTP. This leads to the generation of single-stranded sequences in the vector which are complementary to the single- stranded tails of the PCR product, allowing spontaneous circularization between the product and the vector. This approach inhibits the re-ligation of the parent vector which is often a cause of failure with conventional cloning methods. A schematic showing the theory behind the LIC method is provided in Figure 2.3.

2.6.2.2 The LIC Protocol:

For the generation of SYT-EGFP constructs the LIC method was used unless otherwise stated. The parent LIC-EGFP vector was digested using the restriction enzyme XmaI (New England Biolabs (NEB), Hitchin, UK) and NEB buffer 4 at 37°C for 3 hours. The digested product was run on a 1.5% agarose gel and purified using the GenElute™ Gel

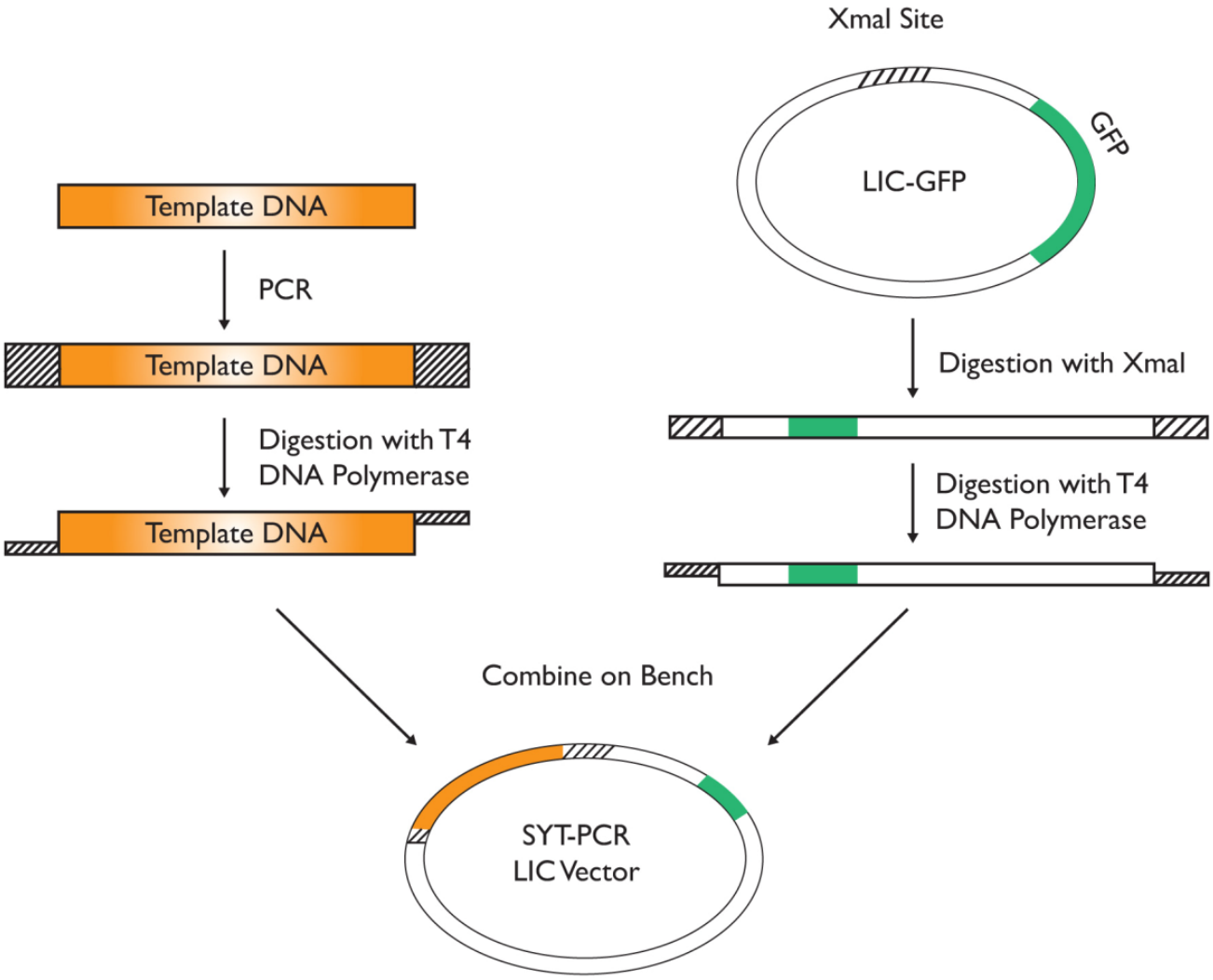

Figure 2.3. The theory behind the LIC method.

Template DNA in the form of SYT image clones was amplified using specific LIC primers. The PCR products were digested using the exonuclease activity of T4 DNA polymerase leaving 5' single-stranded ends. Meanwhile, the parent LIC vector was opened by XmaI digestion followed by further digestion with T4 DNA polymerase. The vector and PCR product now contain complementary single-stranded ends which will anneal spontaneously under the appropriate conditions. Further details are provided in the text.

SYT	Forward Primer	Reverse Primer
III	GCAGGGGCGCAACAGACCCCGGTATGTC AGGAGACTACGAGGA	CCACCAGGCCGGCCAGCACCCGGTCCCTC GGAGTTCTCTTTCTCTG
V	GCAGGGGCGCAACAGACCCCGGTATGTT CCCGGAGCCCCCAAC	CCACCAGGCCGGCCAGCACCCGGTCCGGG CGCAGGCAGCAGCCTCAC
VI	GCAGGGGCGCAACAGACCCCGGTATGC CCTGGAGGAACAAGGA	CCACCAGGCCGGCCAGCACCCGGTCCCAA CCGAGGGTTTCCCTC
VII	GCAGGGGCGCAACAGACCCCGGTATGT ACCGGGACCCGGAGGCGG	CCACCAGGCCGGCCAGCACCCGGTCCGGC CTTCAGCTGGTGCCAC
VIII	GCAGGGGCGCAACAGACCCCGGTATGCT CCACCTGCATGGCTG	CCACCAGGCCGGCCAGCACCCGGTCCGGA GTGGGGCAAGGGCAGGC
XI	GCAGGGGCGCAACAGACCCCGGTATGG CTGAGATCACCAATAT	CCACCAGGCCGGCCAGCACCCGGTCCGTA CTCGCTCAGACTGTGCC
XVII	GCAGGGGCGCAACAGACCCCGGTATGG CGTACATCCAGTTGGA	CCACCAGGCCGGCCAGCACCCGGTCCGGT CACCTCCAGGGAGGCAG

Table 2.4. The sequences of the primers used for the LIC method.

The sequences of the primers for each member of the SYT family known to be expressed in HUVECs are shown. Note that SYT I was cloned using conventional cloning techniques and therefore is not included in the table.

Extraction kit according to the manufacturer's instructions. LIC primers were designed for each SYT isoform known to be expressed in HUVECs with the exception of SYT I according to the theory detailed above (2.6.2.1 The Theory of the LIC Method). The sequences of the LIC primers are shown in Table 2.4. Image clones containing the SYT cDNA sequences were purchased from Source Bioscience (Nottingham, UK) and amplified using the KOD Hot Start DNA Polymerase kit (Merck, Feltham, UK) according to the manufacturer's instructions. The cycling conditions were as follows: 1 heating step to 95°C for 5 minutes followed by 10 x [95°C for 15 seconds, 52°C for 15 seconds, and 70°C for 3 minutes] followed by 30 x [95°C for 15 seconds, 58°C for 15 seconds, and 70°C for 3 minutes] followed by a final step of heating to 70°C for 5 minutes. The PCR products were purified using the GenElute™ PCR Clean-up Kit according to the manufacturer's instructions. Following vector digestion by XmaI and insert amplification by PCR, the T4 digestion reactions were set up. For the vector, 4 pMol of purified vector were added to 4 µL of T4 DNA polymerase buffer (Promega Madison, WI, USA), 4 µL of 25 mM dTTP, 2 µL of 100 mM DTT, 6 µL of T4 DNA polymerase (New England Biolabs, Hitchin, UK), and the mixture was made up to 40 µL with dH_20. For the insert, 2 pMol of purified PCR fragment were added to 2 µL of T4 DNA polymerase buffer, 2 µL of 25 mM dATP, 1 µL of 100 mM DTT, 3 µL of T4 DNA polymerase, and the mixture was made up to 20 µL with dH_20. The reactions were incubated at room temperature for 30 minutes followed by incubation with either 2.2 µL (insert) or 4.4

µL (vector) of 50 mM EDTA for 20 minutes at 75°C. The individual reactions were then purified using the GenElute™ PCR Clean-up kit according to the manufacturer's instructions with the exception that the products were eluted with 30 µL of dH_20 instead of elution buffer. Then, 1 µL of insert and 2 µL of vector were combined and left at room temperature for 15 minutes followed by the addition of 2 µL of 100 mM EDTA. The mixture was then heated to 75°C for 3 minutes. The tubes were removed from the heat block, wrapped in tin foil, and allowed to cool slowly for 1 hour at room temperature. The samples now contain SYT-EGFP LIC constructs and were used to transform competent bacteria as described (2.6.4 The Transformation of Competent Bacteria). All constructs were purified by maxiprepping (see 2.6.7 Maxiprepping) and sequenced to confirm their identities.

2.6.3 Site-Directed Mutagenesis:

Site-directed mutagenesis was performed using the Stratagene QuikChange® Site-Directed Mutagenesis Kit according to the manufacturer's instructions (Agilent Technologies UK Limited, Cheshire, UK). High-purity primers were designed with the aid of an on-line primer design tool (http://labtools.stratagene.com/QC). To generate the SYT V calcium-insensitive mutant the following primers were used: 5'-ggtcatggcggtgtacagcttcgaccgcttctct-3' (forward primer) and 5'-agagaagcggtcgaagctgtacaccgccatgacc-3' (reverse primer). To generate the dominant-negative cytoplasmic SYT V mutants the following primers were used: 5'-gcaggggcgcaacagaccccggtatgtgctgtttctgtctctacc-3' (forward primer) and 5'-ccaccaggccggccagcacccggtccgggcgcaggcagcagcctcac-3' (reverse primer). To generate the SYT VII calcium-insensitive mutant the following primers were used: 5'- tctacctccaagtcctg-agctatgaccgcttcagcc-3' (forward primer) and 5'-ggctgaagcggtcatagctcaggacttggaggtaga-3' (reverse primer). To generate the dominant-negative cytoplasmic SYT VII mutants the following primers were used: 5'-gcaggggcgcaacagaccccggtatgtgtcagcgcaaactgggcaaa-3' (forward primer) and 5'-ccaccaggccggccagcacccggtccggccttcagctggtgccac-3' (reverse primer).

2.6.4 The Transformation of Competent Bacteria:

DH5α competent bacteria (Invitrogen, Paisly, UK) were incubated on ice with a variable quantity of target DNA for 30 minutes. They were then heat-shocked at 42°C for 45 seconds and immediately placed on ice for 2 minutes. 1 mL of SOC media (NIMR, London,

UK) was added and the mixture was incubated at 37°C with shaking at 1,000 RPM for 1 hour. Tubes were then spun for 1 minute at 13,000 RPM, the majority of the supernatant was removed, and the bacterial cell pellet was re-suspended in the remaining SOC media (approximately 100 µL). The suspension was plated onto pre-dried agar plates containing the appropriate antibiotic using aseptic technique. Plates were incubated overnight at 37°C.

2.6.5 Liquid Cultures:

To grow transformed bacteria in small liquid cultures (2.5 mL), individual colonies were picked from agar plates using ethanol-sterilized tweezers and aseptic technique. Colonies were incubated overnight with 2.5 mL of L-broth (NIMR, London, UK) containing the appropriate antibiotic at 37°C and with vigorous shaking. Liquid cultures were then processed for miniprepping as described below (2.6.6 Miniprepping). To grow transformed bacteria in large liquid cultures (250 mL), 50 µL of bacterial suspension from a small liquid culture were incubated with 250 mL of L-broth containing the appropriate antibiotic at 37°C and with vigorous shaking. Samples were then processed for maxiprepping as described below (2.6.7 Maxiprepping).

2.6.6 Miniprepping:

The alkaline lysis method was used to isolate plasmid DNA from transformed bacteria according to the theory and protocol detailed in Brinboim and Dolly (1979) with minor modifications. This method will be referred to herein as 'miniprepping.' Briefly, 1.5 mL of bacterial suspension from a small liquid culture was centrifuged at 13,000 RPM for 30 seconds. The supernatant was removed and the pellet was re-suspended in 250 µL of cold STE (100 mM Tris-HCL pH 8, 100 mM NaCl, 1 mM EDTA). The solution was centrifuged at 13,000 RPM for 30 seconds and the supernatant was removed. The bacterial pellet was re-suspended in 100 µL of Solution I (50 mM glucose, 25 mM Tris-HCL pH 8, and 10 mM EDTA) and 200 µL of freshly-prepared Solution II (200 mM NaOH, 1% SDS). The mixture was incubated at room temperature for 10 minutes. 150 µL of Solution III (60 mL 5M KAc, 11.5 mL HAc, made up to 100 mL in dH_20) was then added and the mixture was incubated on ice for 10 minutes. The samples were then spun at 13,000 RPM for 5 minutes. The supernatant was removed and transferred to a fresh 1.5 mL eppendorf. 2 volumes of 100% ethanol were added and the samples were incubated at -20°C for 1 hour, followed by

centrifugation for 5 minutes at 13,000 RPM. The supernatant was removed and the cell pellet was washed with 500 µL of 70% ethanol. The samples were centrifuged one final time at 13,000 RPM for 5 minutes and the supernatant was removed. The pellets were allowed to dry at room temperature and were then dissolved in 30 µL of TE buffer (10 mM Tris-HCL pH 9, 1 mM EDTA).

2.6.7 Maxiprepping:

'Maxiprepping' is a technique which allows the isolation of large amounts of pure plasmid DNA from a large liquid culture and was performed according to the protocol detailed in Molecular Cloning 3rd Edition (Sambrook and Russell, 2001). Briefly, the bacterial suspension from a large liquid culture (2.6.5 Liquid Cultures) was pelleted at 3,000 RPM for 10 minutes at 4°C in a Beckman JS 4.2 centrifuge (Beckman Coulter, High Wycombe, UK). The bacterial pellet was re-suspended in 25 mL of ice-cold STE and the bacteria were pelleted once again at 3,000 RPM for 10 minutes at 4°C in a Beckman JS 4.2 centrifuge. The supernatant was removed and the pellet was re-suspended in 10 mL of Solution I. 1 mL of 10 mg/ml lysosyme (Sigma-Aldrich, St. Louis, USA) made up in Solution I was added and the mixture was incubated at room temperature for 10 minutes. 20 mL of freshly-prepared Solution II were added and the mixture was incubated at room temperature for 10 minutes. Lastly, 15 mL of ice-cold Solution III were added and the mixture was incubated on ice for 10 minutes followed by centrifugation at 4,200 RPM for 15 minutes at 4°C. The supernatant was filtered through home-made glass wool filters and 27 mL of isopropanol were added. The mixture was then incubated at room temperature for 10 minutes and centrifuged at 4,200 RPM for 30 minutes at 22°C. The pellet was washed with 70% ethanol and allowed to dry at room temperature. Dry pellets were then dissolved in 6 mL TE buffer and the weight of the DNA solution was calculated. For each 1 g of solution, 1.1 g of solid CsCl (Invitrogen) were added and the sample was mixed until homogenous. At this point, 120 µL of ethidium bromide (Biorad, Hemel Hempstead, UK) were added and the samples were incubated in the dark for 15 minutes. The tubes were centrifuged at 3,000 RPM for 15 minutes at 22°C. The red supernatant was transferred to 2 x 3.9 mL QuickSeal tubes (Beckman Coulter, High Wycombe, UK) which were then spun in a TLN-100 ultracentrifuge (Beckman Coulter, High Wycombe, UK) at 100,000 RPM overnight at 22°C. The thin band of plasmid DNA was removed from the QuickSeal tubes, placed in a 15 mL centrifuge tube, and 6 mL of water-saturated N-butanol were added. The solution was shaken vigorously to

encourage phase separation. The top organic layer was removed from the tube and an additional 6 mL of N-butanol were added. This procedure was repeated until no ethidum bromide remained in solution. The aqueous phase was transferred to a fresh 15 mL tube and made up to 5 mL with dH_20. 10 mL of 100% ethanol were added and the tubes were incubated on ice for 15 minutes. The samples were spun at 3,000 RPM for 15 minutes at 4°C. The pelleted plasmid DNA was then washed with 70% ethanol and allowed to dry at room temperature. Finally, the plasmid DNA was dissolved in TE buffer and made up to 2 mg/ml.

2.7 The Enzyme-Linked Immunosorbent Assay (ELISA) Protocol:

2.7.1 Sample Collection:

HUVECs were transfected with either a DNA construct or with SYT siRNA according to the protocol detailed previously (2.2.3 The Nucleofection™ Protocol). At the same time, control cells were transfected with either a non-functional cytoplasmic construct or with non-targeting siRNA. Cells were seeded onto 6-well plates in such a way as to ensure that equal numbers of wells were designated as 'stimulated' and 'unstimulated' and each condition was replicated at least three times. A schematic of the experimental design for media collections is shown in Figure 2.4. Transfected HUVECs were grown to confluency and were used 8 – 48 hours following transfection depending on the expression properties of the construct. To initiate sample collection, 1 mL of release media (consisting of bicarbonate free M199 (Gibco® Life Technologies, Invitrogen, Paisley, UK) and 20 mM HEPES, pH 7.4), was added to each well and the HUVECs were allowed to acclimatize to the media for 50 minutes at 37°C. This was then removed and replaced with fresh release media. After 10 minutes, the media was collected in 1.5 mL eppendorfs and replaced with 1 mL of fresh media containing either 1 µM ionomycin calcium salt (Sigma-Aldrich, St. Louis, USA) or an equivalent volume of 100% ethanol to act as the control non-stimulating solution. After 10 minutes, the release media was collected into 1.5 mL eppendorfs. The samples were spun for three minutes at 13,000 RPM to remove cellular debris and the supernatants were transferred to fresh 1.5 mL eppendorfs. The cell lysates were then collected by incubating the wells with 1 mL/well of lysis buffer (made up of release media, protease inhibitors (1:100 dilution) and 1% TX-100) on ice for five minutes. Lysates were collected by scraping and samples were spun for 5 minutes at 13,000 RPM to remove cellular debris. The supernatants were transferred to fresh 1.5 mL eppendorfs and if necessary frozen at -20°C.

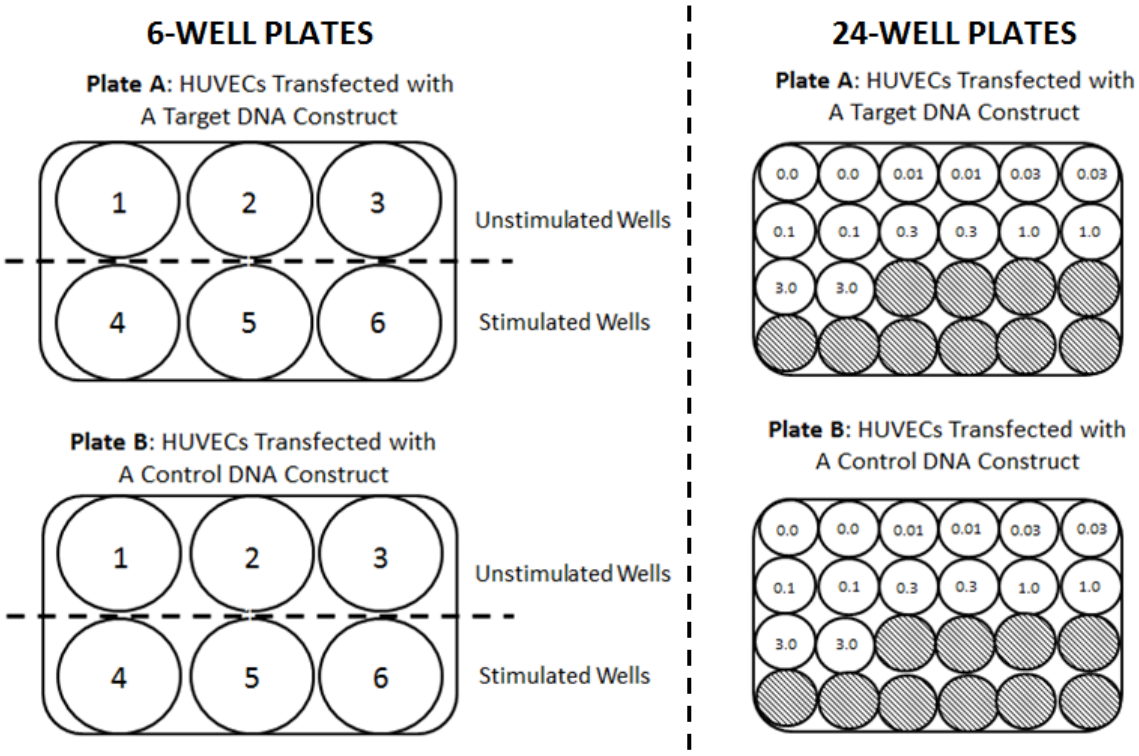

Figure 2.4. The experimental design for media collections.

The experimental set-up for 6-well plates is shown on the left and that for 24-well plates is shown on the right. For the 6-well plates, equal numbers of wells were designated as 'unstimulated' and 'stimulated.' Unstimulated wells were exposed to the ethanol control solution whereas stimulated wells were exposed to 1 µM ionomycin. Each condition was replicated three times. For the 24-well plates, HUVECs were exposed to varying concentrations of ionomycin. The number within each well indicates the applied dose of ionomycin (µM). Each condition was done in duplicate, and the shaded wells were excess.

2.7.2 VWF ELISAs:

VWF ELISAs were used to determine the quantity of VWF secreted by stimulated and unstimulated cells in the presence or absence of either an over-expressed protein or SYT siRNA. 96-well plates (Thermo Scientific, Rochester, NY, USA) were coated with a rabbit anti-VWF antibody (DAKO, Catalogue Number A0082) diluted to 1:600 in PBS. After an overnight incubation in the dark, the anti-VWF antibody was removed and the wells were blocked for 1 hour with 300 µL of Tween-ELISA buffer (TWEB; 0.2% w/v gelatin, 1 mM EDTA, 0.1% Tween-20, made up in PBS). Following blocking, the TWEB was removed and 100 µL of sample was added to each well. Lysates were diluted 1:8 with lysis buffer prior to loading. A standard curve was constructed using a known concentration of VWF (derived from HEK-474 cells over-expressing VWF) serially diluted in a 1:1 ratio 11 times in either release media or lysis buffer. For each plate, a blank containing un-modified release media or lysis buffer was included at the end of the standard curve. The standard curve and the samples were placed on a titramax-100 (Heidolph Instruments, Saffron Walden Essex) for 1 hour at 750 RPM, after which point the samples were removed and the wells were washed 3 times with TWEB. To each well, 100 µL of HRP-conjugated rabbit anti-VWF (DAKO, Catalogue Number P0226) diluted to 1:1000 in TWEB were added. Samples were again placed on the titramax-100 for 1 hour at 750 RPM, after which point they were removed and each well was washed three times with TWEB and three times with PBS. To develop the reaction, 100 µL of CPT buffer (100 mM citric acid, 0.2 M Na_2HPO_4, 0.1% TX-100) supplemented with one 1,2-phenyldiamine dihydrochloride (OPD) tablet (Sigma-Aldrich) and 8 µL of 30% hydrogen peroxide (Sigma-Aldrich) were added to each well. The plates were immediately placed in a VersaMax plate reader (Molecular Devices, Sunnyvale, CA, USA). Data was analysed using Softmax Pro 4.8 software (Molecular Devices, Sunnyvale, CA, USA), and the quantity of VWF in each sample was determined from the standard curve.

2.7.3 Proregion ELISAs:

Proregion ELISAs were used to determine the quantity of proregion secreted by stimulated and unstimulated cells in the presence or absence of either an over-expressed protein or SYT siRNA. 96-well plates (Thermo Scientific, Rochester, NY, USA) were coated with the CLB proregion-35 antibody (a kind gift from Professor M.J.A van Mourik (Sanquin Research, Amsterdam)) diluted to 1:1000 in PBS. After an overnight incubation in the dark,

the proregion-35 antibody was removed and the wells were blocked for 1 hour with 300 µL of TWEB. Following blocking, the TWEB was removed and 100 µL of sample was added to each well. Lysates were diluted 1:8 with lysis buffer prior to loading. A standard curve was constructed using a known concentration of proregion (derived from HEK-475 cells over-expressing proregion) serially diluted in a 1:1 ratio 11 times in either release media or lysis buffer. For each plate, a blank containing un-modified release media or lysis buffer was included at the end of the standard curve. The standard curve and the samples were placed on a titramax-100 for 1 hour at 750 RPM, after which point the samples were removed and the wells were washed 3 times with TWEB. To each well, 100 µL of an affinity-purified antibody specific to the C-terminus of proregion (Hewlett *et al.* 2011) diluted to 1:1000 in TWEB were added. Samples were again placed on the titramax-100 for 1 hour at 750 RPM, after which point they were removed and each well was washed three times with TWEB. To each well, 100 µL of HRP-conjugated anti-rabbit antibody (Stratech Scientific Ltd, Catalogue Number 711-035-152) diluted to 1:500 in TWEB were added. After a 1 hour incubation on the titramax-100 at 750 RPM the samples were removed and the wells were washed 3 times with TWEB and three times with PBS. To develop the reaction, 100 µL of CPT buffer supplemented with 1 OPD tablet (Sigma-Alrich) and 8 µL of 30% hydrogen peroxide (Sigma-Aldrich) were added to each well. The plates were immediately placed in a VersaMax plate reader (Molecular Devices, Sunnyvale, CA, USA). Data was analysed using Softmax Pro 4.8 software (Molecular Devices, Sunnyvale, CA, USA), and the quantity of proregion in each sample was determined from the standard curve.

2.7.4 Dose-Response ELISAs:

HUVECs were transfected with either a DNA construct or with SYT siRNA according to the protocol detailed previously (2.2.3 The Nucleofection™ Protocol). At the same time, control cells were transfected with either a cytoplasmic control construct or with non-targeting siRNA. Cells were seeded onto 24-well plates and allowed to grow to confluency for 48 hours. To initiate sample collection, 300 µL of release media (consisting of bicarbonate free M199 (Gibco® Life Technologies, Invitrogen, Paisley, UK) and 20 mM HEPES, pH 7.4), were added to each well and the HUVECs were allowed to acclimatize to the media for 50 minutes at 37°C. The release media was removed and the HUVECs were incubated for a further 10 minutes in 300 µL of fresh release media. This was discarded and the cells were then exposed to 300 µL of release media containing varying concentrations of

ionomycin calcium salt (Sigma-Aldrich) for 10 minutes according to the schematic shown in Figure 2.4. Each concentration was performed in duplicate on each plate. The 0 µM solution contained 0.6 µL of 100% ethanol and served as a non-stimulating ethanol control. After a 10 minute stimulation, the release media from each well was collected in 1.5 mL eppendorfs. The samples were spun for three minutes at 13,000 RPM to remove cellular debris. The cell lysates were collected by incubating the wells with 300 µL/well of lysis buffer (made up of release media, protease inhibitors (1:100 dilution) and 1% TX-100) on ice for five minutes. Lysates were collected by scraping and samples were spun for 5 minutes at 13,000 RPM to remove cellular debris. The media and lysates were immediately processed for proregion ELISAs according to the protocol detailed previously (2.7.3 Proregion ELISAs).

2.8 Data Analysis:

The data was plotted using Origin 8 software (OriginLab®, Northampton, MA, USA) and is presented as mean ± standard deviation. Statistical analysis was by nonparametric student's *t* test using GraphPad Prism Version 5.0 (GraphPad Software Inc, La Jolla, CA, USA). Data was considered to be statistically significant when it generated a p-value < 0.05.

Chapter Three

The Expression and Endogenous Localization of the SYTs in HUVECs

3.1 Chapter Overview:

The SYTs are the most extensively-characterized family of calcium sensors and have well-established roles in the regulation of the Ca^{2+}-dependent exocytosis of secretory organelles from a variety of cell types (reviewed in Sudhof, 2002). Therefore, I propose that the exocytosis of WPBs from endothelial cells is regulated by one or more members of this family. In order to investigate this hypothesis it was initially necessary to determine which of the 17 SYTs are expressed in HUVECs as to date nothing is known regarding the expression profile of this family in endothelial cells. Firstly, an RT-PCR expression screen was performed using isoform-specific primers and HUVEC mRNA as detailed in '2.3 Reverse-Transcription PCR.' Once it had been established which members of the SYT family are found at the mRNA level in our model endothelial cells, Western blotting was performed with the aim to verify that these SYTs are also present as proteins in HUVEC lysate. Lastly, attempts were made to determine the endogenous subcellular localization of those SYTs which are expressed in endothelial cells.

3.2 The Expression of SYT mRNA in HUVECs:

3.2.1 The Strategy:

For each of the seventeen SYT genes two sets of primers were designed with each set recognizing a different section of cDNA sequence. The purpose of this was primarily to allow the verification of results by repeating reactions using different primer sets. Additionally, the use of multiple primer sets ensured that, should one set fail to recognize its target sequence and therefore yield a false-negative result, the other set should in theory rectify this and produce a positive result providing that the target sequence is present in the reaction mix.

In addition to HUVEC RNA, RNA derived from HEK-293 cells was included as a template for PCR. In my experience HEK cells express a wide range of the SYTs and therefore the inclusion of RNA from this cell line provides a mechanism for validating the functionality of the primers. All bands produced by RT-PCR were sequenced to verify their

identities. In cases whereby neither HUVEC nor HEK RNA yielded a positive result for the presence of a SYT image clones were purchased and used as the template for PCR to confirm the functionality of the primers. Lastly, for each SYT a negative control was included in the PCR screen. This consisted of the entire PCR with the exception of the template RNA, the purpose of which was to control for the presence of contaminating environmental nucleic acids. This strategy is detailed in full in Figure 3.1.

3.2.2 RT-PCR Analysis of SYT Expression in HUVECs:

An RT-PCR screen for the presence of SYT mRNA in HUVECs was performed according to the strategy detailed in Figure 3.1. The principal findings of this are shown in Figure 3.2. As can be seen, I have demonstrated that HUVECs express eight members of the SYT family: SYTs I, III, V, VI, VII, VIII, XI, and XVII. Of these, SYTs VIII, XI, and XVII are Ca^{2+}-independent. HEK cells express SYTs I, II, III, V, VI, VII, VIII, IX, XII, XIII, XIV, XV, and XVI (data not shown) and therefore have proved to be a useful positive control cell line. I have been unable to demonstrate the presence of SYT IV mRNA in either HUVECs or HEK cells. Before concluding that SYT IV is not expressed in either of these cell types it was essential to demonstrate that the primers are capable of recognizing SYT IV transcripts when they are known to be present in a sample. Therefore, an image clone of the SYT IV gene was purchased and this was used as a template for RT-PCR. The results of this are shown in Figure 3.3. As can be seen, the SYT IV primers are indeed capable of recognizing and amplifying the SYT IV transcript and furthermore it is clear that SYT IV is not expressed by either HUVECs or HEK cells.

This work has provided a comprehensive expression screen of SYT mRNA in both HUVECs and HEK cells, the results of which are summarized in Figure 3.4. The eight endothelial-expressed SYTs have now been identified as strong potential candidates for the role of the calcium sensor regulating WPB release from endothelial cells. The presence of SYT XVII mRNA in HUVECs is of particular interest as to my knowledge this represents one of the first observations of the endogenous expression of this member of the SYT family in any cell type.

3.3 The Expression of SYT Protein in HUVECs:

3.3.1 The Strategy:

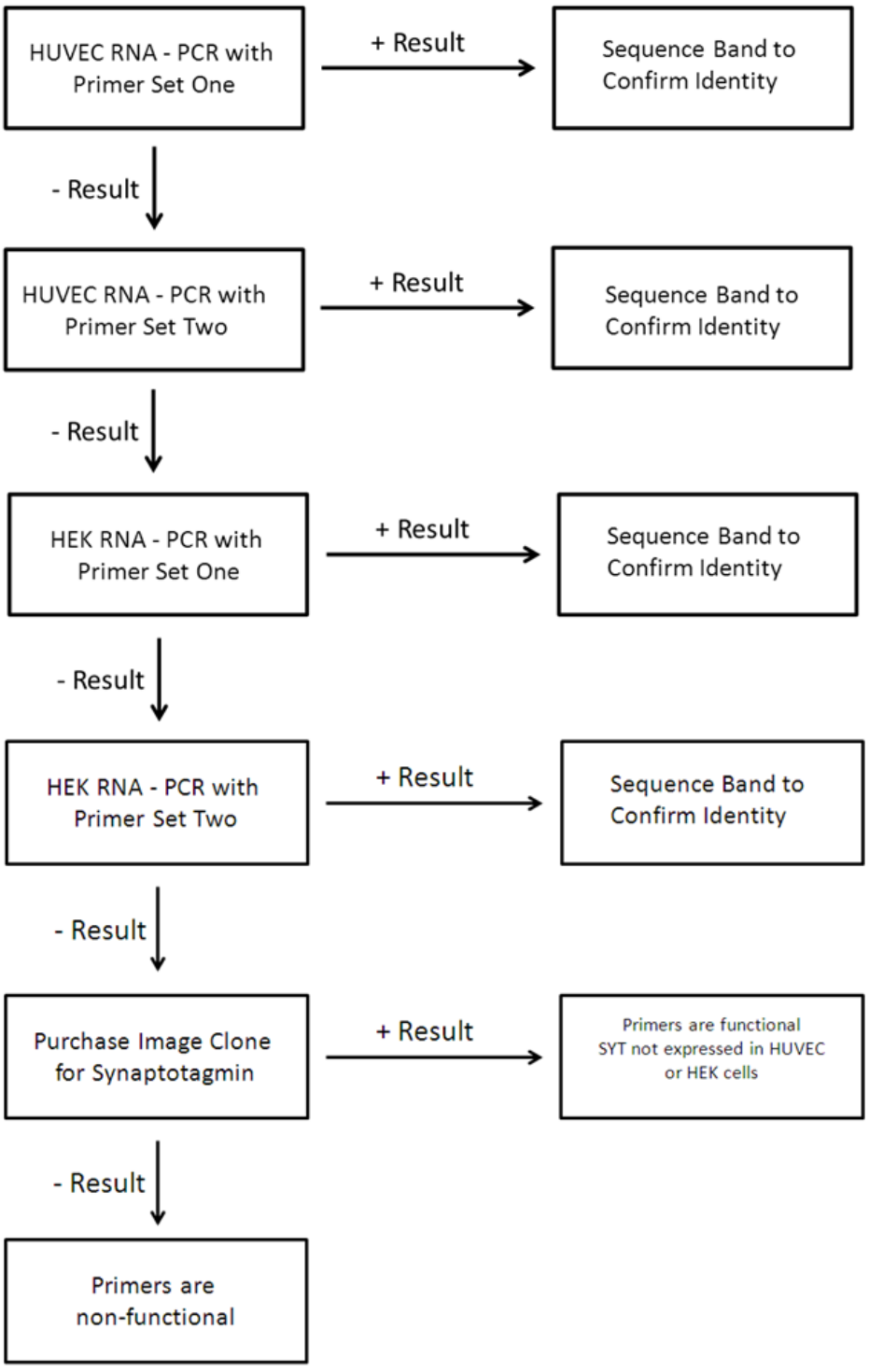

Figure 3.1. The Strategy for Determining the Expression of SYT mRNA in HUVECs. The rationale behind the RT-PCR screen is shown. The use of two primer sets for each gene provides a means of validating results and also guards against false-negatives. The use of HEK RNA provides a positive control for a number of the SYTs. This strategy ensures that the primers are tested against their target template to verify their efficiency. Any bands obtained by PCR were sequenced to confirm their identity. See text for details.

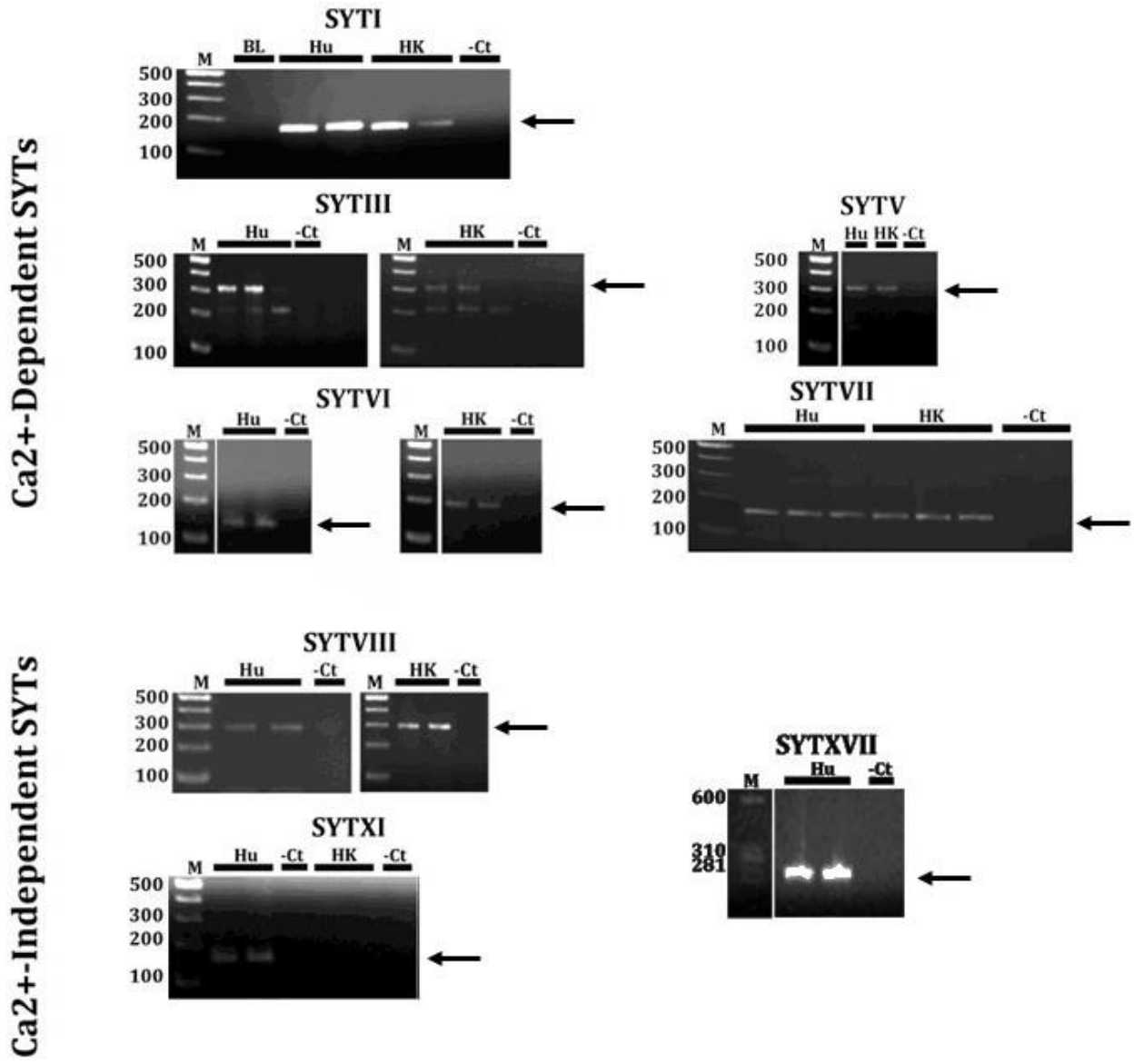

Figure 3.2. The Expression of the SYTs in HUVECs

Representative agarose gels showing the expression of the Ca^{2+}-dependent and Ca^{2+}-independent SYTs in HUVECs by RT-PCR are provided. HUVEC (Hu) and HEK (HK) RNA was probed with primers against the SYT cDNA sequences. A negative control (-Ct) lacking template RNA was included in each case to control for environmental contamination. The sizes of the marker (M) are indicated (in bps). BL: Blank Lane. The arrows indicate products which represent SYT mRNA. These bands were sequence-verified to confirm their identities.

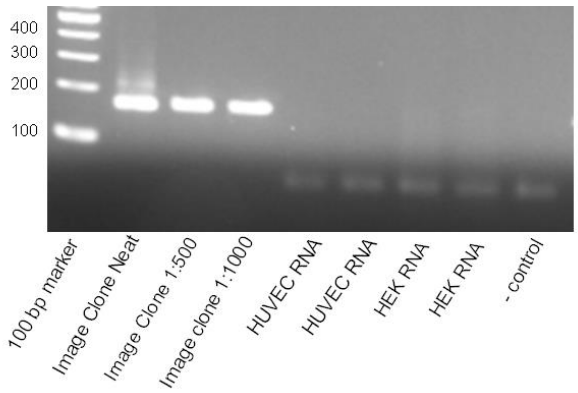

Figure 3.3. SYT IV is not expressed by HUVECs or HEK cells.
SYT IV was amplified from varying dilutions of a sequence-validated Image Clone as indicated. A strong single band of the anticipated size appears on the gel. This band is absent when HUVEC and HEK RNA are used as templates. The sizes of the marker are shown on the left.

It is now known that HUVECs express eight members of the SYT family at the mRNA level, three of which are Ca^{2+}-independent. However, these mRNA transcripts may not necessarily be translated to yield functional proteins and therefore it was essential to determine if these SYTs are also present at the protein level in HUVECs. For this purpose, commercial α-SYT antibodies were purchased (the details of which are available in Table 2.1). Initially, it was necessary to screen the antibodies to determine their optimum working concentrations using the Miniblotter® device as detailed in '2.4.2 Immunoblotting.' Once the optimum dilutions of the primary antibodies had been determined Western blotting was performed to test for the presence of each endothelial-expressed SYT in HUVEC lysate. Lastly, in order to demonstrate that each α-SYT primary antibody is capable of detecting its target protein, SYT-EGFP fusion proteins produced as described in '2.6.2.2 The LIC Protocol' were expressed in HEK-293 cells. This cell line produces large quantities of over-expressed protein and therefore is a convenient tool for demonstrating the functionality of antibodies for both Western blotting and ICC. Lysates from SYT-EGFP-transfected HEK cells were extracted and subjected to Western blotting. Should the antibody in question recognize its target protein then the α-SYT antibody and an α-GFP antibody will both recognize the over-expressed SYT-EGFP construct. This strategy therefore allows the demonstration that each commercial α-SYT antibody is capable of detecting its target protein when it is known to be present in a lysate sample.

This approach was used to screen for the presence of each SYT which is known to be present at the mRNA level in HUVECs and the results are summarized in the following sections. For SYT I, the strategy detailed above is presented in full. However, in the interest of brevity for the remaining seven SYT family members only the essential data is provided.

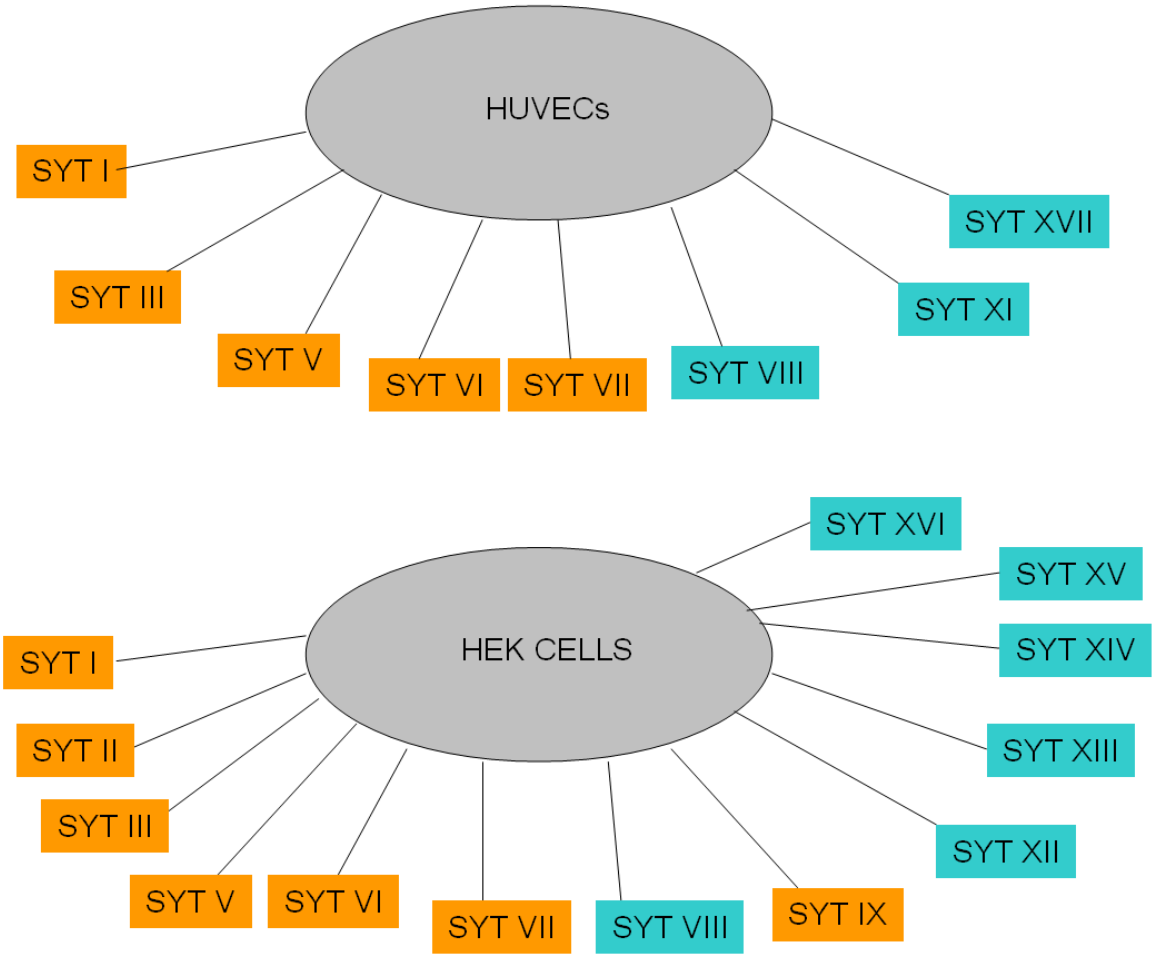

Figure 3.4. The expression of the SYT family in HUVECs and HEK cells.
HUVECs express eight members of the SYT family: SYTs I, III, V, VI, VII, VIII, XI, and XVII. HEK cells express thirteen members of the SYT family: SYTs I, II, III, V, VI, VII, VIII, IX, XII, XIII, XIV, XV and XVI. The SYTs shown in orange are Ca^{2+}-dependent. Those shown in blue are Ca^{2+}-independent.

3.3.2 The Expression of the Ca^{2+}-dependent SYTs at the Protein Level in HUVECs:

The first ten members of the SYT family (SYTs I – X) are for the most part Ca^{2+}-dependent, having the ability to bind free Ca^{2+} ions via specific negatively-charged residues in their C2 domains (von Poser *et al.* 1997). The exceptions to this are SYTs IV and VIII which lack the essential aspartate residues required for calcium binding. The primary sensor mediating the Ca^{2+}-induced exocytosis of WPBs from endothelial cells will logically by Ca^{2+}-dependent and therefore my efforts initially focused on demonstrating the expression of the Ca^{2+}-dependent SYT proteins in HUVECs.

3.3.2.1 SYT I:

A primary antibody against the C-terminal portion of SYT I was purchased from Synaptic Systems. This reagent was raised in mice against amino acids 80 to 421 of the rat SYT I sequence and shows reactivity with human protein. Initially, it was necessary to screen the antibody using the Miniblotter® device to determine its optimum working concentration. A range of dilutions of the primary antibody were tested and the results of this initial screen are shown in Figure 3.5. A primary band of approximately 55 kDa has been identified. Based on these results it was decided to perform all subsequent Western blots using the SYT I antibody at a dilution of 1:200. An example of such a blot is shown in Figure 3.6, and as can be seen a single band of approximately 55 kDa has been detected, replicating the results shown in Figure 3.5. The detection of only one band suggests that HUVECs express one isoform of the SYT I protein.

This work indicates that SYT I is indeed found in HUVECs at the protein level. However, it was necessary to demonstrate that the commercial antibody is capable of recognizing SYT I when it is known to be present in a lysate sample. Therefore, a fluorescent construct of SYT I (SYTI-EGFP) was expressed in HEK-293 cells. Lysate from these cells was extracted and used for Western blotting with the SYT I primary antibody. The blots were also probed with an α-GFP antibody. The results of this are shown in Figure 3.7. As can be seen, a clear band appearing at approximately 95 kDa has been detected by both the SYT I and GFP antibodies, suggesting that the SYT I antibody is indeed capable of recognizing its target antigen. No additional bands have been detected by the SYT I antibody which are not also identified by the GFP antibody, suggesting that the recognition of SYT I is relatively

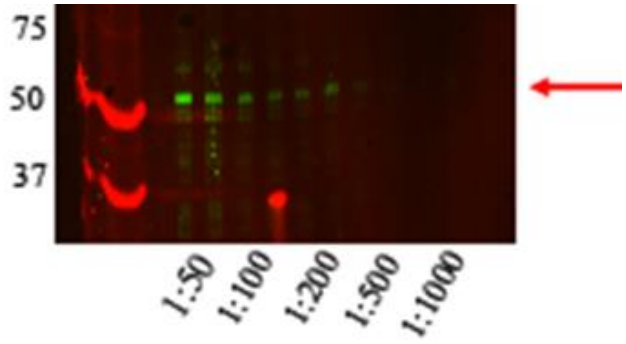

Figure 3.5. The optimum dilution of the SYT I antibody is 1:200.
A representative Western blot produced by probing HUVEC lysate with the SYT I primary antibody at varying concentrations is shown. Each condition is shown in duplicate as indicated. The sizes of the protein marker are shown on the left of the figure (kDa). The red arrow indicates the appearance of a band which is thought to represent the SYT I protein.

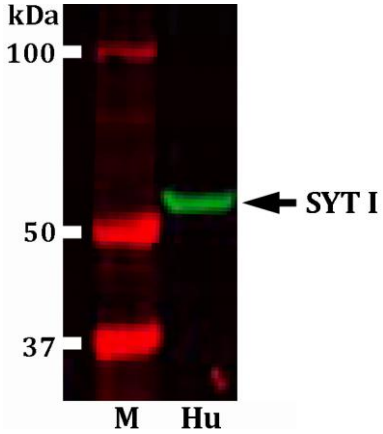

Figure 3.6 The SYT I protein is present in HUVECs.
A representative Western blot produced by probing HUVEC (Hu) lysate with the SYT I primary antibody at a concentration of 1:200 is shown. The sizes of the marker (M) are shown on the left. Notice the appearance of a strong band at approximately 55 kDa which is thought to represent the SYT I protein.

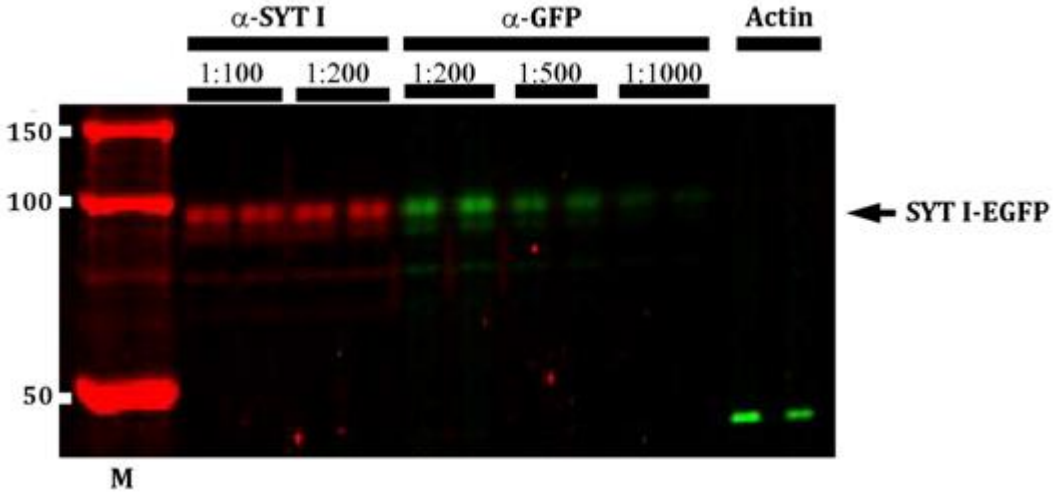

Figure 3.7. The α-SYT I antibody recognizes SYTI-EGFP in HEK lysate.
SYTI-EGFP-expressing HEK lysate was run on the Miniblotter® device. Lanes have been probed with either the SYT I primary antibody (red) or with the α-GFP antibody (green) at varying dilutions as indicated. An actin transfer control has been included and the sizes of the molecular marker (M) (kDa) are shown on the left of the figure. The arrow indicates a band (the SYTI-EGFP construct) which is clearly seen in both the SYT I- and GFP-probed lanes.

specific. However, care must be taken with this interpretation as this method is not an absolute test of antibody specificity. It is possible that α-SYT antibodies cross-react with other members of the SYT family.

3.3.2.2 SYT III:

A primary antibody against SYT III was purchased from Synaptic Systems. This reagent was raised in rabbits against a recombinant peptide corresponding to amino acids 86 to 169 of the human SYT III protein. The optimum dilution of this antibody was determined to be 1:200 (data not shown) and the results of Western blotting with the α-SYT III antibody used at this dilution are shown in Figure 3.8. As can be seen, a series of bands has been detected by the SYT III primary antibody, the strongest of which appears at approximately 63 kDa. This corresponds with the expected size of the largest SYT III isoform. Additional bands are visible at 45 and 50 kDa. It is possible that a number of splice variants of SYT III are expressed simultaneously within HUVECs, or alternatively these multiple bands may represent breakdown products of the original protein (see Discussion). Following the Western blotting of lysates derived from HEK-293 cells expressing SYTIII-EGFP, both the α-GFP and α-SYT III antibodies recognized an identical band of approximately 100 kD (data not shown). Therefore the α-SYT III commercial antibody is capable of recognizing its target protein when it is known to be present in a lysate sample.

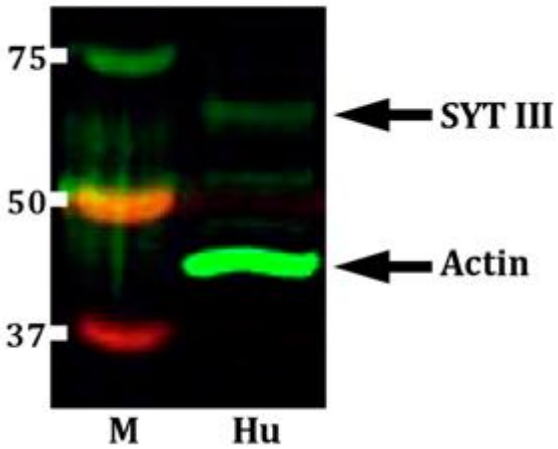

Figure 3.8. The SYT III protein is present in HUVECs.
HUVEC (Hu) lysate was probed with the α-SYT III antibody at a dilution of 1:200. The sizes of the marker are shown on the left of the figure (kDa). The top arrow indicates the most prominent band appearing at 63 kDa which is thought to represent the endogenous SYT III protein. The bottom arrow shows the actin transfer control.

3.3.2.3 SYT V:

A primary antibody generated in rabbits from a synthetic peptide spanning resides 127 to 167 of the human SYT V sequence was purchased from abcam®. The optimum dilution of this antibody for Western blotting was determined to be 1:200 (data not shown). A representative blot of HUVEC lysate probed with the α-SYT V antibody is shown in Figure 3.9. A clear band which appears at approximately 45 kDa has been identified and this corresponds with the expected size of the SYT V protein. A number of other bands of larger sizes were also observed (see discussion). However only the 45 kDa band was lost following siRNA depletion of SYT V (see Chapter 6), indicating that this band most likely represents endogenous SYT V. The blotting of lysates derived from HEK cells over-expressing SYTV-EGFP demonstrated that this commercial antibody is capable of detecting its target protein when it is known to be present in a lysate sample (data not shown).

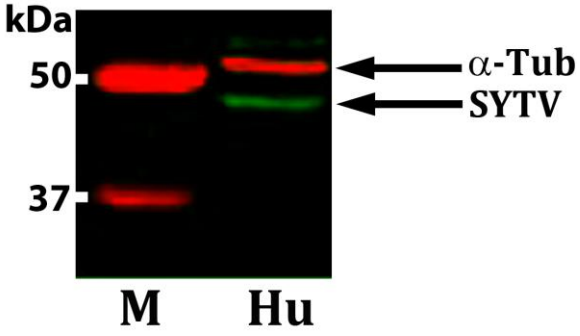

Figure 3.9. The SYT V protein is present in HUVECs.
HUVEC (Hu) lysate was probed with the α-SYT V antibody at a dilution of 1:200. The sizes of the marker (M) are shown on the left. A tubulin transfer control is included (in red). Note the strong band appearing at approximately 45 kDa which is thought to represent SYT V.

3.3.2.4 SYT VI:

A primary antibody against SYT VI was purchased from abcam®. This reagent was raised in rabbits against a recombinant protein corresponding to amino acids 85 to 510 of the human SYT VI sequence. Its optimum dilution was determined to be 1:200 (data not shown). The results of probing HUVEC lysate with the SYT VI antibody at this concentration are shown in Figure 3.10. As can be seen, a number of bands have been detected, the most prominent of which appear at approximately 55, 60, and 70 kDa. Multiple isoforms of the SYT VI protein are known to exist (Fukuda and Mikoshiba, 1999) and equally numerous reports have published conflicting observations regarding the molecular mass of the SYT VI

protein as it appears on Western blots (see Discussion). Therefore, as the data presented here suggests it is likely that SYT VI exists as a series of splice variants in HUVECs.

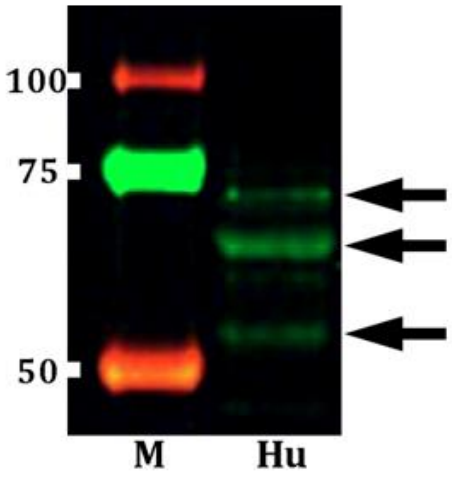

Figure 3.10. The SYT VI protein is present in HUVECs.
HUVEC (Hu) lysate was probed with the α-SYT VI antibody at a dilution of 1:200. The sizes of the marker (M) (kDa) are shown on the left of the image. A number of bands have been identified by the α-SYT VI antibody as indicated by the arrows on the right.

3.3.2.5 SYT VII:

A commercial α-SYT VII antibody was purchased from Synaptic Systems. This reagent was raised in rabbits against a recombinant peptide corresponding to amino acids 46 to 133 of the rat SYT VII sequence and is reported to recognize human protein. The optimum dilution of this antibody was determined to be 1:200 (data not shown), and a representative example of HUVEC lysate probed with the α-SYT VII antibody at this concentration is shown in Figure 3.11. Surprisingly, the SYT VII antibody displayed unusual cross-reactivity with the protein marker. However, despite this a major band of approximately 65 kDa is consistently seen on SYTVII-probed Western blots. This is considerably larger than the predicted mass of 45 kDa for the SYT VII protein. However, it is likely that post-translational modifications affect the observed size of the protein and equally it is possible that a larger isoform of SYT VII is expressed in HUVECs than that which is commonly reported in other cell types (see Discussion). In Figure 3.11, a number of additional bands are visible and these may represent either minor isoforms of the SYT VII protein or possibly proteolytic products of a larger variant. However it was my concern that these bands may be a by-product of the unusual cross-reactivity of the primary antibody with the marker protein. Therefore, a control blot was run which included HUVEC lysate but no marker protein (Figure 3.11, panel ii). An identical staining pattern to that seen when the marker is present

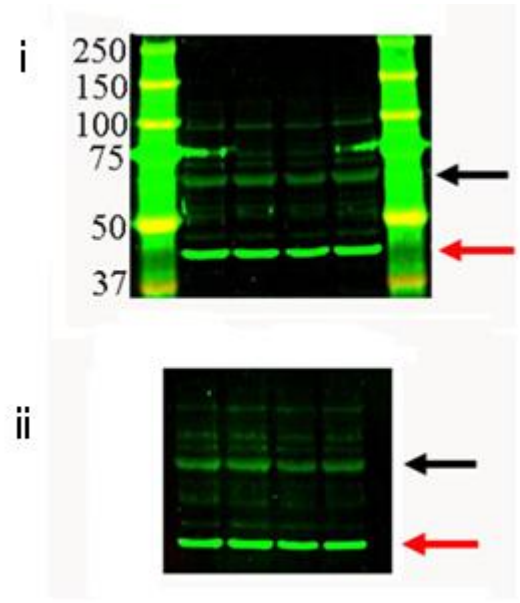

Figure 3.11. The SYT VII protein is found in HUVECs.
HUVEC lysate was probed with the α-SYT VII antibody at a dilution of 1:200. The black arrows indicate a major band appearing at approximately 65 kDa while the red arrows indicate the actin transfer controls. The sizes of the protein marker are indicated on the left (kDa). In Panel (i) notice the intense cross-reactivity of the SYT VII antibody with the marker protein. Panel (ii) shows a blot which has been run in an identical manner to that shown in Panel (i) with the exception that the marker has been omitted. The bands are identical to those seen in Panel (i), suggesting that the reactivity of the SYT VII antibody with the marker protein does not affect the staining pattern produced.

was produced and so the bands observed on α-SYTVII-probed blots are not artifacts of marker reactivity but instead may represent the presence of the SYT VII protein in HUVECs. In support of this, Western blotting lysates derived from HEK cells expressing SYTVII-YFP demonstrated that the commercial antibody is capable of detecting its target protein when it is known to be present in a lysate sample (data not shown).

3.3.3 The Expression of the Ca^{2+}-independent SYTs at the Protein Level in HUVECs:

I have now established which Ca^{2+}-dependent SYTs are expressed in HUVECs at both the mRNA and protein levels and therefore I moved on to address the expression of the Ca^{2+}-independent SYTs. Although these proteins cannot bind Ca^{2+} directly they are known to play a modulatory role in the regulation of secretory events (Sudhof, 2002) and therefore are potential candidates for the role of the protein sensor regulating WPB exocytosis.

3.3.3.1 SYT VIII:

An antibody against SYT VIII was purchased from Acris Antibodies. This reagent was raised in rabbits against a recombinant peptide corresponding to amino acids 67 to 96 of

the human SYT VIII protein. The optimum dilution of this antibody was determined to be 1:200 (data not shown) and the results of a representative experiment probing HUVEC lysate for SYT VIII are shown in Figure 3.12. As can be seen, the SYT VIII antibody has detected three bands, one of which is dominant and appears at approximately 75 kDa. The smaller, fainter bands are seen at approximately 80 and 45 kDa. It is possible that these bands represent three different isoforms of the SYT VIII protein, and indeed numerous variants of SYT VIII have been reported to exist (see Discussion).

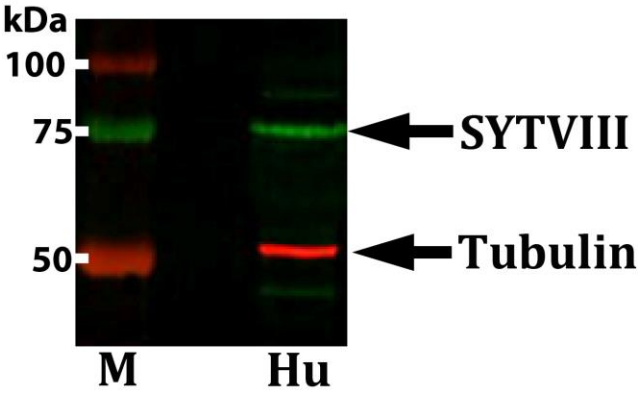

Figure 3.12. The SYT VIII protein is present in HUVECs.
HUVEC (Hu) lysate was probed with the α-SYT VIII antibody at a dilution of 1:200. The sizes of the marker are shown on the left of the image. The tubulin transfer control appears in red. The major band representing the SYT VIII protein is indicated by an arrow.

3.3.3.2 SYT XI:

A mouse monoclonal primary antibody raised against recombinant human SYT XI protein was purchased from Santa Cruz. When attempting to determine the optimum dilution of the SYT XI antibody I was unable to detect any reactivity in HUVEC lysate regardless of the concentration tested (shown in Figure 3.13, Panel (i)). Before any firm conclusions could be drawn as to the presence or absence of the SYT XI protein in HUVECs it was essential to demonstrate that the primary antibody is capable of detecting its target protein when it is known to be present in a lysate sample. Therefore, HUVECs were transfected with a SYTXI-EGFP construct and the resulting lysate was probed with the α-SYT XI antibody. No bands were generated to indicate the recognition of over-expressed SYT XI protein (data not shown) suggesting that the SYT XI antibody does not recognize its target antigen. However, it may also indicate that a high concentration of SYT XI is required for successful detection. To test this possibility HEK-293 cells were transfected with the SYTXI-EGFP construct and allowed to grow to confluency. The resulting lysates were probed with either the SYT XI

primary antibody or with an α-GFP antibody. The results of this are shown in Figure 3.13 panel (ii), and as can be seen both antibodies have recognized a band of approximately 75 kDa. Therefore, this work suggests that the α-SYT XI commercial antibody is capable of recognizing its target antigen but requires high levels of expression for successful detection.

As a final attempt to detect the presence of endogenous SYT XI protein in HUVECs TX-114 lysate partitioning was performed. This method allows the enrichment of integral membrane proteins in a lysate sample and therefore yields a more concentrated source of SYT protein than conventional lysate extraction techniques. The results of Western blotting following TX-114 partitioning are shown in Figure 3.13, panel (iii). As can be seen, despite its ability to concentrate membrane proteins in a lysate sample this method has not allowed the detection of the endogenous SYT XI protein in HUVECs.

This work has been inconclusive as I have been unable to demonstrate the presence of the endogenous SYT XI protein in HUVECs. However, I have shown that the commercial antibody is unable to detect SYT XI when it is specifically up-regulated in HUVECs and so is clearly ineffective. At this stage it is impossible to draw any conclusions as to the expression of the SYT XI protein in endothelial cells.

3.3.3.3 SYT XVII:

A primary antibody against SYT XVII was purchased from abcam®. This reagent was raised in rabbits against a synthetic peptide corresponding to the human SYT XVII protein sequence. The optimum dilution of this reagent was determined to be 1:500 (data not shown) and the results of probing HUVEC lysate with the α-SYT XVII antibody at this concentration are shown in Figure 3.14. A single strong band has been detected at approximately 60 kDa. The estimated size of the SYT XVII protein is 54 kDa and so it is likely that SYT XVII undergoes post-translational modifications in HUVECs (see Discussion). The over-expression of SYTXVII-EGFP in HEK-293 cells demonstrated that the primary α-SYT XVII antibody is indeed capable of detecting its target protein when it is known to be present in a lysate sample (data not shown).

3.4. Determining the Distribution of Endogenous SYT Protein in HUVECs:

As it has now been established that a number of the SYT family members are expressed in HUVECs at both the mRNA and protein levels I attempted to determine the

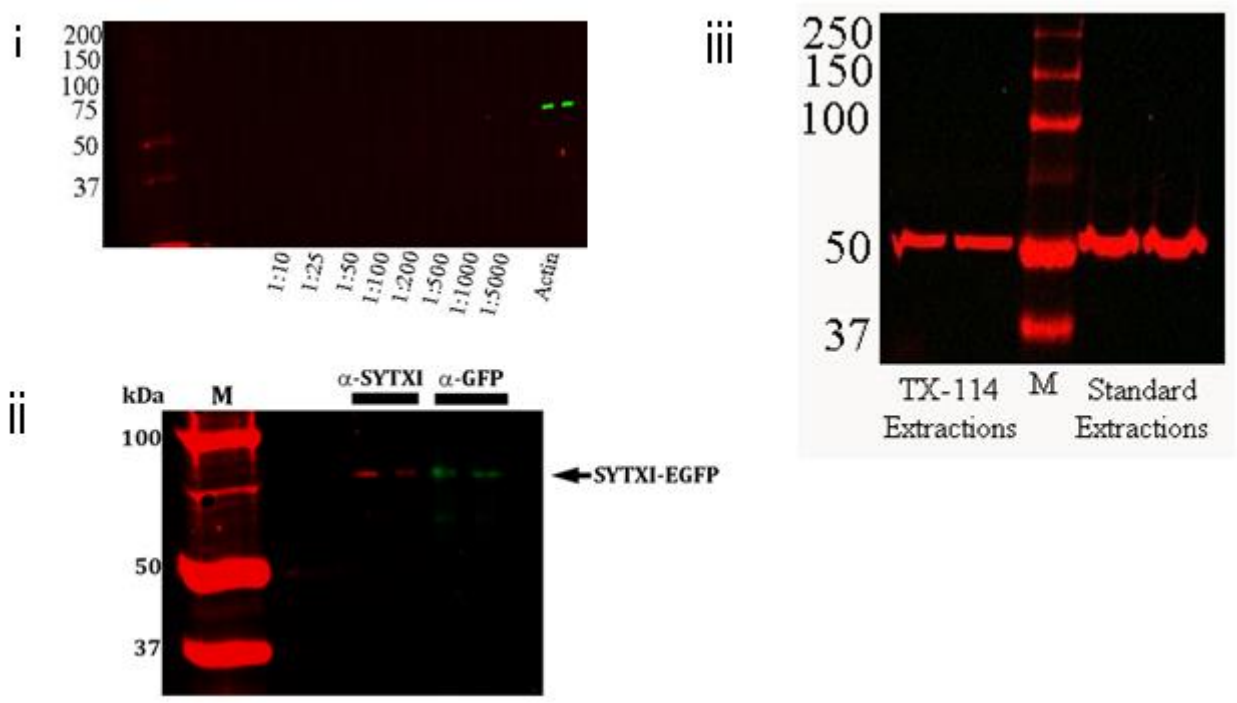

Figure 3.13. The SYT XI antibody does not detect SYT XI protein in HUVEC Lysate.
The SYT XI antibody does not detect SYT XI protein in HUVEC lysate despite repeated attempts to optimize the lysate extraction protocol. It does identify SYTXI-EGFP when over-expressed in HEK cells but not in HUVECs. In Panel (i) HUVEC lysate has been probed with varying dilutions of the SYT XI primary antibody as indicated at the base of the figure. An actin transfer control has also been included. No bands have appeared for the SYT XI protein. The sizes of the molecular marker are shown on the left of the image (kDa). In Panel (ii) a Western blot produced by probing HEK lysate over-expressing SYTXI-EGFP with primary antibodies against either SYT XI (red; 1:200) or GFP (green; 1:1000), is shown. The sizes of the marker (M) are shown on the left of the figure (kDa). In Panel (iii) the results of Western blotting for the endogenous SYT XI protein in HUVEC lysate derived from a TX-114 extraction procedure are shown. No bands have been detected representing the SYT XI protein. The strong band appearing at approximately 50 kDa is the tubulin transfer control. The blotting of HUVEC lysate produced as detailed in '2.4.1.1 Conventional Lysate Extraction' is shown on the right (labeled 'Standard Extractions'). The sizes of the molecular marker (M) are shown on the left (kDa).

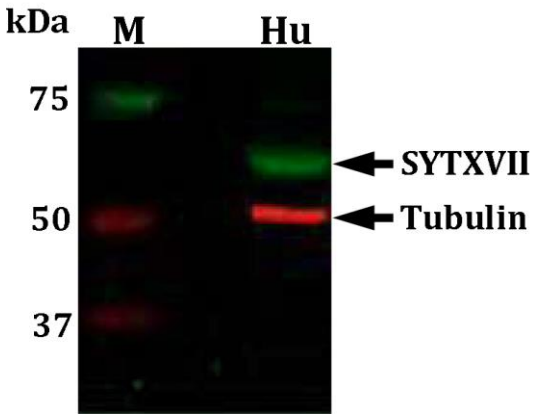

Figure 3.14. The SYT XVII protein is present in HUVECs.
HUVEC (Hu) lysate was probed with the α-SYT XVII antibody at a dilution of 1:500. The tubulin transfer control appears in the red channel. The sizes of the marker are shown on the left. The top arrow indicates the appearance of a band thought to represent the SYT XVII protein at 60 kDa.

distribution of endogenous SYT protein in HUVECs by ICC. As with Western blotting it was initially necessary to optimize this procedure for the detection of endothelial SYT protein. Therefore, for each SYT family member a number of cell fixation methods were trialed along with a range of dilutions of the primary α-SYT antibody. Unfortunately, this approach was on the whole unsuccessful and I failed to determine the endogenous distribution of the majority of the SYTs. Representative examples of PFA/Saponin-fixed HUVECs stained with the SYT antibodies at dilutions of 1:100 are shown in Figure 3.15. As can be seen, only a uniform background staining pattern has been produced for the SYTs which likely represents either the non-specific binding of the primary antibodies or auto-fluorescence from intracellular structures. In contrast, the VWF stain has clearly identified numerous rod-shaped WPBs. Similar results were obtained with methanol and TX-100-fixed HUVECs and with all SYT antibody dilutions tested (data not shown).

Two possibilities explain this failure to detect endogenous SYT protein in HUVECs. Firstly, it is possible that the proteins are in fact not present in HUVECs although this is in disagreement with the Western blot data presented previously. It is more likely that the commercial antibodies used here are unable to recognize endothelial SYT proteins and in order to test this possibility I constructed SYT-EGFP fusion vectors and over-expressed these in HUVECs and HEK cells. The transfected cells were fixed and stained with the commercial α-SYT antibodies and with an antibody against GFP. Should the SYT antibodies be capable of detecting their target proteins then they should co-stain the over-expressed fluorescent constructs with the α-GFP antibody. The results of this for each SYT are shown in Figure 3.16. As can be seen, the antibodies against SYTs I, III, VI, and VII are capable of

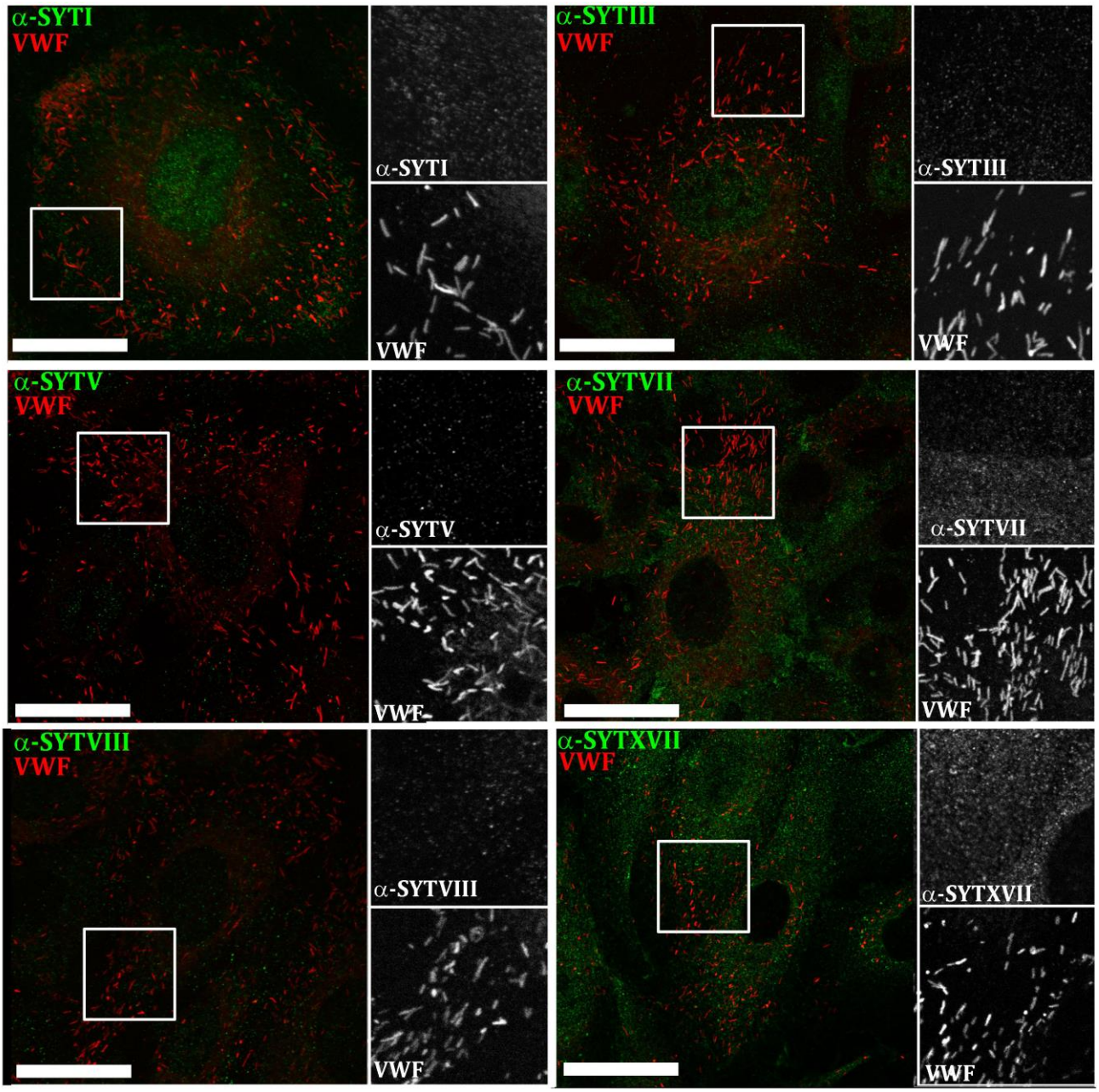

Figure 3.15. The SYT antibodies do not detect endogenous SYT protein in HUVECs.

PFA/Saponin-fixed HUVECs were stained with antibodies against SYTs I, III, V, VII, VIII, and XVII (green, all used at 1:100) as indicated and counter-stained for VWF (red). Areas indicated by the white boxes are shown in grey-scale to the right of the colour images. Scale bars are 20 μm.

recognizing their over-expressed antigens whereas the antibodies against SYTs V, VIII, XI, and XVII do not recognize even highly-expressed protein. A more detailed example of this for the α-SYT VII antibody is shown in Figure 3.17. In this case, the antibody is capable of detecting SYTVII-YFP when it is over-expressed in HEK cells but not in HUVECs. As HEK cells synthesize unusually high quantities of foreign protein this suggests that the α-SYT VII antibody only recognizes its target antigen by ICC when it is present in a highly-concentrated form. HUVECs do not produce sufficient quantities of the SYT VII protein for its recognition by ICC even when it is specifically up-regulated by over-expression. Therefore, my inability to detect endogenous SYT protein in HUVECs by ICC is most likely the result of an insufficient expression level of these proteins in endothelial cells.

There were two exceptions to the general failure of the commercial antibodies to recognize endogenous SYT proteins in HUVECs. Firstly, when optimizing the ICC protocol for the SYT VI protein numerous vesicular structures were seen to be stained by the α-SYT VI antibody. It was shown that this commercial antibody is capable of high-fidelity recognition of its target antigen as it clearly detected over-expressed SYTVI-EGFP in HEK cells (Figure 3.16). Therefore I suspected that these vesicular structures were the result of the specific recognition of the SYT VI protein by the α-SYT VI antibody. In order to determine the identity of these subcellular compartments I performed a full localization screen using markers of various organelles. The results of this screen will not be shown in full but it will suffice to say that the vesicular organelles detected by the SYT VI antibody were shown to be early endosomes as they stained positively for the marker protein EEA-1. An example of the co-staining between EEA-1 and SYT VI is shown in Figure 3.18. Hence, endogenous SYT VI can be found as a component of the early endosomes in HUVECs.

Lastly, while optimizing the ICC protocol for the SYT XI protein large globular masses were observed following the staining of HUVECs with the α-SYT XI antibody. An example of this is shown in Figure 3.19. As can be seen, these aggregates were numerous and concentrated around the perinuclear area. No explanation could be offered as to the provenance of these masses. It is possible that they were the result of impurities in the fixation solutions although I would consider this unlikely as they appeared in HUVECs fixed by both the PFA/Saponin and TX-100 methods. Additionally, these globular masses are not seen in the VWF stain, suggesting that they are specific for the SYT XI antibody. Therefore, it is possible that SYT XI localizes to large vesicles in the perinuclear area and it may be that these vesicles are components of either the endoplasmic reticulum or the Golgi apparatus.

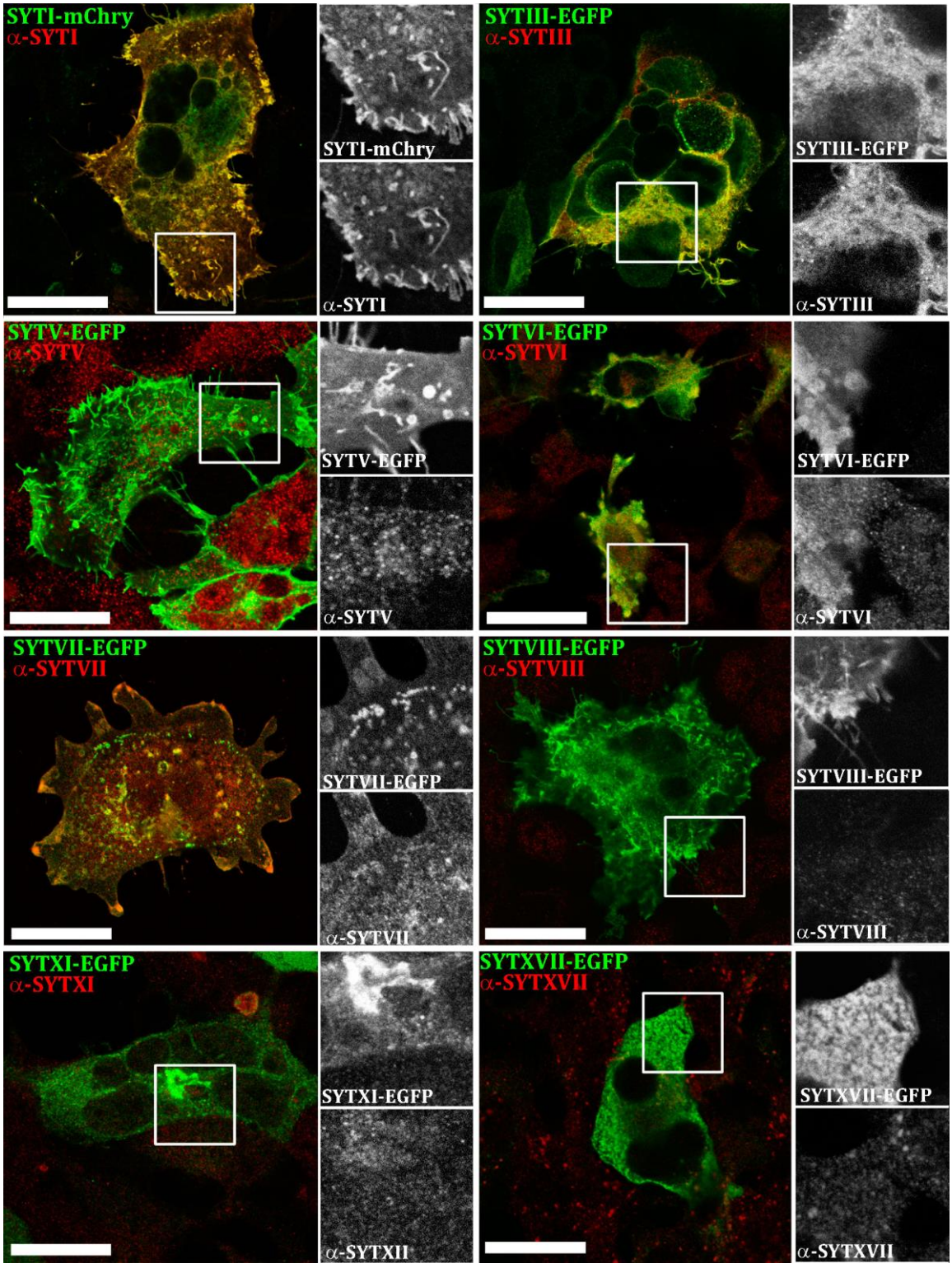

Figure 3.16. The commercial α-SYT antibodies do not reliably detect over-expressed SYT protein in HEK cells.

HEK cells transfected with fluorescent SYT constructs were co-stained with α-SYT antibodies as indicated (red) and an α-GFP antibody (green). Co-localization between the two was visible in only half of cases (SYTs I, III, VI, VII). Scale bars are 20 µm.

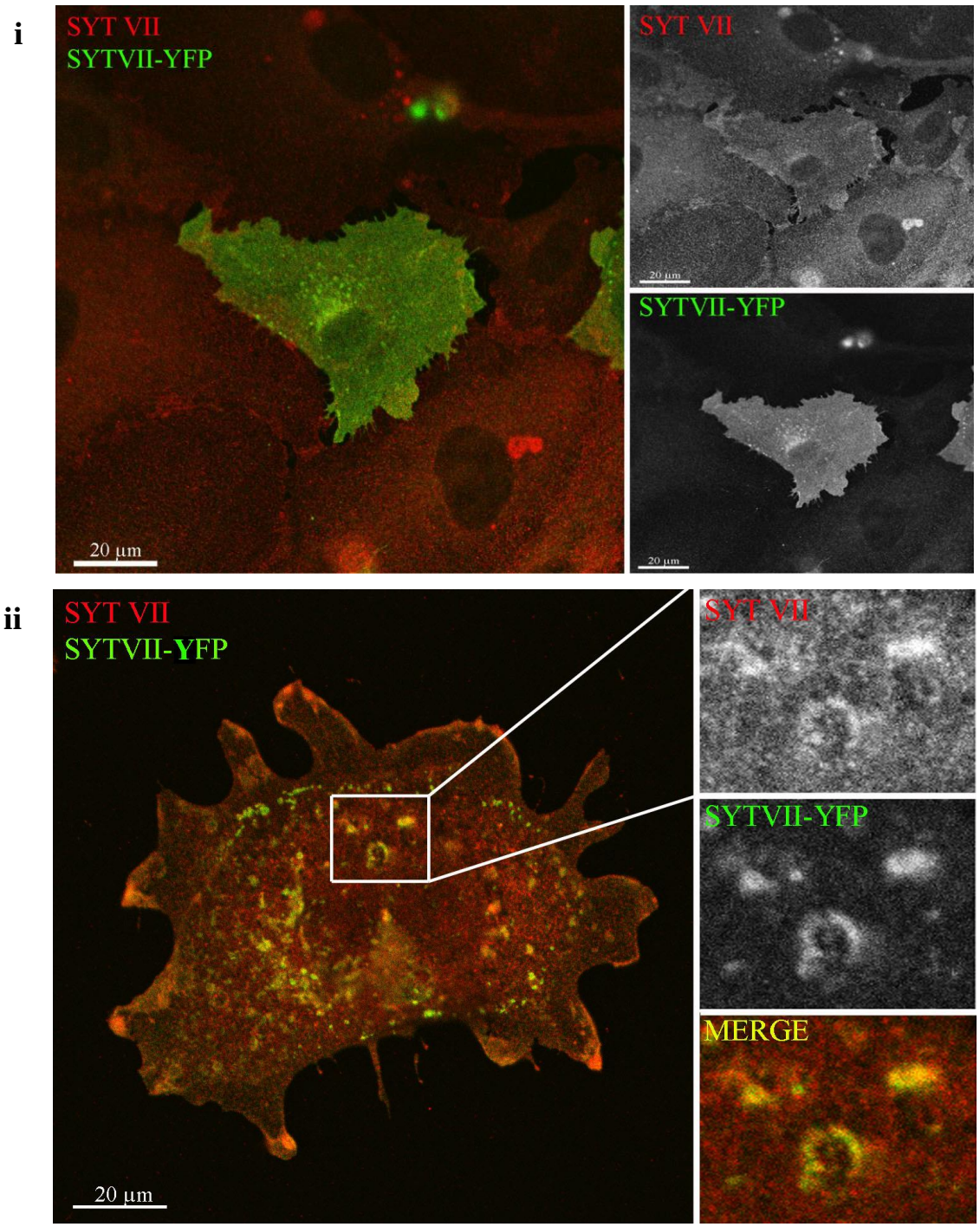

Figure 3.17. The SYT VII antibody recognizes SYTVII-YFP when it is expressed in HEK cells but not in HUVECs.

Representative images of HUVECs (Panel (i), Top) and HEK cells (Panel (ii), Bottom) over-expressing SYTVII-YFP and stained with antibodies against GFP and SYT VII are shown. In Panel (i) the merged image is shown on the left and grey-scales of the two stains are shown on the right. Note the central cell which is strongly expressing the SYTVII-YFP construct. However, as is clear from the red channel the SYT VII primary antibody is unable to distinguish this cell from the rest of the monolayer, demonstrating that the antibody does not recognize the SYTVII-YFP construct. In Panel (ii) the merged image is shown on the left and an enlarged section of the cell as indicated by the white rectangle is shown on the right. Note the evidence of co-localization as seen by the appearance of yellow in the merged image. Therefore the SYT VII antibody is able to recognize the SYTVII-YFP construct when it is over-expressed in HEK cells but not in HUVECs.

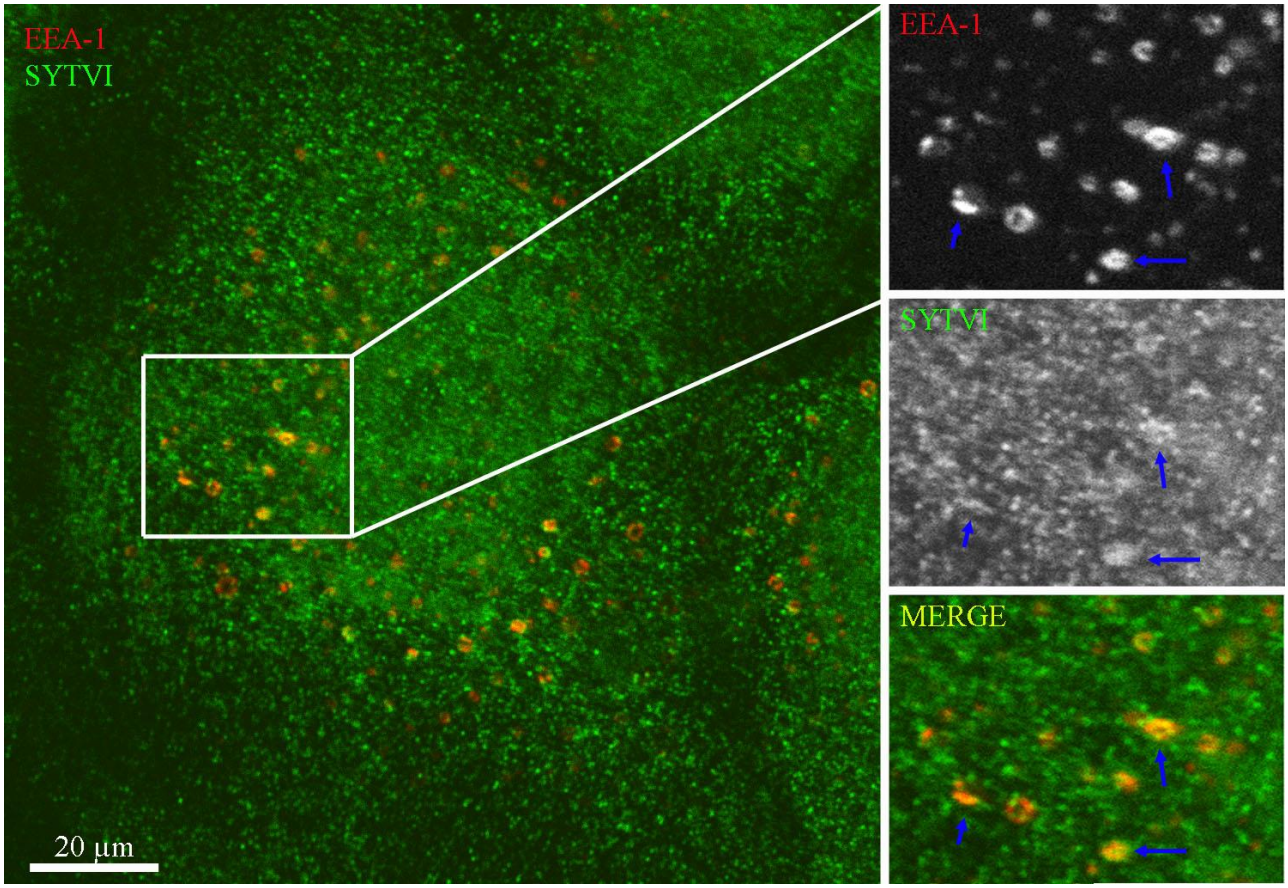

Figure 3.18. Endogenous SYT VI is a component of the early endosomes.
A HUVEC stained for EEA-1 (red) and SYT VI (green) is shown. The merged image is shown on the left. An enlarged section of the cell as indicated by the white rectangle is shown on the right. Note the clear co-localization between these two proteins. The blue arrows in the enlarged panels on the right identify numerous examples of this co-staining.

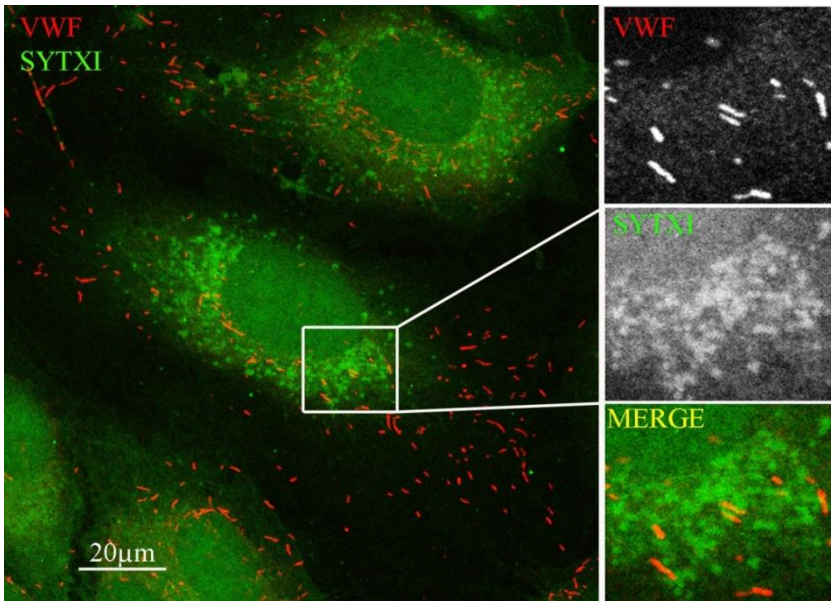

Figure 3.19. Globular structures are seen in HUVECs following staining for SYT XI.
The results of staining TX-100-fixed HUVECs with the VWF (red) and SYT XI (green) antibodies are shown. The merged image is shown on the left. An enlarged section of the cell as indicated by the white rectangle is shown on the right. Note the large aggregates in the perinuclear area which have appeared following the SYT XI stain.

3.5 Discussion and Conclusions:

3.5.1 SYT I:

I have shown that SYT I exists as both an mRNA transcript and as a protein of 55 kDa in HUVECs. This is slightly larger than the predicted mass of 47.5 kDa for the SYT I protein, although it is likely that cell-specific post-translational modifications affect the observed size of the protein. Indeed, SYT I was originally identified as a protein of 65 kDa on synaptic vesicles (Matthew *et al.* 1981) and so clearly its predicted size does not necessarily correlate with experimental observations. The 55-kDa band detected here is specifically diminished following the treatment of HUVECs with SYT I siRNA (see Chapter 8), providing supporting evidence that it is representative of the SYT I protein.

A hazy, diffuse background stain was produced following ICC attempting to determine the distribution of SYT I in HUVECs (see Figure 1.15). A control screen examining the effects of omitting either the SYT I primary antibody or the α-mouse CY-2 secondary antibody revealed that these reagents do not generate a significant degree of background auto-fluorescence (data available in Appendix 3.0). Therefore a subcellular localization screen using markers of various intracellular structures was performed with the aim to identify any co-localization between the vague SYT I stain and specific cell structures. No co-localization was identified between SYT I and any of the organelle markers screened (data not shown). Therefore I conclude that the diffuse stain generated by the α-SYT I antibody results from non-specific binding and thus is not representative of the distribution of SYT I in HUVECs. The antibody was able to recognize SYTI-EGFP following its over-expression in HEK cells (Figure 3.16). This suggests that either SYT I is present at too low a concentration in HUVECs to allow its successful recognition by the commercial antibody or that the endogenous protein is found in a complex with other molecules, rendering it inaccessible to its antibody.

The specific recognition of endogenous SYT I by ICC could be facilitated by the stimulation of HUVECs with agonists which induce an activated, pro-thrombotic state. Indeed, it is known that the expression of a number of secretory proteins such as t-PA, IL-8, and exotaxin-3 is up-regulated by the pre-conditioning of HUVECs with pro-inflammatory reagents such as TNF-α and IL-1β (Huber *et al*. 2002, Utgaard *et al.* 1998, Oynebraten *et al*. 2004). It would be of interest to determine the effect of stimulation on the expression of the

SYT family members in HUVECs as it is likely that their expression may be up-regulated, and this in turn might allow their successful detection by ICC.

3.5.2 SYT III:

This work has demonstrated that SYT III is present in HUVECs as an mRNA transcript and as a protein thereby adding endothelial cells to the growing list of secretory cells which express this Ca^{2+}-dependent member of the SYT family. Western blotting revealed that SYT III is present in HUVECs as a major variant of 63 kDa in keeping with previous observations (Falkowski *et al.* 2011). However, weaker bands of 45 and 50 kDa were also detected following the immunoblotting of HUVEC lysate. These may be a consequence of the cross-reactivity of the α-SYT III primary antibody or they may represent the presence of numerous SYT III splice variants in HUVECs. Indeed, SYT III has been reported to exist as a 78-kDa isoform in the goldfish retia (Berntson and Morgans, 2003) and as a number of isoforms of 46, 66, and 80 kDa in rodent brain homogenates (Brown *et al*. 2000, Grimberg *et al*. 2002). Additionally, following the Western blotting of HEK-293 lysates a single band of 80 kDa representing the SYT III protein was detected (data not shown), suggesting that the numerous bands identified on blots of HUVEC lysate are specific for this cell type rather than being a result of non-specific binding by the primary antibody. Therefore it is likely that within endothelial cells SYT III exists as a number of splice variants or alternatively undergoes extensive post-translational modifications.

ICC aiming to determine the subcellular distribution of the SYT III protein in HUVECs was unsuccessful despite numerous attempts to optimize the protocol for the detection of this protein. However, the commercial α-SYT III antibody was able to identify SYTIII-EGFP following its over-expression in HEK cells (Figure 3.16). Therefore it is likely that the concentration of SYT III in HUVECs is too low to allow its recognition by its antibody. Alternatively, in HUVECs the SYT III protein may exist in a form which is inaccessible to the antibody. For example it may be present as part of a larger complex and indeed analysis of the crystal structure of the SYT III C2AB domain has led to the suggestion that the protein binds to the *trans*-SNARE complex in resting cells (Vrijic *et al.* 2010).

3.5.3 SYT V:

I have demonstrated that SYT V mRNA is present in HUVECs and that the endogenous protein can be visualized by Western blotting as a band of 43 kDa. This band was diminished following SYTV-siRNA treatment of HUVECs (see Chapter 6). A second band was observed at approximately 80 kDa and it is possible that this represents dimeric SYT V. Indeed it is known that over-expressed SYT V forms SDS-resistant aggregates in other cell types (Iezzi *et al*. 2004, Saegusa *et al.* 2002). Hence, it is likely that SYT V forms aggregates in HUVECs and the band seen following Western blotting represents an SDS-resistant SYT V dimer. Additionally, I have obtained similar results following the blotting of lysates derived from HEK cells over-expressing SYTV-EGFP (data not shown). Here, bands were detected of 43 kDa (representing monomeric endogenous SYT V), 70 kDa (representing over-expressed SYTV-EGFP) and 80 kDa (thought to represent dimeric endogenous SYT V).

ICC attempting to identify the subcellular distribution of endogenous SYT V in HUVECs was unsuccessful and this was most likely the result of an inability of the commercial α-SYT V antibody to recognize the endogenous protein. Indeed, the antibody failed to identify the SYTV-EGFP construct following its over-expression in HEK cells (Figure 3.16) and so is clearly unable to detect the SYT V protein when it is known to be present at high concentrations in a lysate sample.

3.5.4 SYT VI:

The Western blotting of HUVEC lysate suggested that SYT VI exists as a series of splice variants within endothelial cells, with bands representing the SYT VI protein seen at 55, 60, and 70 kDa. SYT VI is unique among the SYTs in that it can exist as both a transmembrane and cytosolic protein (Craxton and Goedert, 1999). The molecular weight of the SYT VI isoforms has been reported to be 58 kDa for the full-length protein in PC12 cells (Fukuda and Mikoshiba, 1999), 50 kDa for the ΔTM variants (Fukuda and Mikoshiba, 1999), and 66 kDa in sperm cell lysate (Michaut *et al.* 2001). Therefore, it is likely that numerous variants of SYT VI are expressed simultaneously within HUVECs and cell-specific post-translational modifications may further influence their observed molecular weights. Indeed, the simultaneous presence of four separate splice variants of the protein has been reported in the mouse cerebellum (Fukuda and Mikoshiba, 1999). Therefore, as the data presented here and in previous studies suggests it is possible that SYT VI exists as a series of splice variants in HUVECs.

ICC with a commercial antibody suggested that endogenous SYT VI can be found predominantly as a component of the early endosomes and is absent from other subcellular structures. In order to more accurately determine the subcellular distribution of endogenous SYT VI in HUVECs I performed preliminary co-localization analysis of this protein with markers of the various subcellular organelles. The Pearson's correlation coefficient generated for SYT VI and EEA-1 (0.14 ± 0.043) suggested that no significant co-localization exists between these two proteins. This is in contrast to the conclusions derived from visual analysis of the data. However, the intense background fluorescence generated by the α-SYT VI antibody makes accurately determining the subcellular distribution of SYT VI challenging. Additionally, the major SYT VI splice variant expressed within HUVECs may well be the cytoplasmic ΔTM variant and therefore this background fluorescence may be the result of the cytosolic protein. At this point, the true distribution of endogenous SYT VI in HUVECs is unclear and requires further investigation. Ideally, the identity of its various splice variants in HUVECs should be determined as this would allow sensible predictions to be made as to the likely distribution of the SYT VI proteins(s) in endothelial cells.

3.5.5 SYT VII:

RT-PCR has demonstrated that SYT VII mRNA is expressed in HUVECs. This in itself is unsurprising as SYT VII is believed to be ubiquitously expressed. However, there are a number of isoforms of the SYT VII gene and my preliminary investigations have shown that SYTVII-α and SYTVII-β are specifically expressed in HUVECs (data available to view in Appendix 2.0). Similar to the findings reported in other cell types (Fukuda *et al.* 2002) SYTVII-α is the major isoform found within HUVECs whereas the larger variant SYTVII-β is also present but to a much lesser extent. It is important to consider that different isoforms of SYT VII have different and often antagonistic functions and therefore the ratio of expression of the various isoforms can alter the observed function of SYT VII (Gauthier *et al*. 2008). It would be of interest to determine if and how the ratio of expression of these two isoforms varies, particularly in response to antagonistic stimulation of the endothelium. For example, it may be that the ratio of expression shifts following its exposure to inflammatory versus vaso-protective stimuli, thus altering the calcium sensitivity of WPB exocytosis. It is likely that additional isoforms of SYT VII are present in HUVECs and it would be of interest to determine the full extent of SYT VII gene splicing in the future using variant-specific PCR.

Western blotting has demonstrated that a 65-kDa protein representing SYT VII is present in HUVEC lysate, and indeed this is the precise size for SYTVII-α (Fukuda *et al.* 2002). An additional band of 100 kDa was identified and this may represent either SYTVII-β or perhaps a larger uncharacterized transcript. As the SYT VII protein is now known to be present in HUVECs ICC was attempted with the aim to determine the distribution of the endogenous protein within our model endothelial cells. Unfortunately this was unsuccessful with no recognition of the SYT VII protein achieved despite considerable attempts to optimize the ICC protocol. It was later shown that the commercial α-SYT VII antibody was able to detect SYTVII-YFP following its over-expression in HEK cells but not in HUVECs, demonstrating that the reagent requires a concentrated source of antigen for recognition. Hence, the endogenous ICC failed due to limitations in the efficiency of the primary antibody.

3.5.6 SYT VIII:

Western blotting has demonstrated that the SYT VIII protein is expressed in endothelial cells as two major isoforms of 75 and 80 kDa and furthermore bands representing these two proteins are specifically diminished following the knock-down of SYT VIII in HUVECs (see Chapter 7). This result was not entirely surprising as previous studies have reported the existence of numerous isoforms of SYT VIII. Indeed, it has been reported in mouse sperm cells as a protein of 70 kDa (Hutt *et al.* 2002), in the rat renal cortex as a protein of 52 kDa (Kishore *et al.* 1998), and in PC12 cells as isoforms with molecular weights of 40 and 50 kDa (Monterrat *et al.* 2006). Therefore it is probable that the SYT VIII exists either as a series of splice variants or as one protein which undergoes extensive post-translational modifications affecting its observed molecular weight. Interestingly, when the SYTVIII-EGFP construct was over-expressed in HEK-293 cells and the resulting lysates were subjected to Western blotting two bands of 80 and 90 kDa were identified by both the α-GFP and α-SYT VIII antibodies (data not shown). This suggests that the over-expressed protein undergoes post-translational modifications leading to the generation of two pools of protein with different molecular weights. Specific PCR would be needed to determine the number and identity of the splice variants of the SYT VIII gene which are expressed in our model endothelial cells.

ICC attempting to determine the localization of endogenous SYT VIII in HUVECs was unsuccessful and indeed the commercial antibody failed to detect over-expressed

SYTVIII-EGFP in HEK-293 cells (Figure 3.16). This implies that the antibody is unable to recognize its antigen under the conditions used in our laboratory even when it is present at high concentrations in a cell culture.

3.5.7 SYT XI:

I have shown by RT-PCR that SYT XI is present in HUVECs as an mRNA transcript. Unfortunately my attempts to demonstrate the expression of the SYT XI protein in HUVECs were unsuccessful. This was despite using a variety of lysate extraction techniques including TX-114 partitioning which provides a more concentrated source of membrane proteins. However the commercial α-SYT XI antibody failed to detect over-expressed SYTXI-EGFP in transfected HUVEC lysate and therefore is unable to recognize SYT XI when it was known to be present in an endothelial lysate sample. In contrast, the antibody did recognize SYTXI-EGFP in transfected HEK cells, demonstrating that it requires a highly concentrated source of antigen for successful recognition. In the likely event that SYT XI protein is present endogenously within HUVECs its concentration would be too low to allow detection by the antibody.

ICC examining the distribution of the endogenous SYT XI protein in HUVECs was on the whole unsuccessful although unusual intracellular aggregates were identified. Initially, I presumed that these aggregates were a by-product of fixation or possibly a consequence of cell debris. However, over-expression studies revealed that these unusual aggregates are also seen in HUVECs and HEK cells following their transfection with SYTXI-EGFP (data not shown). It is possible that these aggregates may be a result of the time-dependent aggregation of the SYT XI protein. They may also be representative of subcellular vesicles although my attempts to identify them using an organelle marker screen were unsuccessful.

3.5.8 SYT XVII:

SYT XVII was shown to be present in HUVECs as an mRNA transcript and to my knowledge this is the first observation of the endogenous expression of SYT XVII in any cell type. SYT XVII is also thought to be present in HUVECs as a protein of 60 kDa. The predicted size of the human SYT XVII protein according to the Uniprot database is 54 kDa (http://www.uniprot.org/uniprot, entry Q9BSW7) and so it is likely that either a splice variant of the SYT XVII gene is expressed in HUVECs or the protein undergoes post-translational

modifications which lead to discrepancies between its observed and predicted molecular weights. As I have shown, both of these eventualities are commonplace in the SYT family and as no other studies have attempted to determine the number of isoforms of SYT XVII in existence or their approximate sizes at this point I cannot comment on which possibility is more likely. ICC aiming to determine the distribution of endogenous SYT XVII in HUVECs was unsuccessful due to the failure of the commercial antibody to recognize the SYT XVII protein even when it was over-expressed in HEK-293 cells (Figure 3.16). This was unfortunate as this would have been the first determination of the distribution of endogenous SYT XVII in any cell type.

3.5.9 Conclusions:

I have demonstrated that our model endothelial cells express SYTs I, III, V, VI, VII, VIII, XI, and XVII at both the mRNA and protein levels. Therefore these eight members of the SYT family are strong candidates for the role of the Ca^{2+} sensor regulating WPB exocytosis. Although SYTs VIII, XI, and XVII do not bind Ca^{2+} ions directly they are likely to play a modulatory role in the regulation of secretory events (Sudhof, 2002). The expression of SYT XVII in HUVECs is noteworthy as to my knowledge this represents the first observation of the expression of this member of the SYT family in a specific cell type.

My attempts to determine the endogenous distribution of these proteins in HUVECs by ICC have been on the whole unsuccessful. It is likely that the SYTs are either not expressed at a sufficient level in HUVECs to allow their recognition by commercial antibodies or they are present as a complex with other proteins and so are inaccessible. In any case, as endogenous ICC is clearly inefficient the subcellular localization of the endothelial SYTs will be determined by the over-expression of fluorescent SYT constructs. The remainder of this report will focus on characterizing the subcellular distributions and functional roles of the endothelial SYTs with the aim to determine if one or more members of this family are involved in regulating the Ca^{2+}-driven exocytosis of WPBs from HUVECs.

Chapter Four

Determining the Subcellular Localization of the Endothelial SYTs

4.1 Chapter Overview:

Thus far, I have demonstrated that a number of the SYTs are expressed in our model endothelial cells and although the presence of SYT protein in HUVECs has been demonstrated by Western blotting attempts to determine the subcellular distribution of endogenous SYTs by ICC have been unsuccessful. It appears that in most cases the endogenous protein is not present in sufficient quantities to allow recognition by the commercial antibodies. Therefore, in order to determine the subcellular distribution of the SYTs I constructed fluorescent constructs of each family member which has been shown to be expressed in HUVECs. To achieve this I initially attempted a conventional method as described in '2.6.1 Conventional Ligation-Dependent Cloning.' However, with the exception of the production of the SYTI-mCherry and SYTI-EGFP vectors this approach was unsuccessful. Despite repeated attempts to optimize the protocol by, for example, altering the ratio of vector to insert during the ligation reaction, increasing the quantity of template DNA for PCR, purchasing image clones of the SYTs, and varying the concentration of Mg^{2+} in the reactions I was repeatedly unable to produce SYT constructs through conventional means. Therefore, I used the ligation-independent (LIC) method as described in '2.6.2 Ligation-Independent Cloning.' This approach proved successful and EGFP fusion vectors for SYTs III, V, VI, VII, VIII, XI, and XVII were created and sequence-verified.

In order to determine the subcellular localization of the SYTs in endothelial cells the fluorescent constructs were expressed in HUVECs. ICC was performed with the aim to determine to which subcellular organelles the fluorescent proteins are trafficked. For each transfection, HUVECs were stained for either GFP or mCherry to emphasize the localization of the construct and for markers of various subcellular organelles. The marker proteins used in this study are listed in Table 4.1 and shown in Figure 4.1. They included VWF (a marker of WPBs), LAMP1 (for lysosomes), CD63 (for multivesicular bodies, WPBs, and lysosomes), PECAM (a marker for plasma membrane), TGN-46 (for the *trans* Golgi network), PDI (for the endoplasmic reticulum (ER)), EEA-1 (for the early endosomes) and the transferrin receptor (tfR; for the recycling endosomes). In some cases, HUVECs were also stained for Rab27a (to distinguish between mature and immature WPBs), VAMP3 (a

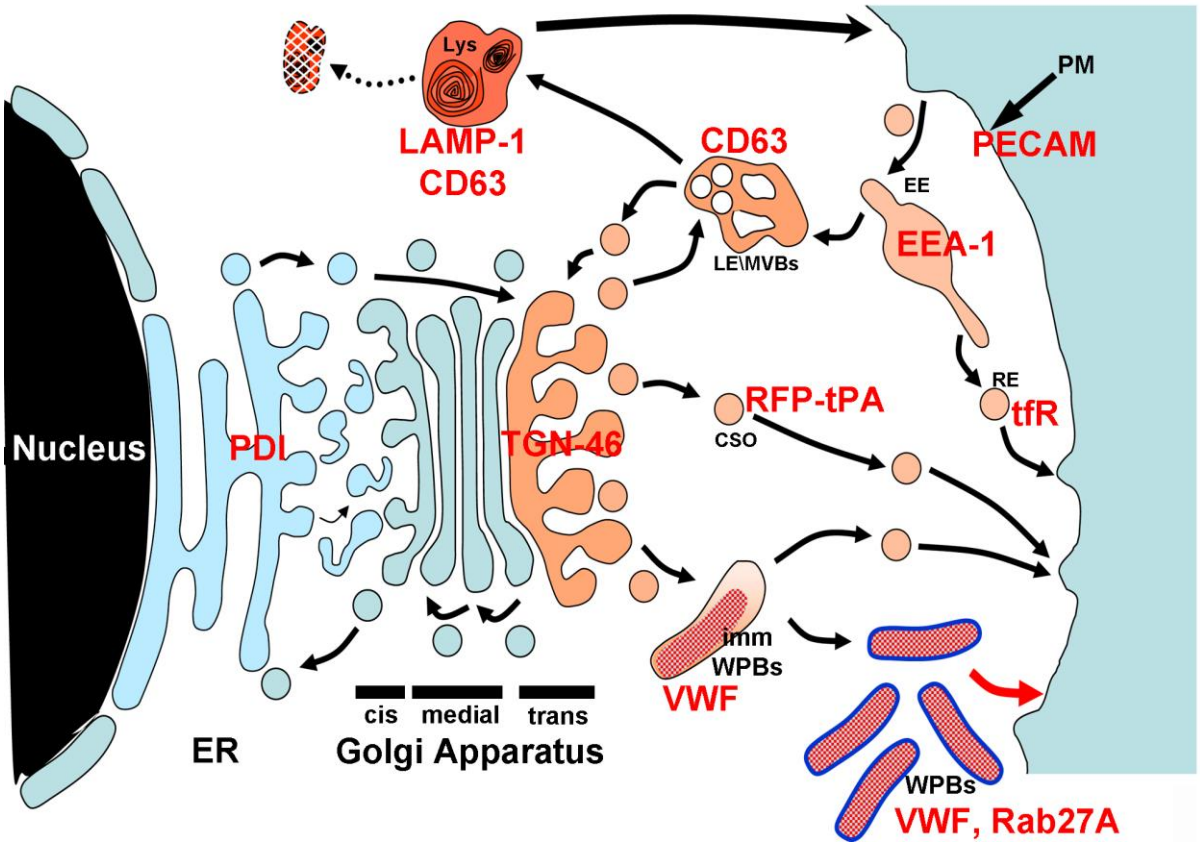

Figure 4.1. Antigens associated with compartments of the secretory pathway

The image shows the major subcellular compartments (black text) of the secretory pathway in endothelial cells and the antigens (**red text**) used to identify them. **ER**; endoplasmic reticulum (**PDI**), **Golgi Apparatus**, comprising cis, medial and trans (**TGN-46**) compartments, **immWPBs**; immature Weibel-Palade bodies (**VWF**), **WPBs**; mature Weibel-Palade bodies (**VWF, Rab27A)**, **CSO**; constitutive secretory organelles (**tPA**), **PM**; plasma membrane (**PECAM**), **EE**; Early Endosomes (**EEA-1**), **RE**; Recycling Endosomes (**tfR**), **LE\MVBs**; late endosomes\multivesicular bodies (**CD63**), **Lys**; Lysosomes (**LAMP1, CD63**).

Marker Protein	Full Name	Organelle / Structure
VWF	von Willebrand Factor	WPBs
LAMP1	Lysosomal-Associated Membrane Protein 1	Lysosomes
CD63	N/A	Multivesicular Bodies, WPBs, Lysosomes
PECAM	Platelet Endothelial Cell Adhesion Molecule	Plasma Membrane
TGN-46	Trans Golgi Network-46	*trans* Golgi Network
PDI	Protein Disulfide Isomerase	Endoplasmic Reticulum
EEA-1	Early Endosome Antigen-1	Early Endosomes
tfR	Transferrin Receptor	Recycling Endosomes
Rab27a	N/A	Mature WPBs
VAMP3	Vesicle-Associated Membrane Protein 3	WPBs
tPA	Tissue Plasminogen Activator	Constitutively-Secreted Small Vesicles

Table 4.1. Various antigens were used to identify subcellular compartments.
The abbreviated and full name of the marker proteins used throughout this study and the subcellular structure(s) which they identify are listed.

SNARE protein resident on WPBs) and tPA (to identify small constitutively-secreted vesicles). Because the subcellular distribution of an over-expressed protein can vary depending on the growth time after transfection, HUVECs were cultured for 6 - 48 hours depending on the SYT prior to fixation. This approach allowed me to determine the subcellular localization of over-expressed SYTs and by extrapolation to identify the likely distribution of the endogenous protein in HUVECs.

4.2 Results:

4.2.1 SYT I:

HUVECs were transfected with SYTI-mCherry and cultured for 24 or 48 hours prior to fixation. Figure 4.2 shows a HUVEC double-stained for mCherry and endogenous VWF. SYTI-mCherry did not label WPBs at either 24 or 48 hours. Instead it appeared to localize to the plasma membrane and to VWF-negative vesicular structures. The plasma membrane localization of SYTI-mCherry was confirmed by co-staining with PECAM (Figure 4.3). At 48 hours post-transfection SYTI-mCherry was less strongly-associated with the plasma membrane and more strongly-associated with the vesicle-like structures (Figure 4.3 bottom

panel). To determine the identity of these structures HUVECs were stained 48 hours following transfection with antibodies directed against different compartments of the endocytic and recycling pathways. Immunolabeling with markers of the early and recycling endosomes showed little evidence of co-localization at either time point (Figure 4.4), indicating that SYTI-mCherry is largely absent from these compartments. Next, HUVECs were stained for markers of the multivesicular bodies and lysosomes (Figure 4.5). As can be seen, SYTI-mCherry co-localized with a subset of CD63-positive organelles and strongly with LAMP1-positive structures. In contrast immunolabeling for the ER and TGN showed no evidence of SYTI-mCherry localization to these compartments (Figure 4.6). Together, the data shows that SYTI-mCherry localizes to the plasma membrane at early time-points following transfection and is present predominantly in multivesicular bodies and lysosomes at more extended times.

4.2.2 SYT III:

SYTIII-EGFP expression peaked early after transfection (8-12 hours) and showed prominent perinuclear localization, labeling of vesicular structures, and what appeared to be a plasma membrane distribution (Figure 4.7). At 24 hours, the number of expressing cells was greatly reduced and by 48 hours no cells could be detected expressing the construct. Based on these results an 8 hour time-point was chosen at which to screen the cells with organelle-specific markers.

To test whether the SYTIII-EGFP-positive vesicular structures might represent WPBs cells were co-stained for VWF (Figure 4.8). No co-localization was detected between SYTIII-EGFP and VWF. The plasma membrane localization of SYTIII-EGFP was confirmed by co-staining with PECAM (Figure 4.9, top panel) and the intense perinuclear signal co-localized with TGN-46 (Figure 4.9, bottom panel). No evidence for co-localization of SYTIII-EGFP with the ER marker PDI was found (Figure 4.10). To determine the identity of the SYTIII-EGFP positive vesicle-like structures cells were co-stained with antibodies against either EEA-1 (Figure 4.11, top panel), tfR (Figure 4.11 bottom panel), CD63 (Figure 4.12 top panel) or LAMP1 (Figure 4.12 bottom panel). SYT III-EGFP clearly co-localized with EEA-1 but only very weakly with the tfR. However, the tfR staining was at times indistinct and so reaching definitive conclusions based on these images is difficult. SYTIII-EGFP also co-localized with a subset of CD63-positive organelles and could be detected in some but not all of the LAMP1-positive structures (Figure 4.12).

Figure 4.2

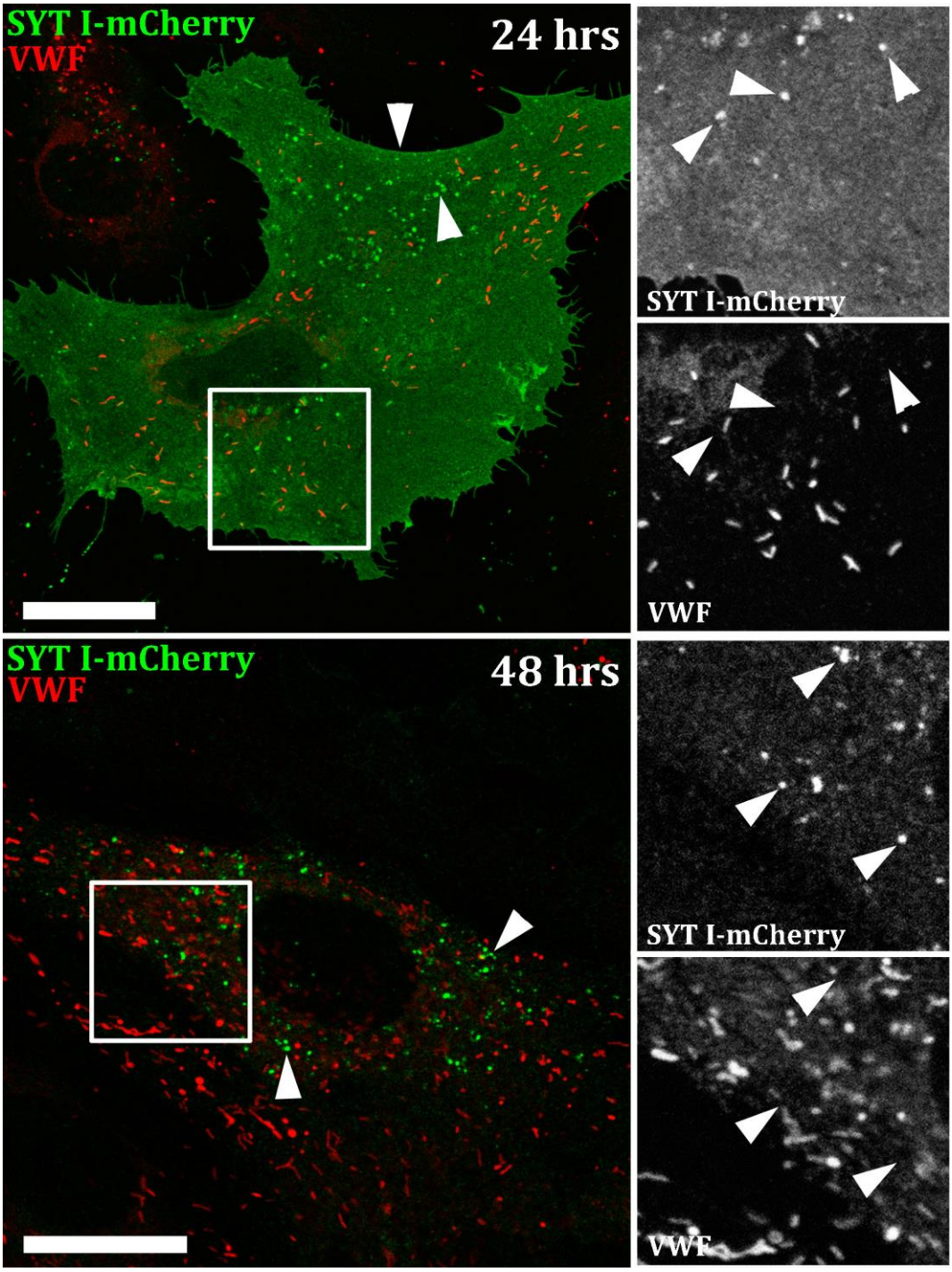

Figure 4.2 SYTI-mCherry labels the plasma membrane and VWF-negative vescicle-like structures in HUVECs.

Images show HUVECs expressing SYTI-mCherry (green) and counter-stained with a specific antibody to VWF (red) at 24 (top) or 48 hours (bottom) post-transfection. The arrows indicate the localization of SYTI-mCherry to the plasma membrane or to VWF-negative vesicular structures. Scales bars are 20 μm.

Figure 4.3

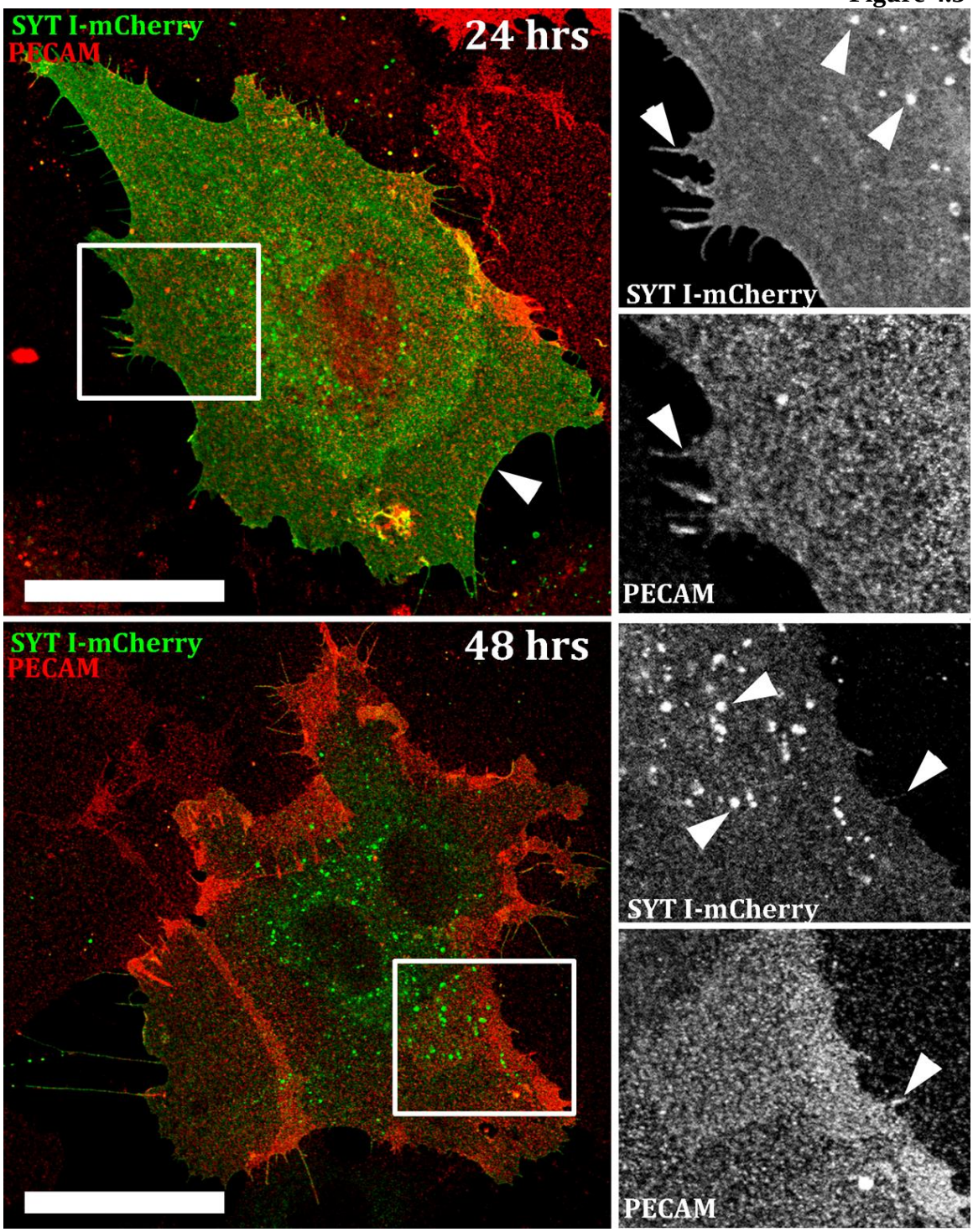

Figure 4.3. SYTI-mCherry is present on the plasma membrane.

Images show HUVECs expressing SYTI-mCherry (green) and counter-stained with a specific antibody to PECAM (red) at 24 (top) or 48 hours (bottom) post-transfection. The arrows indicate SYTI-mCherry-labeled plasma membrane and\or vesicular structures. Scales bars are 20 μm.

Figure 4.4

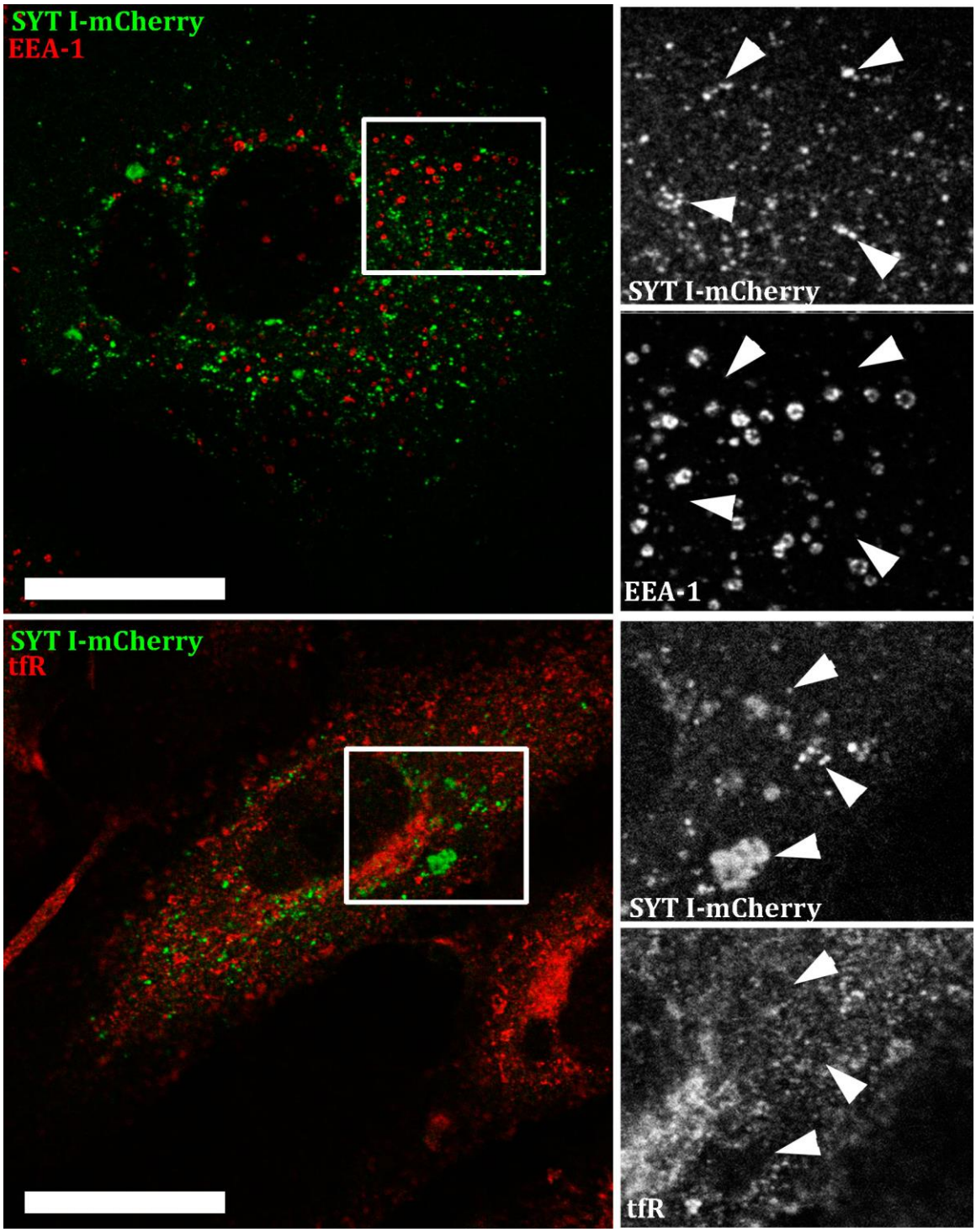

Figure 4.4. SYTI-mCherry is not detectable in the endosomal system in HUVECs.
Images show HUVECs expressing SYTI-mCherry (green) and counter-stained (red) with specific antibodies to EEA-1 (top) or the tfR (bottom) 48 hours post-transfection. Scales bars are 20 μm.

Figure 4.5

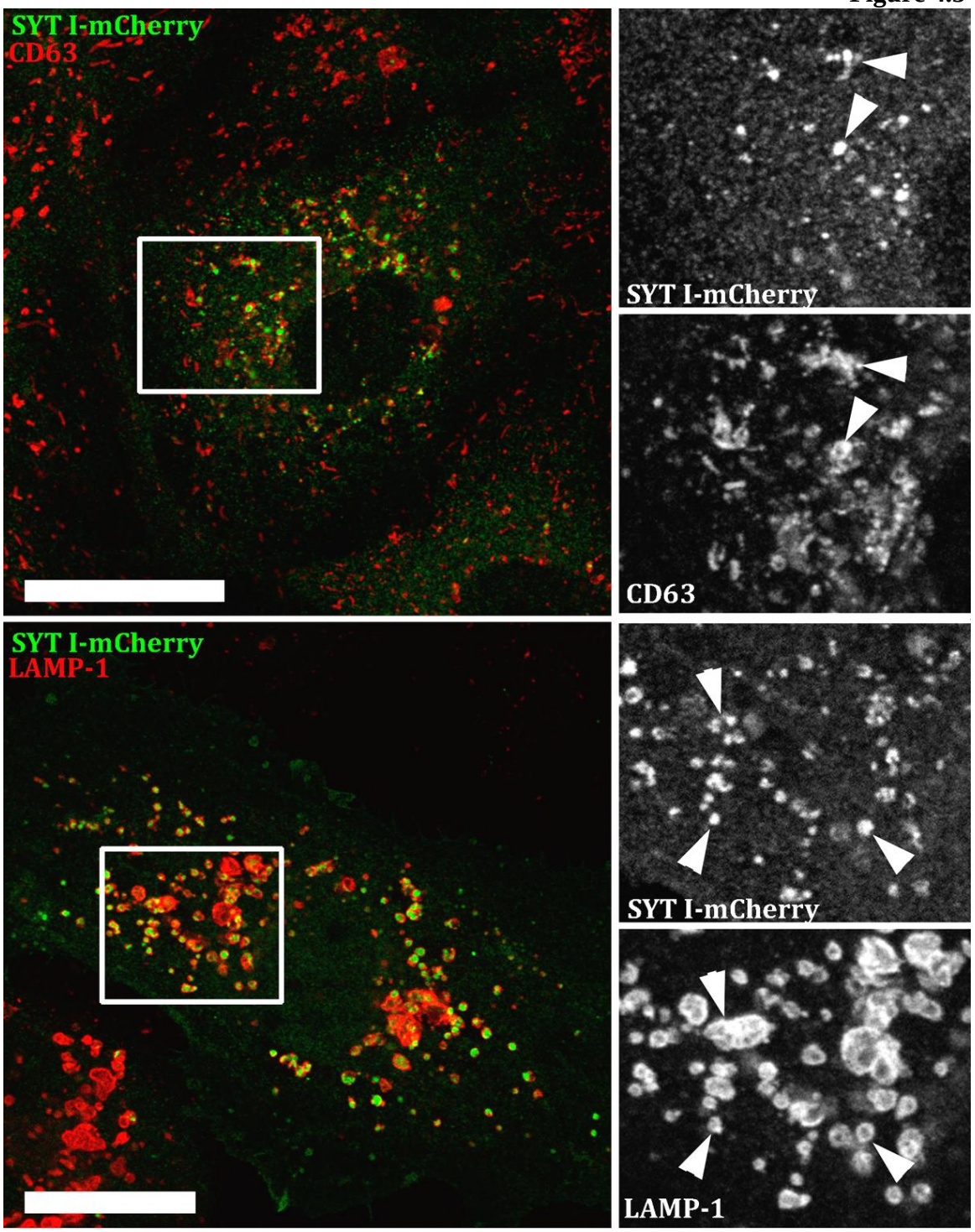

Figure 4.5. SYTI-mCherry is found on the multivesciular bodies and lysosomes in HUVECs.

Images show HUVECs expressing SYTI-mCherry (green) and counter-stained (red) with specific antibodies to CD63 (top) or LAMP1 (bottom) 48 hours post-transfection. Scales bars are 20 μm.

Figure 4.6

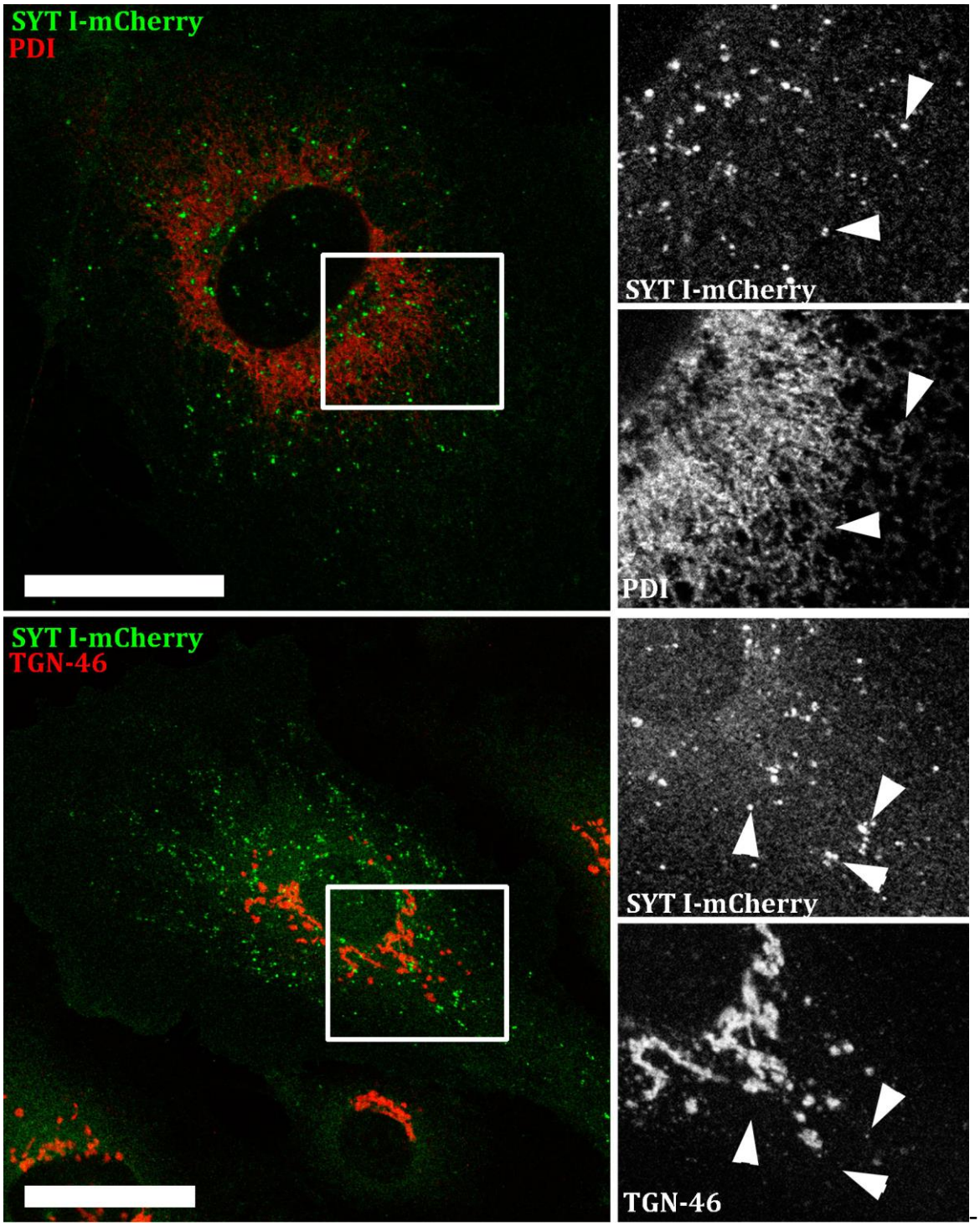

Figure 4.6 SYTI-mCherry does not co-localize with ER or TGN markers.
Images show HUVECs expressing SYTI-mCherry (green) and counter-stained (red) with specific antibodies to PDI (top) or TGN-46 (bottom) 48 hours post-transfection. Scales bars are 20 μm.

Figure 4.7

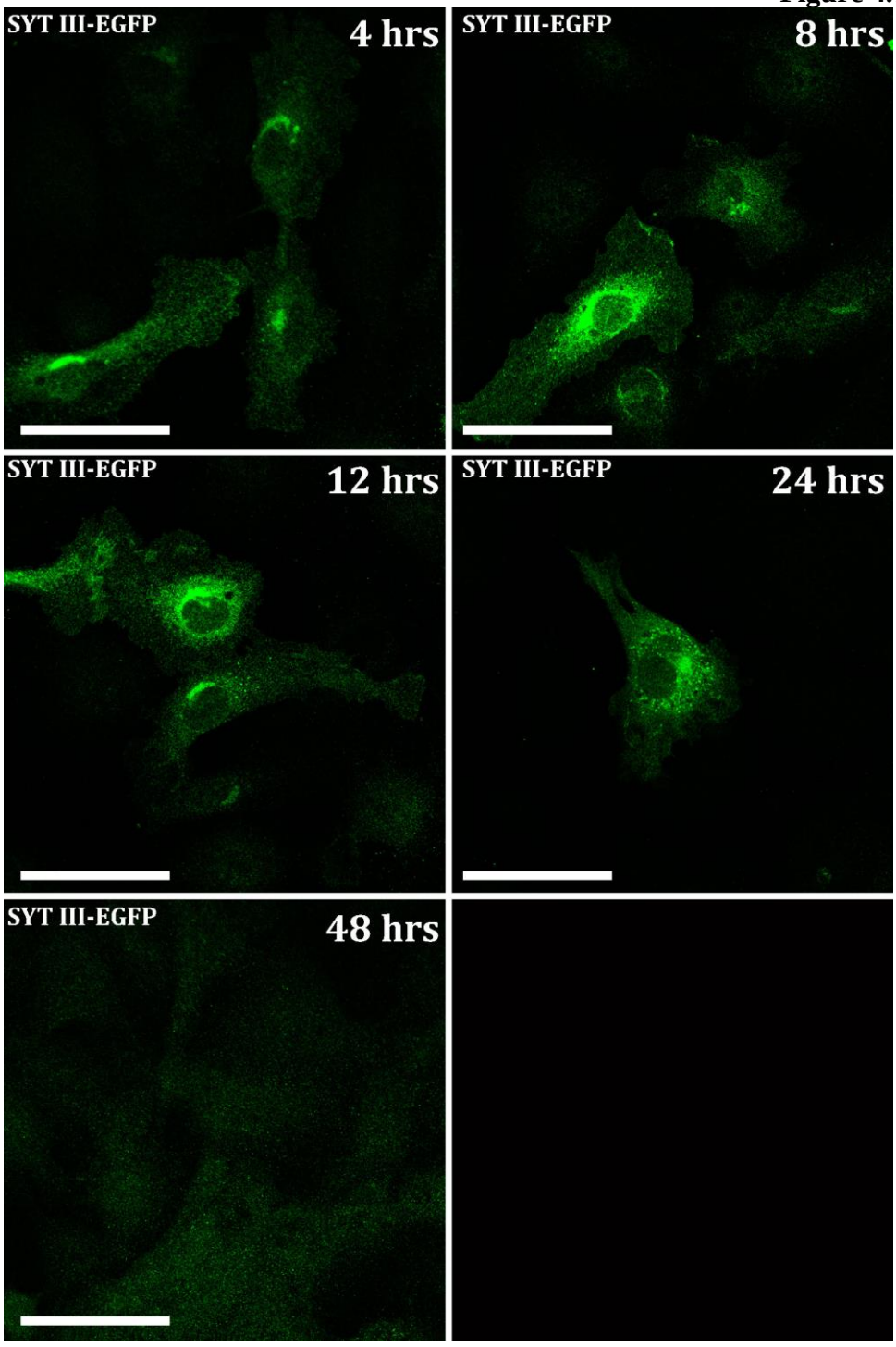

Figure 4.7. Time course of SYTIII-EGFP expression in HUVECs. Images show HUVECs expressing SYTIII-EGFP (green) at 4, 8, 12, 24 and 48 hours post-transfection as indicated. Scales bars are 50 μm.

Figure 4.8

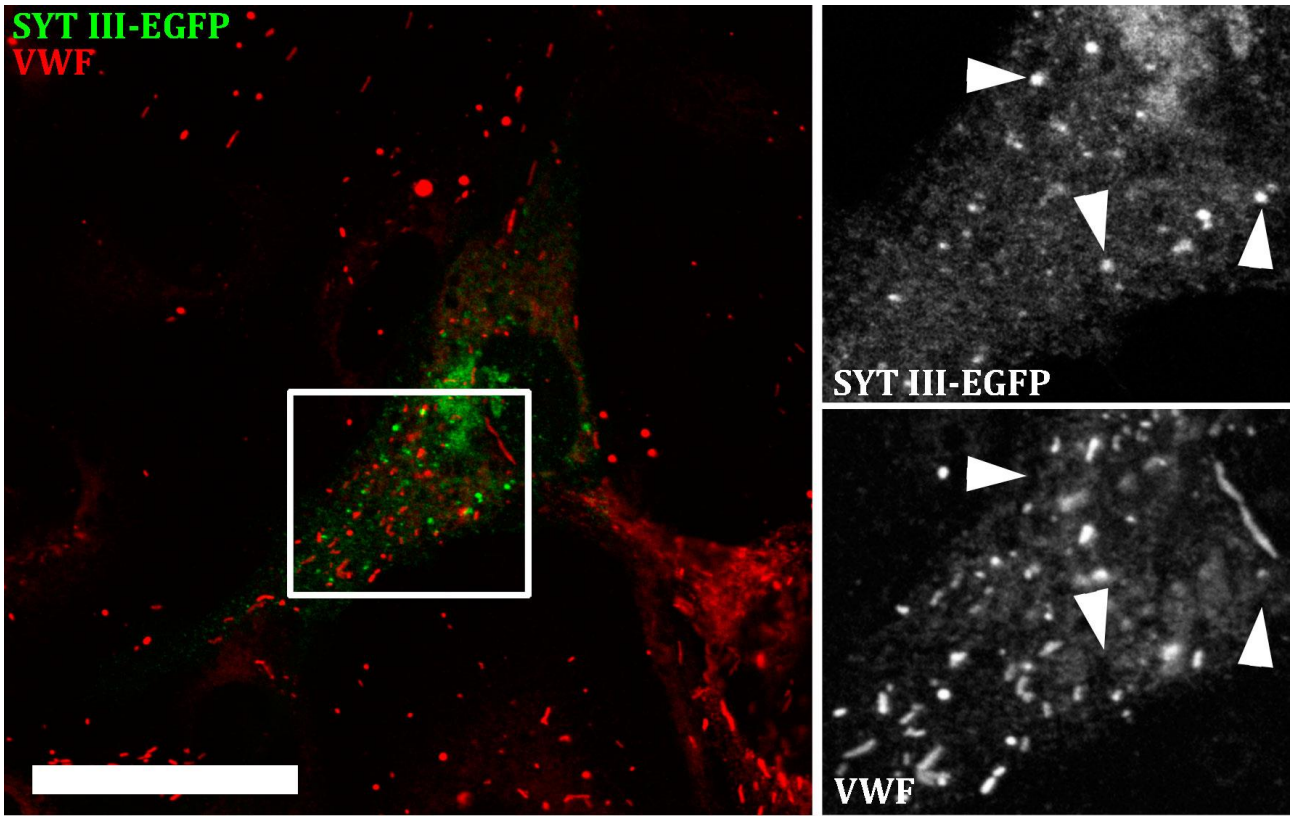

Figure 4.8. SYTIII-EGFP does not co-localize with endogenous VWF.

Images show HUVECs expressing SYTIII-EGFP (green) and counter-stained with a specific antibody to VWF (red) 8 hours post-transfection. Arrows indicate SYTIII-EGFP labeling of punctuate VWF-negative vesicular structures. Scale bar is 30 μm.

Figure 4.9

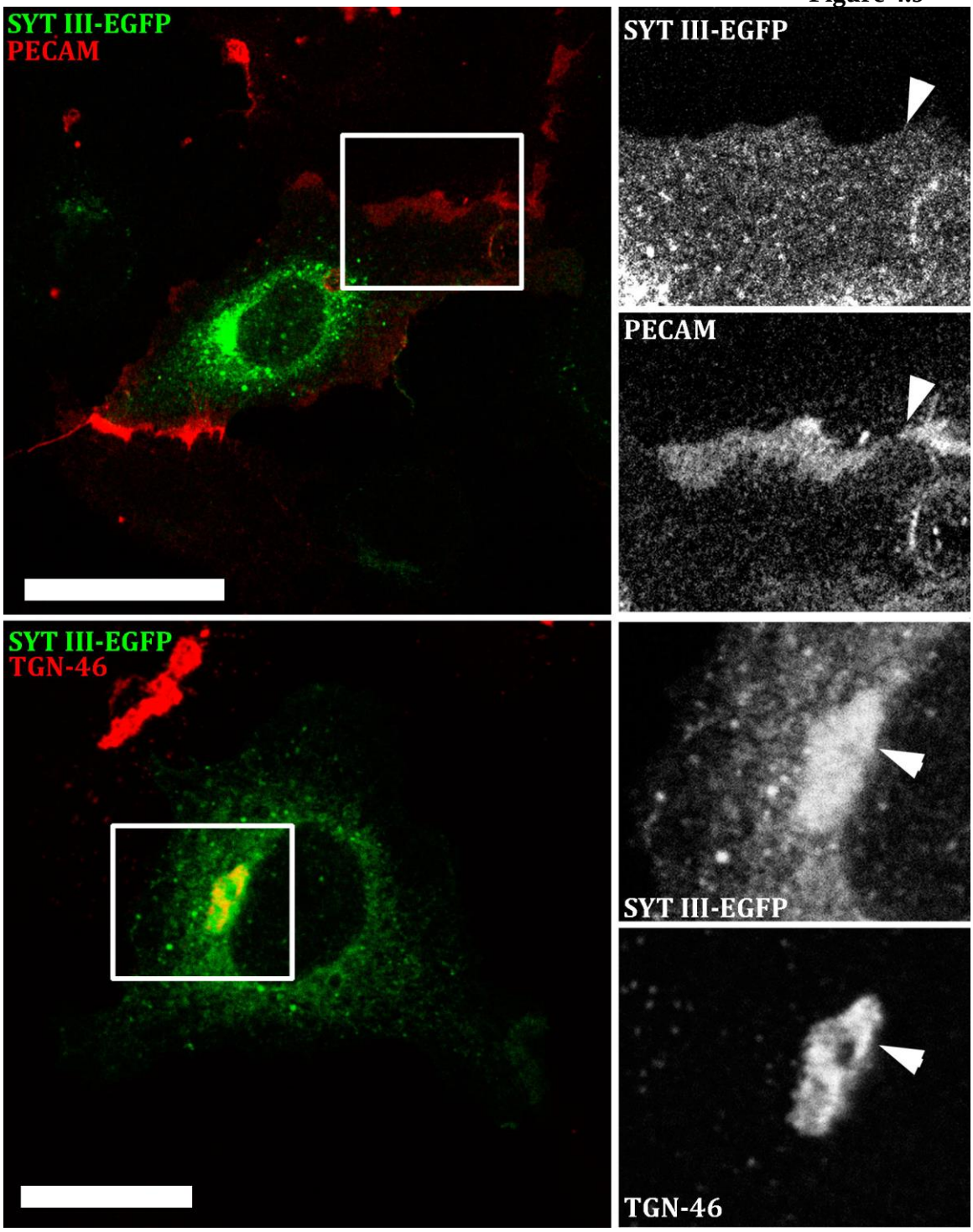

Figure 4.9. SYTIII-EGFP is present at low levels on the plasma membrane and in the TGN.

Images show HUVECs expressing SYTIII-EGFP (green) and counter-stained (red) with a specific antibodies to PECAM (top) or TGN-46 (bottom) 8 hours post-transfection. Arrows indicate SYTIII-EGFP-labeling of the plasma membrane (top) or TGN (bottom). Scale bars are 20 μm.

Figure 4.10

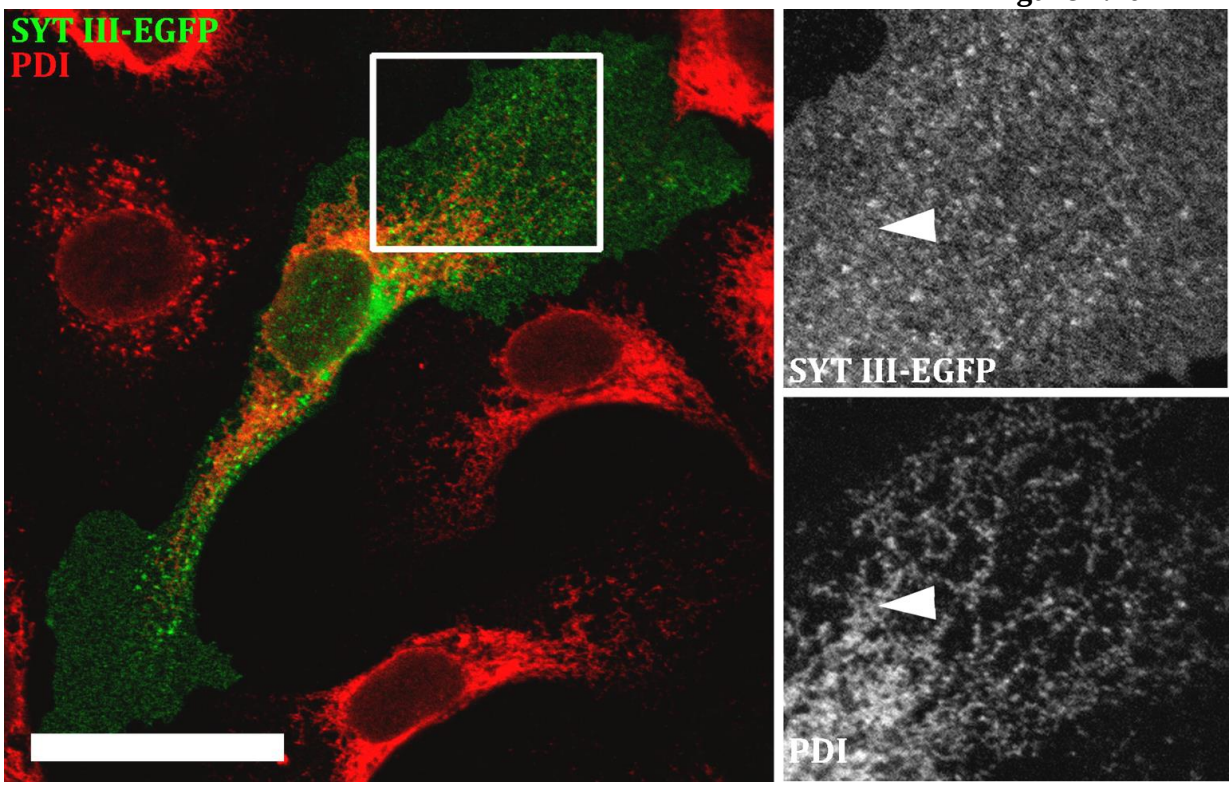

Figure 4.10 SYTIII-EGFP does not co-localize with the ER marker PDI.

Images show HUVECs expressing SYTIII-EGFP (green) and counter-stained with a specific antibody to PDI (red) 8 hours post-transfection. There was no evidence for co-localization of SYTIII-EGFP with PDI (shown by arrow). Scale bar is 20 μm.

Figure 4.11

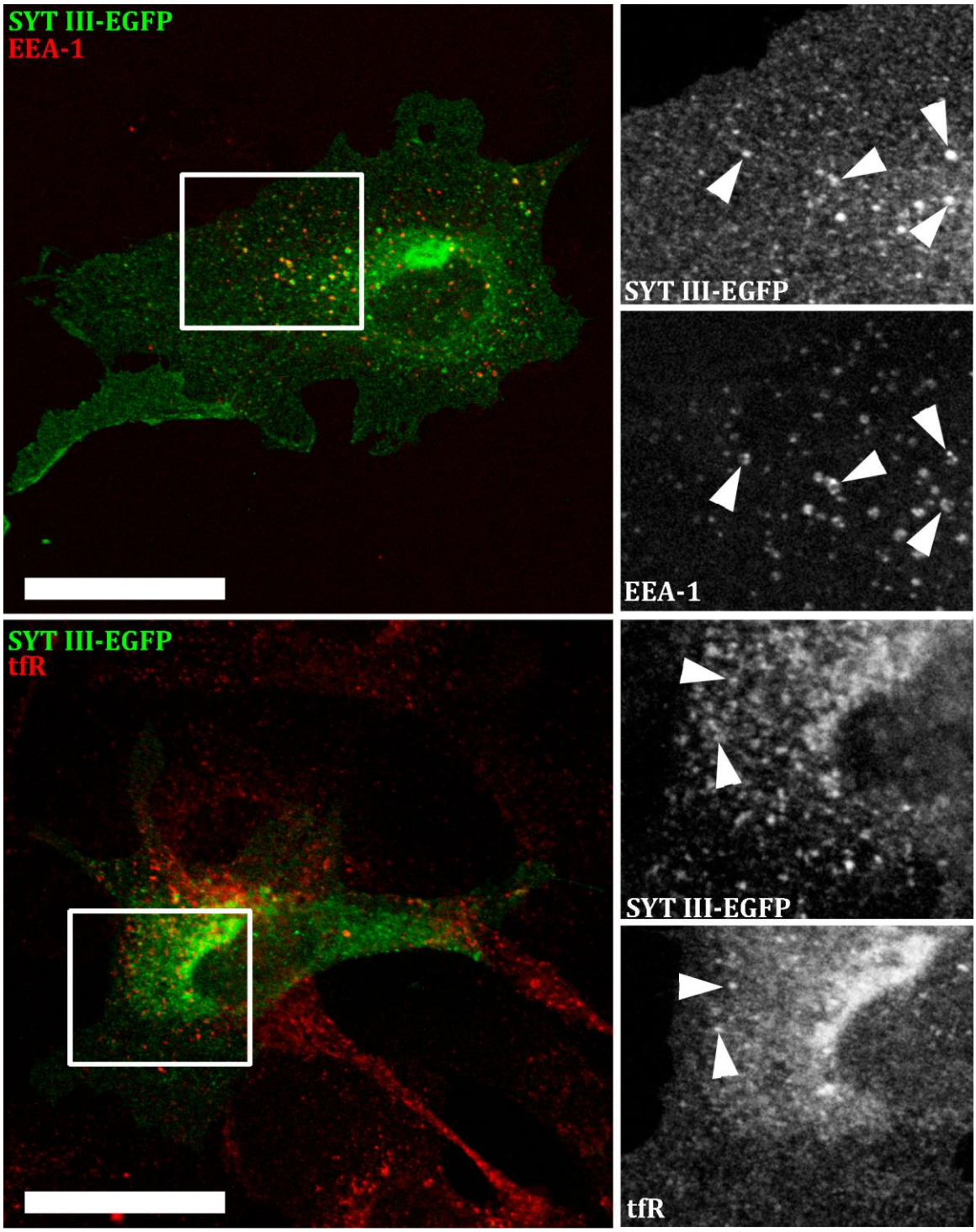

Figure 4.11. SYTIII-EGFP is present in early and possibly recycling endosomes.

Images show HUVECs expressing SYTIII-EGFP (green) and counter-stained (red) with specific antibodies to EEA-1 (top) or tfR (bottom) 8 hours post-transfection. Arrows indicate examples of co-localization between the proteins. Scale bars are 20 μm.

Figure 4.12

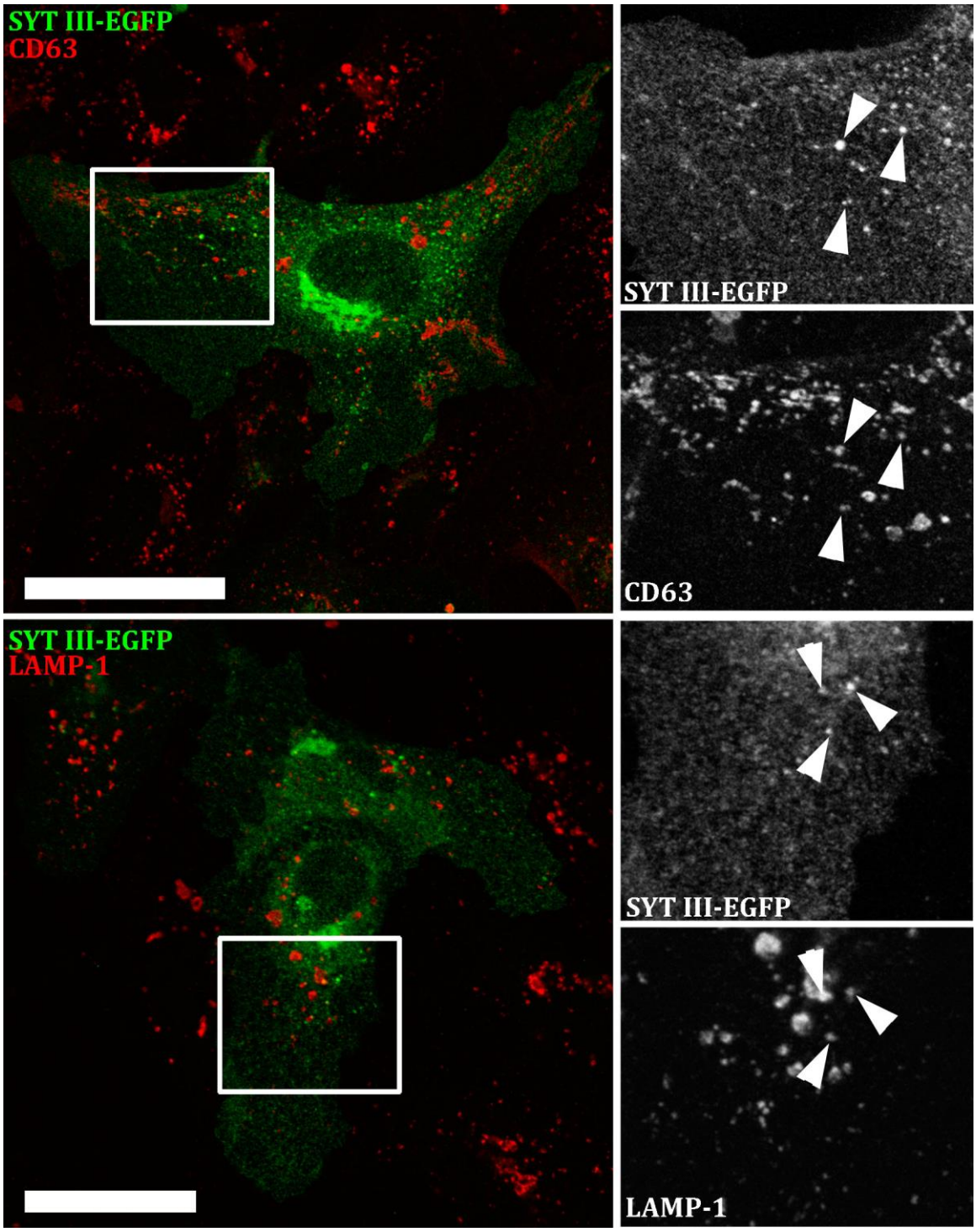

Figure 4.12. SYTIII-EGFP is present in a sub-population of multivesicular bodies and lysosomes.

Images show HUVECs expressing SYTIII-EGFP (green) and counter-stained (red) with specific antibodies to CD63 (top) or LAMP1 (bottom) 8 hours post-transfection. Arrows indicate examples of co-localization between the proteins. Scales bars are 20 μm.

4.2.3 SYT V:

Expressed SYTV-EGFP localised almost exclusively to distinctive rod-like structures which co-stained with endogenous VWF and so were confirmed to be WPBs (Figure 4.13). Some SYTV-EGFP fluorescence was also detectable on the plasma membrane (Figure 4.14) and in the TGN (Figure 4.14, bottom panel) at 24 hours post-transfection (top left in Figure 4.14). Closer inspection of cells labeled with TGN-46 suggested that SYTV-EGFP is present on WPBs as they emerge from this compartment indicating that SYT V may enter the WPB membrane at this point in the secretory pathway. Consistent with a WPB localisation SYTV-EGFP was detected on rod-shaped CD63- and VWF-positive WPBs but was only occasionally seen on smaller, more spherical CD63-positive VWF-negative structures that presumably represent the lysosomes and multivesicular bodies (Figure 4.15). No co-localisation was found between SYTV-EGFP and the organelle markers PDI, EEA-1 (Figure 4.16), tfR or LAMP1 (Figure 4.17).

4.2.4 SYT VI:

The expression of SYTVI-EGFP resulted in a diffuse pattern of fluorescence that was excluded from the nucleus. Co-staining of transfected HUVECs with PECAM or PDI indicated that SYTVI-EGFP is present on the plasma membrane and may also be found in the ER (Figure 4.18) although the latter was not clear. No evidence for the co-staining of SYTVI-EGFP with VWF, EEA-1, tfR, CD63 or LAMP1 was detected (Figure 4.18).

4.2.5 SYT VII:

The SYTVII-YFP construct was a kind gift from Professor Norma Andrews (University of Maryland). The expression of SYTVII-YFP in HUVECs resulted in the appearance of striking rod-like structures which co-localized with endogenous VWF demonstrating that these are representative of WPBs (Figure 4.19). Triple labeling of YFP, VWF and the WPB-specific Rab protein Rab27a (Figure 4.20A) or the v-SNARE VAMP3 (Figure 4.20B) showed that SYTVII-YFP was present on mature WPBs. Close inspection of these images suggested that SYTVII-YFP was also present on some immature Rab27a-negative WPBs (Figure 4.20A). This suggests that SYTVII-YFP may enter the WPB

Figure 4.13

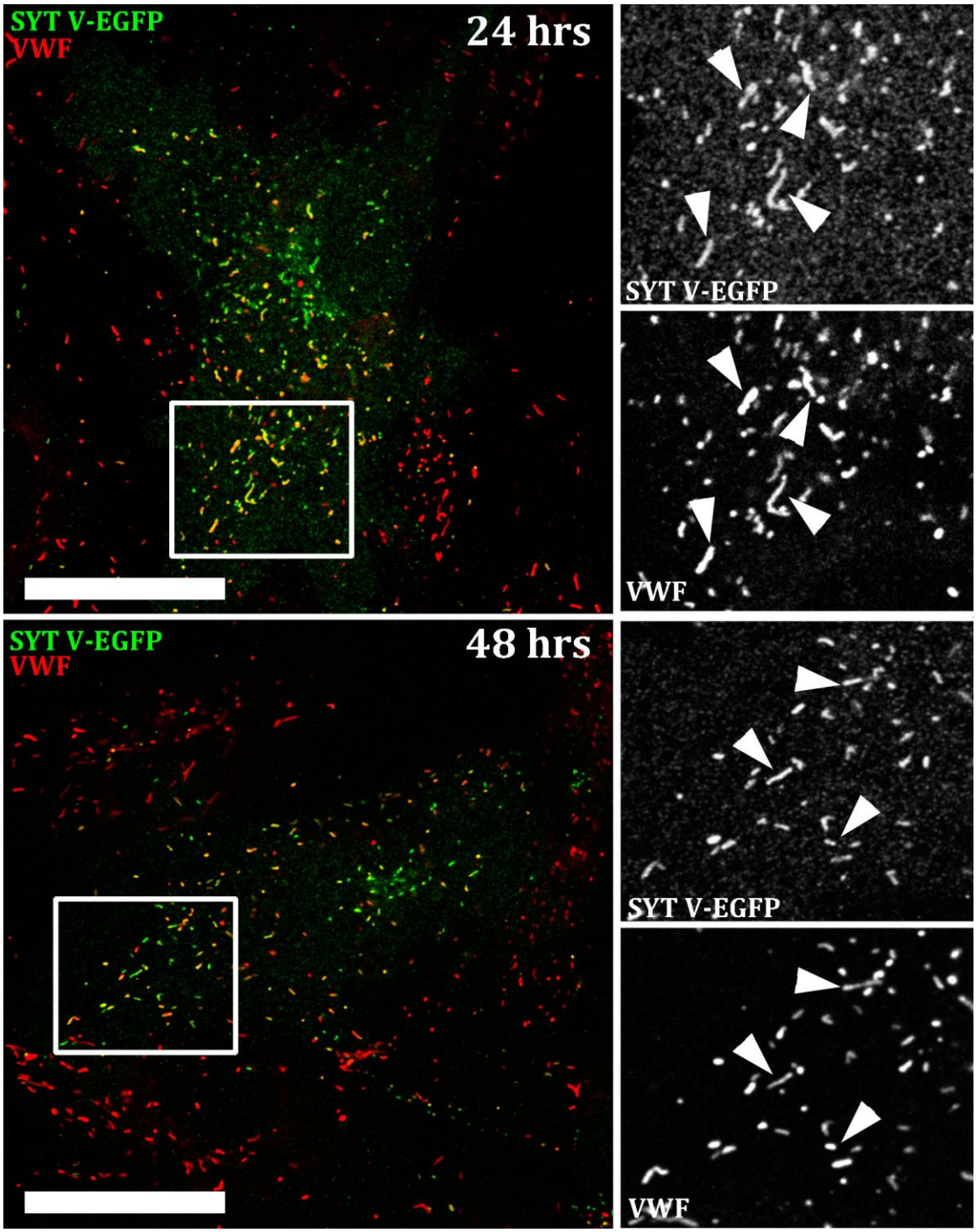

Figure 4.13. SYTV-EGFP is present on WPBs.

Images show HUVECs expressing SYTV-EGFP (green) and counter-stained with a specific antibody to VWF (red) at 24 (top) or 48 (bottom) hours post-transfection. Arrows show co-localization between SYTV-EGFP and endogenous VWF. Scale bars are 20 μm.

Figure 4.14

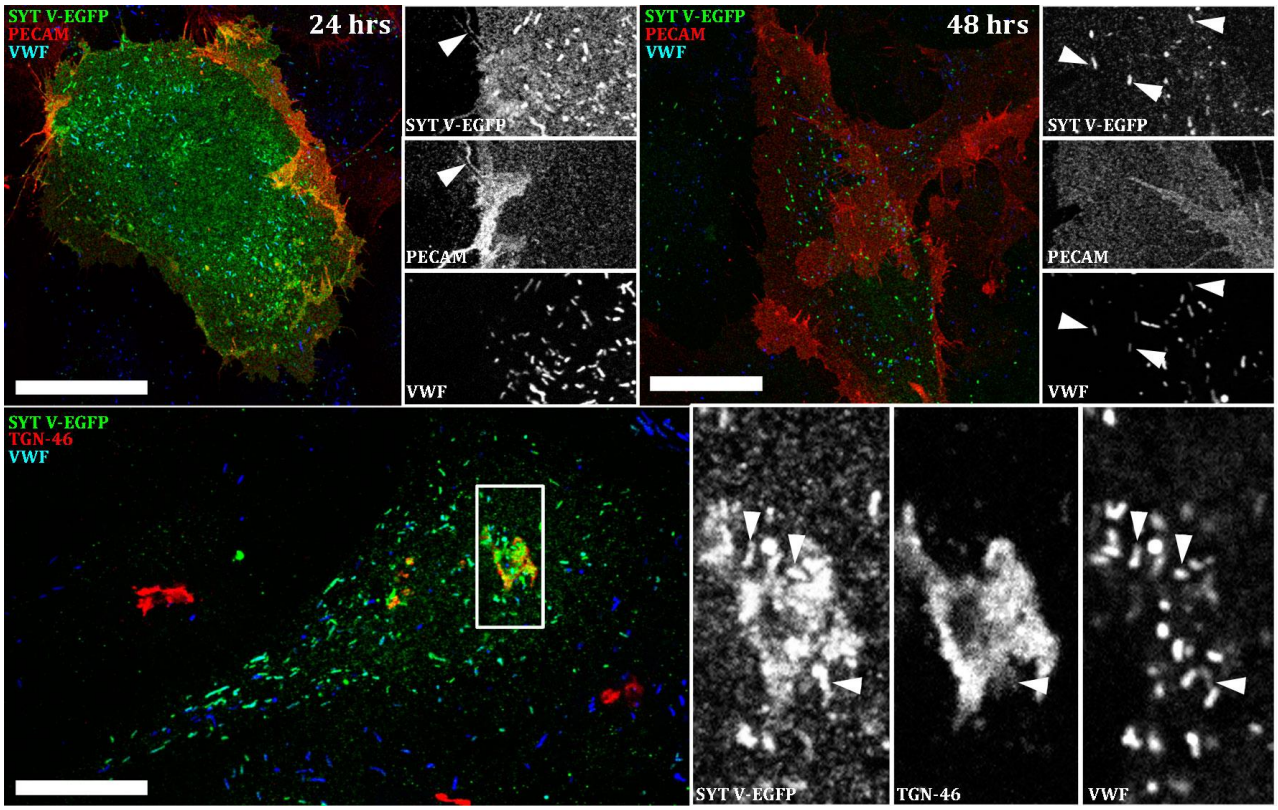

Figure 4.14 SYTV-EGFP is present on the plasma membrane and TGN at early time-points.

Images show HUVECs expressing SYTV-EGFP (green) and counter-stained with specific antibodies to PECAM (red) and VWF (blue) at 24 (top left) or 48 hours (top right) post-transfection. Bottom: SYTV-EGFP-expressing (green) HUVECs counter-stained with specific antibodies to TGN-46 (red) and VWF (blue) at 24 hours post-transfection. Arrows show the co-localization of SYTV-EGFP with endogenous VWF in the TGN region of the cell. Scale bars are 20 μm.

Figure 4.15

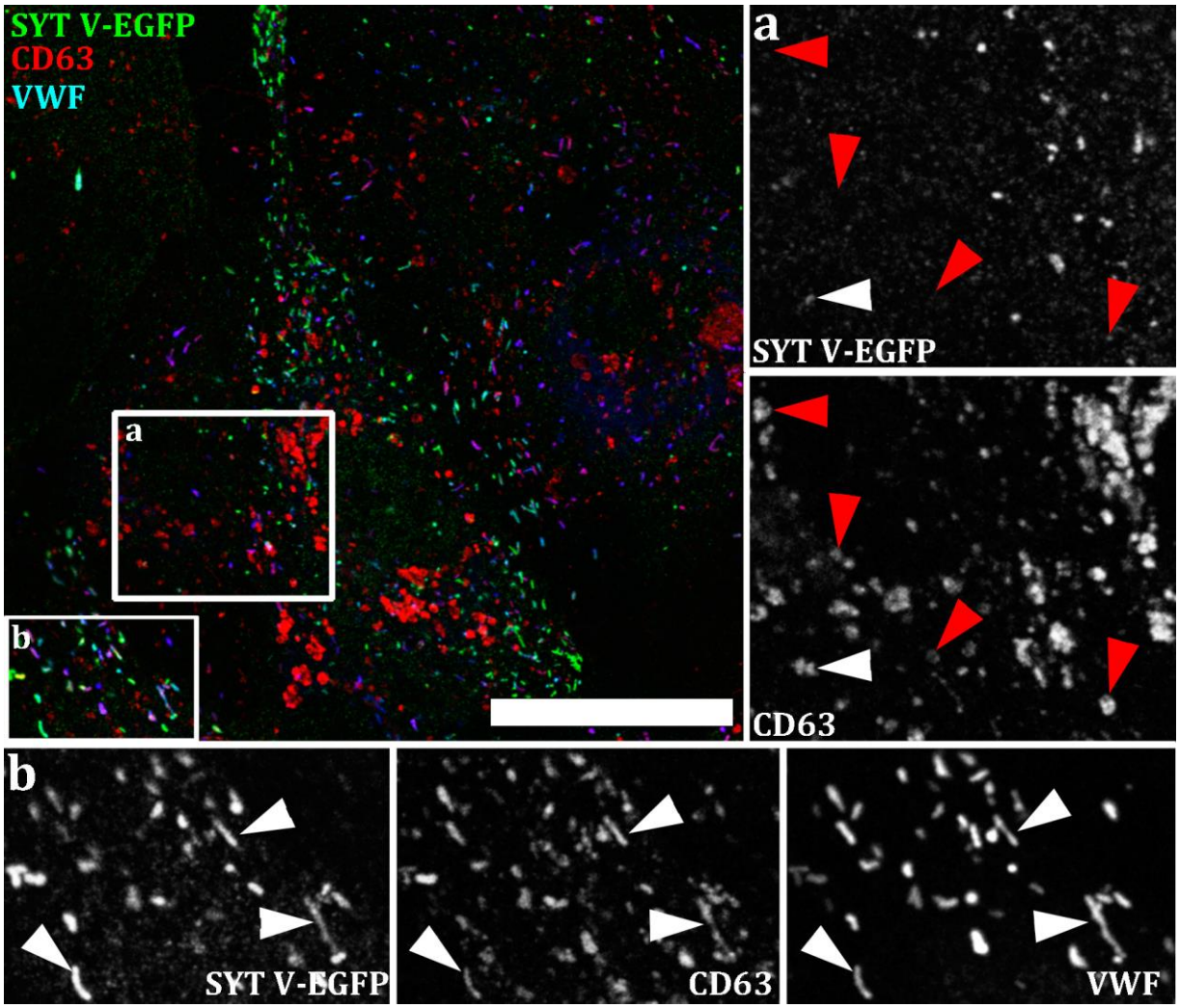

Figure 4.15. SYTV-EGFP is largely absent from multivesicular bodies.

Images show HUVECs expressing SYTV-EGFP (green) and counter-stained with specific antibodies to CD63 (red) and VWF (blue). Scale bar is 20 μm. Grey scale images from region (a) shows SYTV-EGFP (top) and endogenous CD63 (bottom). Red arrows show that most small, rounded CD63-positive organelles largely lack SYTV-EGFP. These organelles are negative for VWF (not shown). Only rarely was there some evidence of co-localization of SYTV-EGFP and endogenous CD63 in these structures (e.g. white arrow). Grey scale panels from region (b) show SYTV-EGFP in rod-shaped CD63-positive WPBs.

Figure 4.16

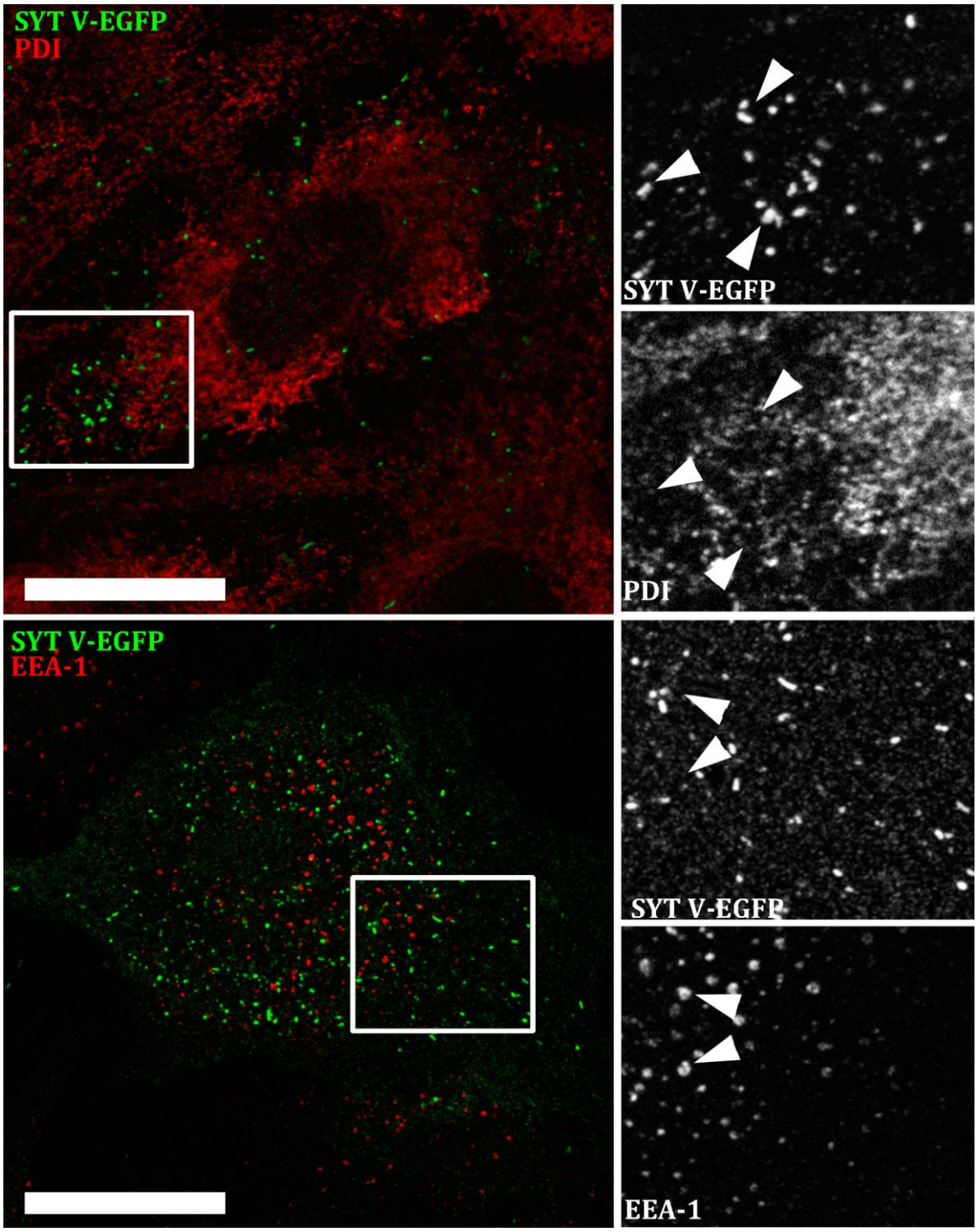

Figure 4.16. SYTV-EGFP does not co-localize with either PDI or EEA-1.

Images show HUVECs expressing SYTV-EGFP (green) and counter-stained (red) with specific antibodies to PDI (top) or EEA-1 (bottom). Arrows show the lack of co-localization of SYTV-EGFP with the ER or early endosomes. Scale bars are 20 μm.

Figure 4.17

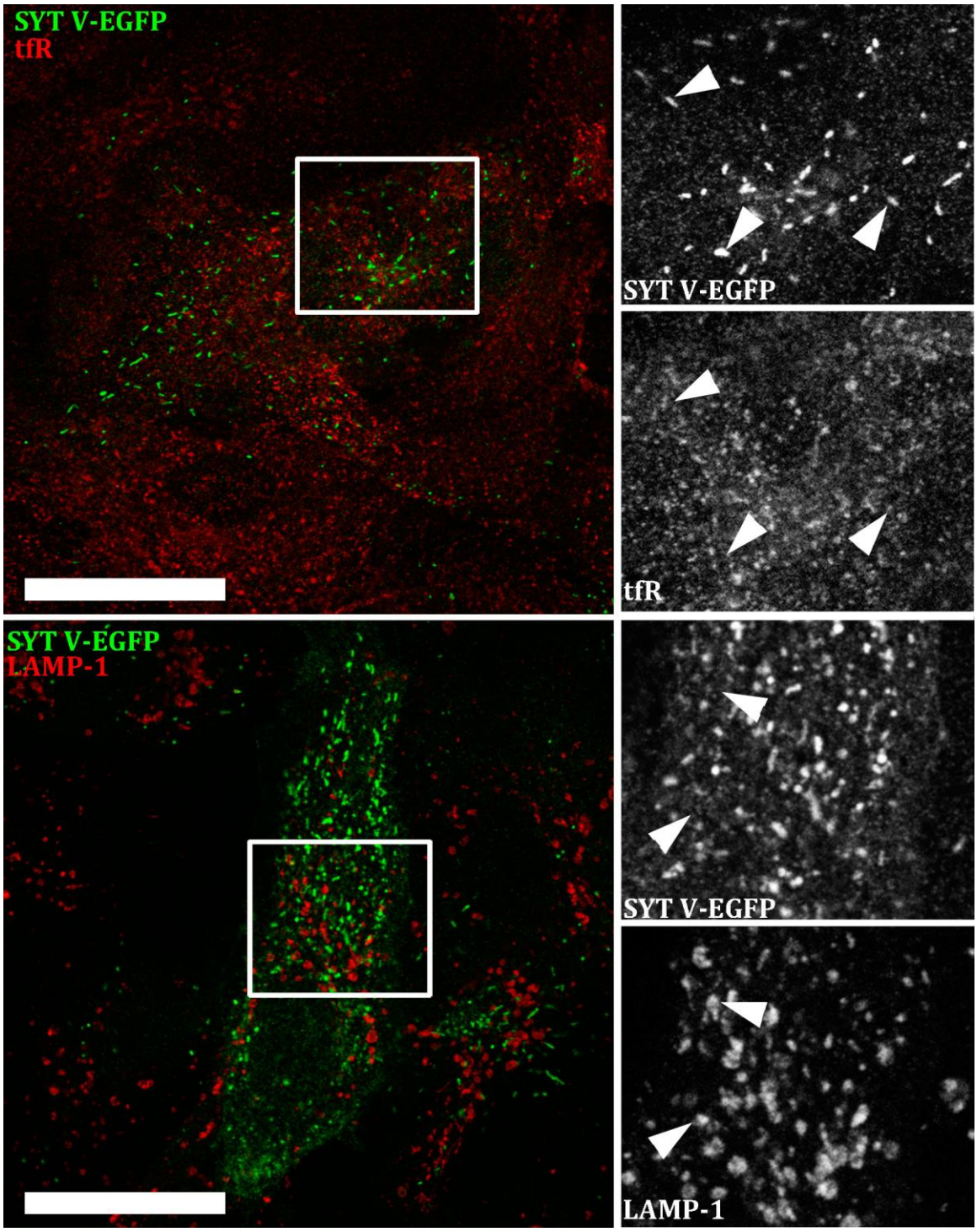

Figure 4.17. SYTV-EGFP does not co-localize with either the tfR or LAMP1.

Images show HUVECs expressing SYTV-EGFP (green) and counter-stained (red) with specific antibodies to tfR (top) or LAMP1 (bottom). Arrows show the lack of co-localization of SYTV-EGFP with recycling endosomes or lysosomes. Scale bars are 20 μm.

membrane at the level of TGN. Triple staining for YFP, VWF and CD63 or LAMP1 revealed that SYTVII-YFP was also present on lysosomes (Figure 4.21). No clear evidence for the co-localization of SYTVII-YFP with the plasma membrane or endosomal system was found (Figure 4.22). The co-expression of SYTVII-YFP with mRFP-tPA, a component of constitutive secretory granules in HUVECs (Knipe *et al* 2010), showed that SYTVII-YFP was absent from these organelles and therefore does not enter the constitutive pathway (data not shown).

4.2.6 SYT VIII:

The expression of SYTVIII-EGFP in HUVECs resulted in the appearance of a perinuclear fluorescence signal and the labeling of a subset of striking rod-like structures. These co-stained with α-VWF antibodies demonstrating that they are WPBs (Figure 4.23). Closer inspection of these images suggested that SYTVIII-EGFP may be present in the WPB membrane as the organelle emerges from the TGN region (Figure 4.23) indicating that it could be recruited to the granules at the level of Golgi. Triple staining for GFP, VWF and CD63 or LAMP1 revealed that SYTVIII-EGFP is absent from the lysosomes although as expected CD63-positive WPBs were shown to contain the construct (Figure 4.24). No evidence for the co-localization of SYTVIII-EGFP with the plasma membrane or endosomal system was found (Figure 4.25).

4.2.7 SYT XI:

The expression of SYTXI-EGFP in HUVECs resulted in the appearance of a strong perinuclear fluorescence signal and a reticular pattern of peripheral fluorescence. The perinuclear fluorescence co-localized with TGN-46 (Figure 4.26, bottom) and to some extent with PDI (Figure 4.26, top). No evidence for the co-localization of SYTXI-EGFP with WPBs (VWF/CD63), the plasma membrane (PECAM), early endosomes (EEA-1), recycling endosomes (tfR) or lysosomes (LAMP1/CD63) was identified (Figure 4.27).

Figure 4.18

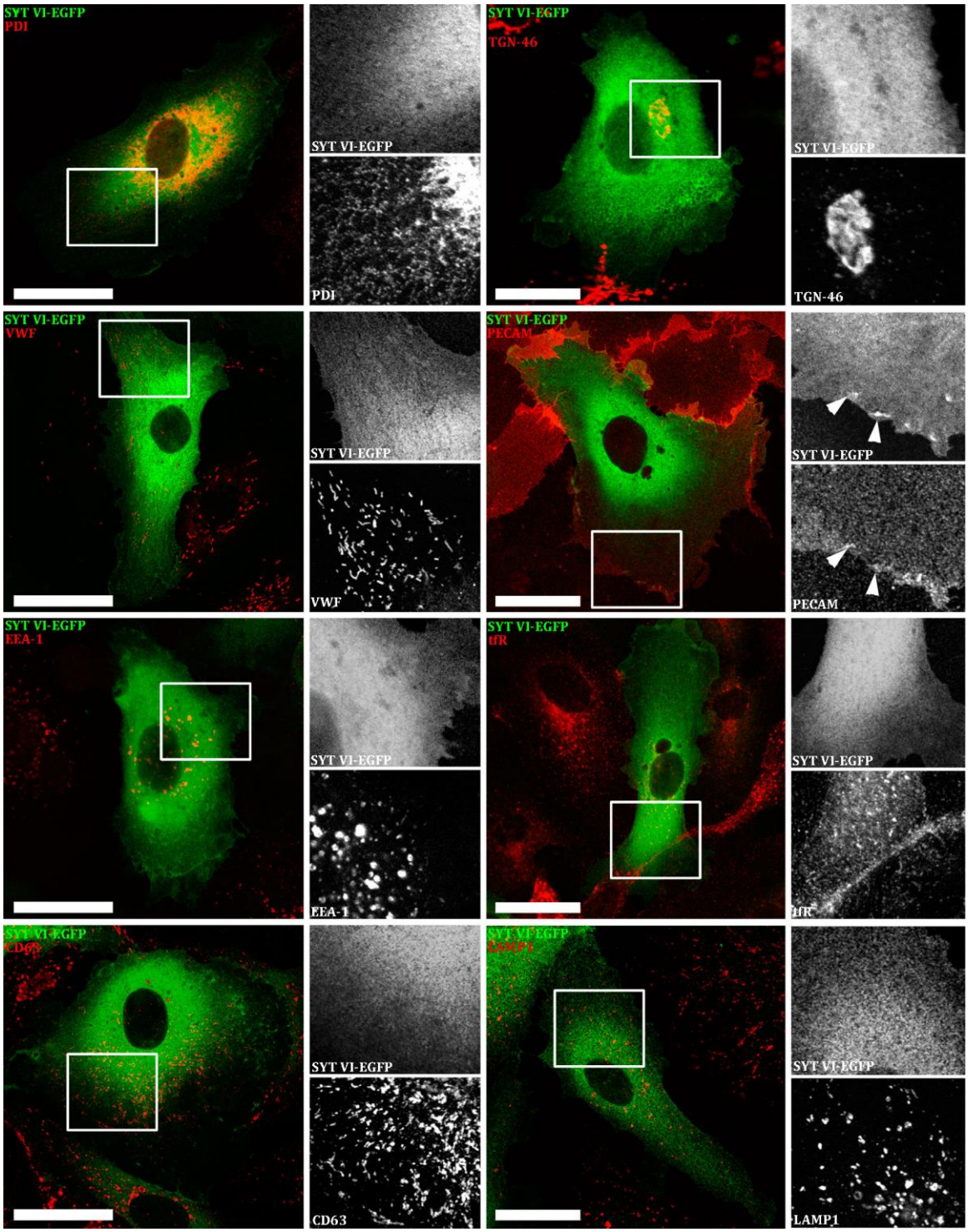

Figure 4.18. SYTVI-EGFP may be present on the plasma membrane but does not clearly co-localize with any other cellular compartment.

Images show HUVECs expressing SYTVI-EGFP (green) and counter-stained (red) with specific antibodies to PDI, TGN-46, VWF, PECAM, EEA-1, tfR, CD63 or LAMP1 as indicated. Arrows in the PECAM panel show the putative localization of SYTVI-EGFP to the plasma membrane. Scale bars are 20 μm.

Figure 4.19

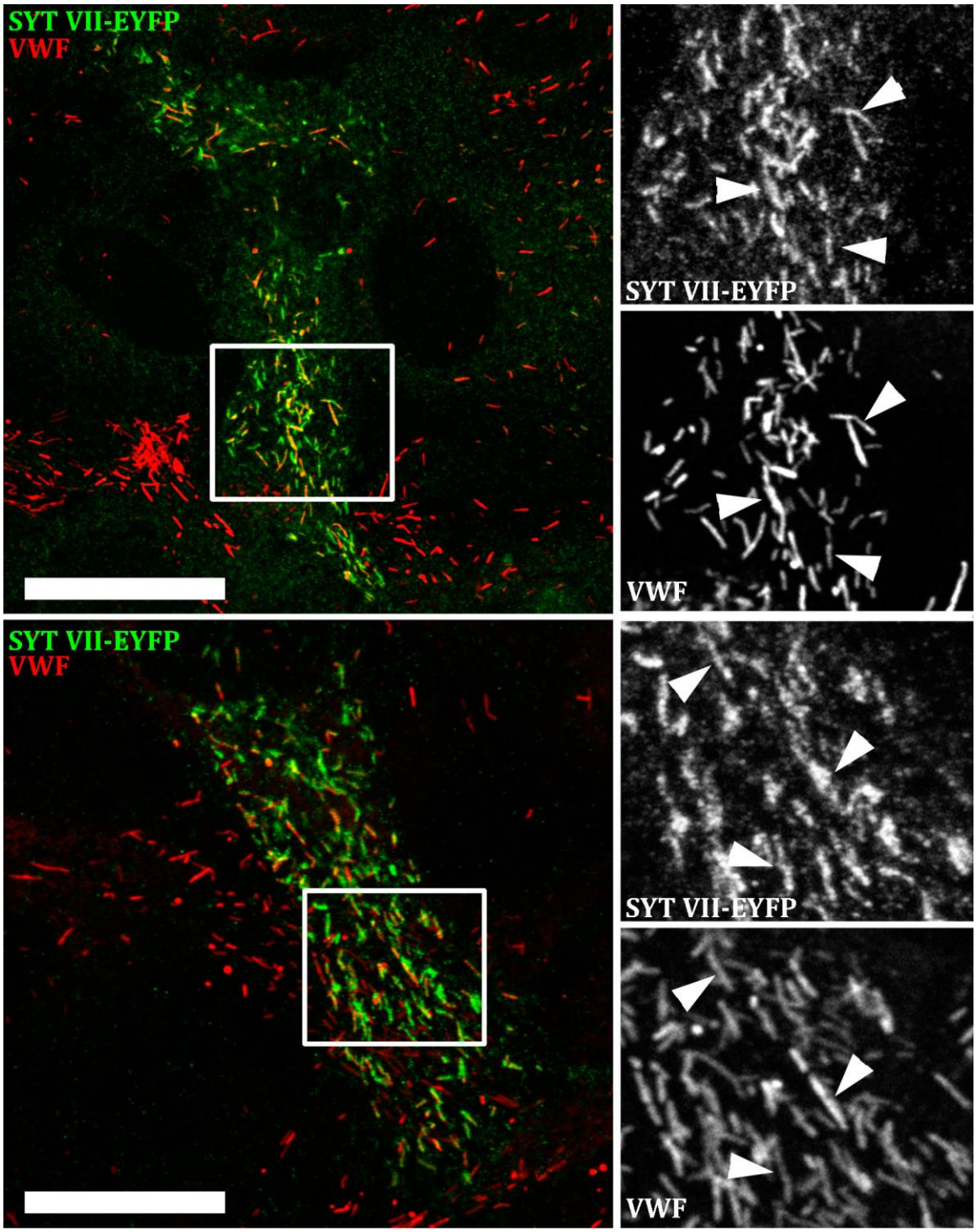

Figure 4.19. SYTVII-YFP is present on WPBs.

The figure shows two examples of HUVECs expressing SYTVII-YFP (green) and counter-stained with a specific antibody to VWF (red) 48 hours post-transfection. Arrows show the co-localization of SYTVII-YFP with endogenous VWF. Scale bars are 20 μm.

Figure 4.20A

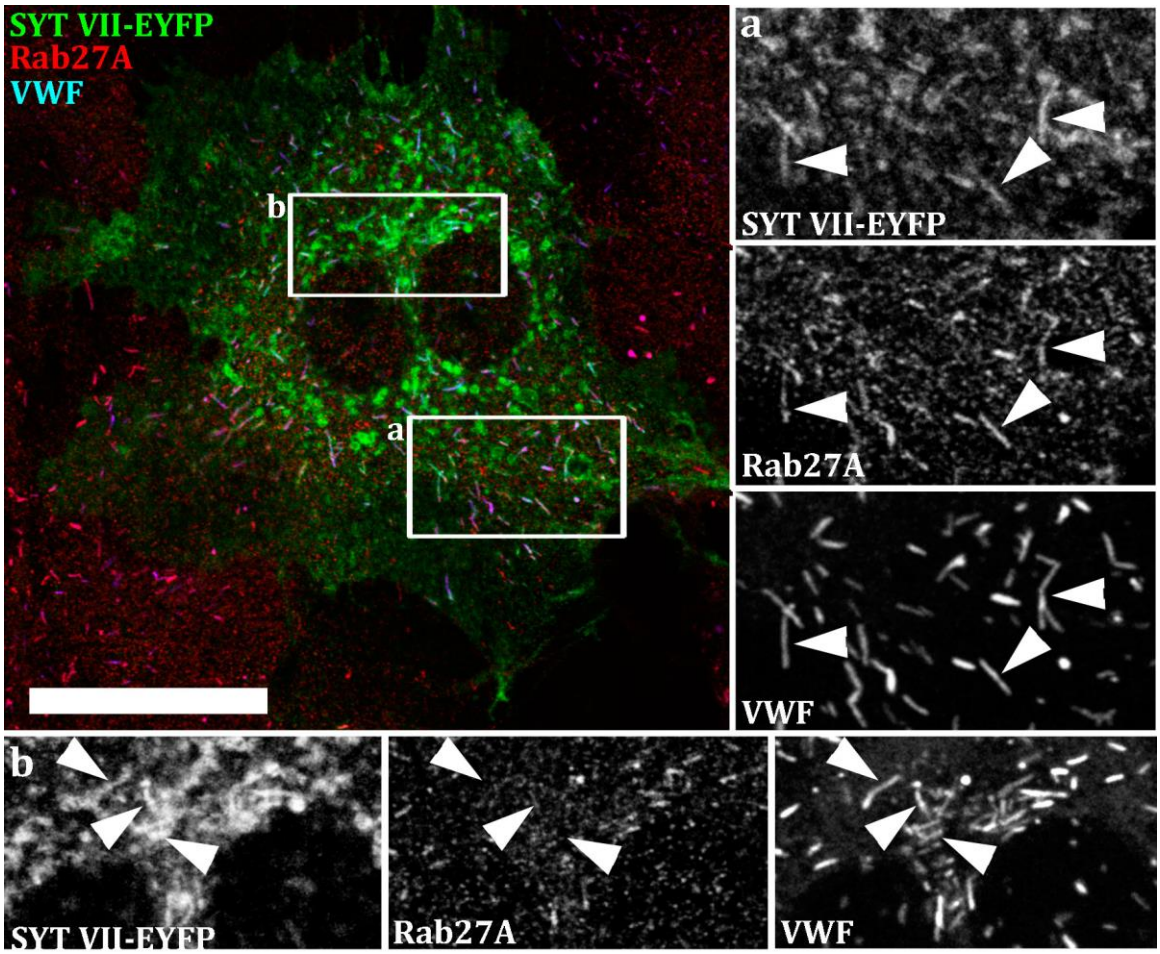

Figure 4.20A. SYTVII-YFP is present on both mature Rab27A-positive and immature Rab27A-negative WPBs.

The image shows HUVECs expressing SYTVII-YFP (green) and counter-stained with specific antibodies to endogenous Rab27A (red) and VWF (blue) 48 hours post-transfection Scale bar is 20 μm. The arrows in region (a) show SYTVII-YFP on mature Rab27A-positive WPBs while in region (b) SYTVII-YFP can be seen on immature Rab27A-negative WPBs emerging from the TGN region of the cell.

Figure 4.20B

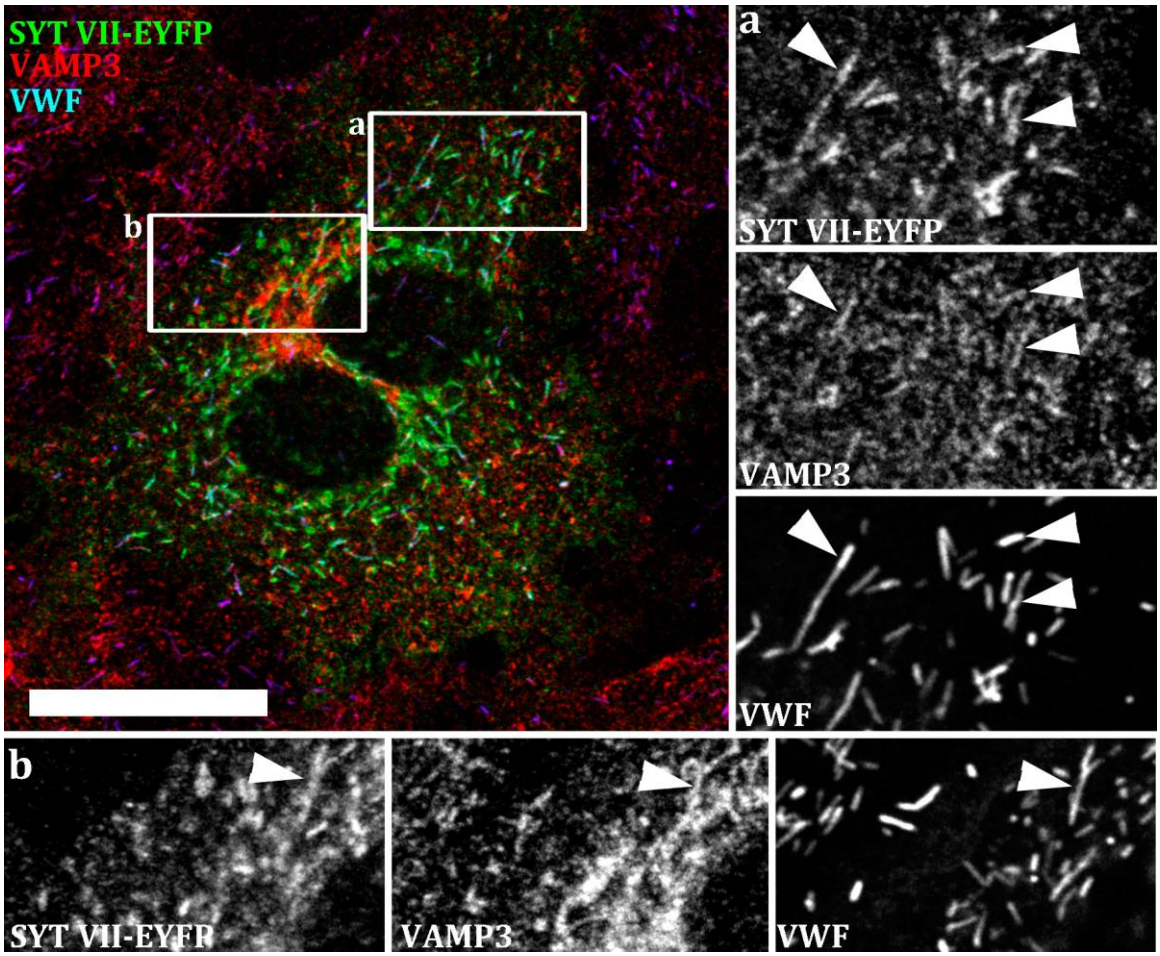

Figure 4.20B. SYTVII-YFP co-localizes with VAMP3-positive WPBs

HUVECs expressing SYTVII-YFP (green) were counter-stained with specific antibodies to endogenous VAMP3 (red) and VWF (blue) 48 hours post-transfection. Scale bar is 20 μm. Arrows in region (a) show SYTVII-YFP on VAMP3-positive WPBs. Arrows in region (b) show SYTVII-YFP on VAMP3-positive WPBs emerging from the TGN region of the cell.

Figure 4.21

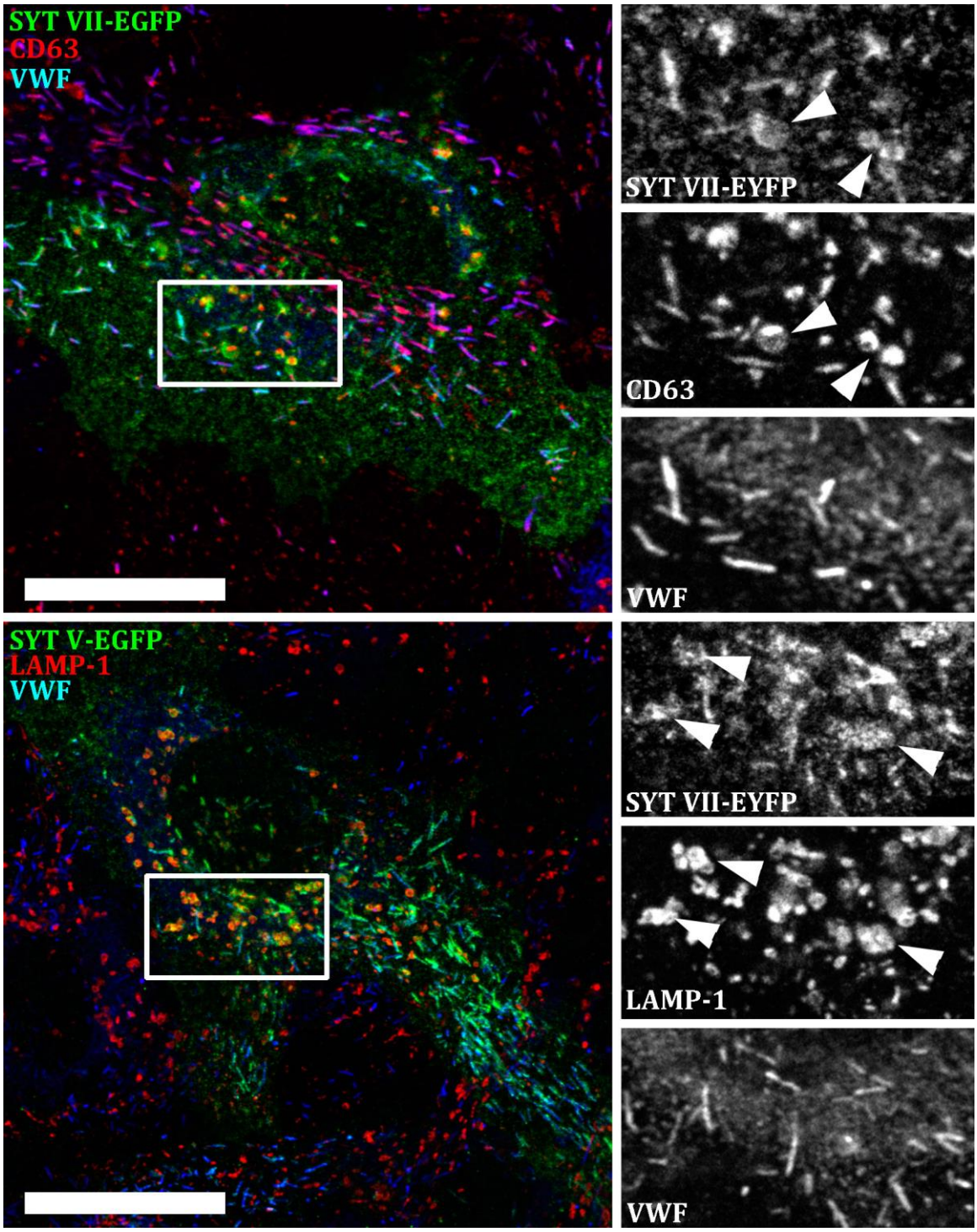

Figure 4.21. SYTVII-YFP co-localizes with CD63- and LAMP1-positive VWF-negative organelles.

HUVECs expressing SYTVII-YFP (green) were counter-stained (red) with specific antibodies to endogenous CD63 (top), LAMP1 (bottom) and VWF (blue) 48 hours post-transfection. Scale bar is 20 μm. Arrows show SYTVII-YFP on CD63- or LAMP1-positive organelles.

Figure 4.22

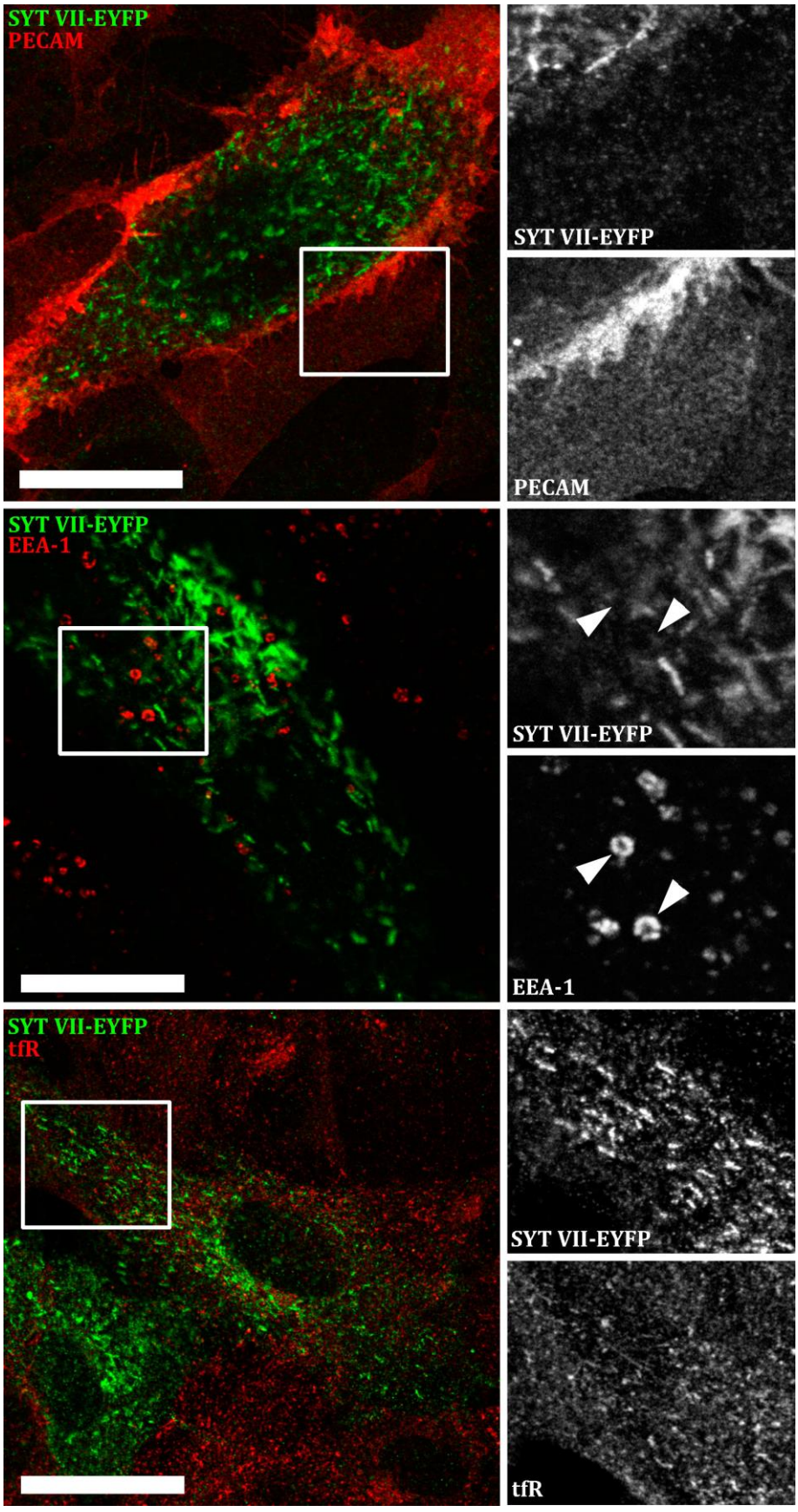

Figure 4.22. SYTVII-YFP does not co-localize with PECAM, EEA-1 or the tfR.
Image shows HUVECs expressing SYTVII-YFP (green) and counter-stained (red) with specific antibodies to endogenous PECAM (top), EEA-1 (middle) or tfR (bottom) 48 hours post-transfection. Scale bar is 20 μm.

Figure 4.23

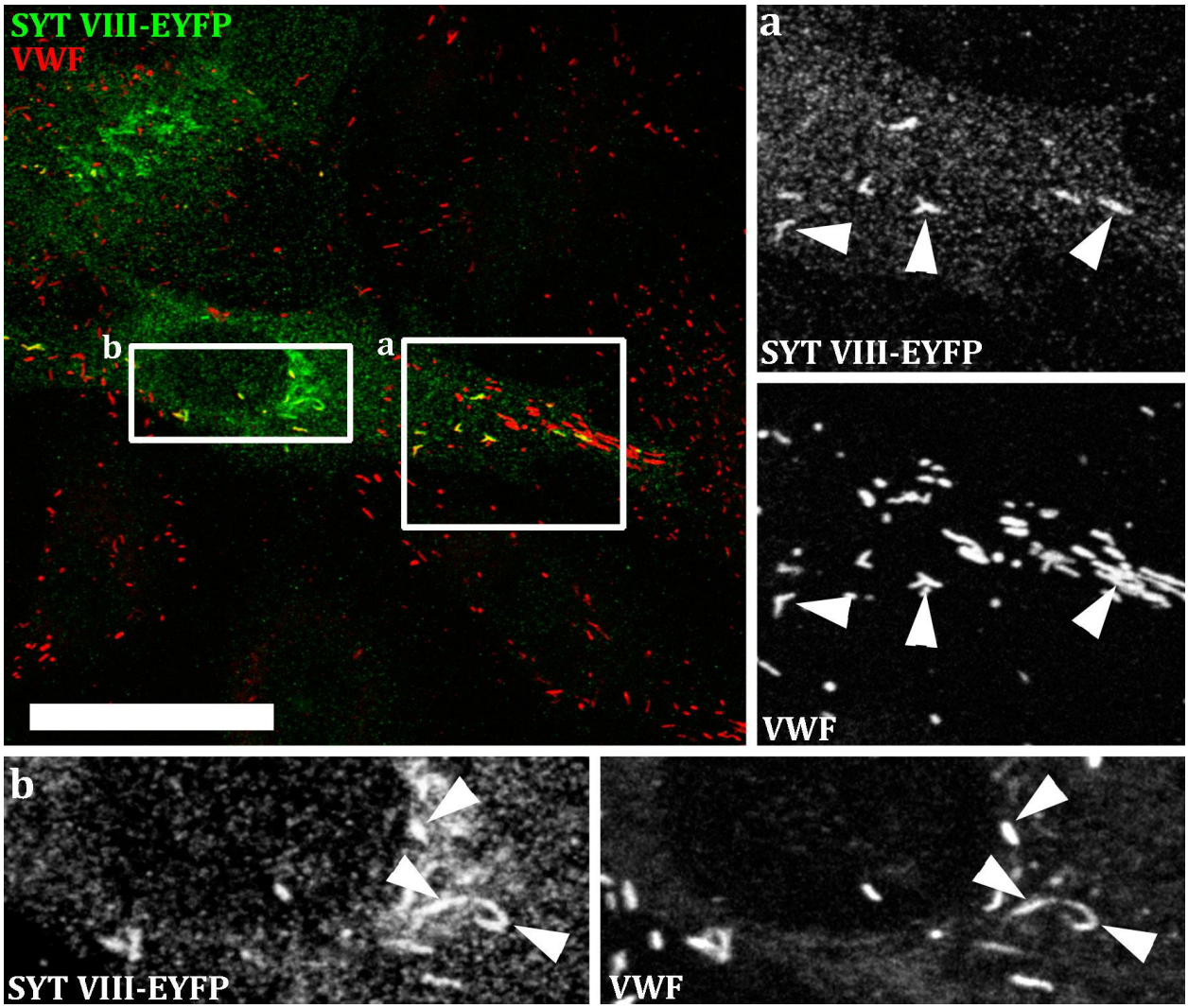

Figure 4.23. SYTVIII-EGFP co-localizes with VWF in WPBs.

HUVECs expressing SYTVIII-EGFP (green) were counter-stained with a specific antibody to endogenous VWF (red) 48 hours post-transfection. Scale bar is 20 μm. Arrows in (a) show the localization of SYTVIII-EGFP to the WPBs and in (b) show the presence of SYTVIII-EGFP on WPBs emerging from the TGN region of the cell.

Figure 4.24

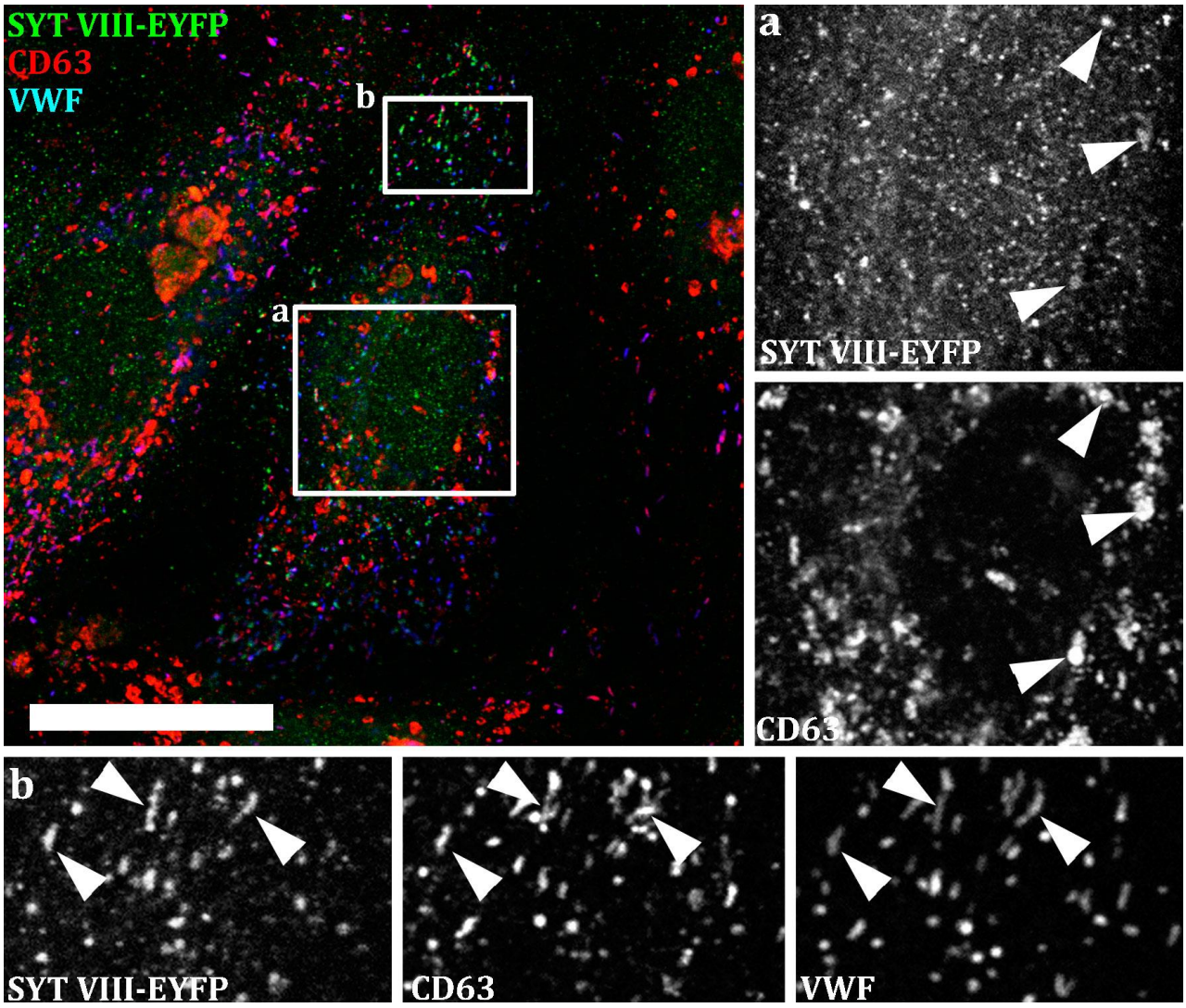

Figure 4.24. SYTVIII-EGFP is only weakly detected in some multivesicular bodies. HUVECs expressing SYTVIII-EGFP (green) were counter-stained with specific antibodies to endogenous CD63 (red) or VWF (blue) 48 hours post-transfection Arrows in region (a) indicate a weak co-localization of SYTVIII-EGFP with large CD63-positive (VWF-negative; not shown) organelles and in (b) co-localization with CD63-positive WPBs. Scale bar is 20 μm.

Figure 4.25

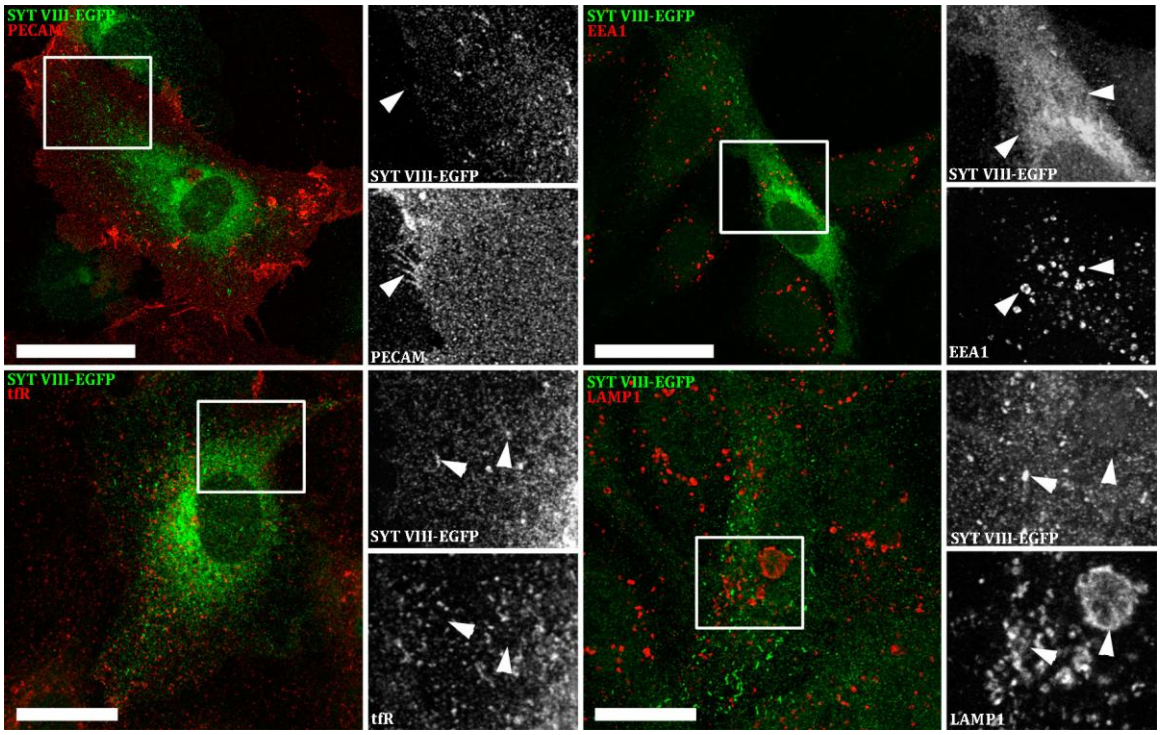

Figure 4.25. SYTVIII-EGFP was not detected on the plasma membrane, in the endosomal system or in the lysosomes.

HUVECs expressing SYTVIII-EGFP (green) were counter-stained (red) with specific antibodies to endogenous PECAM, EEA-1, tfR and LAMP1 48 hours post-transfection. Scale bars are 20 μm. The arrows indicate the absence of co-localization between the proteins.

Figure 4.26

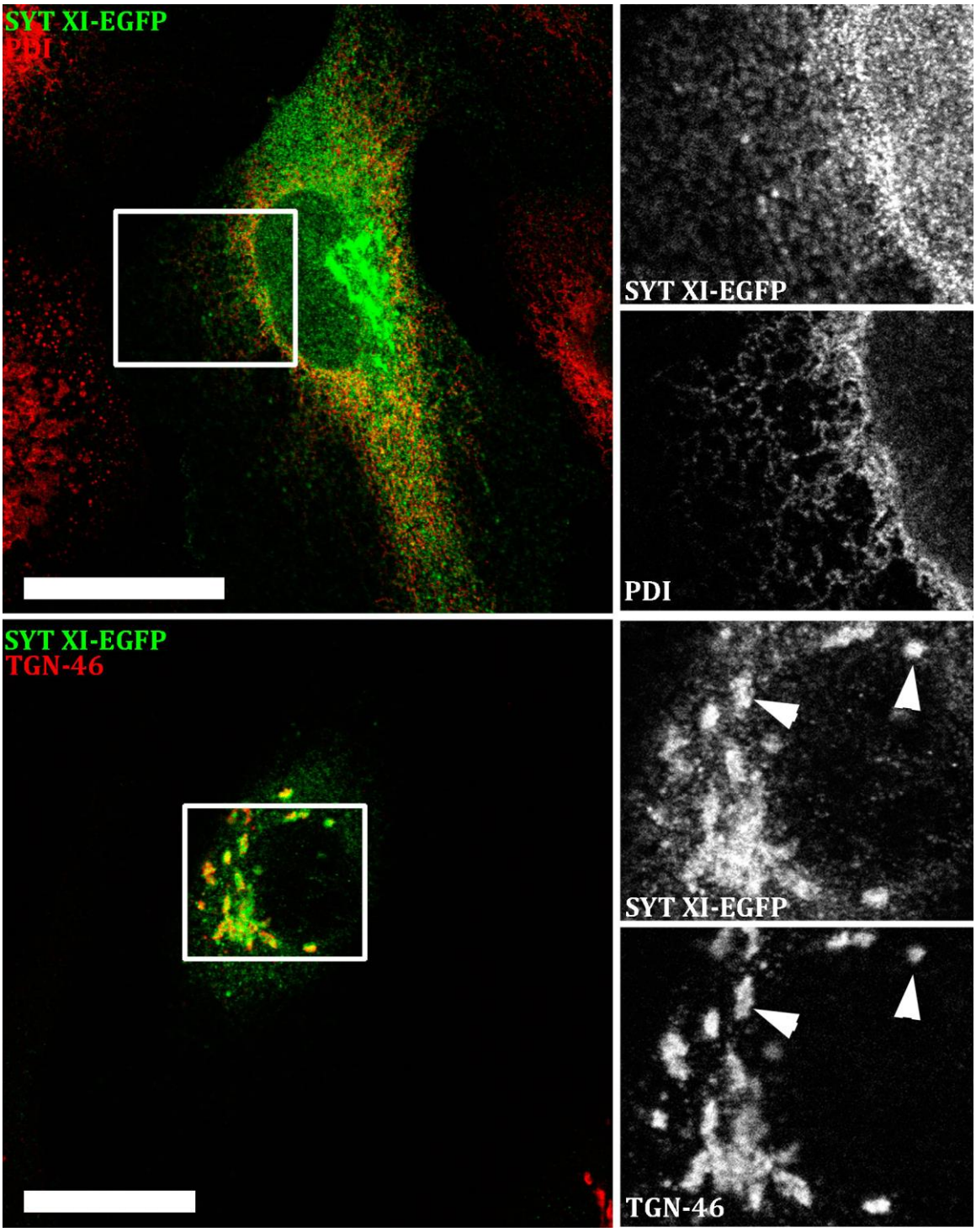

Figure 4.26. SYTXI-EGFP is present in the ER and TGN.

The images show HUVECs expressing SYTXI-EGFP (green) and counter-stained (red) with specific antibodies to endogenous PDI (top) and TGN-46 (bottom). Arrows show the localization of SYTXI-EGFP to the ER or TGN. Scale bars are 20 μm.

Figure 4.27

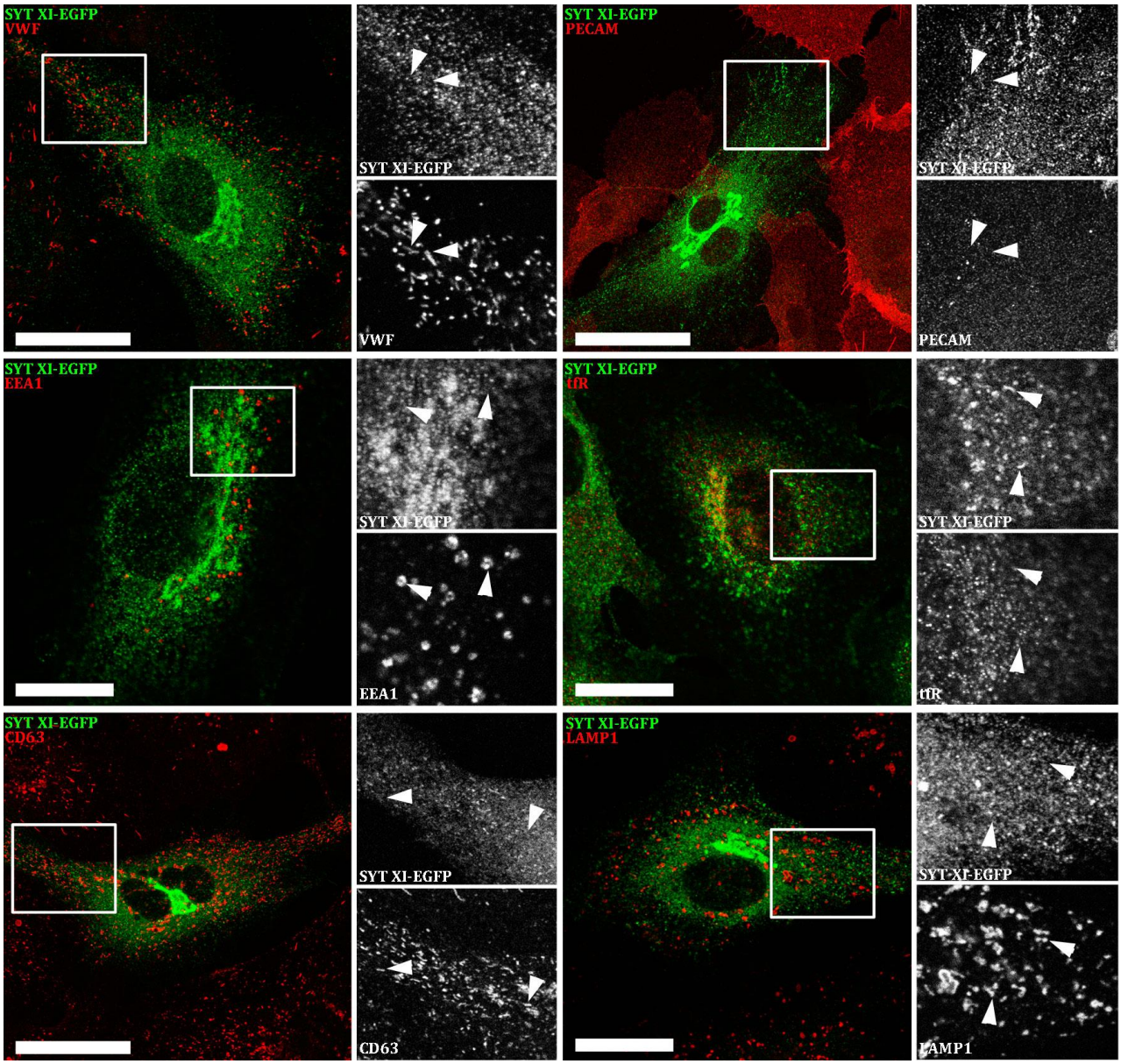

Figure 4.27. SYTXI-EGFP does not co-localize with markers of the WPBs, plasma membrane, early endosomes, recycling endosomes, multivesicular bodies or lysosomes. HUVECs expressing SYTXI-EGFP (green) were counter-stained (red) with specific antibodies to endogenous VWF, PECAM, EEA-1, tfR, CD63 or LAMP1 as indicated. Arrows show the lack of co-localization between SYTXI-EGFP and any of the organelle markers used. Scale bars are 20 μm.

4.2.8 SYT XVII:

SYT XVII is the most recently discovered member of the SYT family and thus far very little work has been done to determine its tissue distribution, subcellular localization, or function. To my knowledge, the data presented below is the first attempt to determine the subcellular localization of SYT XVII in any cell type.

SYTXVII-EGFP expression labeled a wide variety of subcellular structures, the most striking of which were the WPBs (Figure 4.28). Localization was also apparent in the TGN (Figure 4.29), the early and recycling endosomes (Figure 4.30), and the lysosomes and multivesicular bodies (Figure 4.31). Surprisingly, no clear evidence of co-localization between SYTXVII-EGFP and the plasma membrane was detected and there was no co-localization with PDI (Figure 4.32).

4.3 Conclusions and Discussion:

4.3.1 Conclusions:

The primary results of this subcellular localization screen examining the distribution of over-expressed fluorescent SYT constructs in HUVECs are summarized in Table 4.2 and shown in Figure 4.33. From this work, a series of candidates for the role of the Ca^{2+}-sensor mediating the exocytosis of WPBs from HUVECs has been identified and therefore the findings described in this chapter have determined the direction of my research.

I have shown that four members of the SYT family (SYTs V, VII, VIII, and XVII) are found localized to the WPBs following their over-expression in HUVECs. Logically these four proteins were identified as being strong candidates for the role of the calcium sensor regulating WPB exocytosis, and within this group two SYTs hold particular promise. First and foremost, SYT VII was shown to traffic to both WPBs and lysosomes and a large body of published literature has established that SYT VII plays a fundamental role in the regulation of the Ca^{2+}-mediated exocytosis of large secretory granules in other cell types (for review see Andrews and Chakrabarti, 2005). With this in mind, and considering the observed distribution of SYTVII-YFP in HUVECs, SYT VII was designated my primary candidate for the role of the calcium sensor regulating WPB exocytosis. Therefore my research initially focused on investigating the function of this member of the SYT family and this work is presented in the following chapter (Chapter 5).

Figure 4.28

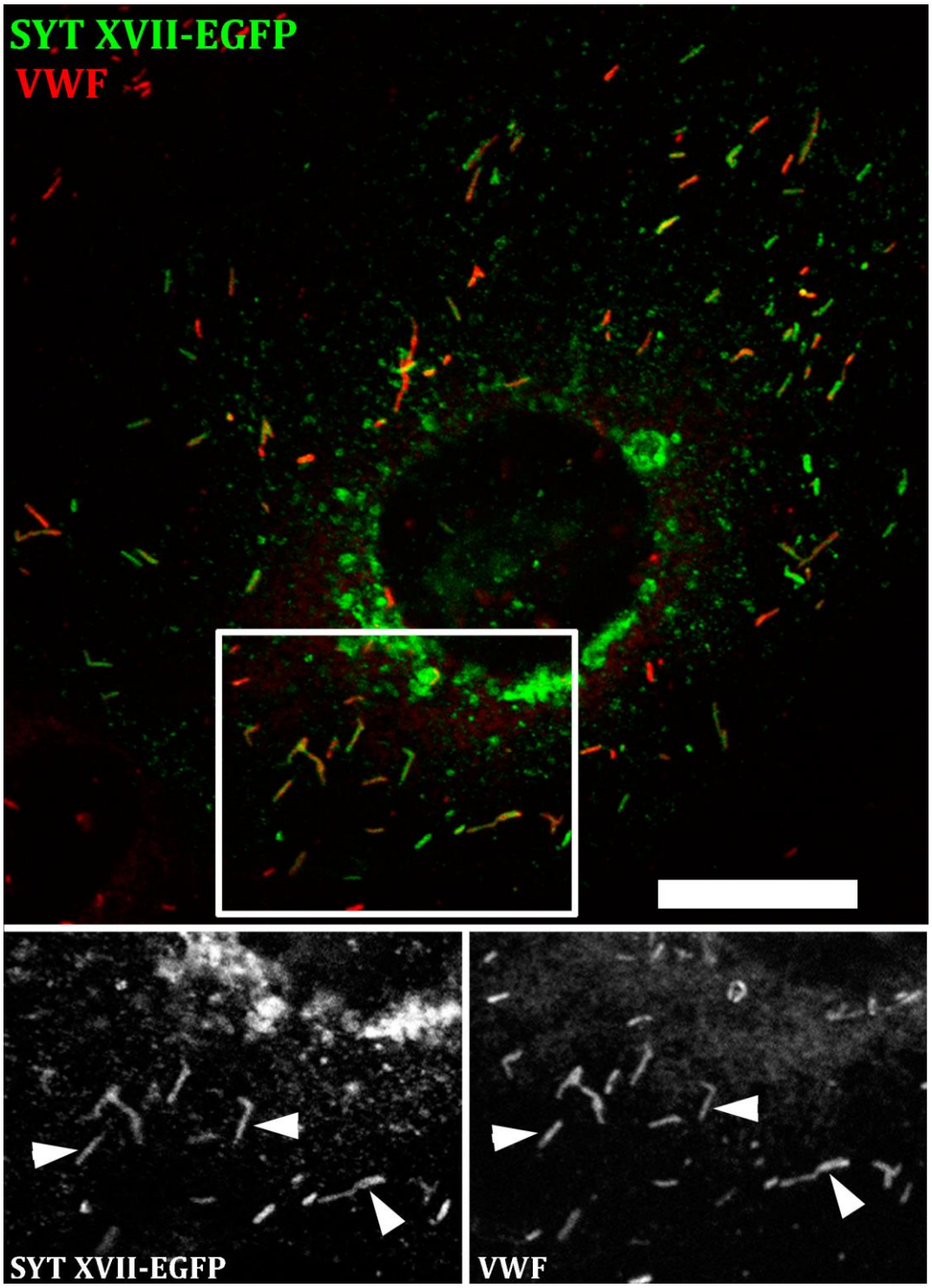

Figure 4.28. SYTXVII-EGFP localizes to the WPBs in HUVECs

The image shows a single HUVEC expressing SYTXVII-EGFP (green) and counter-stained with a specific antibody to endogenous VWF (red). Arrows show co-localization between SYTXVII-EGFP and WPBs. Scale bar is 5 μm.

Figure 4.29

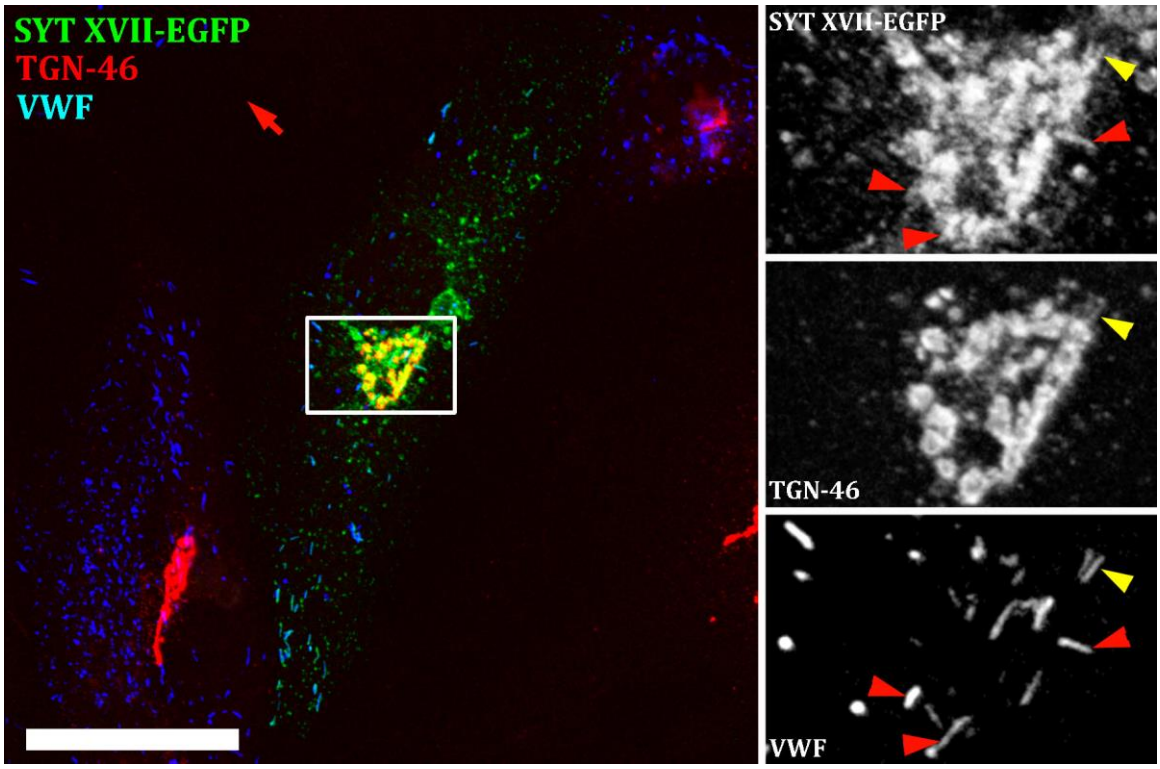

Figure 4.29 WPB localization of SYTXVII-EGFP

Image shows a single HUVEC expressing SYTXVII-EGFP (green) and counter-stained with specific antibodies to endogenous TGN-46 (red) and VWF (blue). Yellow arrow shows two TGN-46 positive WPBs which are emerging from the TGN and contain SYTXVII-EGFP. Red arrows show the localization of SYTXVII-EGFP with TGN-46-negative WPBs closely associated with the TGN region of the cell. Scale bar is 20μm.

Figure 4.30

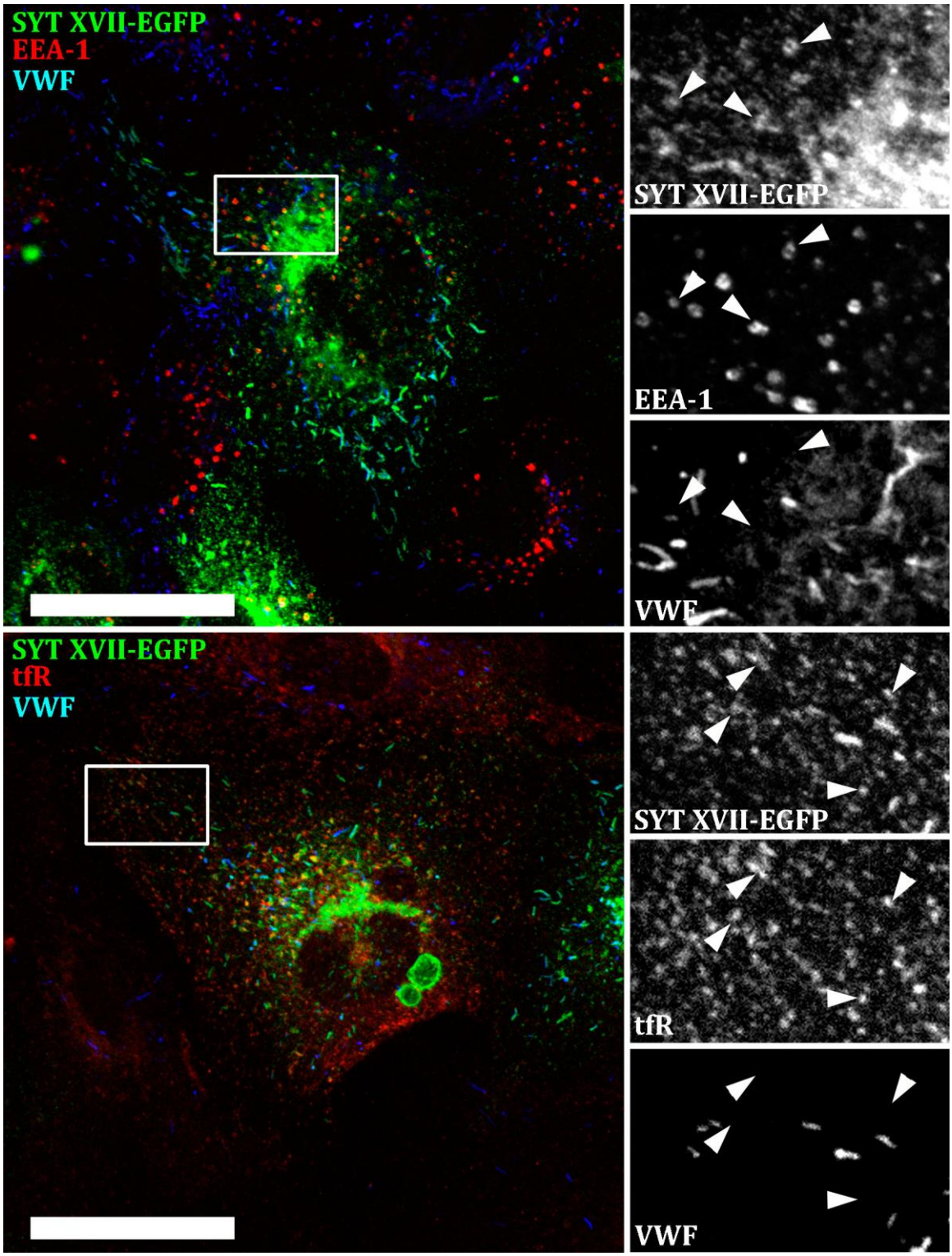

Figure 4.30. SYTXVII-EGFP co-localizes with markers of the endosomal system.

HUVECs expressing SYTXVII-EGFP (green) were counter-stained (red) with specific antibodies to endogenous EEA-1 (top) or tfR (bottom). Arrows show co-localization of SYTXVII-EGFP with the early and recycling endosomes. Scale bars are 20 μm.

Figure 4.31

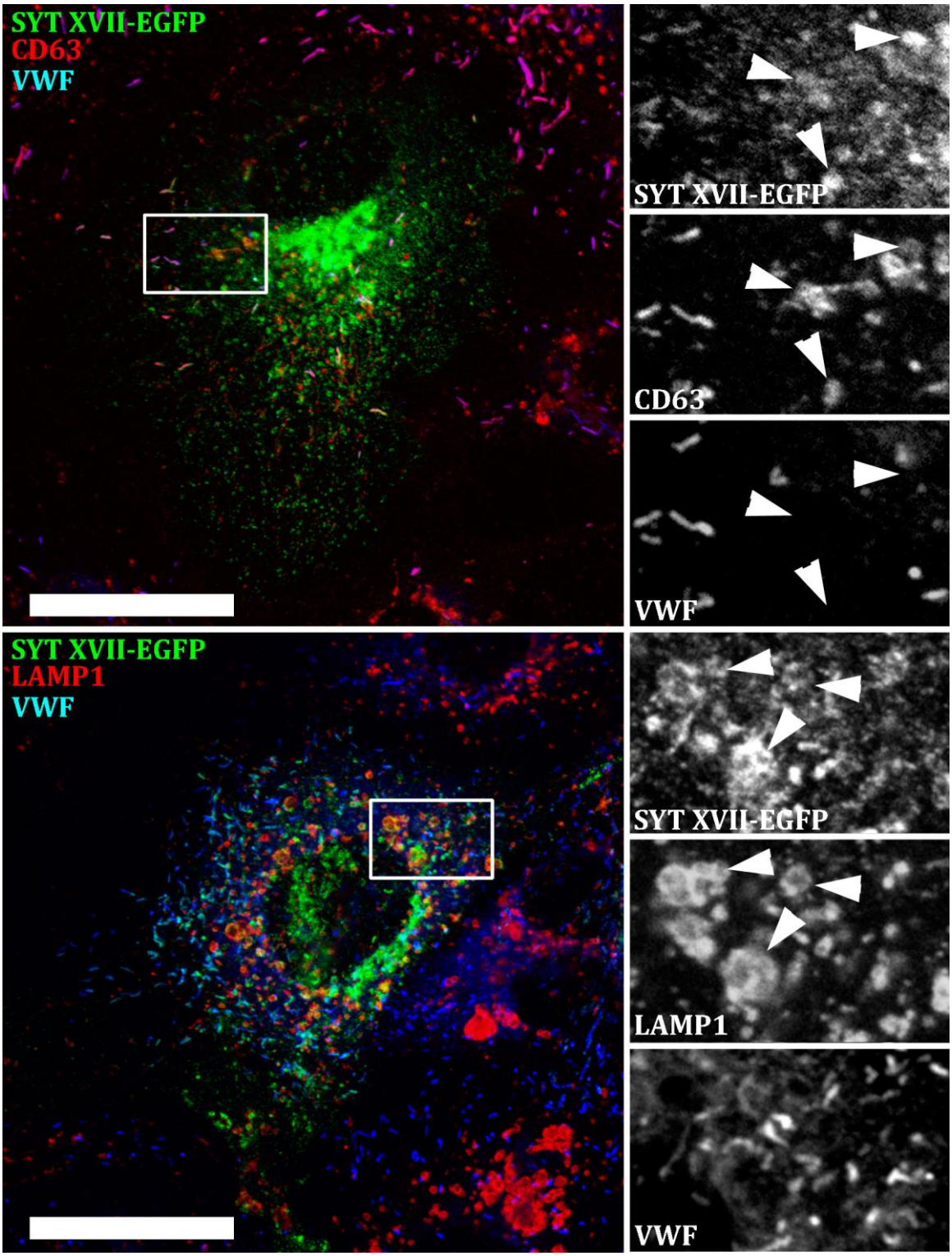

Figure 4.31. SYTXVII-EGFP co-localizes with markers of multivesicular bodies and lysosomes.

HUVECs expressing SYTXVII-EGFP (green) were counter-stained (red) with specific antibodies to endogenous CD63 (top) or LAMP1 (bottom). Arrows show the co-staining of SYTXVII-EGFP and multivesciular bodies or lysosomes. Scale bars are 20 μm.

Figure 4.32

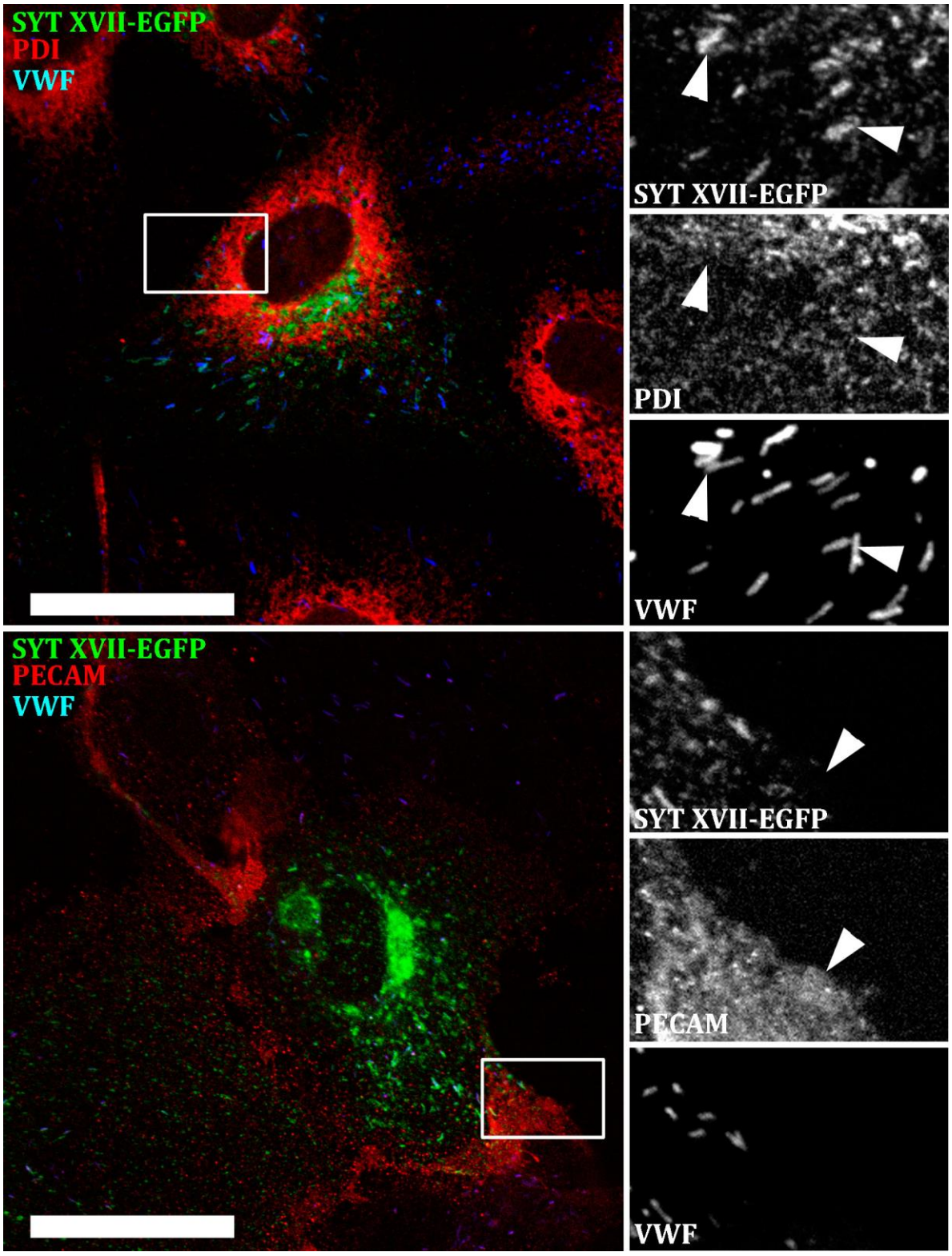

Figure 4.32. SYTXVII-EGFP is not detectable on the plasma membrane or in the ER

HUVECs expressing SYTXVII-EGFP (green) were counter-stained (red) with specific antibodies to PDI (top) or PECAM (bottom). The arrows show the lack of co-localization of SYTXVII-EGFP with PDI or PECAM. Scale bars are 20 μm.

A second Ca^{2+}-dependent SYT, SYT V, was shown to have a strong and almost-exclusive WPB distribution in HUVECs and so was identified as a promising candidate for the role of the WPB Ca^{2+}-sensor. There is currently little known regarding the function of the SYT V protein in other cell types and so unlike SYT VII no evidence is available in the literature suggesting that SYT V may be involved in mediating WPB exocytosis. However, SYT V is expressed in HUVECs and given its strong localization to WPBs following over-expression it is certainly possible that this protein is involved in the regulation of WPB exocytosis. Therefore extensive functional studies were performed with the aim to ascertain the function to SYT V in endothelial cells and these are presented in Chapter 6.

Two additional members of the SYT family (SYTs VIII and XVII) were shown to traffic to WPBs following their over-expression in HUVECs. These two proteins are Ca^{2+}-insensitive and so are not likely to be to be the primary regulators of Ca^{2+}-mediated WPB exocytosis. It is however entirely feasible that they may function as modulators of exocytosis and so were pursued as proteins of interest for the purposes of this investigation. Firstly, SYTVIII-EGFP traffics exclusively to WPBs in HUVECs although its distribution pattern forty-eight hours following transfection led me to believe that the protein is progressively removed from the organelles. Therefore it is possible that the observed localization of the construct to WPBs is an artifact of over-expression. Secondly, SYTXVII-EGFP traffics to the WPBs following its over-expression in HUVECs but is also found as a component of the lysosomes, endosomes, and Golgi network. Two possibilities explain this observation; either the trafficking of SYTXVII-EGFP to WPBs is not specific or this member of the SYT family plays a fundamental but as-yet unknown role in endothelial cell biology, hence its wide distribution. In any case, the initial experimental evidence suggesting that SYTs VIII and XVII are involved in WPB exocytosis is not as strong as for SYTs V and VII. However they cannot be excluded on this basis and so functional studies were pursued attempting to determine the role of these Ca^{2+}-insensitive proteins in HUVECs. This work is presented in Chapter 7.

Finally, four additional SYT family members (SYTs I, III, VI and XI) are found in HUVECs but do not localize to WPBs when over-expressed. Therefore these proteins are not located in a subcellular position where they could easily regulate the final stage of WPB exocytosis. However, it is entirely possible that they are involved in the biosynthesis, budding, maturation, or trafficking of WPBs. Therefore, more-limited functional studies were attempted aiming to determine the relationship between these SYTs and WPB biology. These results will be presented in Chapter 8.

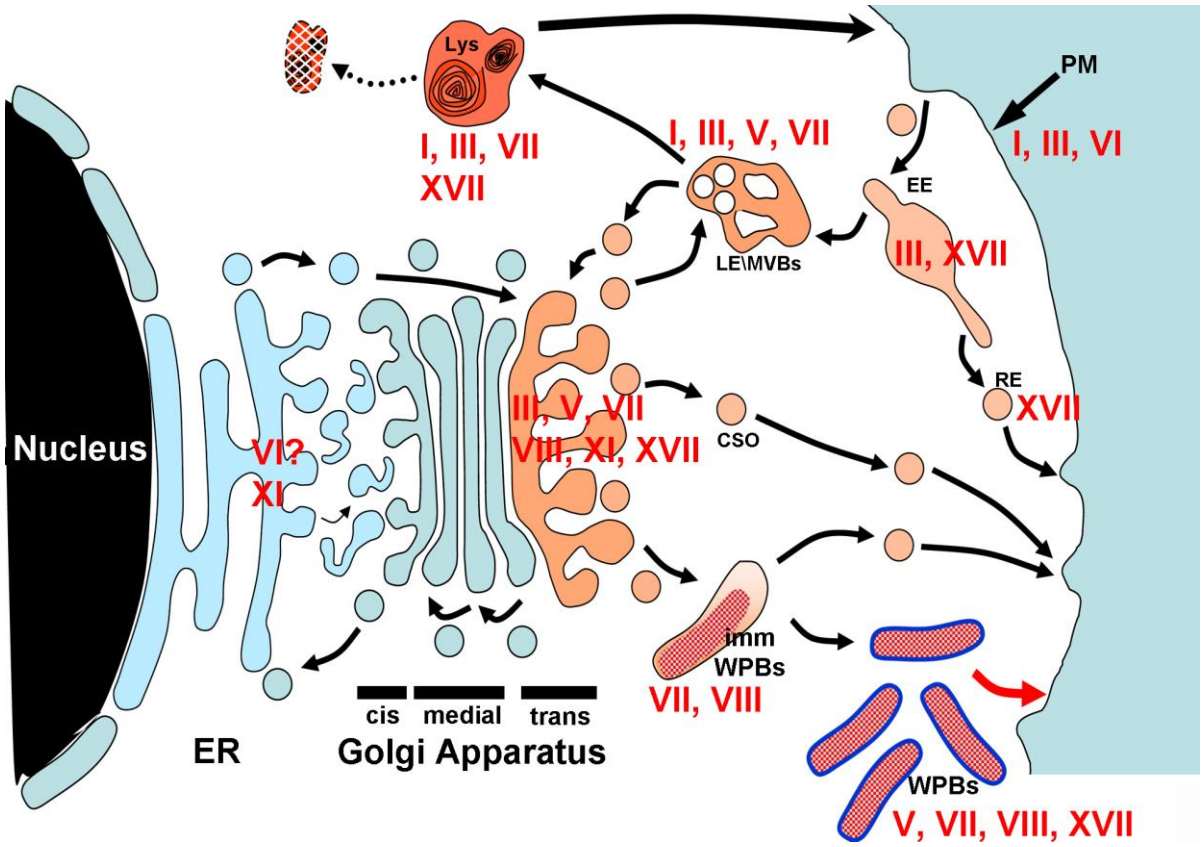

Figure 4.33. The SYTs show an extensive distribution pattern in HUVECs.

The image summarizes the distribution of fluorescent SYTs (**Red Text**) associated with the major subcellular compartments (Black Text) of the secretory pathway in endothelial cells.

SYT	Subcellular Localization
I	Plasma Membrane Lysosomes
III	Plasma Membrane / Early Endosomes / TGN
V	WPBs / TGN
VI	ER/ Plasma Membrane
VII	WPBs Lysosomes
VIII	WPBs / TGN
XI	TGN / ER
XVII	WPBs Lysosomes Endosomes TGN

Table 4.2. The SYTs show an extensive distribution pattern in HUVECs.

The subcellular localization of the endothelial-expressed SYTs is summarized.

4.3.2 Discussion:

4.3.2.1 SYT I:

SYT I is a component of synaptic vesicles in neurons (Matthew *et al.* 1981) and LDCVs in PC12 cells (Lynch and Martin, 2007), pancreatic acinar cells (Falkowski *et al.* 2011), and mast cells (Baram *et al.* 2001). Here, the probable distribution of endogenous SYT I in HUVECs has been determined by the over-expression of SYTI-mCherry which was shown to localize to the plasma membrane and lysosomes at both twenty-four and forty-eight hours following transfection. Interestingly, the reported localization of the construct to the plasma membrane was considerably stronger at earlier time-points suggesting that SYT I may have a short half-life in HUVECs leading to its rapid internalization and degradation. Alternatively, this observation may simply be an expression property of the construct and therefore not biologically relevant. This distribution of SYT I in HUVECs suggests that it may play role in the regulation of WPB exocytosis as SYTs found on opposing membrane are able to form oligomers when in close apposition and thus function cooperatively to regulate fusion events (Sugita *et al.* 2001).

4.3.2.2 SYT III:

This work has shown that the SYT III protein is largely absent from the WPBs, lysosomes, multivesicular bodies, and the endoplasmic reticulum in HUVECs. However, interestingly SYTIII-EGFP was shown to localize strongly to EEA1-positive early endosomes and was also detected at low levels on the plasma membrane. This is in keeping with published observations showing that SYT III is found endogenously on rab11-positive perinuclear endocytic recycling endosomes in RBL-2H3 cells (Grimberg *et al*. 2002). Here, SYT III was shown to be essential for the *de novo* formation of recycling endosomes at the plasma membrane. Therefore it is highly likely that SYT III is involved in regulating the formation of early endosomes in endothelial cells and indeed it would be of interest to determine if it can be found co-localized with rab11 in HUVECs. In contrast to published observations (Falkowski *et al.* 2011, Masztalerz *et al.* 2006), SYT III was not found to co-localize with LAMP1 in HUVECs. However, following the transfection of HEK cells with SYTIII-EGFP the construct was seen to traffic to LAMP1-positive structures (data not

shown), indicating that its absence in these organelles in HUVECs is likely to be a specific feature of its over-expression in this cell type.

4.3.2.3 SYT V:

There is currently little known regarding the subcellular distribution of SYT V although it has been reported to be a component of secretory granules in pancreatic α-cells (Iezzi *et al.* 2004) and LDCVs in PC12 cells (Saegusa *et al.* 2002). Here, I have shown that SYT V traffics strongly to WPBs when over-expressed in HUVECs and therefore this member of the SYT family is in an ideal subcellular position to regulate the exocytosis of WPBs. Additionally, a proportion of the construct was observed on the plasma membrane and in the Golgi body. It is possible that following the basal release of WPBs from HUVECs the SYT V protein is trafficked from the plasma membrane to the Golgi body via the recycling pathway where it is loaded onto forming granules. A time-course experiment examining the trafficking of the SYT V protein following stimulation would be necessary to verify this hypothesis. Additionally, it is known that in other cell types the localization of the SYT V protein varies depending on the stimulation state of the cell (Vinet *et al*. 2008). It would be of interest to determine if the observed distribution of SYTV-EGFP is altered following HUVEC stimulation with ionomycin or histamine.

4.3.2.4 SYT VI:

The typical subcellular localization of endogenous SYT VI is currently unclear as the majority of investigators use over-expressed protein to determine its distribution in their cells of interest (Dean *et al.* 2012, Saegusa *et al*. 2002, Fukuda and Mikoshiba, 1999). Here, the over-expression of the SYTVI-EGFP protein in HUVECs suggests the construct localizes predominantly to the plasma membrane and the ER. This is in contrast to my previous observation that endogenous SYT VI is found as a component of the early endosomes (see Chapter 3). However, it should be noted that the template DNA used to construct the SYTVI-EGFP vector was derived from a single image clone of SYT VI and so would only represent one variant of the protein. It is possible that this variant shows a more restricted distribution than has been observed for the endogenous protein(s). Indeed, it is known that different variants of the SYT VI protein show unique localization patterns following their over-expression as full-length SYT VI is trafficked to the ER and Golgi when over-expressed in

PC12 and COS cells whereas a transmembrane-lacking variant is found within the cytosol and as a component of internal membranes (Fukuda and Mikoshiba, 1999). Interestingly, within HEK cells over-expressed SYTVI-EGFP also localizes to the ER and is excluded from other structures (data not shown). Therefore, the subcellular localization of SYT VI in HUVECs is currently debatable although no evidence has been provided to suggest that the protein is found within WPBs. Therefore, SYT VI is not located in a subcellular position which would allow its regulation of WPB fusion with the plasma membrane.

4.3.2.5 SYT VII:

The ubiquitously-expressed protein SYT VII appears to have a fundamental role in the exocytosis of large secretory granules and has been found as a component of lysosomes in fibroblasts (Martinez *et al.* 2000), phagosomes in macrophages (Czibener *et al*. 2006), LDCVs in T-cells (Fowler *et al.* 2007), and insulin- and glucagon-containing granules in pancreatic cells (Gao *et al.* 2000, Gustavsson *et al.* 2009). Here, I have shown that SYTVII-YFP co-localizes with both VWF and VAMP3 on WPBs and with LAMP1 on lysosomes. In HUVECs which express the construct, SYTVII-YFP traffics to virtually every granule. However closer inspection reveals that it localizes most strongly to the tips of many WPBs and in some cases is also seen concentrated at regular intervals along their length. It is tempting to speculate that these regions may represent potential sites of compound fusion events between individual granules, or possibly may distinguish sites of fusion between WPBs and other cellular structures such as lysosomes and multivesicular bodies. Hence, SYT VII may play a specific role in mediating intracellular fusion events between WPBs and other organelles.

SYTVII-YFP was detected on both mature (Rab27a-positive) and immature (Rab27a-negative) granules, demonstrating that it is likely to be loaded onto WPBs as they form at the TGN rather than being recruited from other subcellular structures following granule budding. The construct could not be detected in the Golgi body, ER, endosomal system, or as a component of the plasma membrane. Therefore, the specific trafficking of SYTVII-YFP to WPBs has implicated this member of the SYT family in the regulation of WPB exocytosis, a proposition which is supported by the current literature. Interestingly, the tetraspanin CD63 is found as component of the WPB membrane (Vischer and Wagner, 1992) and this protein has been reported to bind to and traffic SYT VII to lysosomes in fibroblasts via a palmitoylation-dependent interaction (Flannery *et al.* 2010). It is conceivable that a similar mechanism

occurs in HUVECs whereby CD63 is responsible for the delivery of SYT VII to WPBs and lysosomes. In the future it would be of interest to test this by eliminating the CD63 protein and determining the effect on the subcellular distribution of SYT VII. Equally co-immunoprecipitation experiments may demonstrate a physical interaction between CD63 and SYT VII as well as identifying other binding partners of SYT VII in HUVECs.

4.3.2.6 SYT VIII:

The subcellular distribution of endogenous SYT VIII in other cell types is currently unknown with the exception that it is found in the acrosomal crescent of murine sperm cells (Hutt *et al.* 2002). Here, I have shown that SYTVIII-EGFP is trafficked exclusively to the WPBs and TGN and is excluded from the lysosomes, the plasma membrane, the ER, and the endosomal system. However, at forty-eight hours following transfection only a small proportion of HUVECs were seen to be expressing the construct and within this population of cells only a minority of WPBs were positive for SYTVIII-EGFP. In contrast, at twenty-four hours the construct is expressed by a greater proportion of HUVECs and shows a more extensive WPB distribution. These discrepancies may simply be the result of an expression property of the construct or they may represent the progressive removal of SYTVIII-EGFP from WPBs. This would suggest that either SYTVIII-EGFP enters WPBs as a result of a default pathway or its presence in the organelles is due to inefficient exclusion at the level of the Golgi. However, the lack of trafficking of the construct to other organelles argues against this theory. An additional consideration is that the SYTVIII-EGFP construct, having been derived from an image clone, represents only one isoform of the SYT VIII protein. It is known that different variants of SYT VIII show unique localization patterns (Monterrat *et al.* 2006) and so it would be of interest to produce fusion constructs of the endothelial-specific SYT VIII isoforms from pools of HUVEC cDNA to determine their precise subcellular distributions. Unfortunately my attempts to do this were unsuccessful but it would be a useful avenue for future research.

4.3.2.7 SYT XI:

I have shown that SYTXI-EGFP consistently localizes to the Golgi body in HUVECs. This is in-keeping with the published finding that SYTXI-EGFP localizes to the Golgi body in PC12 cells (Fukuda and Mikoshiba, 2001). As two unrelated SYTXI-GFP constructs have

been shown to localize to the Golgi body in different cell types it is likely that the endogenous SYT XI protein is indeed found within this compartment. However, it is also possible that the observed distribution of SYT XI is the result of uncontrolled aggregation of the over-expressed protein in the TGN. Equally, it is possible that SYT XI lacks a binding partner in PC12 and endothelial cells which it requires for transport out of the Golgi. However, as the SYT mRNA expression screen has demonstrated that SYT XI mRNA is expressed endogenously in HUVECs this option seems unlikely.

4.3.2.8 SYT XVII:

I have shown that SYTXVII-EGFP has a broad distribution pattern in our model endothelial cells, localizing to the WPBs, lysosomes, early endosomes, recycling endosomes, and the Golgi body. Indeed, the only structures which stain negatively for the over-expressed protein are the ER and the plasma membrane. This extensive distribution suggests that either the construct is trafficked non-specifically to a number of organelles in HUVECs and therefore these observations are an artefact of over-expression or that SYT XVII does in fact play a fundamental role in endothelial cell biology. Only one other study has attempted to determine the distribution of SYT XVII using a fluorescent construct over-expressed in hippocampal neurons and these results were inconclusive (Dean *et al.* 2012). Therefore given the lack of any available literature concerning the distribution of SYT XVII in other cell types it is impossible at this point to comment further on my findings.

Chapter 5
Investigating the Function of SYT VII in HUVECs

5.1 Background Information:

5.1.1 The Regulation of Expression of the SYT VII Gene:

The rat cDNA sequence for SYT VII was first determined in 1995 (Li *et al.* 1995). The human equivalent of the rat SYT VII gene was localized to chromosome 11q13 in 1998 as a result of an attempt to identify candidate genes responsible for the degenerative eye disease Best vitelliform macular dystrophy (Cooper *et al.* 1998). Initial attempts to characterize the tissue distribution of this novel transcript by Northern blotting revealed that SYT VII mRNA is found extensively in adult and foetal tissue, with particularly high levels reported in the brain, liver, heart, and thymus (Cooper *et al.* 1998). SYT VII is now known to be ubiquitously expressed with its mRNA found in the rodent cerebrum, cerebellum, olfactory bulb, intestine, kidney, pancreas, heart, lung, and spleen (Li *et al*. 1995, Han *et al.* 2004).

The signalling pathways which regulate the expression of the SYT VII gene have been partially elucidated in recent years, and indeed SYT VII mRNA levels are known to fluctuate in patients suffering from certain medical conditions. For example, in pancreatic islets derived from patients suffering from type II diabetes SYT VII mRNA levels are decreased (Andersson *et al.* 2012). Additionally, it is likely that SYT VII mRNA levels fluctuate during pregnancy as they have been reported to increase in developing mouse follicles following exposure to pregnant mare serum gonadotropin (PMSG) (Choi *et al.* 2012).

It has become clear in recent years that the expression of the SYT VII gene is heavily influenced by the dopaminergic signalling pathway. As a consequence SYT VII mRNA levels become dysregulated following the onset of Parkinson's disease and as a result of chronic drug use. In the caudoputamen and the striatum, acute cocaine administration results in the activation of extracellular signal-regulated kinase (ERK), which leads to the expression of the immediate early gene *c-fos* and ultimately to alterations in the level of SYT VII mRNA (Zhang *et al.* 2004, Zhang and Zu, 2006). The expression of the SYT VII gene is activated by the dopamine D1 receptor via the stimulation of adenylyl cyclases and repressed by the D3

receptor via the inhibition of adenylyl cyclases. Interestingly, the SYT VII promoter contains cAMP-response element binding (CREB) protein- and AP-1 transcription complex-binding consensus sequences, indicating that the expression of SYT VII is likely to be mediated by either the CREB or AP-1 transcription complexes following cocaine administration.

As a consequence of its regulation by the dopaminergic pathway, evidence has been provided suggesting that SYT VII may play a role in the pathogenesis of Parkinson's disease (PD). Rats treated with 6-hydroxydopamine to deplete their striatal dopamine levels show an almost complete loss of SYT VII mRNA and this can be reversed following treatment with either L-dopa or with the D1 agonist SKF82958 (Glavan and Zivin, 2005). Additionally, the treatment of hemiparkinsonian rats with L-dopa increases the expression of SYT VII mRNA, suggesting that the use of L-dopa as a therapeutic for PD may lead to elevated levels of SYT VII mRNA in the striatum. This may partly explain the neurological abnormalities which result from chronic L-dopa administration (Glavan, 2008).

5.1.2 The Splice Variants of SYT VII:

At least three isoforms of SYT VII have been reported to exist in human, mouse, and rat tissue, and these variants are designated SYTVII-α ,β, and γ (Fukuda *et al.* 2002). SYTVII-α is the major isoform, appearing as a 65-kDa protein on Western blots, and is found expressed predominantly in non-neuronal tissues. SYTVII-β and SYTVII-γ are minor isoforms and are primarily expressed in neuronal tissue. These two variants contain inserts of 44 and 116 amino acids respectively in the spacer domain between the transmembrane region and the C2 domains. The three isoforms are present in a ratio of 77:20:3 (α:β:γ) in the mouse brain, and therefore SYT VII-γ is relatively uncommon. Indeed, it is rarely detected in tissues outside the brain. In PC12 cells, SYTVII-α was reported to co-stain with TGN-38 in the perinuclear region and was also seen to reside on endosomes and on dense-core vesicles in the tips of neuritis (Fukuda *et al.* 2002).

A subsequent study has reported the presence of an additional SYT VII isoform, SYTVII-δ, in pancreatic β-cells and INS-1E cells (Gauthier *et al*. 2008). This novel isoform is composed only of exons 1 to 5 of the SYT VII gene and therefore lacks the C2 domains necessary for calcium binding. SYTVII-α and -β are also expressed in the pancreas, with the ratio of expression being 11:3.8:0.5 (α:β:δ). However, SYTVII-δ was not detected by Western blotting and indeed it is possible that this minor isoform is not translated into a stable protein. When SYTVII-α is over-expressed in INS-1E cells it is trafficked to the

plasma membrane and results in decreased insulin content of the LDCVs (Gauthier *et al*. 2008). In contrast, capacitance studies revealed that the over-expression of SYTVII-β has no effect on insulin secretion. Following the transfection of INS-1E cells with siRNA against the various isoforms, it was shown that the loss of SYTVII-α results in a decrease in insulin secretion whereas the knock-down of SYTVII-β results in a slight increase in secretion (Gauthier *et al*. 2008). It is possible that SYTVII-β functions as an antagonist of SYTVII-α, and therefore the ratio of expression of the various isoforms in a cell may modulate the observed overall function of SYT VII. It is important to bear in mind that the precise number of SYT VII isoforms has yet to be determined fully, and indeed it is known that rostral brain regions express up to six different SYT VII variants (Sugita *et al*. 2001, Han *et al*. 2004).

5.1.3 The SYT VII Protein: Structure, Calcium Sensitivity, Oligomerization and Internalization:

Structurally, the C2B domain of SYT VII is remarkably similar to that of SYT I, with both domains showing 48 % sequence identity. However, a prominent difference is that the SYT VII C2B domain binds three Ca^{2+} ions whereas the SYT I C2B domain binds two Ca^{2+} ions (Xue *et al.* 2010). These three calcium-binding sites are formed by loops 1-3 of the SYT VII C2B domain and the bound ions are coordinated by five aspartate residues, one serine residue, and three backbone carbonyl groups. The SYT I C2B domain lacks this crucial serine residue and hence only binds two Ca^{2+} ions. Additional differences in the SYT VII C2B domain are that only one of two prominent α-helices present in the SYT I C2B domain (the HA helix) is seen in the SYT VII protein. These relatively subtle structural differences between the two SYTs lead to dramatic functional consequences. The C2 domains are not only essential for determining the overall function of the SYT VII protein but are also crucial for ensuring its stability. If both C2 domains of SYT VII are mutated to render them insensitive to calcium, the expression level of the SYT VII protein is only 20-30 % of that of the wild-type protein, suggesting that calcium-binding is essential for the stabilization of the protein (Maximov *et al.* 2008).

As indicated, SYT VII is a Ca^{2+}-sensitive SYT, and like SYTs IX and XI its C2B domain shows strong IP_4 binding activity demonstrating that this member of the SYT family is capable of high-affinity interactions with internal membranes (Ibata *et al.* 1998). Indeed, the Ca^{2+}-mediated sensitivity of membrane binding for the SYT VII C2A domain is much higher than that for the SYT I C2A domain, with $Ca_{1/2}$ values of 31 ± 2 μM for the SYT I

C2A domain versus 1.7 ± 0.2 μM for the SYT VII C2A (Brandt *et al.* 2012). This observed heightened sensitivity is the result of the slow membrane dissociation rate of the SYT VII C2A domain, as although the rate of association with target membranes is 2-fold slower than that of the SYT I C2A domain, dissociation rates are 60-fold slower. Dissociation can be slowed by treatment with solutes which enhance the hydrophobic effect such as trehalose or Na_2SO_4, and hence it is though that the SYT VII C2A domain first associates with target membranes in an electrostatic manner requiring Ca^{2+} ions and anionic membrane lipids and then inserts into the membrane through a slow hydrophobic process. Indeed, the SYT VII C2A domain forms a stronger interaction with membranes containing higher quantities of the anionic lipid phosphatidylserine, demonstrating the importance of electrostatic interactions in membrane binding. Additionally, the SYT VII C2A domain maintains its association with liposomes following NaCl titration whereas the SYT I C2A domain dissociates rapidly, demonstrating the importance of strong non-electrostatic forces in SYT VII membrane binding. It is likely that the stronger binding affinity of the SYT VII C2A domain compared with the SYT I C2A domain is due to the presence of two phenylalanine residues at positions 167 and 229 of the SYT VII C2A region. These sites are located at the ends of two Ca^{2+}-binding loops, and in the SYT I C2A domain are occupied by methionine and phenylalanine respectively. As phenylalanine shows a stronger affinity for lipid membranes due to its inherent hydrophobicity, it is most likely this extra phenylalanine residue which allows the SYT VII C2A domain to insert deeper into target membranes.

The SYT VII protein shows robust Ca^{2+}-dependent oligomerization at the cytoplasmic domain with EC_{50} values of about 155 μM Ca^{2+} and can also form weak Ca^{2+}-independent oligomers (Fukuda *et al.* 2000). Indeed, the SYT VII cytoplasmic domain displays the strongest Ca^{2+}-dependent oligomerization activity in the SYT family (Fukuda *et al.* 2001). This strong multimerization ability is the result of an asparagine residue in the SYT VII C2B domain (ASN328). In other SYTs, this site is occupied by threonine. SYT VII preferentially forms Ca^{2+}-dependent oligomers with SYTs V, VI, and X, can produce weak oligomers with SYTs I, II, and IX, and does not interact with the other members of the SYT family. For most SYTs, oligomerization of the cytoplasmic domain is only possible if the proteins are tethered at the N-terminus. However, the co-expression of both full-length and cytoplasmic portions of the SYT VII protein revealed that SYT VII is able to oligomerize without anchoring at the N-terminus.

The mechanism of oligomerization of the SYT VII protein is different to that of SYT I, as both C2 domains contribute to Ca^{2+}-dependent hetero- and homo-oligomerization

(Fukuda *et al*. 2001). The SYT VII C2A domain can bind to itself and to the C2A domain of SYT VI but not to the SYT VII C2B domain. Likewise the C2B domain of SYT VII can bind to itself and to the C2B domain of SYT II but not to the SYT VII C2A domain. Hence, it has been proposed that SYT VII has two calcium-binding 'hands' and so oligomerizes more strongly than other SYT isoforms. Indeed, a chimera consisting of the SYT VII protein containing the SYT I C2A domain showed only weak Ca^{2+}-dependent oligomerization, and hence pairing of the two hands of SYT VII is essential for multimerization (Fukuda *et al*. 2002).

The precise mechanism behind the unique Ca^{2+}-mediated oligomerization activity of SYT VII has been further studied by site-directed mutagenesis, and it was demonstrated that three aspartate residues in loops 1 and 3 of the SYT VII C2 domains (ASP172, ASP303, and ASP357) function cooperatively to induce oligomerization (Fukuda *et al*. 2002). The mutation of any of these three residues abolishes the calcium-dependent hetero- and homo-oligomerization of SYT VII.

Rotary-shadowing electron microscopy has revealed that SYT VII oligomers are large unbranched linear structures of various lengths as opposed to aggregates (Fukuda *et al*. 2002). However, in the absence of calcium the free SYT VII molecules do form globular structures. A Ca^{2+}-independent mutant of SYT VII (D172N/D303N) is unable to form linear oligomers and instead remains in a globular form. The Ca^{2+}-induced linear oligomer of SYT VII may be involved in the opening of the fusion pore. Interestingly, the expression of tandem cytoplasmic domains of wild-type SYT VII but not the D172N/D303N mutant in PC12 cells was able to inhibit the Ca^{2+}-dependent release of neuropeptide Y by 50%. Hence, oligomerization is likely to be crucial for the function of SYT VII.

The C2B domains of both SYT I and SYT VII contain a WHXL internalization motif and hence are likely to interact with the endocytic proteins dynamin and eps15 (Dasgupta and Kelly, 2002). However, within the C2B domain of SYT VII a further motif is located within the 37 amino acids which constitute the first two β-strands, and this functions to inhibit the WHXL internalization signal. Therefore, although the SYT VII C2 domain contains internalization signals, in contrast to SYT I the SYT VII protein is not actively internalized in PC12, fibroblast, or epithelial cells. Interestingly, the SYT VII C2A domain contains a unique non-tryptophan-based internalization signal which is independent of both dynamin and AP-2, and indeed if the C2A domain is expressed in isolation it undergoes endocytosis at a rate comparable to SYT I (Dasgupta and Kelly, 2002). It has been proposed that SYT VII functions to couple exocytosis and endocytosis via these conflicting internalization signals.

The theory states that in resting cells SYT VII does not undergo endocytosis as its internalization motifs are masked by the C2B inhibitory sequence. However, in response to an as-yet unknown stimuli these signals are unmasked and SYT VII is internalized. It is possible that internalization requires either phosphorylation or dephosphorylation of SYT VII or may require the binding of an accessory protein. The presence of two unique internalization signals requiring different signalling mechanisms suggests that SYT VII may be directed to different intracellular compartments under different conditions.

5.1.4 The Function of SYT VII:

5.1.4.1 The SYT VII Knock-Out Mouse:

SYT VII has been highly conserved throughout evolution and is one of only three members of the SYT family which is present in both *C. elegans* and drosophila (Aldolfsen *et al.* 2004). With this in mind, and considering the ubiquitous tissue distribution of SYT VII mRNA, it would be reasonable to assume that SYT VII plays a central and essential role in the regulation of secretory events. However, the SYT VII $^{-/-}$ mouse is viable, has a normal lifespan, and shows no obvious phenotypic differences to the wild-type mouse (Chakrabarti *et al*. 2003, Maximov *et al*. 2008). Initially, the only reported abnormality of the SYT VII $^{-/-}$ mouse was a slightly limited reproductive potential in later life (Chakrabarti *et al*. 2003). However, more recent work has revealed that SYT VII $^{-/-}$ mice display a lower body weight, reduced body fat content, a higher basal metabolic rate, and an increased rate of lipolysis compared with wild-type mice (Lou *et al.* 2011). Therefore, SYT VII is likely to be involved in the regulation of metabolism.

5.1.4.2 SYT VII in the Nervous System:

SYT VII is expressed throughout the nervous system where it is known to be involved in the regulation of neurite outgrowth during synaptogenesis and in the secretion of LDCVs from PC12 and dopaminergic neurons. However, it is currently unclear what role if any SYT VII plays in the regulation of fast synaptic transmission.

SYT VII is involved in the process of neurite outgrowth during development, as superior cervical ganglion neurons derived from SYTVII-deficient mice show defective neurite outgrowth and arborisation when explanted onto Matrigel matrices in the presence of

Nerve Growth Factor (NGF) (Arrantes and Andrews, 2006). In sympathetic neurons, SYT VII is present on VAMP7/LAMP-1-containing lysosomes in the cell body and in neuronal processes and is secreted onto the plasma membrane following ionomycin stimulation. The inability of neurons from SYTVII-deficient mice to develop correctly may be a result of the failure of neuronal lysosome secretion, resulting in a deficit of membrane available to add to the tips of growing processes. Indeed, SYT VII is known to be a key regulator of lysosome exocytosis in other cell types (Martinez *et al*. 2000).

In addition to its role in synaptogenesis and neurite outgrowth, SYT VII is known to be involved in regulating the secretion of LDCVs from PC12 cells. In this cell type, SYT VII is found on the plasma membrane and is specifically concentrated at active zones where it co-localizes with the synaptic vesicle protein synaptoporin (Sugita *et al*. 2001). Peptides against the C2A and C2B domains of SYT VII inhibit exocytosis from PC12 cells. Additionally, the over-expression of SYT VII in this cell line results in the increased sensitivity of catecholamine secretion in response to the divalent cations Ca^{2+}, Ba^{2+}, and Sr^{2+} (Wang *et al*. 2005). Conversely the knock-down of SYT VII in PC12 cells leads to a decrease in the sensitivity of secretion. It has been proposed that members of the SYT family function in a similar manner to SNARE proteins whereby SYTs located on opposing membranes form oligomers which are essential for the opening of the fusion pore (Sugita *et al*. 2001). It is possible that SYT VII localizes to the plasma membrane in PC12 cells and in response to Ca^{2+} binding forms oligomers with either SYT I or II on synaptic vesicles, allowing the fusion pore to open and in this way regulating exocytosis.

It is currently unclear if SYT VII plays a role in the regulation of Ca^{2+}-mediated fast synaptic transmission at axon terminals. In PC12 cells and hippocampal neurons, SYT VII has been reported to localize to the plasma membrane and is also enriched at the active zones of presynaptic neurons. However, EGFP-SYTVII localizes to lysosomes and LDCVs and not to synaptic vesicles (Aldolfson *et al*. 2004). Likewise, ICC performed in Drosophila suggests that SYT VII does not co-localize with SYT I on synaptic vesicles and instead is found on larger granules and within the soma. Therefore, in neurons SYT VII is not in an ideal intracellular position to regulate synaptic transmission and instead appears to localize to lysosomes and LDCVs.

In the SYT VII $^{-/-}$ mouse, the extent of fast synchronous release, slow asynchronous release, and short-term plasticity are unaffected, indicating that SYT VII is not involved in these aspects of synaptic transmission. SYT VII deletion does not suppress asynchronous release in SYT I $^{-/-}$ mice (Maximov *et al.* 2008), and equally in SYT I $^{-/-}$ Drosophila the over-

expression of SYT VII cannot rescue the loss of fast synaptic transmission or their locomotive defects (Aldolfson *et al*. 2004), indicating that these two members of the SYT family perform non-overlapping functions in the regulation of synaptic transmission. However, it has been shown that SYT VII regulates the asynchronous release of neurotransmitters at the zebrafish neuromuscular, as SYT VII-deficient zebrafish show fewer asynchronous release events (Wen *et al.* 2010).

In adrenal chromaffin cells, truncated transcripts of SYT VII are expressed and these are thought to be involved in the slow phase of synaptic transmission. When adrenal chromaffin cells are treated with siRNA against SYT VII, the slow phase of exocytosis is decreased by 50% (Schonn *et al*. 2007). Interestingly, when both SYT I and SYT VII are knocked-out in adrenal chromaffin cells, overall exocytosis is reduced by 70% and only very slow secretory events persist. However, it is possible that SYT VII plays an indirect role in the regulation of slow synaptic transmission by influencing the endocytosis and re-filling of synaptic vesicles. Therefore, the likely conclusion from this work is that SYT VII does not play a direct role in the regulation of fast synaptic transmission and instead its role in the nervous system is in the regulation of LDCV secretion.

5.1.4.3 SYT VII and Endocytosis:

It is known that SYT VII contains numerous internalization signals which allow it to interact with endocytic proteins under certain conditions and therefore it is likely that SYT VII is involved in the regulation of endocytosis (Dasgupta and Kelly, 2002). Indeed, variants of SYT VII which lack the C2 domains increase the rate of recycling of synaptic vesicles when over-expressed in neurons (Virmani *et al.* 2003). By contrast, the over-expression of wild-type SYT VII decreases the rate of endocytosis through a mechanism which is dependent on the dimerization of SYT VII. Therefore, SYT VII may act as a molecular switch, with different splice variants directing vesicles to either a fast or a slow recycling pathway depending on their length.

5.1.4.4 SYT VII and the Regulation of Lysosome Exocytosis:

SYT VII is a resident protein on lysosomes and is heavily involved in regulating their fusion with the plasma membrane. Initially, SYT VII was reported to localize to lysosomes in rat NRK cells, human HEK-293 cells, mouse 3T3 cells, and hamster CHO cells (Martinez *et*

al. 2000). In NRK fibroblasts, the Ca^{2+}-dependent secretion of lysosomes could be inhibited by their exposure to either antibodies or peptides against the C2A domain of SYT VII. SYT VII is now thought to be trafficked to lysosomes via a palmitoylation-dependent interaction with the tetraspanin CD63 (Flannery *et al.* 2010). The palmitoylation sites of SYT VII have been identified as three cysteine residues within and directly adjacent to the transmembrane domain. If these sites are mutated, SYT VII is retained within the Golgi body whereas CD63 traffics to lysosomes as expected. Conversely, if the tyrosines in the lysosome targeting motif of CD63 are disrupted, both CD63 and SYT VII are trafficked as a complex to the plasma membrane. In macrophages, SYT VII is trafficked with CD63 to growing phagosomes from lysosomes in a Ca^{2+}-dependent process. It is thought that this association with CD63 allows SYT VII to be trafficked to both lysosomes and the plasma membrane in response to cytoplasmic Ca^{2+} increases.

5.1.4.5 SYT VII and Membrane Repair:

Membrane injury results in the uncontrolled influx of Ca^{2+} across the plasma membrane into the cell. This will lead to either apoptosis of the cell or wound healing via the Ca^{2+}-dependent exocytosis of lysosomes, which occurs at cytosolic Ca^{2+} concentrations of between 1- 5 µM (Gerasimenko *et al.* 2001). SYT VII plays a pivotal role in membrane repair by inducing the exocytosis of lysosomes. Indeed, in fibroblasts membrane repair can be inhibited by the addition of antibodies against the C2 domains of SYT VII. Additionally, murine embryonic fibroblasts (MEFs) derived from mice whose SYT VII gene has been disrupted with a neomycin cassette show impaired lysosome exocytosis and plasma membrane resealing following wounding (Chakrabarti *et al*. 2003). Interestingly, these mice develop a condition which is similar to the human autoimmune diseases polymyositis and dermatomyostitis, characterized by fibrosis of the skin and skeletal muscle, endomysial collagen deposition, increased levels of serum creatine kinases, and the invasion of muscle fibres by leukocytes. However, there are no obvious defects in the brain, liver, heart, pancreas, spleen or kidneys suggesting that the inflammation is restricted to the skeletal muscle. This may be due to the fact that skeletal muscle constantly undergoes mechanical stress resulting in rupture of the plasma membrane and therefore the loss of the SYT VII protein would have a more severe impact in this tissue.

5.1.4.6 SYT VII and Phagocytosis:

SYT VII is involved in the Ca^{2+}-dependent process of phagocytosis by regulating the delivery of membrane from lysosomes and late endosomes to the forming phagocytic cup. Indeed, a progressive inhibition of particle uptake as particle load increases is seen in macrophages from SYT VII $^{-/-}$ mice compared to those derived from wild-type mice (Czibener *et al*. 2006). This effect can be rescued by the over-expression of wild-type but not Ca^{2+}-insensitive SYT VII. Additionally, the recruitment of LAMP-1 to forming phagosomes is inhibited in SYT VII $^{-/-}$ mice, demonstrating the failure of phagolysosome fusion.

As a consequence of its role in mediating phagolysosome fusion in phagocytic cells, SYT VII is also involved in preventing the replication of pathogens within cells. For example, *Trypanosoma cruzi* G strain (type I) amastigotes are the causative agents of Chagas' disease and induce phagocytosis in mammalian cells with the same efficiency as professional phagocytes (Fernandes *et al.* 2013). The knock-down of either SYT VII or CD63 inhibits amastigote internalization, indicating that the delivery of lysosomes to the forming phagosome cup is essential for *T. cruzi* uptake.

In dendritic cells, the function of SYT VII appears to be unique as it is not involved in mediating phagocytosis in this cell type. Dendritic cells are able to undergo phagocytosis, but their primary function is to act as antigen-presenting cells. Unlike macrophages, dendritic cells undergo a maturation phase following stimulation and it appears that SYT VII is involved in this maturation phase rather than in the uptake of antigens. Indeed, no inhibitory effects on phagocytosis are seen in cells derived from SYT VII $^{-/-}$ mice (Becker *et al.* 2009). In dendritic cells, SYT VII is located on the periphery of lysosomes as is the case in macrophages. However, SYT VII expression is up-regulated following LPS stimulation and the protein is seen to translocate to the plasma membrane. Dendritic cells derived from SYT VII $^{-/-}$ mice show delayed trafficking of MHC class-II molecules to the plasma membrane, and therefore it is likely that SYT VII regulates the fusion of MHC class-II-containing vesicles with the plasma membrane rather than phagocytosis in this cell type.

5.1.4.7 SYT VII and Bone Formation:

SYT VII is associated with cathepsin-K-containing lysosomes in osteoclasts and bone matrix protein-containing vesicles in osteoblasts (Zhao *et al.* 2008). In SYT VII $^{-/-}$ mice, catepsin K secretion is inhibited as is the formation of the ruffled border in osteoclasts. Additionally, bone matrix protein deposition is impaired in SYT VII $^{-/-}$ osteoblasts. The lack

of proper exocytosis from osteoblasts and osteoclasts leads to morphological abnormalities in SYT VII $^{-/-}$ mice. Resorptive pits and ruffled membranes are small and irregular, and calcarial primary osteoblasts derived from SYT VII $^{-/-}$ mice are defective in nodule formation and collagen secretion. Additionally, SYT VII-deficient mice are osteopeninc, having a dramatic decrease in trabecular bone volume, thickness, and increased trabecular separation. As a consequence, bone formation rates are decreased by almost three-fold. Osteoclastogenesis however is not affected, indicating that SYT VII is not involved in osteoclast differentiation. The transduction of a retrovirus containing SYT VII into osteoclasts and osteoblasts completely rescues the defects seen in SYT VII $^{-/-}$ cells, indicating that they are due entirely to the loss of this member of the SYT family.

5.1.4.8 SYT VII and the Secretion of LDCVs from T-cells:

SYT VII has been shown to have an as-yet undefined but essential role in the secretion of lytic granules from cytotoxic T-lymphocytes (CTLs) (Fowler *et al*. 2007). SYT VII localizes to granzyme-containing lytic granules following CTL activation. SYTVII $^{-/-}$ CTLs show impaired cytotoxicity and indeed SYT VII $^{-/-}$ animals cannot effectively clear an infection by the *Listeria monocytogenes* pathogen. It is thought that SYT VII is essential for the perforin/granzyme-mediated destruction of pathogens by mediating lytic granule exocytosis, although its precise role is currently unclear.

5.1.4.9 SYT VII and the Regulation of Insulin and Glucagon Secretion:

It is now well-established that SYT VII is involved in regulating insulin and glucagon secretion and therefore plays a significant role in the regulation of metabolism. SYT VII mRNA is found in rat islets and BTC3 and RINm5F cell lines whilst the SYT VII protein is found on insulin-containing granules in pancreatic β-cells (Gao *et al.* 2000). The SYT VII transcript is also present at high levels in mouse islets and in the INS-1 cell line, and in mouse pancreatic β-cells SYT VII is seen to co-localize with insulin (Gustavsson *et al.* 2007). If SYT VII is over-expressed in RINm5F cells, the result is increased insulin secretion (Gao *et al.* 2000). Equally, SYT VII $^{-/-}$ mice show impaired insulin secretion and glucose intolerance (Gustavsson *et al.* 2007).

It is now know that the loss of SYT VII in pancreatic islet cells impairs GLUT4 trafficking following an insulin challenge (Li *et al.* 2007). GLUT4 is responsible for insulin-

stimulated glucose uptake, and following stimulation GLUT4 translocates from an intracellular compartment to the plasma membrane of fat and skeletal muscle cells in a Ca^{2+}-dependent manner. In SYT VII $^{-/-}$ mice, GLUT4 is constitutively secreted to the plasma membrane of fat and skeletal muscle cells and there is no significant increase in GLUT4 translocation to the plasma membrane following an insulin challenge. Therefore, in addition to regulating Ca^{2+}-dependent insulin secretion, SYT VII also functions to translocate GLUT4 to the plasma membrane of fat and skeletal muscle cells, allowing glucose to be absorbed from the bloodstream.

SYT VII is found co-localized with glucagon in mouse α-cells, and indeed SYT VII is now known to be the principal Ca^{2+}-sensor for Ca^{2+}-induced glucagon exocytosis from α-cells in the pancreas (Gustavsson *et al.* 2009). Indeed, the deletion of SYT VII inhibits glucagon secretion from α-cells in an *in vivo* mouse model. Equally, in an *in vitro* model involving isolated intact pancreatic islets derived from SYT VII $^{-/-}$ mice an 80% impairment in glucagon secretion was reported. Finally, SYT VII-deficient mice show an impaired response to insulin-induced hypoglycaemia. Therefore, substantial evidence has been provided to demonstrate that SYT VII is heavily involved in the secretion of glucagon from α-cells.

The loss of normal insulin and glucagon secretion in SYT VII $^{-/-}$ mice has significant phenotypic consequences. SYT VII $^{-/-}$ mice display a lower body weight, lower body fat content, higher oxygen consumption, higher core body temperatures, and a higher basal metabolic rate compared with control mice (Lou *et al.* 2011). They also require an increased quantity of lipid for energy production as their respiratory exchange ratio is lower than control mice. Indeed, SYT VII $^{-/-}$ mice display increased lipolysis and an increased capacity for fatty acid transport and oxidation. Therefore, it appears that SYT VII $^{-/-}$ mice employ compensatory mechanisms allowing adaptation to a persistent low glucagon level which require increased fat consumption leading to a lower overall body weight.

5.1.4.10 SYT VII and Cell Migration:

SYT VII and SYT V were identified through an RNA-mediated interference screen as having positive effects on chemotaxis following chemokine stimulation. Both SYT V- and SYT VII-deficient T- and THP-2 cells display less migration following CXCL12 exposure *in vitro* than wild-type cells (Colvin *et al.* 2010). Equally, chemoattractant-induced Ca^{2+}-dependent lysosome fusion was impaired in SYT VII-deficient neutrophils. Lymphocytes

from SYT VII $^{-/-}$ mice show an accumulation of lysosomes in their uropods (the trailing edges of the cell membrane which form during cell migration), and these lysosomes also show impaired release. Finally, SYT VII $^{-/-}$ T-cells are more adherent than those derived from wild-type animals, with 81.48% of SYT VII $^{-/-}$ T-cells displaying an adherent phenotype compared with 6.14% of wild-type cells. Hence, SYT VII is involved in regulating the adhesive properties of cells. It is likely that SYT VII mediates cell migration by inducing the fusion of lysosomes with the plasma membrane, allowing the addition of membrane to the leading edge of migrating cells in response to chemokine stimulation.

5.1.5 SYT VII and the Fusion Pore:

A popular theory suggests that members of the SYT family regulate exocytic events by forming oligomers which influence the formation and physical structure of the fusion pore (Tucker and Chapman, 2002). The effect of the SYT VII protein on the opening and dilation of fusion pores in chromaffin cells has been analysed using patch amperometry in both wild-type and SYT VII mutant chromaffin cells (Segovia *et al*. 2010). Amperometic measurements demonstrated that the foot signal which is used to examine the early steps of fusion pore formation was unchanged between control, SYT VII $^{-/-}$, and SYT VII mutant chromaffin cells, indicating that SYT VII does not affect the early formation of the fusion pore. However, in both SYT VII $^{-/-}$ and SYT VII mutant cells, the lifetime of the fusion pore was significantly extended by up to 3-fold, demonstrating that SYT VII is indeed involved in fusion pore structure. In chromaffin cells expressing a Ca^{2+}-insensitive mutant of SYT VII a significant increase in kiss-and-run events was reported. It is possible that Ca^{2+} binding to the C2A domain of SYT VII is sufficient to initiation the opening of the fusion pore, but in the absence of Ca^{2+} binding to the C2B domain the pores become unstable and collapse.

This work has been extended to demonstrate that SYT VII restricts the expansion of the fusion pore. In murine embryonic fibroblasts (MEFs) derived from SYT VII $^{-/-}$ mice 45% of lysosomes undergo complete exocytosis compared with wild-type MEFs from which only 21% of vesicles undergo full secretion (Jaiswal *et al*. 2004). Additionally, secretion occurs on average 28 seconds earlier than in wild-type mice. Interestingly, it was noted that secreted membrane proteins of wild-type mice remain clustered in close proximity to the fusion pore following exocytosis, whereas membrane proteins from SYTVII $^{-/-}$ mice rapidly diffuse away from the site of exocytosis. Hence, SYT VII is required to cluster lysosome membrane

proteins in the area proximal to the initial site of fusion and also functions to limit the size of the fusion pore and increase the time required for its formation.

5.1.6 The Binding Partners of SYT VII:

Currently, it is unclear which proteins SYT VII interacts with in order to form the fusion apparatus, and of course the components of this complex will undoubtedly vary depending on the cell type in question. In lysates derived from NRK cells, isolated SYT VII interacts with the v-SNARE VAMP7 and the t-SNAREs syntaxin-4 and SNAP-23 (Rao *et al*. 2004). Specifically, the C2A domain of SYT VII binds SNAP-23 via a mechanism that is enhanced by the H3 domain of syntaxin-4. Additionally, the exocytosis of lysosomes from NRK cells is inhibited by peptide fragments of syntaxin-4 and VAMP-7 and also following SNAP-23 cleavage by *Botulinum* neurotoxin. However, the specificity of these reported interactions has been questioned, as SYT VII can also bind to syntaxin-2, syntaxin-3, and to heterodimers consisting of SNAP-25 and syntaxin1a. Equally, SYT I binds to syntaxin-2 and syntaxin-3. However, it does not bind to syntaxin-4 and therefore it is likely that the SYT VII:syntaxin-4 interaction is more specific. Ultimately, it is probable that SYT VII has a number of SNARE binding partners, although work done in NRK cells suggests that a fusion complex consisting of SYT VII, syntaxin-4, VAMP7, and SNAP-23 mediates lysosome exocytosis.

In adrenal chromaffin cells, a 45-kDa isoform of SYT VII was found to be expressed and localized to chromogranin A-containing secretory granules (Osborne *et al.* 2007). It is likely that SYT VII is involved in mediating the exocytosis of the slowly releasable pool of granules from chromaffin cells whereas SYT I mediates the release of the readily releasable pool (RRP) (Schonn *et al*. 2007). An affinity pulldown screen using highly purified chromaffin granules from bovine adrenal medulla demonstrated that SYT VII interacts with phosphatidylinositol 4,5-bisphosphate (PIP_2) via its C2B domain in the absence of calcium and via the C2A and C2B domains in the presence of calcium (Osborne *et al.* 2007). A polylysine stretch consisting of K320, K321, and K325 in the C2B domain has been identified as being responsible for mediating PIP_2 binding and this interaction is essential for the release of catecholamine from chromaffin cells. It may be that by binding PIP_2 SYT VII is brought into close contact with the vesicle membrane prior to Ca^{2+} binding.

Finally, it is now known that the function of SYT VII is regulated by SUMOylation, either directly or indirectly, and indeed SYT VII interacts with components of the

SUMOylation apparatus such as SUMO1 and the deSUMOylating enzyme SENP1 (Dai *et al*. 2011). Small ubiquitin-like modifier (SUMO) proteins are reversibly attached to proteins to regulate their localization or function in a process called SUMOylation. SUMO1 co-precipitates with SYT VII in lysates derived from INS-1 cells and human islets, although this interaction is transiently lost following glucose stimulation. Binding is enhanced by the overexpression of SUMO1 and is disrupted by SENP1 over-expression. This disruption also enhances the exocytosis of insulin from INS-1 cells. Hence, SUMOylation may impair insulin secretion via a mechanism which involves SYT VII. This effect may be direct, resulting from the SUMOylation of SYT VII itself, or may be indirect, resulting from an as-yet unknown interaction between SYT VII and a SUMOylated binding partner. Equally, it is possible that the deSUMOylation of SYT VII is necessary to allow the exocytosis of insulin to proceed.

5.1.7 SYT VII and a Potential Role in the Regulation of WPB Exocytosis:

Based on the evidence provided in the literature I have identified SYT VII as a strong candidate for the role of the calcium sensor regulating the release of WPBs from endothelial cells. Firstly, SYT VII is known to be involved in the Ca^{2+}-mediated exocytosis of large secretory granules similar to WPBs from a range of cell types (as discussed, see 5.1.4 The Function of the SYT VII Protein). Additionally, WPBs have been detected in the endothelium of hagfish, the living ancestor of vertebrates (Yano *et al.* 2007), and so it is likely that their exocytosis will be regulated by an evolutionally-conserved molecule. SYT VII is one of only three SYTs found in both *C. elegans* and drosophila (Aldolfsen *et al.* 2004), providing further evidence that it may be the calcium sensor regulating WPB exocytosis. Finally, SYT VII is a binding partner for syntaxin-4 and SNAP-23, and these proteins have been implicated as the t-SNAREs responsible for mediating WPB exocytosis with the plasma membrane (Matsushita *et al*. 2003). Therefore, based on the conservation of the SYT VII protein throughout evolution, its established role as a Ca^{2+}-sensor in a number of cell types, and its known ability to interact with components of the WPB fusion apparatus, I propose that SYT VII is the most promising candidate for the role of calcium sensor regulating WPB exocytosis from HUVECs. Hence, I initially focused my efforts on testing this hypothesis through functional studies as will be discussed in the remainder of this chapter.

5.2 SYTVII-YFP Over-Expression ELISAs:

Previous observations have shown that SYT VII can be found in HUVECs at both the mRNA and protein levels and crucially over-expressed SYTVII-YFP localizes to both the WPBs and lysosomes. The trafficking of SYTVII-YFP to the granules supports the hypothesis that this member of the SYT family may be involved in regulating the Ca^{2+}-dependent process of WPB exocytosis from endothelial cells. In order to test this theory, the SYTVII-YFP construct was transfected into HUVECs with the aim to determine if over-expressed SYT VII has any effect on the secretion of WPBs from endothelial cells. Briefly, HUVECs were transfected with either SYTVII-YFP or with the control cytoplasmic construct YFP and allowed to grow to confluency on 6-well plates for 48 hours. Both cultures were then stimulated with either 1 µM ionomycin or with a control non-stimulating solution. The media and lysates were collected from each well, centrifuged to remove cellular debris, and processed for both VWF and proregion ELISAs as described in '2.7 The Enzyme-Linked Immunosorbent Assay (ELISA) Protocol.'

Initially, VWF ELISAs were carried out with the aim to examine the extent of VWF secretion from HUVECs expressing SYTVII-YFP and those expressing YFP. The results of a representative experiment are shown in Figure 5.1 (i). As can be seen, no differences in the extent of VWF secretion are apparent between cells expressing SYTVII-YFP and those expressing the control construct YFP. The samples were then subjected to the more-sensitive proregion ELISA and the results of a representative assay can be seen in Figure 5.1 (ii). Again, it would appear that the over-expression of SYTVII-YFP does not affect the quantity of proregion released from HUVECs. Therefore over-expressed SYT VII does not affect the extent of WPB secretion from endothelial cells in response to 1 µM ionomycin exposure. However, it is important to note that the expression level of the SYTVII-YFP construct in HUVECs is relatively low. It is quite possible that due to this poor transfection efficiency the background secretion of protein from non-expressing cells is too high to allow the detection of even significant alterations to secretion from transfected cells (see Discussion).

5.3 The Effects of SYTVII-YFP Over-Expression on the Calcium Sensitivity of WPB Exocytosis: The Dose-Response Curve

The over-expression of SYTVII-YFP in HUVECs did not have a significant effect on the overall secretion of either VWF or proregion following stimulation with 1 µM ionomycin.

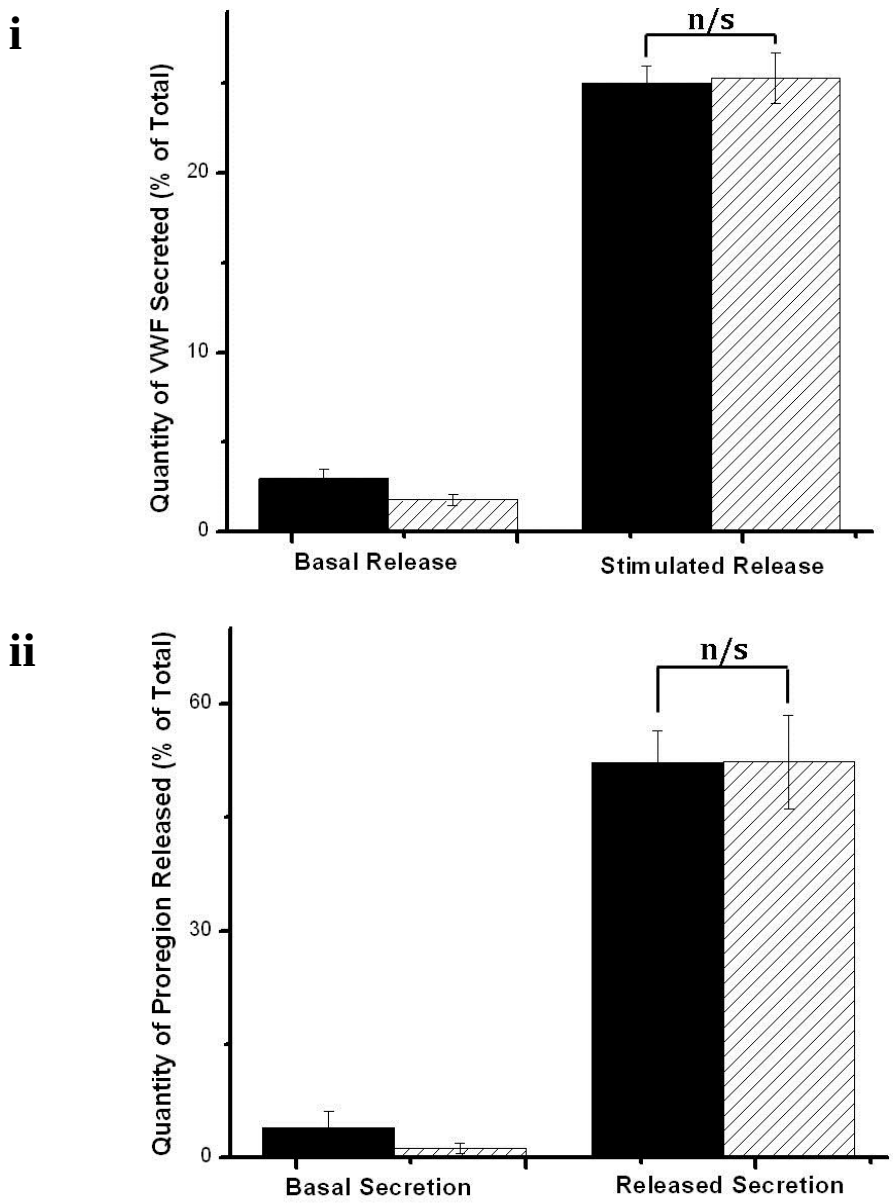

Figure 5.1. SYT VII over-expression does not affect the exocytosis of WPBs.

HUVECs were transfected with either SYTVII-YFP or YFP. Media and lysates were collected from cells after forty-eight hours and processed for VWF and proregion ELISAs. Cells incubated with a control non-stimulating solution provided the data for basal secretion. Cells incubated with 1 µM ionomycin provided the data for stimulated secretion. Panel (i) shows the quantity of VWF released as a percentage of the total quantity of VWF in the cells. Panel (ii) shows the quantity of proregion released as a percentage of the total quantity of proregion in the cells. Black bars represent YFP-transfected cells. Hatched bars represent SYTVII-YFP-transfected cells.

n/s = non-significant (p-value › 0.05)

n = 3 replicates from one vial of HUVECs; data is representative of 3 individual experiments performed on separate vials of HUVECs.

However these assays only allow the examination of WPB exocytosis in response to a single concentration of ionomycin, which in this case is relatively high. It has been reported that a key function of members of the SYT family is to influence the sensitivity of secretory events to low concentrations of calcium (Gao *et al.* 2000, Wang *et al.* 2005), and therefore it is possible that SYT VII may modulate the sensitivity of WPB exocytosis in response to low concentrations of Ca^{2+} ions. I have developed a dose-response assay as a method for determining the effect of the over-expression of constructs on the calcium sensitivity of WPB exocytosis, details of which can be found in Appendix 1.0. This assay was used to test the hypothesis that SYT VII may function to modulate the calcium sensitivity of WPB exocytosis in endothelial cells.

Briefly, HUVECs transfected with either SYTVII-YFP or with a control cytoplasmic construct (YFP) were seeded onto 24-well plates. Cells were allowed to grow to confluency for 48 hours, after which point they were stimulated with varying concentrations of ionomycin. For each transfection, an ethanol control was included to provide the rate of basal secretion. Following the ten-minute stimulation, the media and lysates were collected from each well, the samples were spun down to remove cellular debris, and a proregion ELISA was performed. HUVECs are heterogeneous and each individual culture will secrete different quantities of proregion in response to ionomycin stimulation. Therefore, in order to allow a direct comparison between experiments the data from each replicate was normalized to the secretion recorded from the YFP-expressing control cells exposed to 1 μM ionomycin. The final dose response curve is shown in Figure 5.2. As can be seen, the over-expression of SYTVII-YFP in HUVECs results in a small but significant increase in the calcium sensitivity of WPB exocytosis. At low concentrations of ionomycin the extent of secretion is significantly higher in cells expressing SYTVII-YFP than those expressing the control plasmid YFP. However, for 1 μM ionomycin (i.e. the concentration which was used for the over-expression ELISAs described previously) the extent of proregion secretion is equivalent for both cultures. Therefore, this work suggests that SYT VII does indeed modulate the sensitivity of WPB exocytosis as increased proregion secretion is reported from HUVECs following their exposure to low concentrations of ionomycin when the SYT VII protein is up-regulated.

5.4 The Effects of the Knock-Down of SYT VII on WPB Exocytosis:

The use of the dose-response assay has demonstrated that the up-regulation of SYT

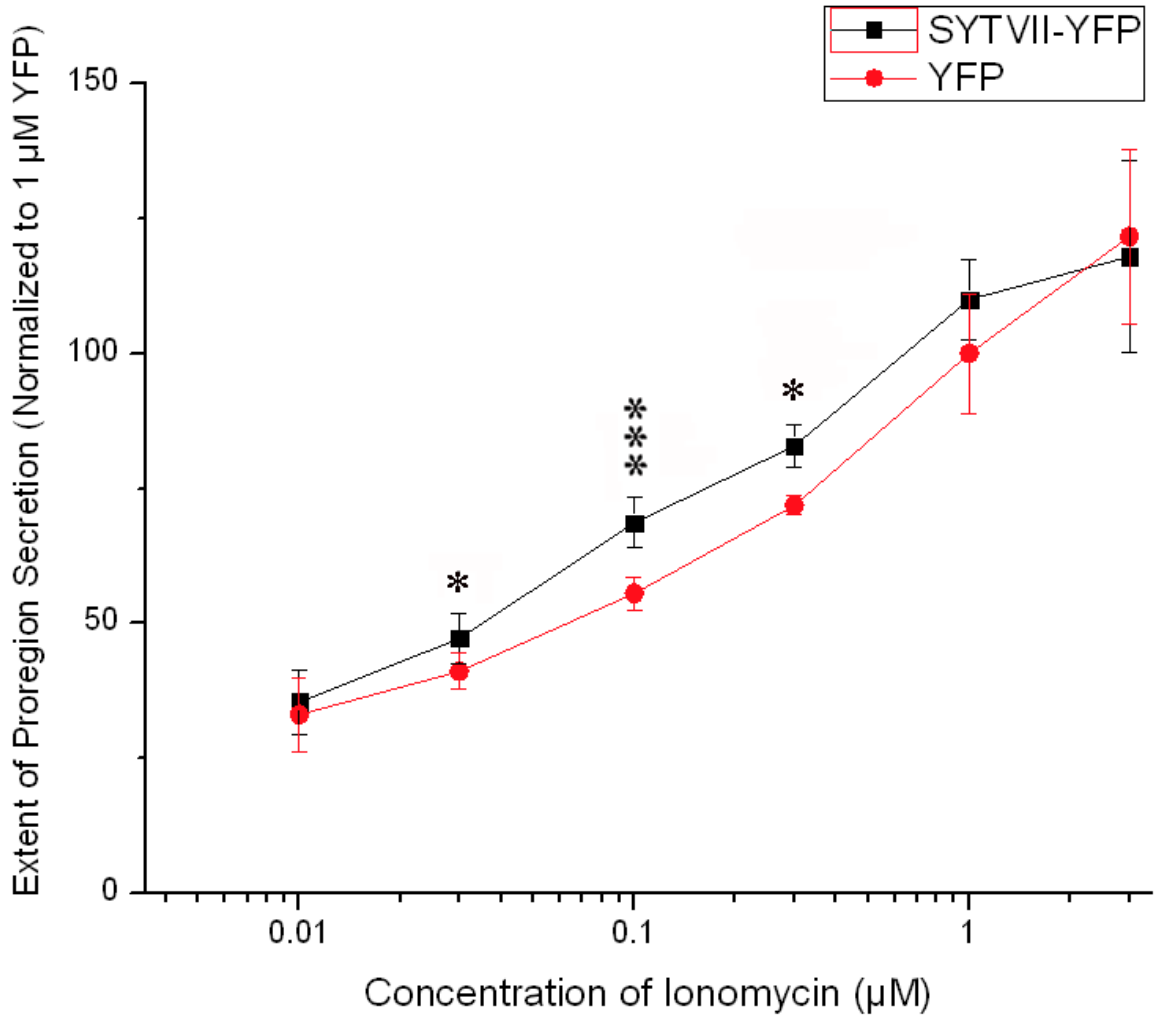

Figure 5.2. Over-expressed SYT VII modulates the calcium sensitivity of WPB exocytosis.
Cells transfected with either SYTVII-YFP or the cytoplasmic control construct YFP were stimulated with varying concentrations of ionomycin as indicated in the x-axis. The quantity of proregion secreted was determine using a proregion ELISA. This procedure was repeated three times. For each transfection, the data was normalized to the extent of proregion secreted from YFP-expressing control cells exposed to 1 µM ionomycin. The data from the three replicates was combined and the means of the normalized values were used to plot the final dose-response curves.

* P-value ‹ 0.05

*** P-value ‹ 0.0005

VII does indeed have a subtle effect on the calcium sensitivity of WPB secretion. However, the overall extent of WPB exocytosis in response to 1 μM ionomycin is not altered in HUVECs expressing SYTVII-YFP compared with those expressing YFP. Over-expression ELISAs are limited in that they rely on a sufficient expression level of the protein in question to overcome the background secretion derived from non-expressing cells. Therefore, it was decided to knock-down the SYT VII protein in HUVECs using siRNA with the aim to determine if diminished levels of the SYT VII protein have an effect on the exocytosis of WPBs from our model endothelial cells.

5.4.1 The Optimization of the Knock-Down Protocol:

Initially, it was necessary to optimize the knock-down protocol for SYT VII siRNA as the ideal conditions for achieving an effective knock-down can vary depending on the target protein. Firstly, HUVECs were transfected with 400 pMol of either SYT VII siRNA or control non-targeting siRNA. After forty-eight hours the lysates were collected and Western blots were performed with the aim to determine the quantity of SYT VII protein present in each culture. Blots were probed with an α-SYT VII antibody and an α-tubulin antibody. The results of this are shown in Figure 5.3. As can be seen, the efficient knock-down of the SYT VII protein is achieved using 400 pMol of SYT VII siRNA. In contrast, the level of tubulin in each culture remains unchanged indicating that an equivalent quantity of total protein was present in each sample. This optimization procedure was repeated using HUVECs transfected with either 200 pMol of either SYT VII siRNA or control non-targeting oligos. However, these conditions failed to yield efficient knock-down of the SYT VII protein (data not shown). Additionally, at time-points less than forty-eight hours no significant knock-down of the SYT VII protein was seen (data not shown). Therefore, the optimum knock-down of the SYT VII protein is achieved when HUVECs are transfected with 400 pMol of SYT VII siRNA and allowed to grow in culture for forty-eight hours.

In order to determine if the knock-down of SYT VII has any obvious morphological effects on the HUVECs or their WPBs, cells were transfected with 400 pMol of either SYT VII siRNA or with control siRNA and were processed for ICC forty-eight hours later. A mock transfection was also performed whereby cells were transfected with 4 μl of dH_20. Each culture was stained with antibodies against both VWF and TGN-46. The results of this are shown in Figure 5.4. As can be seen, each culture has produced a confluent monolayer

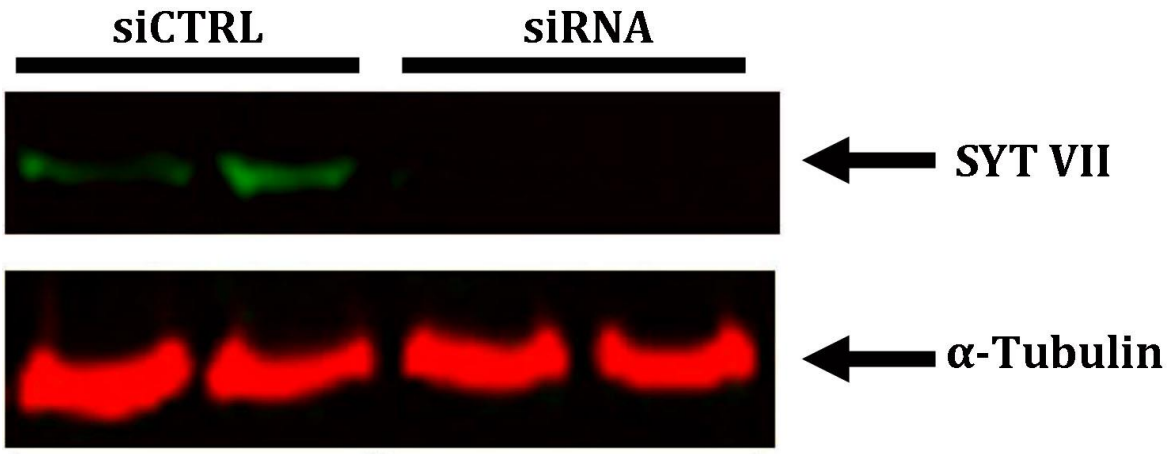

Figure 5.3. The SYT VII protein is depleted in HUVECs following siRNA transfection.

Cells transfected with 400 pMol of either SYT VII siRNA or the control non-targeting oligos (siCTRL) as indicated were grown to confluency for forty-eight hours. Lysates from each culture were extracted and Western blotting was performed. The upper blot shows the results of probing for SYT VII whereas the lower blot shows the corresponding tubulin loading control. As can be seen, efficient knock-down is achieved following transfection with 400 pMol SYT VII siRNA. The extent of the knock-down of SYT VII in SYT VII siRNA-transfected HUVECs is 74.87% of that seen in control siRNA-transfected HUVECs (normalized to the total quantity of protein as determined from the tubulin loading control).

which contains high numbers of rod-shaped WPBs. Hence no obvious effects are apparent on either HUVEC or WPB morphology following transfection with SYT VII siRNA, suggesting that the SYT VII protein does not influence the synthesis or trafficking of WPBs.

5.4.2 SYT VII Knock-down ELISAs:

As it has now been established that 400 pMol of SYT VII siRNA yields an efficient knock-down of the SYT VII protein forty-eight hours following transfection functional studies were performed with the aim to determine if the knock-down of SYT VII affects the exocytosis of WPBs from HUVECs. Firstly, VWF ELISAs were performed and the results of a representative assay are shown in Figure 5.5 (i). As can be seen, no differences in overall VWF secretion are apparent between cells transfected with SYT VII siRNA and those

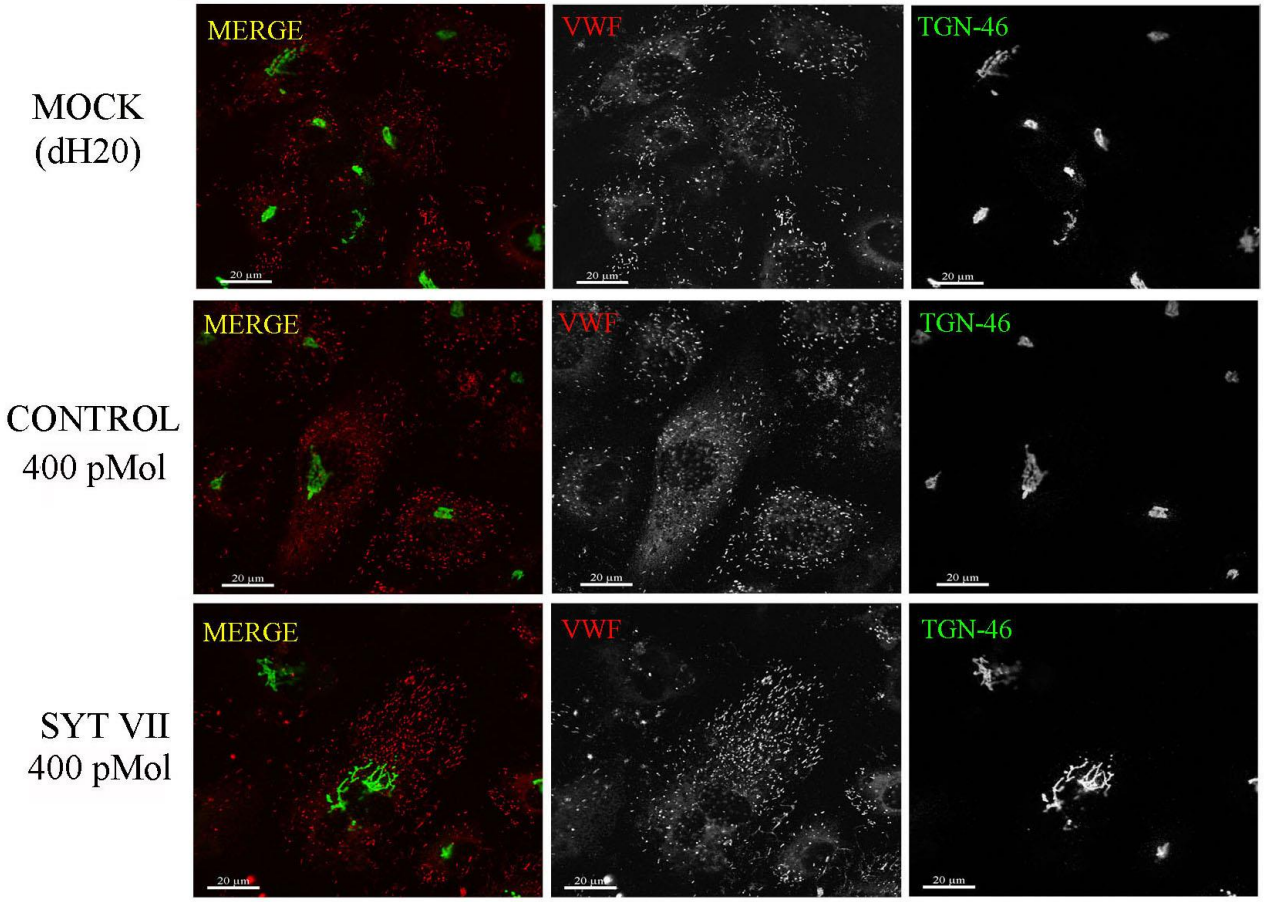

Figure 5.4. The knock-down of SYT VII does not affect the morphology of either HUVECs or their WPBs.

HUVECs transfected with 400 pMol of either SYT VII siRNA or with control non-targeting oligos as indicated were stained with antibodies against both VWF and TGN-46. A mock transfection has also been performed (4 µl of dH_20). The left-hand panels show the merged images, the middle panels show the VWF stain in the red channel, and the right-hand panels show the TGN-46 stain in the green channel. All cultures examined have grown to confluency and HUVECs appear morphologically normal. Likewise, each culture contains high numbers of large, rod-shaped WPBs.

transfected with non-targeting control oligos. The collected samples were then processed for proregion ELISAs and the results of a representative assay are shown in Figure 5.5 (ii). No differences in the total quantity of proregion secreted are visible between HUVECs transfected with SYT VII siRNA and those expressing the control oligos. Therefore the knock-down of SYT VII does not influence the overall extent of WPB exocytosis from HUVECs following their stimulation with 1 µM ionomycin.

5.5 The Effects of SYT VII Knock-Down on the Calcium Sensitivity of WPB Exocytosis: The Dose-Response Curve

The dose-response assay revealed that SYT VII over-expression increases the calcium sensitivity of WPB exocytosis as increased proregion secretion is reported at lower ionomycin concentrations following SYT VII up-regulation. In order to further investigate the role of SYT VII in the regulation of WPB exocytosis the dose-response assay was repeated using HUVECs transfected with 400 pMol of either SYT VII siRNA or control non-targeting siRNA. The purpose of this was to determine if the knock-down of SYT VII has an effect on the calcium sensitivity of WPB exocytosis in response to ionomycin stimulation.

Figure 5.6 shows the dose-response curves for HUVECs transfected with SYT VII siRNA versus those transfected with control siRNA. As can be seen the knock-down of SYT VII in HUVECs does not affect the calcium sensitivity of WPB exocytosis. The dose-response curves generated from both cultures are remarkably similar with no significant differences in the extent of proregion secretion apparent for any of the six ionomycin concentrations tested. Therefore, unlike SYT VII over-expression the knock-down of SYT VII does not alter the calcium sensitivity of WPB exocytosis from HUVECs.

5.6 Discussion:

As SYTVII-YFP traffics to WPBs when over-expressed in HUVECs it is likely that endogenous SYT VII is found as a membrane protein on the granules and so this member of the SYT family has been identified as a prime candidate for the role of the calcium sensor regulating WPB exocytosis from HUVECs. Indeed, SYT VII is known to play a vital role in a number of non-neuronal secretory events such as the regulation of the exocytosis of lysosomes from fibroblasts (Martinez *et al.* 2000), the formation of the phagosomes in

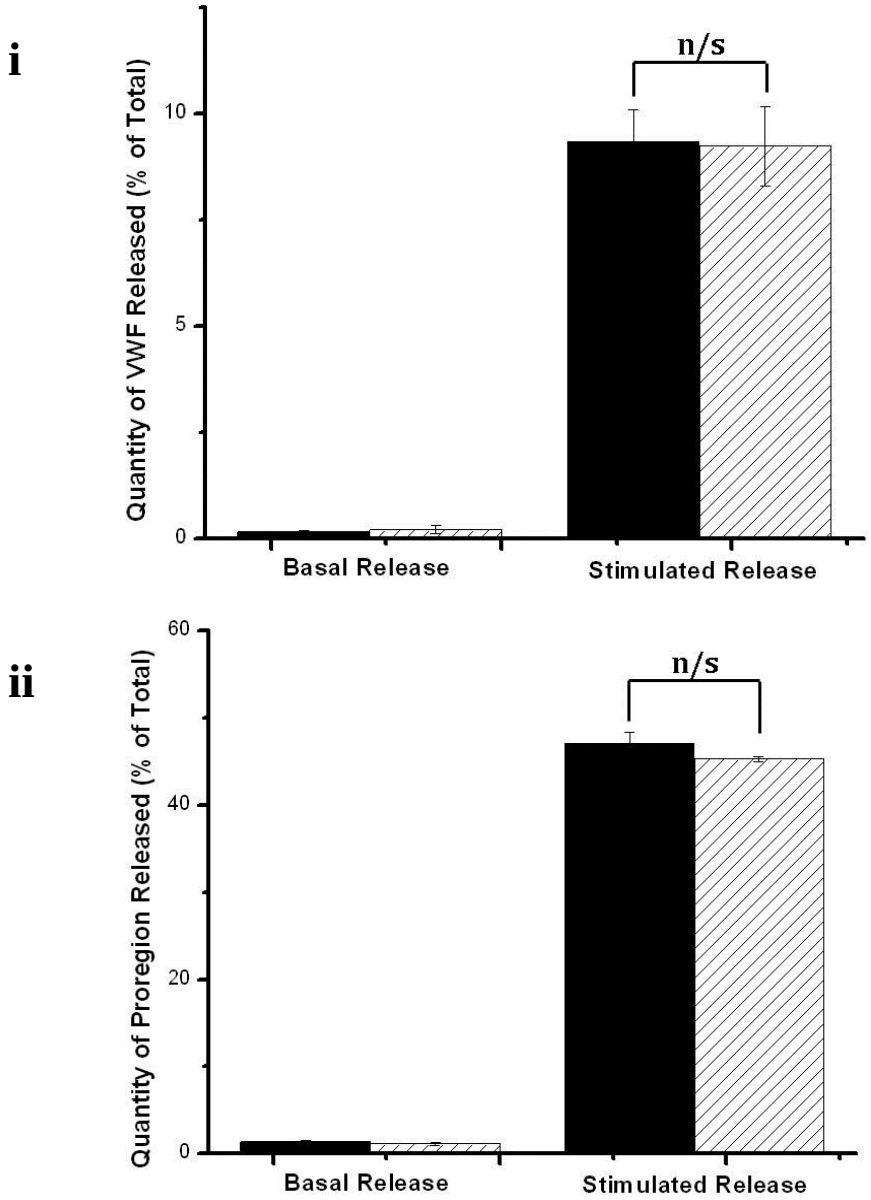

Figure 5.5. SYT VII knock-down does not affect the exocytosis of WPBs.

HUVECs were transfected with either SYTVII siRNA (400 pMol) or control siRNA (400 pMol). Media and lysates were collected from cells after forty-eight hours and processed for VWF and proregion ELISAs. Cells incubated with a control non-stimulating solution provided the data for basal secretion. Cells incubated with 1 µM ionomycin provided the data for stimulated secretion. Panel (i) shows the quantity of VWF released as a percentage of the total quantity of VWF in the cells. Panel (ii) shows the quantity of proregion released as a percentage of the total quantity of proregion in the cells. Black bars represent control siRNA-transfected cells. Hatched bars represent SYTVII siRNA-transfected cells.

n/s = non-significant (p-value › 0.05)

n = 3 replicates from one vial of HUVECs; data is representative of 3 individual experiments performed on separate vials of HUVECs.

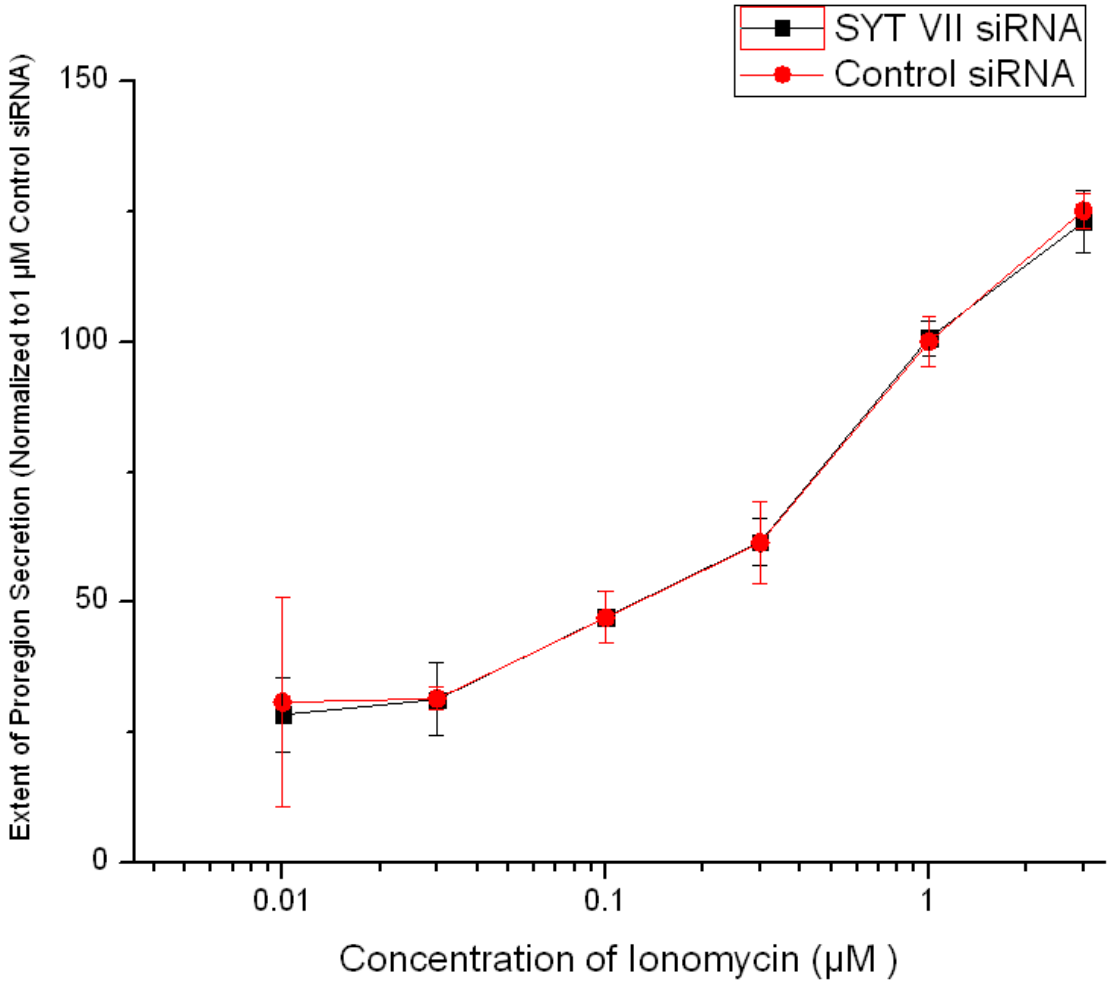

Figure 5.6. SYT VII knock-down does not affect the calcium sensitivity of WPB exocytosis.

HUVECs transfected with either SYT VII siRNA or with control non-targeting siRNA were stimulated with varying concentrations of ionomycin as indicated in the x-axis. The quantity of proregion secreted was determined using a proregion ELISA. This procedure was repeated three times. For each assay, the data was normalized to the secretion of proregion recorded from control cells exposed to 1 µM ionomycin. Data from the three replicates was combined, and the means of the normalized values were used to plot the final dose-response curves.

macrophages (Czibener *et al.* 2006), MHC class II antigen presentation in dendritic cells (Becker *et al.* 2009), bone formation and degradation (Zhao *et al.* 2008), the release of LDCVs from T-cells (Fowler *et al.* 2007), and the exocytosis of both insulin and glucagon from pancreatic cells (Gao *et al.* 2000, Gustavsson *et al.* 2007, Gustavsson *et al.* 2009). Therefore SYT VII has an already-established role in mediating the exocytosis of large secretory granules similar to WPBs. The functional studies performed here attempting to determine the role SYT VII plays within endothelial cells have yielded interesting results. Firstly, SYTVII-YFP over-expression ELISAs demonstrated that the up-regulation of the SYT VII protein does not affect the absolute release of WPBs following exposure to 1 µM ionomycin. However, the dose-response assay revealed that SYTVII-YFP over-expression does increase the calcium sensitivity of exocytosis. Although this effect was relatively small, it is important to consider that the transfection of SYT DNA into HUVECs is inherently inefficient and the majority of the cultured cells will not express the construct. Therefore the high signal-to-noise ratio makes the detection of a functional effect following SYT up-regulation challenging. With this in mind, the observed small effect on calcium sensitivity following SYTVII-YFP over-expression seen here is in reality likely to represent a considerable shift in the kinetics of WPB exocytosis from transfected cells.

SYT VII knock-down studies revealed that the loss of SYT VII in HUVECs does not affect either the absolute secretion of WPBs or the calcium sensitivity of their exocytosis. These results are in contrast to the over-expression studies and suggest that SYT VII is not involved in the regulation of WPB exocytosis. However, it is likely that the extent of knock-down achieved here was not sufficient to result in a functional effect as it could be the case that only a small proportion of the SYT VII protein is required to produce a wild-type phenotype. However, it is also possible that redundancy exists amongst the SYTs, masking the effects of the knock-down of one family member. In future, double knock-down experiments should be performed with particular emphasis on those SYTs which have been reported to traffic to WPBs (SYTs V, VII, VIII, and XVII). It is of interest to consider that SYT VII preferentially forms oligomers with SYT V (Fukuda *et al.* 2001), and therefore these two molecules are likely to interact within the WPB membrane. Therefore a double knock-down involving SYT V and SYT VII may lead to an interesting functional effect.

Although the functional studies discussed here have not provided a definitive role for the SYT VII protein in endothelial cells, they have certainly identified this member of the SYT family as a focal molecule for future studies. Key experiments would focus on live-cell imaging with HUVECs over-expressing SYT VII as this would allow the accumulation of

kinetic secretory data on a single-cell level and thus overcome the limitations of biochemical over-expression studies. Additionally, further analysis of the effect of SYT VII on the calcium sensitivity of WPB exocytosis could be achieved by measuring the Ca^{2+} concentration within living HUVECs using a cell-permeable calcium dye such as fura-2 and correlating this with the kinetics of WPB exocytosis. Lastly, live-cell imaging could be used in combination with amperometry to determine if the knock-down or over-expression of SYT VII influences the formation or stability of the fusion pore. Indeed, it is known that the over-expression of SYT VII in PC12 cells increases the number of LDCVs which undergo full fusion as opposed to kiss-and-run secretory events, suggesting that SYT VII up-regulation may decrease the stability of the fusion pore (Sugita *et al.* 2001). Equally, in chromaffin cells the knock-down of SYT VII restricts fusion pore expansion and increases the time required for its formation (Segovia *et al*. 2010). It is likely that SYT VII may be involved in WPB fusion pore formation in endothelial cells.

Finally, a further avenue for future research which may prove profitable would be to obtain a SYT VII $^{-/-}$ mouse. Endothelial cells from this mouse model could be isolated and grown in culture, providing a source of SYT VII $^{-/-}$ cells which would overcome the limitations of the SYT VII siRNA knock-down studies attempted here. The dose-response assay could be repeated using these cells to determine if the calcium sensitivity of exocytosis is decreased compared with wild-type murine endothelial cells. Additionally, it would be of interest to perform ICC to determine if the biosynthesis and morphology of WPBs is affected by the complete loss of the SYT VII protein. Lastly, a SYT VII $^{-/-}$ mouse model would provide the opportunity to perform platelet-clotting assays to determine if the loss of SYT VII results in a clinical phenotype.

Chapter 6
Investigating the Function of SYT V in HUVECs

6.1 Background Information:

SYT V was the first non-neuronal member of the SYT family to be described in 1995 (Hudson and Birnbaum, 1995, Craxton and Geodert, 1995). This novel SYT was predicted to be Ca^{2+}-dependent, and examination of its distribution in rat tissue showed it to be present in the kidney, lung, heart, adipose tissue, and brain, where it is enriched in synaptic vesicles.

The full sequence of the human SYT V gene and its genomic location were determined in 1997 (Craxton *et al*. 1997). The human gene encodes a protein which is 386 amino acids in length and therefore the predicted molecular mass of human SYT V is 42 kDa. However it has been identified by Western blotting as a protein of 70 kDa (Iezzi *et al*. 2004). The SYT V gene itself is located on chromosome 19q13.4 in close proximity to the SYT III gene, and these two SYTs may indeed be linked. Based on the sequence similarity between SYT V and SYTs III, VI, and X these four family members have been proposed to belong to the same sub-group of SYTs which primarily functions to regulate non-neuronal exocytosis (Saegusa *et al*. 2002). Members of this group are characterized by an N-terminal cysteine cluster which allows dimer formation by disulfide bonding (Saegusa *et al.* 2002).

SYT V is expressed in a number of diverse cell types and its physiological function has been partly characterized. It has been reported to be a component of secretory granules in glucagon-producing pancreatic α-cells but not in insulin-secreting β-cells (Iezzi *et al.* 2004, Saegusa *et al.* 2002) and therefore was proposed to be involved in glucagon but not insulin or somatostatin secretion. However, the knock-down of SYT V in INS-1E cells reduced hormone-stimulated insulin secretion by 79%, and so the true role of SYT V in pancreatic hormone exocytosis is currently unclear (Iezzi *et al*. 2004). In PC12 cells, SYTV-GFP was reported to co-localize with SYT I on dense-core vesicles which were able to undergo Ca^{2+}-dependent exocytosis (Saegusa *et al.* 2002). Additionally, SYT V has been reported to localize to axons in hippocampal neurons, where it can be found on both the plasma membrane and as a component of dense-core granules (Dean *et al.* 2012). SYT V mRNA has been reported in rat basophilic leukaemia cells, although its function in this cell type is currently unknown (Baram *et al.* 2001). Lastly, SYT V has been linked to the regulation of the Ca^{2+}-dependent process of phagocytosis. In resting macrophages, SYT V localizes to

recycling endosomes and to the plasma membrane where it concentrates in protruding filopodia. However, following stimulation, SYT V is rapidly transferred to the phagosomes where it remains throughout their maturation and eventual exocytosis (Vinet *et al*. 2008). The knock-down of SYT V results in a 50 % inhibition of phagocytosis, and this effect is particularly pronounced under conditions of large particle size and high particle number. Hence, it has been suggested that SYT V regulates the focal exocytosis of endosomal structures which provide additional membrane surface area for the formation of large phagosomes.

The bulk of the studies done thus far with the aim to characterize the function of SYT V have focused on the phagocytosis of *Leishmania donovani* by macrophages. *Leishmania* parasites are responsible for the potentially fatal visceral disease leishmaniasis in humans and are spread via infected female sand flies (Lodge and Descoteaux, 2004). Following infection, *Leishmania* promastigotes are phagocytosed by mononuclear phagocytes, and in order to survive and reproduce within human cells the parasite has evolved to inhibit phagosome fusion with components of the endosomal and lysosomal systems. The inhibition of these fusion events depends on the presence of the crucial virulence factor lipophosphoglycan (LPG) which covers the surface of the parasites (Lodge and Descoteaux, 2005). It is thought that, following the internalization of the parasite, LPG is transported from the parasite membrane to the phagosome membrane and disrupts lipid raft microdomains. This ultimately inhibits fusion events between the phagosome and components of the endosomal and lysosomal networks. Hence, the accumulation of membrane proteins essential for the acidification of the phagosome such as NADPH oxidase is inhibited and this allows the parasite to maintain a favourable pH for survival within the host phagosomes.

It is now known that LPG from *Leishmania donovani* promastigotes partly inhibits phagosome maturation by causing the dissociation of SYT V from phagosome membranes (Vinet *et al*. 2009). Indeed, if a mouse macrophage cell line stably expressing SYTV-GFP is infected with *L. donovani* promastigotes the result is a significant decrease in the quantity of SYT V present in the phagosomes of infected cells. The mechanism whereby *L. donovani* is able to remove SYT V from phagosomes depends on the disruption of lipid rafts within the phagosome membrane. SYT V can be found on GM1-containing lipid raft microdomains in phagosomes and indeed phagosomes internalizing zymosan particles show co-localization between SYT V and GM1 (Vinet *et al*. 2009). However, phagosomes internalizing LPG-coated particles show co-localization only between GM1 and LPG. Hence, LPG insertion into the lipid membrane results in the exclusion of SYT V.

The process whereby SYT V is removed from immature phagosomes allows the promastigote to survive as the progressive acidification of the organelle fails. Indeed, SYT V controls phagolysosome biogenesis by regulating the trafficking of cathepsin D and vesicular proton-ATPase (V-ATPase) to the immature phagosomes. The knock-down of SYT V impairs cathepsin D and V-ATPase c subunit recruitment by up to 50 % whereas the recruitment of LAMP1, EEA-1, and cathepsin B is not affected (Vinet *et al.* 2009). The impact of this inhibition on the pH of the maturing phagosome is similar to that seen in the presence of LPG. Hence, SYT V regulates phagosome maturation, possibly by mediating the fusion of immature phagosomes with lysosomes containing cathepsin D and the V-ATPase. The insertion of LPG into the lipid rafts disrupts SYT V localization to phagosomes and therefore inhibits their acidification.

Since its discovery in 1995 as a novel non-neuronal SYT the tissue distribution, subcellular localization, and possible function of SYT V have been partly characterized. Interestingly, a unique role of this SYT seems to be as a regulator of the internal pH of organelles via the recruitment of membrane proteins such as acidifying proton pumps. The work done thus far to characterize this feature of SYT V has been done entirely on phagosomes in macrophages, and therefore it will be of great interest to determine if SYT V is responsible for regulating the internal pH of other organelles.

6.2 SYTV-EGFP Over-Expression ELISAs:

I have shown that SYT V is present in HUVECs at both the mRNA and protein levels and that over-expressed SYTV-EGFP traffics exclusively to the WPBs. Therefore this member of the SYT family is now a prime candidate for the role of the calcium sensor regulating the Ca^{2+}-mediated exocytosis of WPBs from endothelial cells. In order to investigate this hypothesis, functional studies were performed with the aim to identify any role SYT V plays in the regulation of WPB secretion from HUVECs. Initially, these functional studies involved over-expression ELISAs whereby HUVECs were transfected with either the SYTV-EGFP construct or with a control cytosolic construct (YFP). Forty-eight hours following transfection, the now-confluent HUVECs were stimulated with either 1 µM ionomycin or with a control non-stimulating solution. Both the media and lysates were collected and the samples were processed for VWF and proregion ELISAs.

No significant differences in the extent of the stimulated or basal secretion of proregion were apparent between cells expressing SYTV-EGFP and those expressing YFP

(data not shown) suggesting that SYT V up-regulation does not affect the quantity of proregion secreted from stimulated HUVECs. However, the VWF ELISAs performed on the same samples used for the proregion ELISAs yielded conflicting results, as shown in Figure 6.1. The data generated from the first assay (Figure 6.1 (i)) suggests that SYTV-EGFP over-expression in HUVECs leads to a significant increase in VWF secretion in response to ionomycin exposure compared with YFP-expressing cells. However, Figure 6.1 (ii) shows the reverse effect whereby SYTV-EGFP over-expression leads to a significant decrease in VWF secretion compared with control cells. Finally, the third assay (Figure 6.1 (iii)) shows no significant changes in VWF secretion between cells over-expressing SYTV-EGFP and control cells. In my experience, it is unusual for the VWF ELISAs to offer such conflicting data when the proregion ELISAs performed on the same samples suggest that the extent of secretion remains unchanged between conditions. It is possible that SYTV-EGFP over-expression causes the deregulation of VWF secretion from HUVECs. However, the reasons why the release of VWF but not proregion is affected are currently unclear, but may be related to pH changes within the organelle caused by SYTV-EGFP over-expression (see Discussion). Therefore, at this point the data suggests that the up-regulation of SYT V may affect the exocytosis of WPBs, although it appears that the release of VWF is influenced considerably more so than that of smaller WPB-resident proteins such as proregion.

6.3 The Effects of SYTV-EGFP Over-Expression on the Calcium Sensitivity of WPB Exocytosis: The Dose-Response Curve

It has been well-documented thus far that over-expressed SYTV-EGFP localizes to WPBs in HUVECs and previous functional studies have suggested that SYTV-EGFP over-expression may influence the secretion of VWF from HUVECs. In order to better define the function of SYT V in HUVECs I examined the effects of SYTV-EGFP over-expression on the calcium sensitivity of WPB exocytosis using the dose-response curve assay. The experiments were performed as described in '2.7.4 Dose-Response ELISAs.' The raw data obtained from each replicate was normalized to the quantity of proregion secreted from YFP-expressing control cells exposed to 1 µM ionomycin. The final dose-response curve is shown in Figure 6.2. The two curves provided from cells over-expressing either SYTV-EGFP or YFP are broadly similar and show no significant differences in the quantity of proregion secreted in response to any of the six different concentrations of ionomycin examined. Hence,

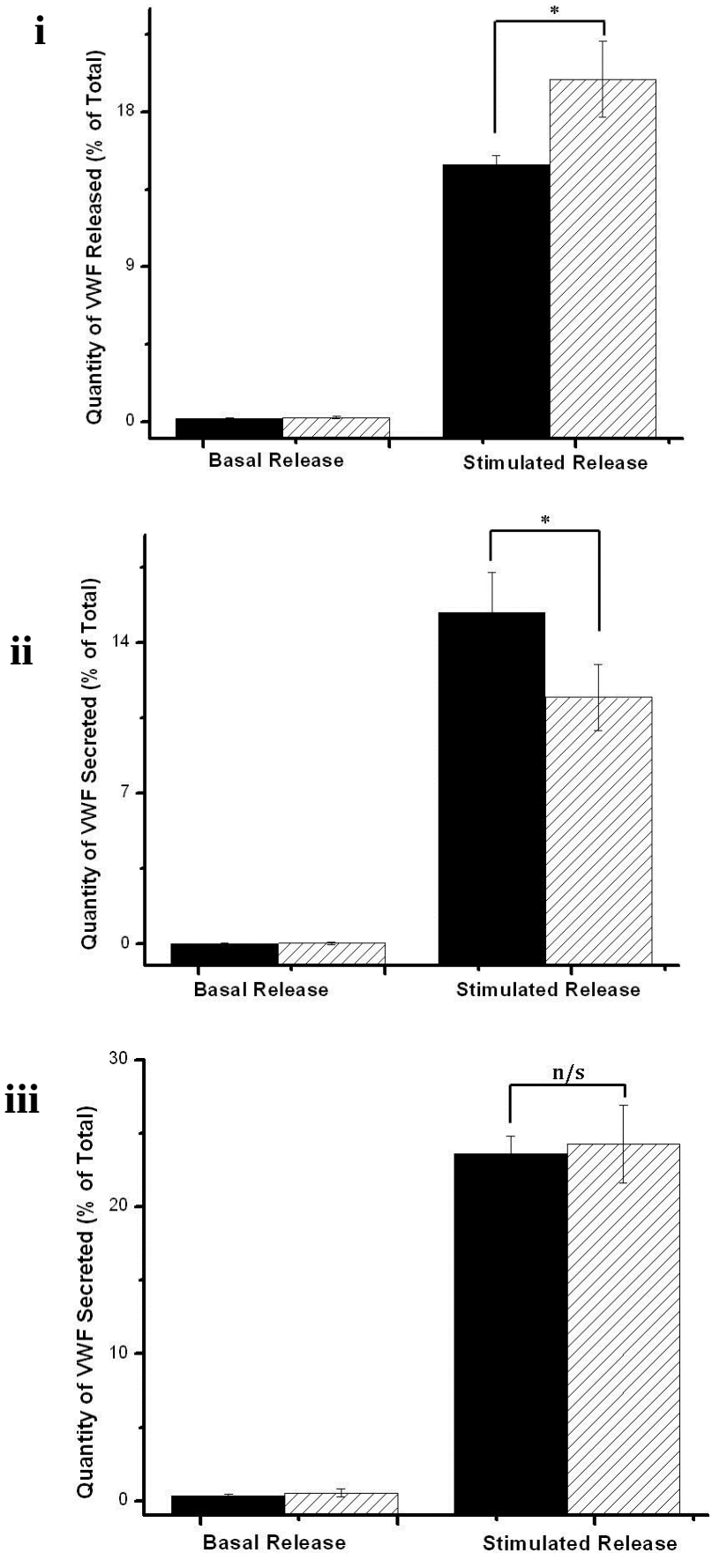

Figure 6.1 SYT V up-regulation influences the extent of VWF secretion from HUVECs.

VWF ELISAs were performed to examine the effects of SYTV-EGFP over-expression on VWF secretion from HUVECs compared with a control construct (YFP). The graphs show the quantity of VWF released as a percentage of the total quantity of VWF in the cells. Cells incubated with a control non-stimulating solution provided the data for the basal release of VWF. Cells incubated with 1 µM ionomycin provided the data for the stimulated release of VWF. Black bars represent YFP-transfected cells. Hatched bars represent SYTV-EGFP-transfected cells. Panels (i), (ii), and (iii) show the results of three separate assays.

* P-value ‹ 0.05.
n/s = non-significant (p-value › 0.05)

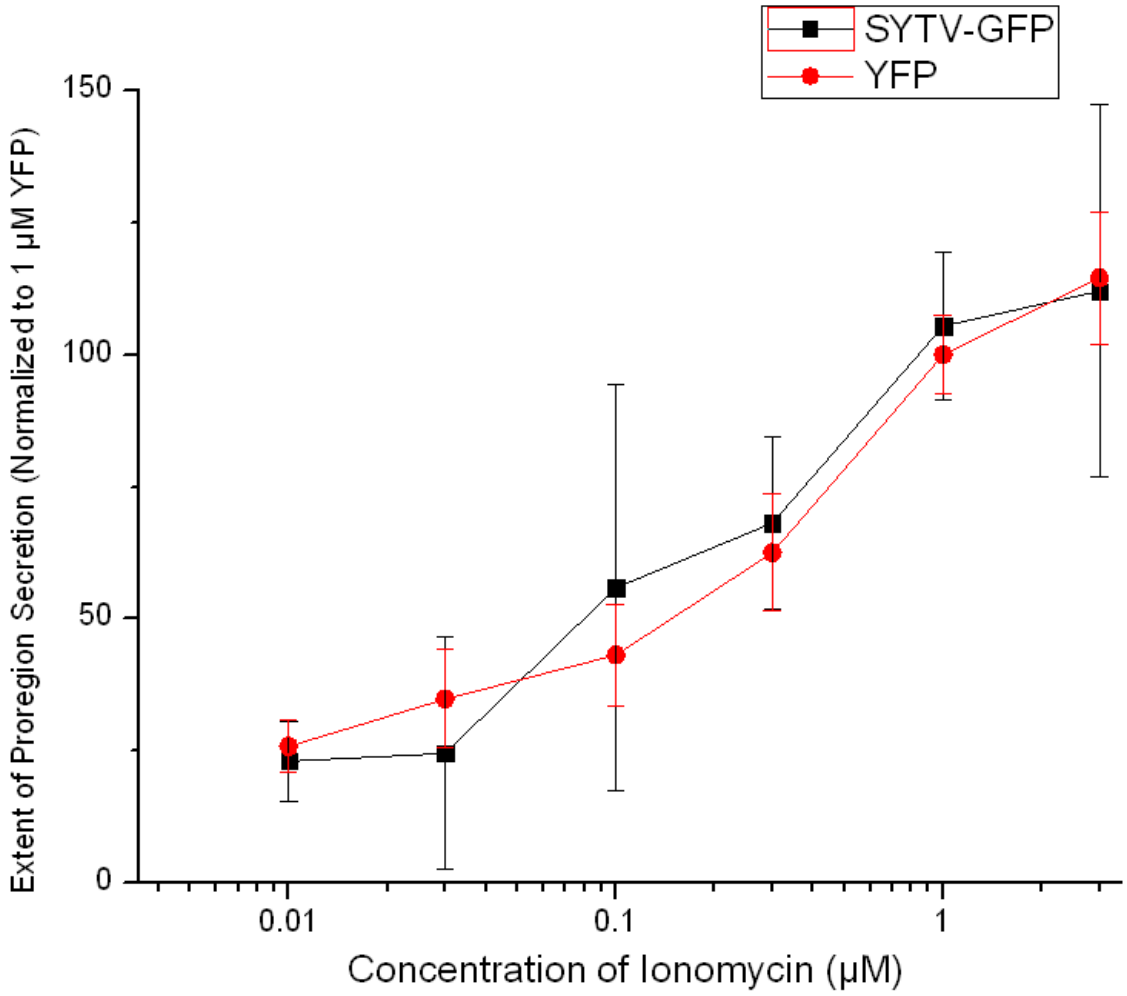

Figure 6.2. SYTV-EGFP over-expression does not influence the calcium sensitivity of WPB exocytosis.

HUVECs transfected with either SYTV-EGFP or with the cytoplasmic control construct YFP were stimulated with varying concentrations of ionomycin as indicated in the x-axis. The quantity of proregion secreted was determined using a proregion ELISA. This procedure was repeated three times. For each transfection, the data was normalized to the extent of proregion secreted from YFP-expressing cells in response to 1 µM ionomycin. Data from the three replicates was combined, and the means of the normalized values were used to plot the final dose-response curves.

it would appear that SYTV-EGFP over-expression does not affect the calcium-sensitivity of WPB exocytosis from HUVECs.

6.4 The Effects of the Knock-Down of SYT V on WPB Exocytosis:

The function of the SYT V protein in the regulation of WPB exocytosis is currently unclear. In order to further investigate this the SYT V protein was knocked-down in our model endothelial cells and functional studies were performed with the aim to determine if the loss of SYT V leads to any significant effects on the extent of WPB exocytosis from HUVECs.

6.4.1 The Optimization of the Knock-Down Protocol:

The knock-down of SYT V was achieved according to the protocol detailed in '2.2.4 The Knock-Down of SYT mRNA.' As the knock-down procedure must be optimized for each individual protein it was initially necessary to screen the siRNA to determine the ideal conditions for the knock-down of SYT V in HUVECs. Figure 6.3 shows the Western blot obtained following the blotting of HUVECs transfected with 200 pMol of either SYT V siRNA or control siRNA with antibodies against SYT V and tubulin. As can be seen, reasonable knock-down of the SYT V protein was achieved when HUVECs were transfected with 200 pMol of SYT V siRNA. I made additional attempts to optimize this effect by varying the quantity of transfected siRNA and the time for which cells were left in culture (data not shown) but I could not improve on that achieved with 200 pMol of SYT V siRNA.

Initially, it was necessary to determine if the knock-down of SYT V in HUVECs has any visible effect on the morphology and biosynthesis of WPBs. Therefore, ICC was performed using HUVECs transfected with 200 pMol of either SYT V siRNA or control non-targeting oligos. The results of this are shown in Figure 6.4. As can be seen, no visible differences are apparent between the transfected cultures as each has produced a confluent monolayer of morphologically-normal HUVECs. Additionally, each culture has generated large numbers of rod-shaped WPBs which are dispersed as expected throughout the cells. Therefore, SYT V knock-down does not yield any striking effects on the biosynthesis or morphology of either HUVECs or their WPBs.

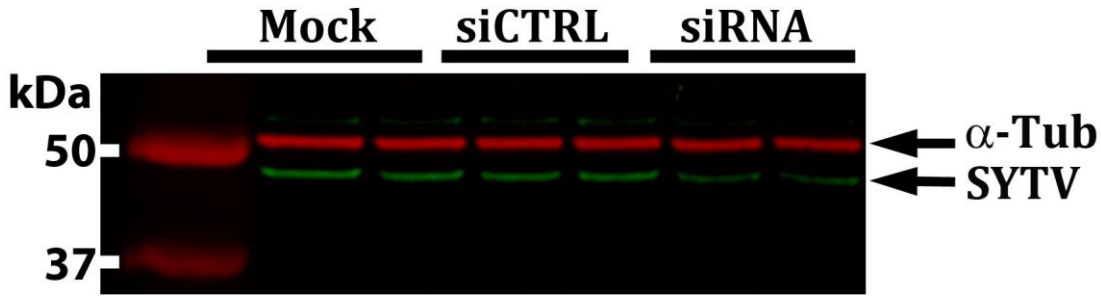

Figure 6.3. The SYT V protein is depleted in HUVECs following siRNA transfection.

Cells were transfected with 200 pMol of either SYT V siRNA or control non-targeting oligos (siCTRL) as indicated and were allowed to grow to confluency for forty-eight hours. A mock transfection was also performed (4 µL dH_2O). Lysates from each culture were extracted and Western blotting was carried out probing for SYT V (green) and tubulin (red). The sizes of the protein marker are indicated on the left of the blot. The knock-down of the SYT V protein is achieved following transfection with 200 pMol of SYT V siRNA. The tubulin loading control shows that an equivalent quantity of total protein was loaded into each well. The extent of the knock-down of SYT V in SYT V-siRNA-transfected HUVECs is 41.28% of that seen in control siRNA-transfected HUVECs (normalized to the total quantity of protein as determined from the tubulin loading control).

6.4.2 SYT V Knock-Down ELISAs:

In order to investigate whether the knock-down of SYT V impacts upon the exocytosis of WPBs from HUVECs functional studies were performed in the form of VWF and proregion ELISAs. The results of a representative VWF ELISA are shown Figure 6.5 (i). As can be seen, SYT V knock-down has no effect on the extent of the overall secretion of VWF from HUVECs, suggesting that SYT V does not influence WPB exocytosis. Proregion ELISAs were then performed using the collected samples and the results of a representative assay are shown in Figure 6.5 (ii). Again, SYT V knock-down has no effect on the overall exocytosis of proregion from transfected HUVECs. Therefore the knock-down of SYT V does not influence the extent of WPB exocytosis from endothelial cells.

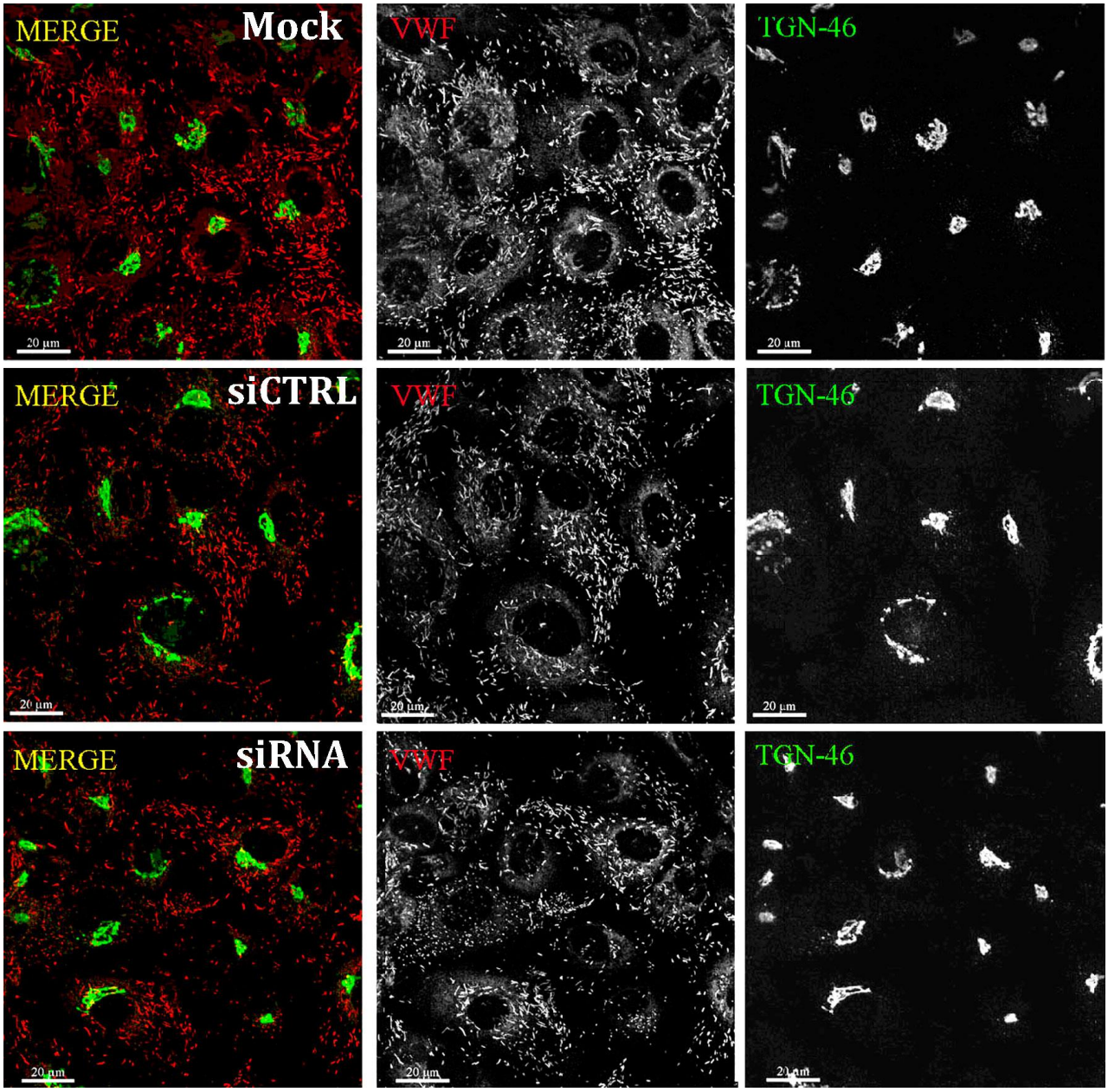

Figure 6.4. The knock-down of SYT V does not affect the morphology of either HUVECs or their WPBs.

HUVECs transfected with 200 pMol of either SYT V siRNA or with control non-targeting oligos as indicated were stained with antibodies against both VWF and TGN-46. A mock transfection was also included (4 µl of dH_20). The left-hand panels show the merged images, the middle panels show the VWF stain in the red channel, and the right-hand panels show the TGN-46 stain in the green channel. All cultures examined have grown to confluency and HUVECs appear morphologically normal. Likewise, each culture contains high numbers of large, rod-shaped WPBs.

6.5 SYT V Mutant Proteins and WPB Exocytosis:

The siRNA studies previously described are limited in that they require a strong knock-down of the target protein to overcome the residual functional effect of the endogenous protein. Therefore, a series of mutants of the SYT V protein were produced with the aim to abolish the normal function of endogenous SYT V in HUVECs. These mutants were over-expressed in HUVECs to determine if SYT V does indeed play a role in WPB exocytosis.

6.5.1 The SYT V Mutant Proteins:

Three fluorescent mutants of SYT V were generated: a cytoplasmic mutant (designated SYTV-EGFPΔTM), a full-length Ca^{2+}-insensitive mutant (designated SYTV-EGFP D/S), and a cytoplasmic Ca^{2+}-insensitive mutant (designated SYTV-EGFPΔTM D/S). SYTV-GFPΔTM is a cytoplasmic variant of SYT V and therefore lacks the transmembrane domain which normally characterizes members of the SYT family as integral membrane proteins (Perin *et al.* 1990). For the human SYT V protein, this transmembrane region is located between amino acids 24 and 45 according to the Uniprot database (entry O00445). In order to generate the SYTV-EGFPΔTM mutant, a forward primer was designed which eliminated both the transmembrane and N-terminal regions of the SYT V protein. Therefore, the final product of cloning will consist only of the linker region and the C2 domains of the SYT V protein and so is expected to be a cytoplasmic variant of the full-length protein.

Secondly, a Ca^{2+}-independent variant of full-length SYT V was generated, designated SYTV-EGFP D/S. Wild-type SYT V is a Ca^{2+}-dependent SYT due to a series of aspartate residues in its C2A domain which function to coordinate Ca^{2+} ions prior to secretory events. However, the Ca^{2+}-independent SYTs such as SYTs IV and XI have a serine residue in place of the third aspartate in the Ca^{2+}-binding motif of the C2A domain, rendering them unable to bind Ca^{2+} ions (von Poser *et al.* 1997). Therefore, a Ca^{2+}-dependent SYT such as SYT V can be converted to a putative Ca^{2+}-independent protein by mutating this essential aspartate. For the SYT V protein, this key residue is ASP197. Hence, in order to generate the SYTV-EGFP D/S mutant nucleotides 589, 590, and 591 (i.e. the codon GAC) of the SYT V cDNA sequence were mutated to AGC, resulting in an aspartate to serine mutation. This approach is illustrated in Figure 6.6.

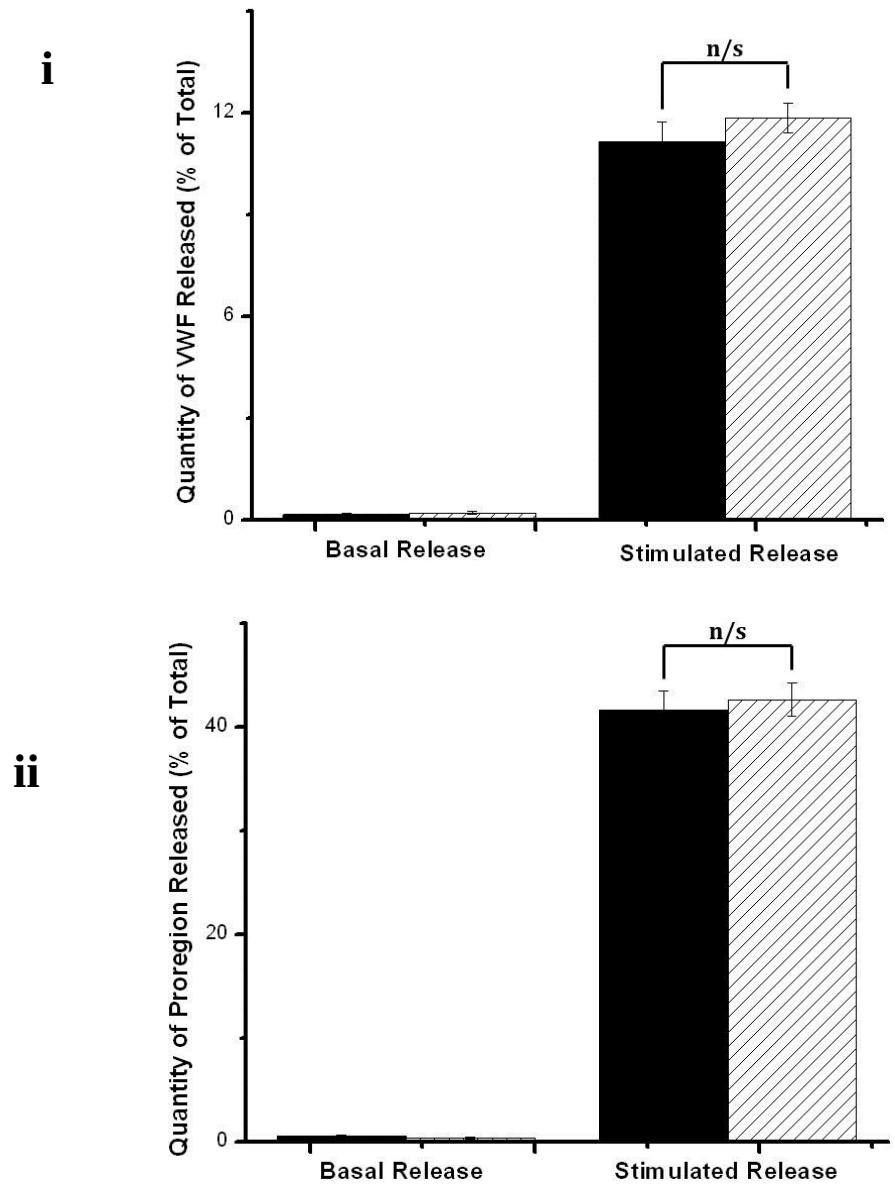

Figure 6.5. SYT V knock-down does not affect the exocytosis of WPBs.

HUVECs were transfected with either SYT V siRNA (200 pMol) or control siRNA (200 pMol). Media and lysates were collected from cells after forty-eight hours and processed for VWF and proregion ELISAs. Cells incubated with a control non-stimulating solution provided the data for basal secretion. Cells incubated with 1 µM ionomycin provided the data for stimulated secretion. Panel (i) shows the quantity of VWF released as a percentage of the total quantity of VWF in the cells. Panel (ii) shows the quantity of proregion released as a percentage of the total quantity of proregion in the cells. Black bars represent control siRNA-transfected cells. Hatched bars represent SYT V siRNA-transfected cells.

n/s = non-significant (p-value › 0.05)

n = 3 replicates from one vial of HUVECs; data is representative of 3 individual experiments performed on separate vials of HUVECs.

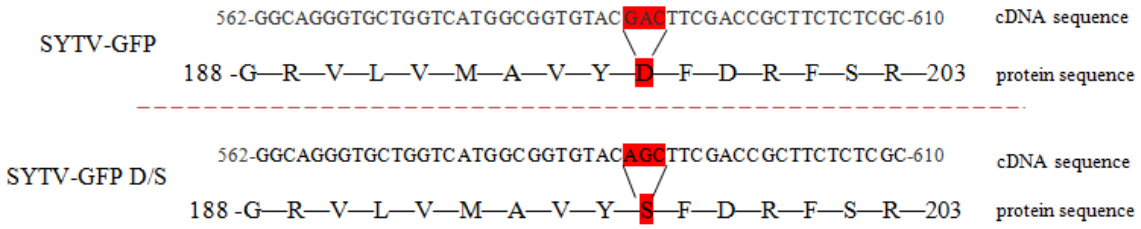

Figure 6.6. SYT V can be converted to a Ca^{2+}-independent SYT by the mutation of one essential aspartate residue in the C2A domain.

A D/S mutation was introduced into SYTV-EGFP to produce SYTV-EGFP D/S. For each construct, the cDNA sequence is provided as indicated while the amino acid sequence is shown underneath. The mutated nucleotides and their corresponding amino acids are emphasized in red.

The final SYT V mutant generated for these assays, designated SYTV-EGFPΔTM D/S, is a cytoplasmic version of the SYTV-GFP D/S mutant and was intended to act as a dominant negative inhibitor of endogenous SYT V. This construct was produced by PCR using the forward primer originally designed to generate SYTV-GFPΔTM to eliminate the N-terminal and transmembrane domains of the SYTV-GFP D/S full-length mutant, thereby generating SYTV-GFPΔTM D/S. An image depicting the creation of these three SYT V mutants is provided in Figure 6.7

6.5.2 The Over-Expression of the SYT V Mutant Proteins in HUVECs:

The three newly-synthesized SYT V mutants were used for proregion over-expression ELISAs with the aim to determine if non-functional variants of the SYT V protein could affect the extent of WPB secretion from HUVECs. The results of a representative assay are shown in Figure 6.7. As can be seen, it would appear that none of the three mutants examined here affect the quantity of proregion secreted from HUVECs as the levels of secretion are not significantly different to that seen from cells expressing the wild-type SYTV-EGFP construct. Therefore, the data provided here and from other functional studies performed to date suggest that SYT V is not involved in the regulation of WPB secretion from endothelial cells.

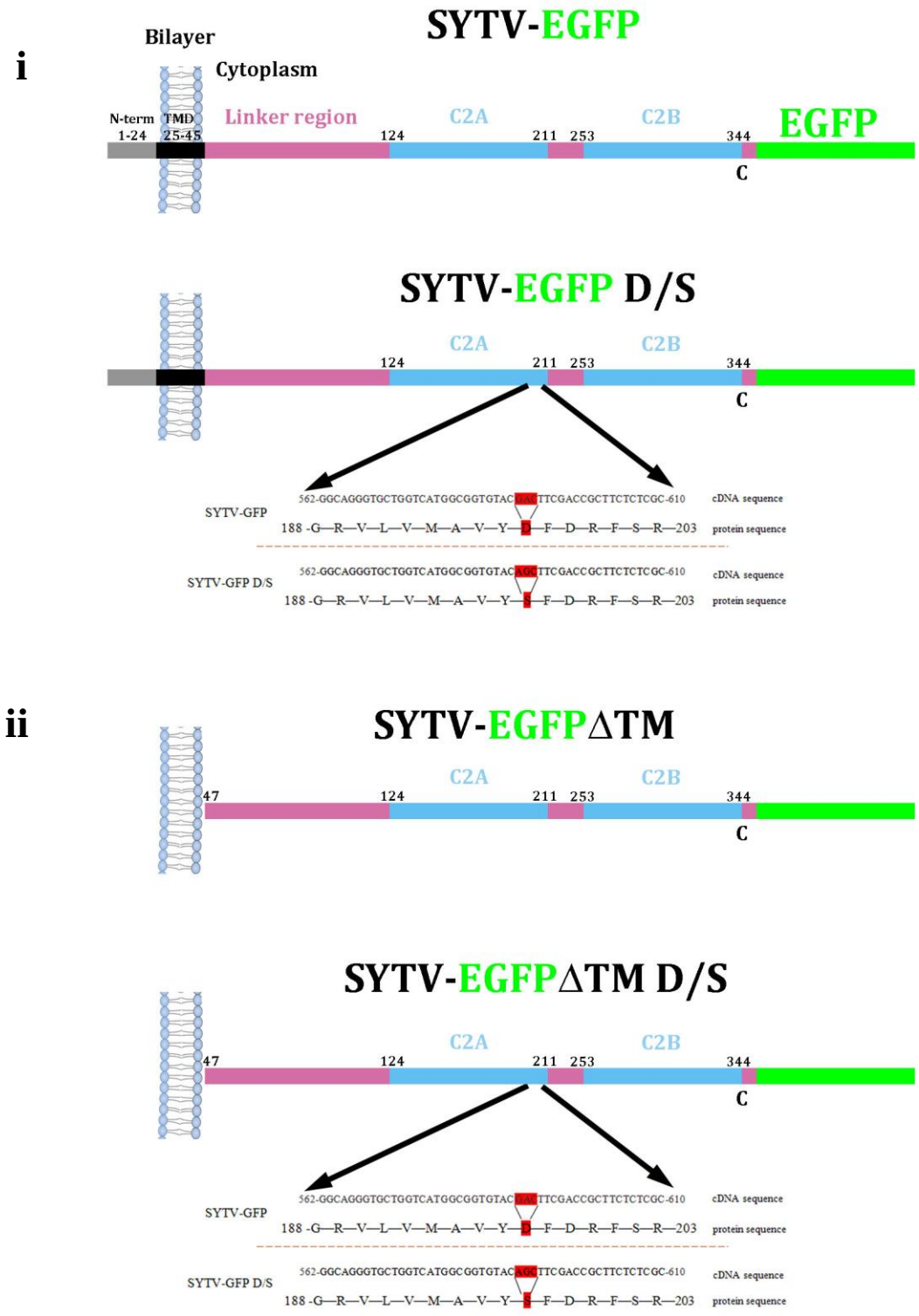

Figure 6.7. Three mutant variants of the SYTV-EGFP construct were created.

Panel (i) depictes the structure of the SYTV-EGFP D/S mutant compared with the SYTV-EGFP construct. Panel (ii) depictes the structures of the SYTV-EGFPΔTM and SYTV-EGFPΔTM D/S constructs. The numbers of the amino acid residues marking the boundaries of each domain of SYT V are shown in black.

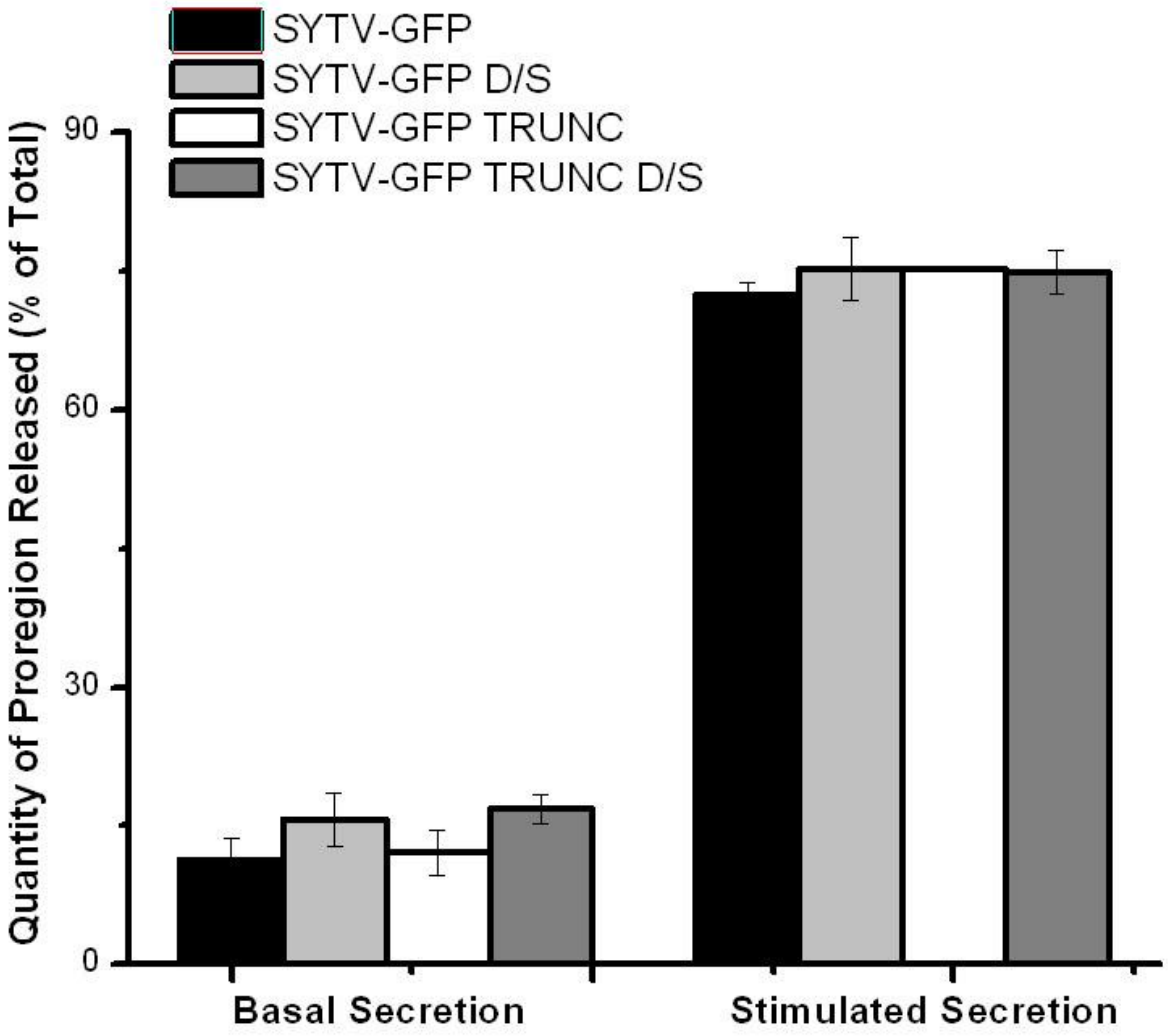

Figure 6.8. The up-regulation of mutant SYT V proteins does not affect the secretion of proregion from HUVECs.

The results of a representative experiment examining the effects of the over-expression of mutants of the SYT V protein on proregion secretion from HUVECs are shown. Media and lysate were collected from cells expressing SYTV-EGFP, SYTV-EGFP D/S, SYTV-EGFPΔTM, or SYTV-EGFPΔTM D/S and a proregion ELISA was performed. The graph shows the quantity of proregion released as a percentage of the total quantity of proregion in the cells. Cells incubated with a control non-stimulating solution provided the data for the basal release of proregion. Cells incubated with 1 µM ionomycin provided the data for the stimulated release of proregion. No significant differences in proregion secretion are apparent between cell expressing wild-type SYT V (SYTV-EGFP) and those expressing any of the three mutant variants of SYT V.

n = 3 replicates from one vial of HUVECs; data is representative of 3 individual experiments performed on separate vials of HUVECs.

6.5.3 The Subcellular Localization of the SYT V Mutants:

It was of interest to identify the subcellular localization of each of the three novel SYT V mutants to determine if the trafficking of these proteins is affected by their mutations. Therefore HUVECs expressing each of the four constructs were fixed forty-eight hours following transfection and processed for ICC. The results of this are shown in Figure 6.9. As can be seen, no obvious differences in the subcellular localization of the SYT V variants are apparent as each plasmid appears to localize strongly to the WPBs. For the SYTV-EGFP D/S mutant this was expected as a single amino-acid substitution is not predicated to be sufficient to alter the subcellular localization of this construct compared with wild-type SYTV-EGFP. For the SYT V variants which lack the transmembrane domain (SYTV-EGFPΔTM and SYTV-EGFPΔTM D/S), it is likely that these protein are trafficking to the WPBs via interactions with integral membrane proteins present on the surface of the organelle. It is probable that these mutant variants of SYT V are peripheral membrane proteins and associate with the WPBs through other membrane proteins (Li *et al*. 1995). However, notice the appearance of diffuse cytoplasmic staining for both SYTV-EGFPΔTM and SYTV-EGFPΔTM D/S in Figure 6.8 suggesting that a proportion of the protein can be found within the cytoplasm. The expression of the three SYT V mutants does not affect the morphology of WPBs as HUVECs expressing these plasmids all contain high numbers of rod-shaped WPBs.

6.6 Discussion:

The general function of SYT V has yet to be determined although it is known to regulate the exocytosis of LDCVs from PC12 cells (Saegusa *et al*. 2002), the formation of phagosomes in macrophages (Vinet *et al.* 2008), and plays an as-yet unclear role in insulin secretion (Iezzi *et al*. 2004). The observation that SYTV-EGFP localizes extensively to WPBs suggests that endogenous SYT V is located in an ideal position to regulate the Ca^{2+}-dependent exocytosis of granules from endothelial cells. In order to further investigate the function of the SYT V protein in HUVECs, over-expression ELISAs were performed which yielded conflicting data. The VWF ELISAs revealed a dysregulation of WPB exocytosis following SYTV-EGFP over-expression whereas the proregion ELISAs performed on the same samples showed no effect of SYT V up-regulation on proregion secretion. There are a number of possibilities which explain these interesting findings. Firstly, it may simply be that

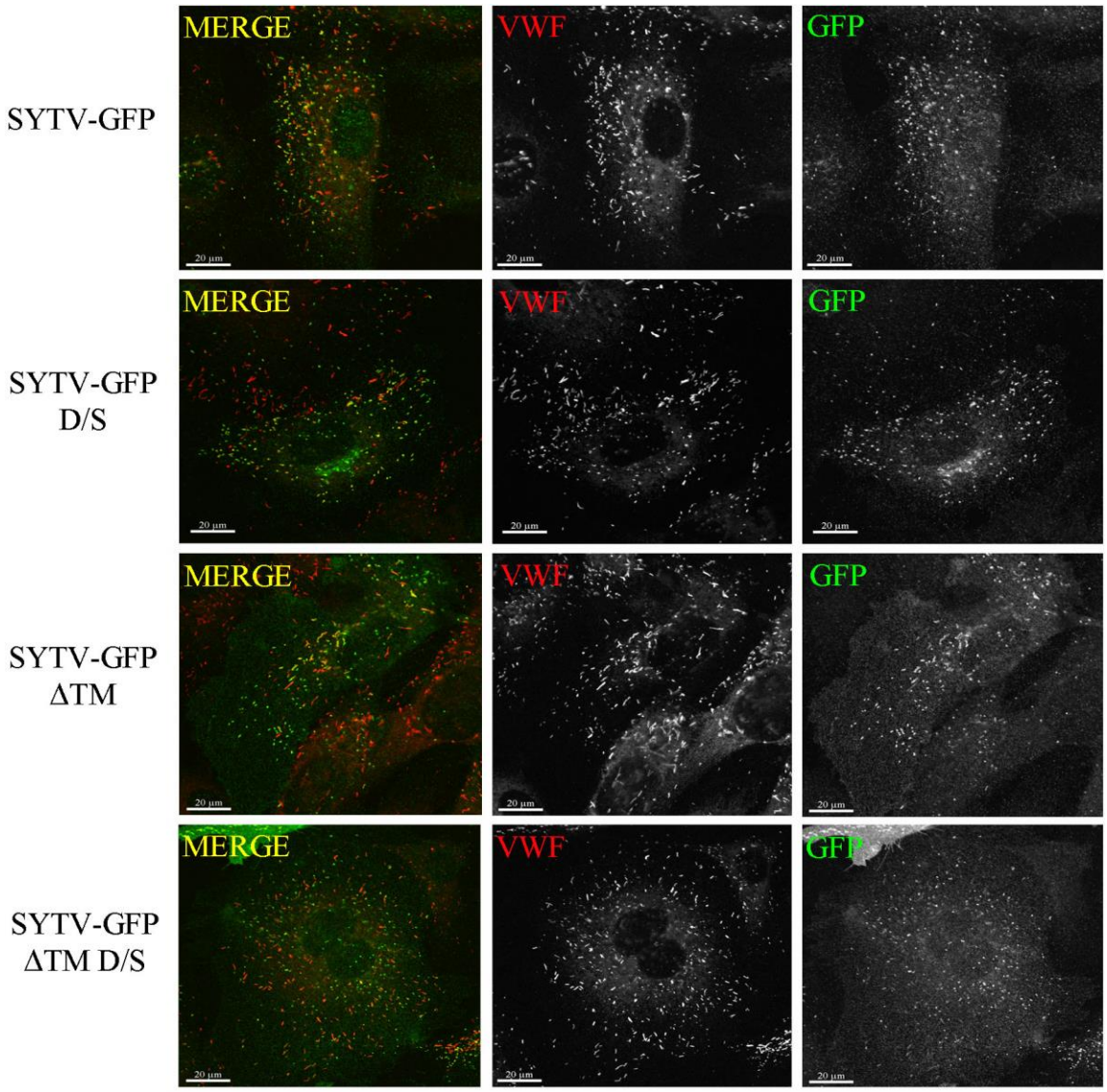

Figure 6.9. Mutant SYT V proteins localize to WPBs.

HUVECs expressing SYTV-EGFP, SYTV-EGFP D/S, SYTV-EGFPΔTM, or SYTV-EGFPΔTM D/S as indicated on the left of the figure were stained for either VWF or GFP. The left-hand panels show the merged images, the middle panels show the VWF stain in the red channel, and the right-hand panels show the GFP stain in the green channel. In all four cultures the constructs localize to the WPBs. Notice the diffuse cytoplasmic staining seen in cells expressing variants of SYT V which lack the transmembrane domain (SYTV-EGFPΔTM and SYTV-EGFPΔTM D/S). All four constructs showed a similar transfection efficiency (approximately 20%) in HUVECs and all showed an optimum expression time of 48 hours.

the proregion ELISAs are more accurate than the VWF ELISAs although such conflicting results have not been observed in other experimental series. In order to test this possibility it is essential that substantially more replicates of the VWF and proregion assays are performed to verify that the unusual effects seen here are consistent and reproducible. Secondly, it is possible that SYT V may be involved in mediating the formation or structure of the fusion pore. In this case, the up-regulation of SYT V in HUVECs may lead to alterations in the size of the fusion pore, allowing the release of proregion but not VWF from transfected cells. Equally, an increase in the number of kiss-and-run events due to fusion pore instability may explain these findings. Live-cell imaging using the SYTV-EGFP construct would be required to test these possibilities. Thirdly, it is possible that SYT V over-expression results in alterations in the internal pH of granules in transfected cells. Indeed, SYT V is known to be involved in the acidification of phagosomes in macrophages by mediating the recruitment of V-ATPase and cathepsin D (Vinet *et al*. 2009). A dysregulation of the internal pH of the WPBs may influence the exocytosis of multimeric VWF more so than the smaller and more mobile proregion. However, increases in the internal pH of WPBs would lead to the rounding-up of the granules, and the lack of any effect of SYTV-EGFP over-expression on the morphology of WPBs argues against this hypothesis. Lastly, it is possible that the over-expression of SYT V influences not the regulated secretion of VWF but rather its release via the constitutive pathway. This would explain the observation that SYTV-EGFP over-expression affects VWF but not proregion secretion, as proregion is found exclusively within WPBs whereas VWF is also found within the constitutive pathway (Arribas and Cutler, 2000). Future work may focus on testing these alternatives to better characterize the function of the SYT V protein in HUVECs.

The SYTV-EGFP construct was also used to establish a dose-response curve with the aim to determine if the up-regulation of SYT V in HUVECs influences the calcium sensitivity of WPB exocytosis. Although recent work has suggested that members of the SYT family can function cooperatively to determine the sensitivity of secretory events (Gao *et al.* 2000, Wang *et al.* 2004), the dose-response curve constructed here demonstrated that SYT V is not involved in determining the calcium sensitivity of WPB exocytosis. To further investigate the function of SYT V in endothelial cells, mutant variants of the SYTV-EGFP construct were produced and over-expressed in HUVECs but again no functional effects on WPB exocytosis were identified. However, it is important to consider that all over-expression studies are limited in that they rely on a high transfection efficiency to overcome the background secretion from non-transfected cells. It is possible that these studies did not

achieve a sufficient level of expression of the SYTV-EGFP construct to allow the identification of a functional effect. Indeed, the issue of the poor transfection of an unrelated SYTV-EGFP construct has been identified as an obstacle in other studies (Iezzi *et al*. 2004). To overcome this problem, knock-down studies were attempted using siRNA specific for SYT V. In keeping with the previous observations, no effects on WPB exocytosis were reported following the knock-down of SYT V in HUVECs. However, this work was compromised as the optimum knock-down of the SYT V protein was low (approximately 40%). It is likely that the extent of the knock-down of SYT V was not sufficient to abolish the function of the endogenous protein as only a small proportion of the total SYT V molecules present in HUVECs may be required to achieve a wild-type phenotype. Additionally, the quantification of the knock-down was challenging as multiple bands representing the SYT V protein were visualized by Western blotting and the commercial antibody failed to detect the endogenous protein by ICC. More accurate quantification of SYT V knock-down in HUVECs could be achieved by using real-time PCR, and indeed this technique could also be useful in further optimizing the knock-down protocol for SYT V mRNA. Lastly, it is possible that following the knock-down of SYT V in HUVECs another member of the SYT family is able to compensate for its loss, and indeed functional redundancy between members of the family has been reported (Lynch and Martin, 2007, Nishiki and Augustine, 2004).

In conclusion, this work has demonstrated that SYT V, despite its strong localization to WPBs in HUVECs, most likely does not play a role in their exocytosis. However, there have been many limitations associated with these functional studies, as has been discussed. The next step in determining the function of SYT V in HUVECs would be to perform live-cell imaging experiments using the SYTV-EGFP construct over-expressed in our model endothelial cells. This would allow the accumulation of real-time secretory data on a single-cell level, overcoming the limitations of the over-expression and knock-down studies. Additionally, as SYT V plays a role in the regulation of pH within phagosomes it would be of interest to determine if SYT V up-regulation influences the internal pH of WPBs through the use of pH-sensitive GFP mutants. Finally, the generation and analysis of a SYT V knock-down mouse would shed more light on the function of SYT V in both endothelial cells and other cell types. Such a mouse model is not available at present but its creation would offer a wealth of possibilities for future research.

Chapter 7

Investigating the Functions of SYTs VIII and XVII in HUVECs

7.1 Chapter Overview:

The Ca^{2+}-independent SYTs VIII and XVII are expressed in HUVECs and both can be found as components of WPBs when over-expressed. Despite this, for reasons which have been discussed neither protein has been identified as an outstanding candidate for the role of the calcium sensor regulating WPB exocytosis from endothelial cells. However, as both SYTs are found within the WPB membrane a series of functional studies were undertaken with the aim to determine if either one of these proteins does indeed play a role in the regulated exocytosis of the granules.

7.2 SYT VIII:

7.2.1 Background Information:

As is the case with many members of the SYT family there has been relatively little work done attempting to characterize the distribution and function of SYT VIII. It is known that this SYT belongs to a group of paralogues consisting of SYTs I, II, V, and VIII (Monterrat *et al*. 2006) and that it contains several mutations in its C2A domain which render it unable to bind Ca^{2+} ions (von Poser *et al.* 1997). Further evidence suggesting that SYT VIII is a Ca^{2+}-insensitive SYT comes from the observation that a fluorescent fragment of SYT VIII, SYT8-C_2AB-eGFP, does not translocate to internal membranes upon a rise in cytosolic calcium levels (Kishore *et al.* 1998). SYT VIII contains two putative PKA phosphorylation sites in its cytoplasmic region and interestingly also contains a histidine-rich region consisting of the sequence HRHRHRK which is not seen in other family members (Kishore *et al.* 1998). The titration of these histidine residues could impact the binding of SYT VIII to other proteins such as SNARES and therefore changing pH levels could be a stimulus for secretory events which are regulated by SYT VIII.

The relatively limited work done to date examining the distribution of SYT VIII suggests that it is broadly expressed in mammals. SYT VIII is found as a 52-kDa protein in the rat renal cortex and inner medulla, and RT-PCR has demonstrated the existence of SYT

VIII mRNA in the rodent kidney, cerebral cortex, liver, lung, and heart (Kishore *et al*. 1998). Indeed, an extensive analysis of the distribution of SYT VIII in the rat kidney showed that the protein could be found in the cortex, outer medulla, and inner medulla. SYT VIII expression has also been reported in the insulinoma cell line HIT-5HT and in PC12 cells (Monterrat *et al*. 2006).

Like many members of the SYT family, SYT VIII exists as a number of isoforms and indeed different variants of the protein show different subcellular localizations. ICC and subcellular fractionation studies have reported the existence of two isoforms of the SYT VIII protein consisting of either 50 or 40 kDa which are distinguished by variations in the N-terminus of the protein (Monterrat *et al.* 2006). The 40 kDa variant is a cytosolic protein in the brain, in PC12 cells, and in clonal β-MIN6 cells whereas the 50 kDa isoform is found in clusters on vesicles and co-localizes with the Golgi SNARE protein Vti1a. In neurons, SYT VIII immunoreactivity is confined to the soma and co-stains with synaptophysin, a marker of synaptic vesicles (Monterrat *et al.* 2006).

The bulk of the work done thus far to determine the function of SYT VIII has focused on its role in the regulation of the secretion of the acrosome from sperm cells. The sperm acrosome is a single large secretory granule which is released in response to the increasing Ca^{2+} levels generated when the sperm surface membrane contacts receptors in the zona pellucida surrounding the egg. SYT VIII has been found at both the mRNA and protein levels in mouse spermatogenic cells (Hutt *et al*. 2002). Fractionation studies have demonstrated that SYT VIII is found specifically in the membrane fraction and co-sediments with markers of the mouse sperm head such as the sperm-specific β-1,4 galctosyl transferase. Furthermore, SYT VIII is localized to the acrosomal crescent and the densitometric analysis of Western blots demonstrated that SYT VIII reactivity diminishes by 54% following stimulation of sperm cells with the calcium ionophore A23187. SYT VIII is now known to bind to syntaxin 2, a SNARE protein which is also expressed in sperm cells and localized to the acrosome (Hutt *et al.* 2005). Recombinant fragments of SYT VIII and syntaxin 2 inhibit the acrosomal reaction in streptolysin O-permeabilized sperm in a dose-dependent manner. The same effect is seen following the addition of antibodies specific for SYT VIII. Therefore, it has been proposed that SYT VIII and syntaxin 2 play a role in the regulation of the secretion of the acrosome from mouse sperm cells.

In conclusion, although little is known concerning the function of SYT VIII, evidence to date suggests that it is a broadly-distributed, Ca^{2+}-insensitive SYT which plays a potentially-vital role in the exocytosis of the acrosome from sperm cells. As with many

members of the SYT family, the presence of numerous isoforms of the protein, each with unique subcellular distributions, makes the study of SYT VIII challenging.

7.2.2 SYTVIII-EGFP Over-Expression ELISAs:

7.2.2.1 Forty-Eight Hours Following SYTVIII-EGFP Transfection:

Studies thus far have demonstrated that SYT VIII can be found at both the mRNA and protein levels in HUVECs and that over-expressed SYT VIII localizes to WPBs. Hence, SYT VIII is a strong candidate for the role of the calcium sensor regulating WPB secretion from endothelial cells. In order to investigate this hypothesis over-expression ELISAs were performed with the aim to examine the effect of the up-regulation of SYT VIII on WPB exocytosis. Briefly, HUVECs were transfected with either SYTVIII-EGFP or with the control cytoplasmic construct YFP and were seeded onto 6-well plates. After forty-eight hours the now-confluent cells were stimulated with either 1 μM ionomycin or with a control non-stimulating solution. The media and lysates were collected from the cells and these samples were processed for ELISAs as detailed in '2.7 The Enzyme-Linked Immunosorbent Assay (ELISA) Protocol.' Both the VWF and proregion ELISAs demonstrated that the over-expression of SYTVIII-EGFP in HUVECs cultured for forty-eight hours does not affect the extent of WPB release compared with cells expressing YFP (data not shown).

7.2.2.2 Twenty-Four Hours Following SYTVIII-EGFP Transfection:

The ELISAs performed at forty-eight hours following transfection have indicated that the up-regulation of SYT VIII in HUVECs does not influence WPB exocytosis. However, the subcellular localization screen examining the distribution of SYTVIII-EGFP described in Chapter Four has demonstrated that the construct shows a higher expression level across the HUVEC monolayer and a more intense perinuclear staining pattern twenty-four hours following transfection. I was interested to see if a shorter culture time following transfection would influence the results of the VWF and proregion ELISAs. Therefore, HUVECs transfected with either SYTVIII-EGFP or YFP were allowed to grow to confluency for twenty-four hours after which point the media collections and ELISAs were repeated. Interestingly, for both the VWF and proregion assays every replicate showed a clear trend towards an increase in the quantity of material secreted from SYTVIII-EGFP-transfected

HUVECs compared with YFP-expressing cells. Example VWF and proregion assays are shown in Figure 7.1. In most cases, however, the difference in secretion between the cultures did not reach statistical significance. It is possible that SYTVIII-EGFP over-expression does influence the secretion of WPBs from HUVECs although an increased number of replicates would be required to confirm this. Additionally, the SYTVIII-EGFP construct has a poor transfection efficiency in HUVECs and it may be that its expression level is too low to allow significant results to be generated from these assays.

7.2.3 The Effects of the Knock-Down of SYT VIII on WPB Exocytosis:

As the previous series of functional experiments has proved inconclusive knock-down ELISAs were performed to determine if the loss of SYT VIII from HUVECs has a significant effect on WPB exocytosis.

7.2.3.1 The Optimization of the Knock-Down Protocol:

As the knock-down procedure must be tailored for individual proteins it was initially necessary to determine the optimum conditions for the efficient elimination of the SYT VIII protein in endothelial cells. A number of conditions were trialed which will not be discussed in detail here. The end-result of this process was that the optimum knock-down of SYT VIII is achieved with 400 pMol of siRNA and an incubation time of forty-eight hours. A representative Western blot showing the reduction in the level of SYT VIII protein in HUVECs treated in this way is shown in Figure 7.2. In keeping with previous observations (see Chapter 3), two bands representing the SYT VIII protein have appeared following Western blotting. The top band of approximately 80 kDa is diminished to a greater extent than the bottom band of 75 kDa. These two bands likely represent two separate isoforms of the SYT VIII protein. Therefore it is possible that the larger isoform has a shorter half-life in endothelial cells than the smaller variant, thus explaining the discrepancy in knock-down efficiency. The implications of this will be considered at a later stage (7.2.4 The Role of SYT VIII in Human Endothelial Cells – A Discussion.)

It was necessary to evaluate the effects of the knock-down of SYT VIII on the morphology of the HUVECs and their resident WPBs. Therefore, HUVECs transfected with 400 pMol of either SYT VIII siRNA or control siRNA were fixed forty-eight hours following transfection. ICC was performed with antibodies against VWF and TGN-46. The

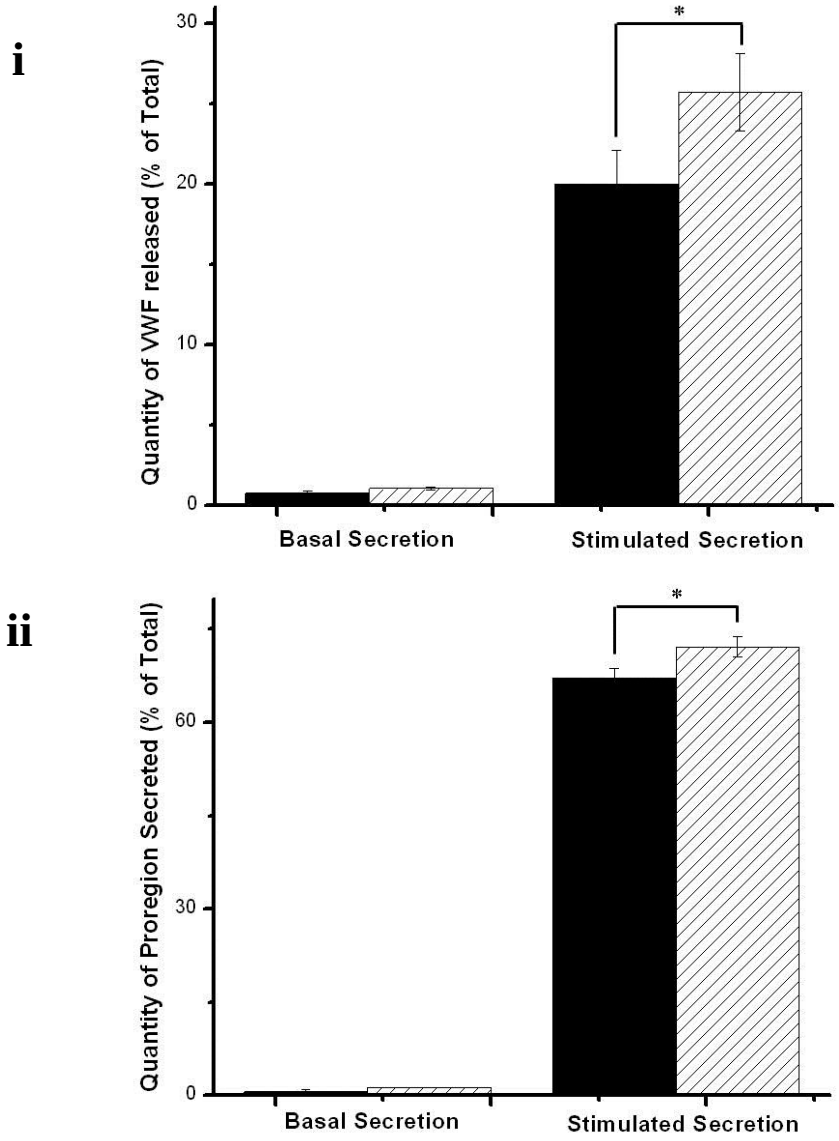

Figure 7.1. SYT VIII over-expression results in a trend for the increased secretion of WPBs from stimulated HUVECs.

HUVECs were transfected with either SYTVIII-EGFP or YFP. Media and lysates were collected from cells after twenty-four hours and processed for VWF and proregion ELISAs. Cells incubated with a control non-stimulating solution provided the data for basal secretion. Cells incubated with 1 µM ionomycin provided the data for stimulated secretion. Panel (i) shows the quantity of VWF released as a percentage of the total quantity of VWF in the cells. Panel (ii) shows the quantity of proregion released as a percentage of the total quantity of proregion in the cells. Black bars represent YFP-transfected cells. Hatched bars represent SYTVIII-EGFP-transfected cells.

* P-value ‹ 0.05.

n = 3 replicates from one vial of HUVECs; data is representative of 3 individual experiments performed on separate vials of HUVECs.

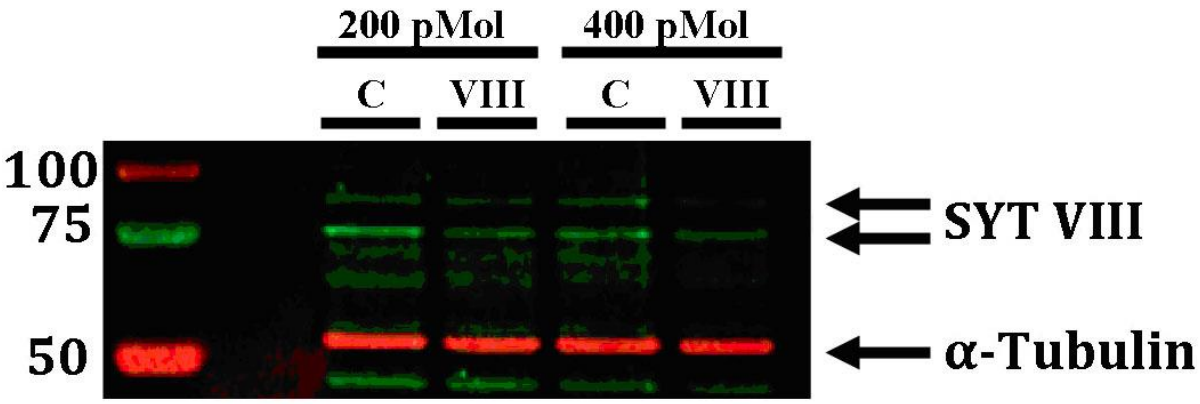

Figure 7.2. The SYT VIII protein is depleted in HUVECs following siRNA transfection.

HUVECs were transfected with either SYT VIII siRNA (VIII) or the control non-targeting oligos (C) and grown to confluency for forty-eight hours. Lysates from each culture were extracted and Western blotting was performed probing for SYT VIII (green) and tubulin (red). Reasonable knock-down of SYT VIII is achieved following transfection with 400 pMol of SYT VIII siRNA. The tubulin loading control shows that an equivalent quantity of protein was loaded into each well. Two isoforms of SYT VIII have been visualized at 80 and 75 kDa, as indicated. The larger isoform showed a knock-down of 66% compared with the loading control. The smaller isoform showed a knock-down of 31% compared to the loading control. The sizes of the marker are indicated on the left (kDa).

results of this are shown in Figure 7.3. As can be seen the cells have formed a confluent monolayer and the WPBs are numerous, large, and rod-shaped as expected. Therefore, this brief investigation suggests that SYT VIII does not influence either the biosynthesis or trafficking of WPBs in endothelial cells.

7.2.3.2 SYT VIII Knock-Down ELISAs:

It has now been established that the reasonable knock-down of SYT VIII can be achieved following the transfection of HUVECs with 400 pMol of SYT VIII siRNA and that this process has no obvious effects on cell morphology. Therefore, VWF and proregion ELISAs were performed with the aim to determine if the loss of the SYT VIII in endothelial

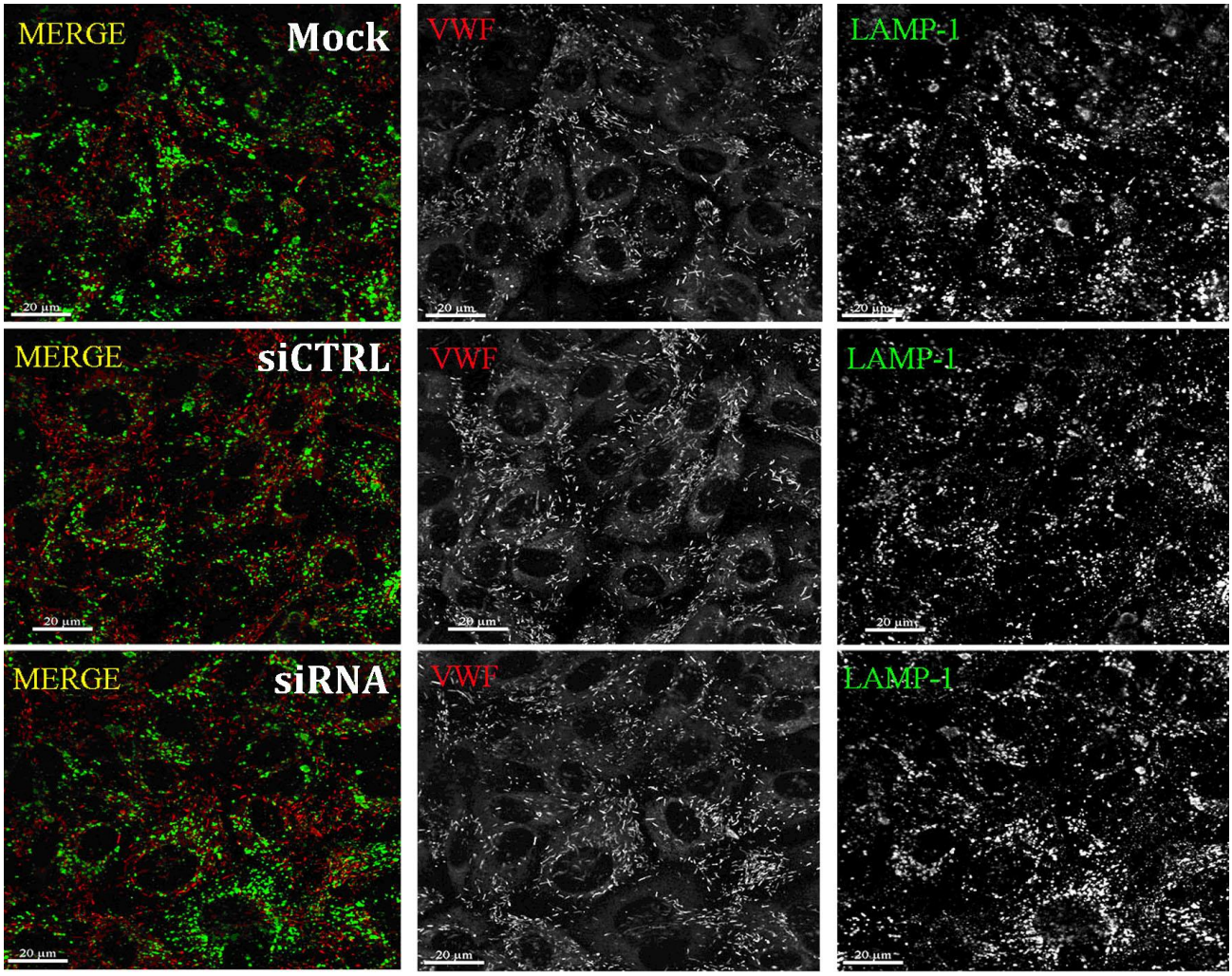

Figure 7.3. The knock-down of SYT VIII does not affect the morphology of either HUVECs or their WPBs.

HUVECs transfected with 400 pMol of either SYT VIII siRNA or control non-targeting oligos (siCTRL) as indicated were stained with antibodies against both VWF and TGN-46. A mock transfection was also included (4 µl of dH_20). The left-hand panels show the merged images, the middle panels show the VWF stain in the red channel, and the right-hand panels show the TGN-46 stain in the green channel. All cultures examined have grown to confluency and HUVECs appear morphologically normal. Likewise, each culture contains high numbers of large, rod-shaped WPBs.

cells has an effect on the exocytosis of WPBs. The results of a representative VWF ELISA are shown in Figure 7.4 (i). The knock-down of SYT VIII does not affect the quantity of VWF secreted from stimulated HUVECs. The results of a representative proregion ELISA are shown in Figure 7.4 (ii). Again, it would appear that the loss of the SYT VIII protein from HUVECs does not influence the overall secretion of proregion. These results suggest that, despite its subcellular localization, SYT VIII does not play a role in the Ca^{2+}-mediated exocytosis of WPBs from HUVECs. However, the knock-down effect achieved here was relatively weak and so it may be the case that the residual endogenous protein is sufficient to maintain a fully functional phenotype following SYT VIII knock-down. Additionally, it appears that numerous isoforms of SYT VIII are present simultaneously within HUVECs and these are inhibited to varying extents following siRNA transfection. The implication of this will be considered further in the following section.

7.2.4 The Role of SYT VIII in Human Endothelial Cells – A Discussion:

It is known that SYT VIII regulates the secretion of acrosomes from sperm cells via an interaction with the SNARE syntaxin-2 (Hutt *et al.* 2005). However the role of SYT VIII in other cell types is currently unclear. Here, I have attempted to determine if SYT VIII plays a role in the regulation of WPB exocytosis from endothelial cells. Firstly, I performed over-expression ELISAs using HUVECs transfected with the SYTVIII-EGFP construct and grown in culture for either forty-eight or twenty-four hours. The up-regulation of SYT VIII in HUVECs grown for forty-eight hours following transfection had no effect on the secretion of either VWF or proregion in response to ionomycin stimulation. In contrast, in HUVECs incubated for only twenty-four hours following transfection the over-expression of SYTVIII-EGFP resulted in a trend for the increased exocytosis of both VWF and proregion following stimulation. However these results did not generally reach statistical significance. A higher number of replicates would be required first and foremost to improve the reliability of this data. Equally, it would be of interest to repeat these ELISAs with HUVECs incubated for 8 or 12 hours following transfection. If SYTVIII-EGFP is progressively removed from WPBs as they mature and move through the secretory pathway then these shorter time periods may yield interesting results. Lastly, as the expression level of the SYTVIII-EGFP construct is notably low live-cell imaging would prove invaluable for the collection of data on a single-cell level. This would also provide an efficient means for rapidly increasing the sample size of SYTVIII-EGFP-expressing cells for statistical analysis without the need for time-

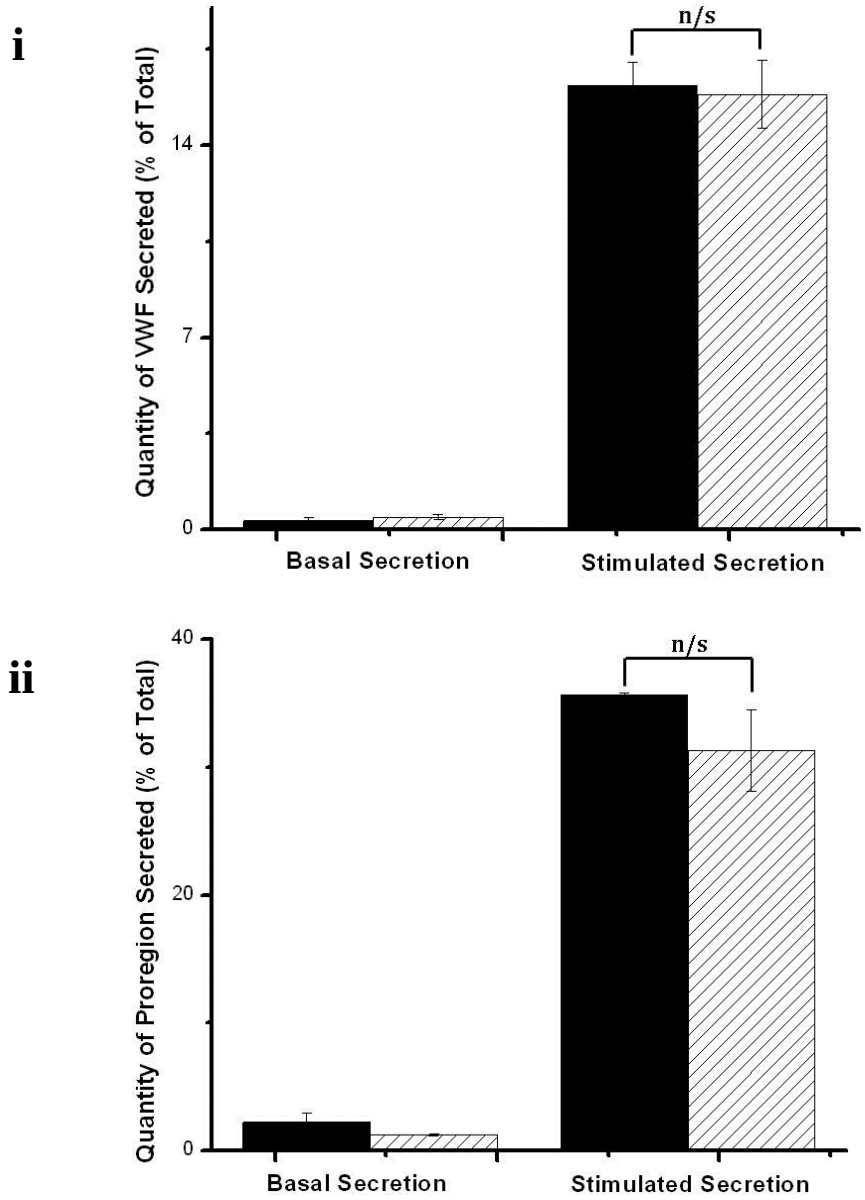

Figure 7.4. SYT VIII knock-down does not affect the exocytosis of WPBs.

HUVECs were transfected with either SYT VIII siRNA (400 pMol) or control siRNA (400 pMol). Media and lysates were collected from cells after forty-eight hours and processed for VWF and proregion ELISAs. Cells incubated with a control non-stimulating solution provided the data for basal secretion. Cells incubated with 1 µM ionomycin provided the data for stimulated secretion. Panel (i) shows the quantity of VWF released as a percentage of the total quantity of VWF in the cells. Panel (ii) shows the quantity of proregion released as a percentage of the total quantity of proregion in the cells. Black bars represent control siRNA-transfected cells. Hatched bars represent SYT VIII siRNA-transfected cells.

n/s = non-significant (p-value › 0.05)

n = 3 replicates from one vial of HUVECs; data is representative of 3 individual experiments performed on separate vials of HUVECs.

consuming biochemical assays.

As the over-expression ELISAs have proved inconclusive as to the involvement of SYT VIII in the regulation of WPB exocytosis I also performed SYT VIII knock-down assays. These studies showed that the knock-down of SYT VIII has no effect on the Ca^{2+}-mediated exocytosis of either VWF or proregion from HUVECs. They were however complicated by the fact that two variants of the SYT VIII protein are knocked-down to different extents following siRNA transfection. Western blotting revealed that the larger 80 kDa SYT VIII isoform was diminished to a greater extent than the smaller 75 kDa isoform. It is possible that the smaller isoform is more stable and has a longer half-life in endothelial cells. Alternatively, it may be that the pools of siRNA target the larger isoform with greater efficiency than smaller variants. Therefore, at this point it is impossible to say if the lack of an effect following SYT VIII siRNA transfection in HUVECs is an accurate observation or is simply the result of the inefficient knock-down of certain isoforms leading to a significant quantity of endogenous protein remaining in culture. These complications could be over-come by the generation of a SYT VIII $^{-/-}$ mouse as this would prove the optimum method for definitively eliminating every isoform of the SYT VIII protein in endothelial cell cultures.

To conclude, this work has demonstrated that SYT VIII is a WPB-associated protein and therefore is a key protein of interest for future work investigating the biosynthesis, trafficking and exocytosis of these organelles from endothelial cells. My attempts to assign a function for the SYT VIII protein have been complicated by the low transfection efficiency of the SYTVIII-EGFP construct and the simultaneous expression of multiple SYT VIII isoforms in HUVECs. However, multiple avenues for future research attempting to better define the role of the SYT VIII protein in endothelial cells have been identified and these would focus on live-cell imaging experiments, the production of a SYT VIII $^{-/-}$ mouse, and the generation of fluorescent constructs of endothelial-specific SYT VIII isoforms.

7.3 SYT XVII:

7.3.1 Background Information:

SYT XVII is the most recently characterized member of the SYT family and to date no studies have been undertaken attempting to determine its physical properties, tissue distribution, subcellular localization, or function. The only exception to this is the observation that following an over-expression screen of the SYT family in hippocampal neurons SYT

XVII localizes to internal vesicles in the axon (Dean *et al.* 2012). The identity of these axonal structures is currently unknown but they are unlikely to be synaptic vesicles. Here, I have demonstrated that SYT XVII is present in HUVECs as both an mRNA transcript and as a protein of approximately 65 kDa. Surprisingly, over-expressed SYTXVII-EGFP was shown to have an extensive distribution in HUVECs, localizing to the lysosomes, TGN, endosomal system, and WPBs. The fact that SYTXVII-EGFP localizes to WPBs suggests that this member of the SYT family may be involved in the regulation of WPB secretion. Therefore functional studies were undertaken with the aim to test this hypothesis. To my knowledge this will be the first study focusing on this Ca^{2+}-independent member of the SYT family.

7.3.2 SYTXVII-EGFP Over-Expression ELISAs:

Firstly, the effect of the up-regulation of SYT XVII on WPB secretion was examined using both VWF and proregion ELISAs performed on samples collected from HUVECs expressing either SYTXVII-EGFP or YFP. The results of the VWF ELISAs are shown in Figure 7.5. In Figure 7.5 (i), SYTXVII-EGFP over-expression has resulted in a significant decrease in the extent of regulated VWF secretion compared with that seen from the control YFP-expressing cultures. However, in the assay shown in Figure 7.5 (ii) the opposite effect is seen whereby SYTXVII-EGFP over-expression results in an increase in VWF secretion. Lastly, Figure 7.5 (iii) shows no significant differences in secretion between SYTXVII-EGFP-expressing HUVECs and control cells. The reasons for these discrepancies are currently unclear although it would appear that SYTXVII-GFP over-expression has resulted in the deregulation of VWF secretion.

As these VWF ELISAs have yielded conflicting results proregion ELISAs were carried out on the collected samples in an attempt to further investigate the effects of SYTXVII-EGFP over-expression on WPB secretion. Surprisingly, for all three assays no significant differences in proregion secretion were identified between cells over-expressing SYTXVII-EGFP and YFP (data not shown). Therefore SYTXVII-EGFP over-expression does not affect the extent of proregion secretion from HUVECs but does seen to have an as-yet unclear effect on VWF secretion. Interestingly, this data is similar to that generated from the ELISAs examining the effect of the over-expression of SYTV-EGFP in HUVECs.

7.3.3 The Role of SYT XVII in Human Endothelial Cells – A Discussion:

The observations that SYT XVII is expressed in HUVECs and traffics to the WPBs when over-expressed imply that this member of the SYT family is a strong candidate for the role of the calcium sensor regulating WPB exocytosis at the plasma membrane. Over-expression ELISAs using the SYTXVII-EGFP construct were performed with the aim to investigate this theory. These showed surprising results whereby the up-regulation of the SYT XVII protein has a very similar effect to that of SYT V. Indeed, each VWF assay performed yielded conflicting results whereas the proregion assays carried out on the same samples showed no effect of SYTXVII-EGFP over-expression on WBP exocytosis. The reasons for these discrepancies are extensive and include changes in the internal pH of the WPBs, dysregulation of the constitutive but not regulated release of VWF, alterations to the size and formation of the fusion pore, or simply being the result of differences in the accuracies of the two assays. These possibilities also explain the effect of the up-regulation of the SYT V protein in HUVECs and have been discussed extensively elsewhere (see 6.6 Discussion). Therefore they will not be re-evaluated here but it will suffice to say that SYT XVII may have an interesting but as-yet unclear role in the regulation of WPB exocytosis. Additionally, Ca^{2+}-independent SYTs are known to function cooperatively with Ca^{2+}-dependent SYTs to regulate secretory events and therefore it may be the case that SYTs V and XVII function as a complex to regulate the exocytosis of WPBs. The over-expression of either protein would have implications for the extent of WPB secretion and this may explain the strikingly similar effects of over-expression of these two SYTs on VWF secretion.

Future work must focus on confirming any role that SYT XVII plays in the regulation of the Ca^{2+}-mediated exocytosis of WPBs from endothelial cells. This would be best achieved at this point through the use of knock-down assays, and indeed I attempted the siRNA-mediated inhibition of SYT XVII in HUVECs but unfortunately could not achieve a knock-down effect greater than 50%. Despite this, I did perform knock-down ELISAs using SYT XVII siRNA which suggested that the loss of the SYT XVII protein from HUVECs does not affect the release of either VWF or proregion (data not shown). Equally ICC implied that the knock-down of SYT XVII in HUVECs does not affect the synthesis or trafficking of WPBs (data not shown). However, as the extent of knock-down of SYT XVII as measured by Western blotting was so poor it is impossible to judge if these negative results are genuine observations or are the result of an inefficient knock-down. Therefore this data has not been presented. In the future the SYT silencing protocol for the SYT XVII protein should be

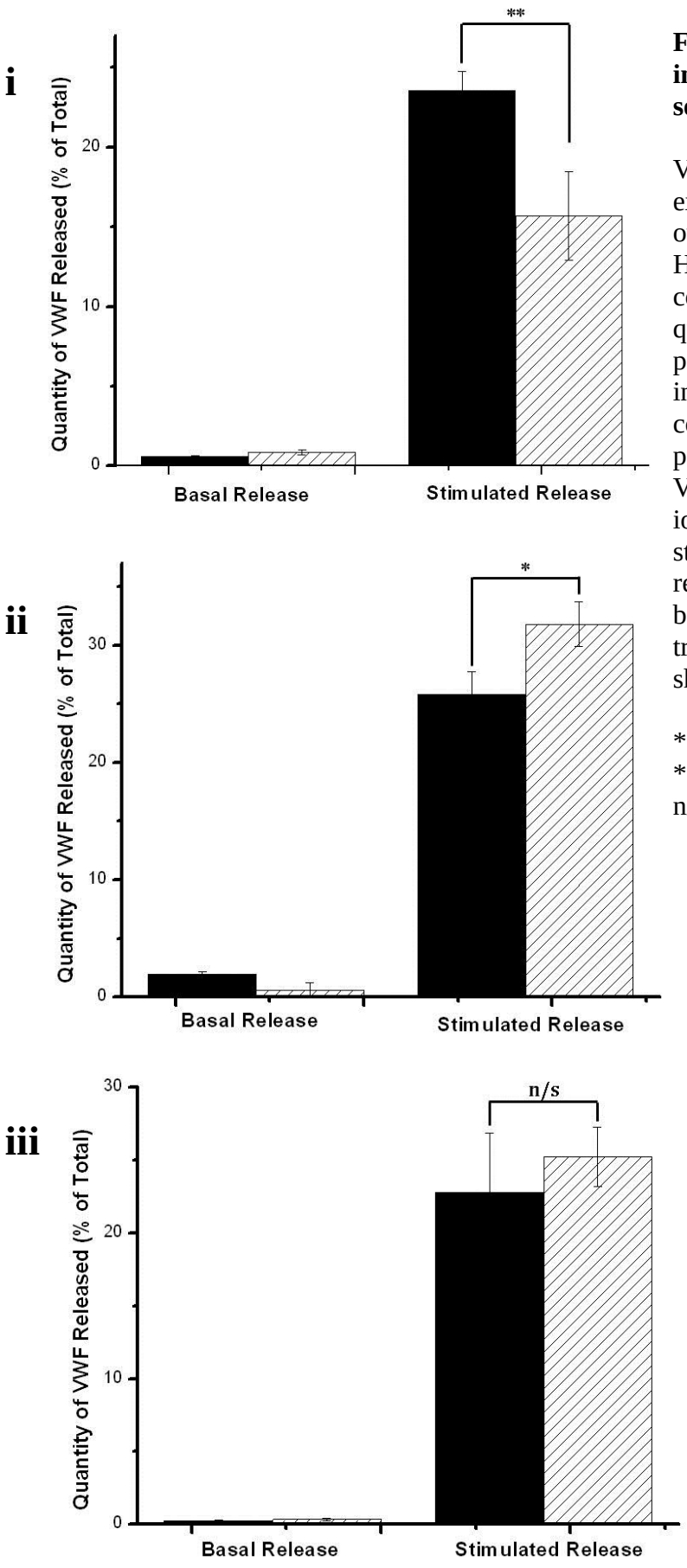

Figure 7.5 SYT XVII up-regulation influences the extent of VWF secretion from HUVECs.

VWF ELISAs were performed to examine the effects of SYTXVII-EGFP over-expression on VWF secretion from HUVECs compared with a control construct (YFP). The graphs show the quantity of VWF released as a percentage of the total quantity of VWF in the cells. Cells incubated with a control non-stimulating solution provided the data for the basal release of VWF. Cells incubated with 1 µM ionomycin provided the data for the stimulated release of VWF. Black bars represent YFP-transfected cells. Hatched bars represent SYTXVII-EGFP-transfected cells. Panels (i), (ii), and (iii) show the results of three separate assays.

* P-value ‹ 0.05.
** P-value ‹ 0.005.
n/s = non-significant (p-value › 0.05)

optimized and these studies repeated once an acceptable level of knock-down has been achieved. Additionally, it would be of great interest to see if the simultaneous knock-down of both SYTs V and XVII has an effect on the exocytosis of WPBs from HUVECs, as the evidence suggests that these two SYT family members may have a similar role in endothelial cell biology. It may be that these two proteins function either cooperatively or redundantly and therefore their joint knock-down may yield a striking biological effect.

This work has been the first of its kind attempting to determine the distribution and role of the SYT XVII protein in any cell type, and therefore the results are of general interest for those working in the field of SYT biology. However before the function of this member of the SYT family can be understood further it is essential to determine the extent of expression of the SYT XVII gene in mammalian tissue and the number of SYT XVII isoforms which may exist in various cell types. As the subcellular localization screen performed here suggests that SYT XVII may have an unexpected fundamental role in organelle biogenesis, trafficking, or exocytosis it would be of particular interest to generate a SYT XVII $^{-/-}$ mouse to determine if such a creature shows any striking phenotypic defects.

Chapter Eight

Investigating the Functions of SYTs I, III, VI, and XI in HUVECs

8.1 An Overview:

The previous functional studies have focused on establishing a role for those endothelial SYTs which are known to localize to WPBs when over-expressed in HUVECs as these proteins are in the optimum subcellular location for the regulation of WPB fusion with the plasma membrane. However, there are four additional members of the SYT family which are expressed in HUVECs but do not localize to the WPBs. These proteins should not be immediately discounted as candidates for the role of the WPB calcium sensor as it has been proposed that members of the SYT family can function in a similar manner to SNAREs whereby different SYTs located on opposing membranes can form complexes which are essential for mediating secretory events. Particularly, the oligomerization of SYTs on closely-positioned membranes may be crucial for the formation of the fusion pore (Sugita *et al.* 2001, Sudhof, 2002). Hence, the fact that a SYT is not found on the WPB membrane does not necessarily imply that it is not involved in the regulation of WPB exocytosis. Indeed, over-expressed SYTI-mCherry localizes to the plasma membrane and so this SYT may be located in an ideal subcellular position to influence WPB secretion. Additionally, these four SYTs may be involved in other aspects of WPB biology such as their biosynthesis, maturation, and trafficking which although not directly relevant to the aims of this investigation could be easily identified by basic biochemical assays. Therefore, I performed limited functional studies aiming to identify any role played by SYTs I, III, VI, and XI in the regulation of WPB secretion.

8.2 The Function of SYT I in HUVECs:

8.2.1 Background Information:

8.2.1.1 Discovery and Initial Characterization:

SYT I was first identified in 1981 in the rat brain as a vesicular protein of 65 kDa present on the outer surface of synaptic vesicles (Matthew *et al.* 1981). This novel protein,

initially named p65, was shown to have a wide distribution in neuronal tissue and was reported to be present at low levels in non-neuronal secretory tissue. Indeed, it is now known that SYT I mRNA is found in the olfactory bulb, hippocampus, amygdala, striatum, hypothalamus, pituitary, cerebellum, throughout the cerebral cortex, and at low levels in the spinal cord (Berton *et al.* 1997, Marqueze *et al.* 1995).

The sequence of rat SYT I was deduced in 1990 and notably this 421-residue protein contains two 116-residue domains which are homologous to the regulatory C2-region of protein kinase C (PKC) (Perin *et al.* 1990). SYT I was therefore predicted to bind Ca^{2+} ions and anionic phospholipids via these C2 domains in a similar manner to PKC, and indeed in 1991 it was shown that SYT I is a putative membrane-bound Ca^{2+}-binding protein (Perin *et al.* 1991). A later study demonstrated that isolated SYT I C2 domains are sufficient for high-affinity Ca^{2+} and anionic phospholipid binding (Davletov and Sudhof, 1993). These domains exhibited strong positive cooperatively for Ca^{2+} binding which suggested multiple binding sites and also bound Ba^{2+} and Sr^{2+} ions at lower affinities. Further studies mapped the human SYT I gene to chromosome 12q21 and demonstrated that this gene is highly conversed between humans, rats, and drosophila (Perin *et al.* 1991).

8.2.1.2 The Role of SYT I in Synaptic Transmission:

Early studies demonstrated that SYT I has an essential role in the regulation of fast synaptic transmission. SYT I $^{-/-}$ *C. elegans* worms exhibit severe behavioural abnormalities related to locomotion, feeding, mating, and defecation resulting from reduced synaptic function (Nonet *et al.* 1993). Additionally, SYT I $^{-/-}$ *Drosophila melanogaster* flies show a high proportion of embryonic lethality and those that do survive exhibit uncoordinated muscle contractions and behaviour abnormalities including an inability to jump and mate. These mutants show impaired synaptic transmission characterized by diminished evoked excitatory junctional potentials whereas the frequency of spontaneous release events increases (Littleton *et al* 1993). Conclusive evidence that SYT I is the major Ca^{2+} sensor for fast synaptic neurotransmission came from the generation of SYT I $^{-/-}$ mice (Geppert *et al.* 1994). This mutation is lethal but hippocampal neurons cultured from embryonic SYT I $^{-/-}$ homozygous mice show severely impaired synaptic transmission. In keeping with the observations generated from the SYT I $^{-/-}$ *Drosophila*, fast synchronous release is inhibited whereas the frequency of asynchronous release including spontaneous activity increases.

It is now known that the primary functions of SYT I in synaptic transmission are to synchronize fast release events and inhibit asynchronous transmission. Indeed, hippocampal neurons derived from SYT I $^{-/-}$ mice secrete a reduced quantity of glutamate via the fast synchronous pathway but an increased quantity through asynchronous events, resulting in no overall changes in glutamate release compared with wild-type neurons (Nishiki and Augustine, 2004). Additionally, SYT I $^{-/-}$ AD4 *drosophila* mutants which have no functional SYT I protein show severely inhibited synchronous secretion and increased asynchronous release events (Yoshihara and Littleton, 2002). SYT I AD1 *drosophila* mutants which express the SYT I C2A domain show partially recovered synchronous release indicating that the C2A domain in isolation is able to stimulate synaptic vesicle fusion.

The importance of SYT I in the regulation of the kinetics and sensitivity of fast synaptic transmission has been demonstrated by a series of elegant mutagenesis studies. A single point mutation (R223Q) in the SYT I protein results in a two-fold decrease in its overall Ca^{2+} affinity, and this in turn results in a two-fold decrease in the both the Ca^{2+} sensitivity and overall probability of release events (Fernandez-Chacon *et al.* 2001). In contrast, a gain-of-function mutation whereby tryptophan residues are introduced into the exposed surface loops of the SYT I C2 domain increasing their inherent hydrophobicity and membrane affinity resulted in enhanced Ca^{2+} sensitivity and probability of synaptic transmission (Rhee *et al.* 2005). Incidentally in both cases spontaneous release events are not affected by these SYT I mutants.

8.2.1.3 The Role of SYT I in the Regulation of Non-Synaptic Secretory Events:

SYT I is found primarily in neuronal cells where it specializes in mediating fast synaptic transmission. However it has been shown to be involved in the regulation of non-neuronal secretory events. For example, SYT I is found in pancreatic acinar cells where it localizes to zymogen granules (Falkowski *et al.* 2011). An anti-SYT I antibody inhibits ancini exocytosis by 35% and so SYT I is involved in the regulation of zymogen exocytosis. Additionally, SYT I functions reluctantly with SYT IX to control the exocytosis of LDCVs from PC12 cells (Lynch and Martin, 2007). Indeed, the regulated exocytosis of LDCVs persists fully in cells which lack only one of these two SYT isoforms but is abolished completely if both proteins are simultaneously knocked-down in PC12 cells. Interestingly, each isoform appears to confer unique kinetic properties to the secretion of LDCVs as the

over-expression of SYT I leads to faster release kinetics whereas that of SYT IX leads to slower release kinetics. Hence, it is likely that the ratio of expression of various SYT isoforms may affect the observed kinetics of a secretory event. Interestingly, this study also demonstrated that SYT I but not SYT IX mediates compensatory endocytosis in PC12 cells. Lastly, when over-expressed in the immortalized mast cell line RBL-2H3 SYT I localizes to secretory granules and results in their increased Ca^{2+}-dependent secretion (Baram *et al.* 2001).

8.2.1.4 Insights into the Regulation and Trafficking of SYT I:

SYT I is phosphorylated on a single residue (T128) found in the lysine-rich linker region between the transmembrane and C2A domains by casein kinase II although the functional implications of this are currently unclear (Davletov *et al.* 1993). However, it is known that the trafficking of SYT I is heavily regulated by the palmitoylation of this crucial linker region. Indeed, the palmitoylation of five cysteine residues directs SYT I to vesicles in rodent cortical and striatal neurons (Kang *et al.* 2004). In contrast, unpalmitoylated SYT I localizes in a diffuse pattern across the axon and increased amounts are found on the plasma membrane. It is likely that palmitoylation regulates the internalization of SYT I from the cell surface and indeed unpalmitoylated SYT I mutant proteins fail to undergo endocytosis from the plasma membrane.

The final 29 N-terminal amino acids of SYT I constitute a crucial signalling peptide as their transplantation to SYT VII can re-direct this protein from the plasma membrane to secretory vesicles (Han *et al.* 2004). Equally, the N-terminus of SYT VII when transplanted to SYT I re-directs this vesicular protein to the plasma membrane. Interestingly, the glycosylation of this region is also essential for the correct trafficking of SYT I, with one asparagine residue (ASN24) playing a particularly central role. Indeed, a randomized N-terminal sequence containing ASN24 inserted onto SYT VII is all that is required to re-direct this protein to the synaptic vesicles. Additionally, N24Q SYT I mutants fails to undergo endocytosis from the plasma membrane indicating that glycosylation is also essential for its internalization. As would be expected, hippocampal neurons expressing the N24Q mutant show diminished synaptic responses as a result of the mis-sorting of SYT I. These observations suggest that glycosylation is crucial for the regulation of both the endocytosis of SYT I and its trafficking to synaptic vesicles. The exact sequence surrounding the glycosylation site appears to be irrelevant.

8.2.2 SYTI-EGFP Over-Expression ELISAs:

It has been established thus far that SYT I is present in HUVECs as both an mRNA transcript and as a protein. Additionally, subcellular localization studies have demonstrated that fluorescently-tagged SYT I traffics to the plasma membrane and to lysosomes when over-expressed. By virtue of its localization to the plasma membrane, it is possible that SYT I may be involved in the regulation of WPB exocytosis from HUVECs. In order to test this hypothesis, VWF and proregion ELISAs were performed with the aim to establish the effects of SYT I over-expression on WBP secretion. Briefly, HUVECs were transfected with either SYTI-EGFP or with a control cytoplasmic construct (YFP). Cells were seeded onto 6-well plates and allowed to grow to confluency for forty-eight hours. HUVECs were then stimulated with either 1 μM ionomycin or with a control non-stimulating solution. Following stimulation, both the media and lysates were collected and spun down to remove cellular debris. Samples were processed for both VWF and proregion ELISAs according to the protocols detailed in '2.7 The Enzyme-Linked Immunosorbent Assay (ELISA) Protocol.'

Initially, VWF ELISAs were performed on samples collected from both SYTI-EGFP and YFP over-expressing cells. The results of this are shown in Figure 8.1. As can be seen SYTI-EGFP over-expression does not affect the quantity of either VWF or proregion released from stimulated HUVECs, indicating that the up-regulation of SYT I does not influence the extent of WPB secretion.

It has been demonstrated that the subcellular localization of the SYTI-EGFP construct varies depending on the time after transfection that HUVECs are fixed and examined (see Chapter 4). After forty-eight hours, the SYTI-EGFP construct localizes to lysosomes and to the plasma membrane. However, at twenty-four hours following transfection the construct shows a much stronger plasma membrane distribution. Therefore, the VWF and proregion ELISAs were repeated using HUVECs cultured for twenty-four hours following transfection. The results of this did not differ from those seen at forty-eight hours following transfection (data not shown).

8.2.3 The Effects of the Knock-Down of SYT I on WPB Exocytosis:

Over-expression ELISAs are limited in that they rely on a sufficient expression level of the construct to overcome the background exocytosis of WPBs from non-expressing cells. With this in mind, and considering that SYT I has a well-characterized role in the Ca^{2+}-

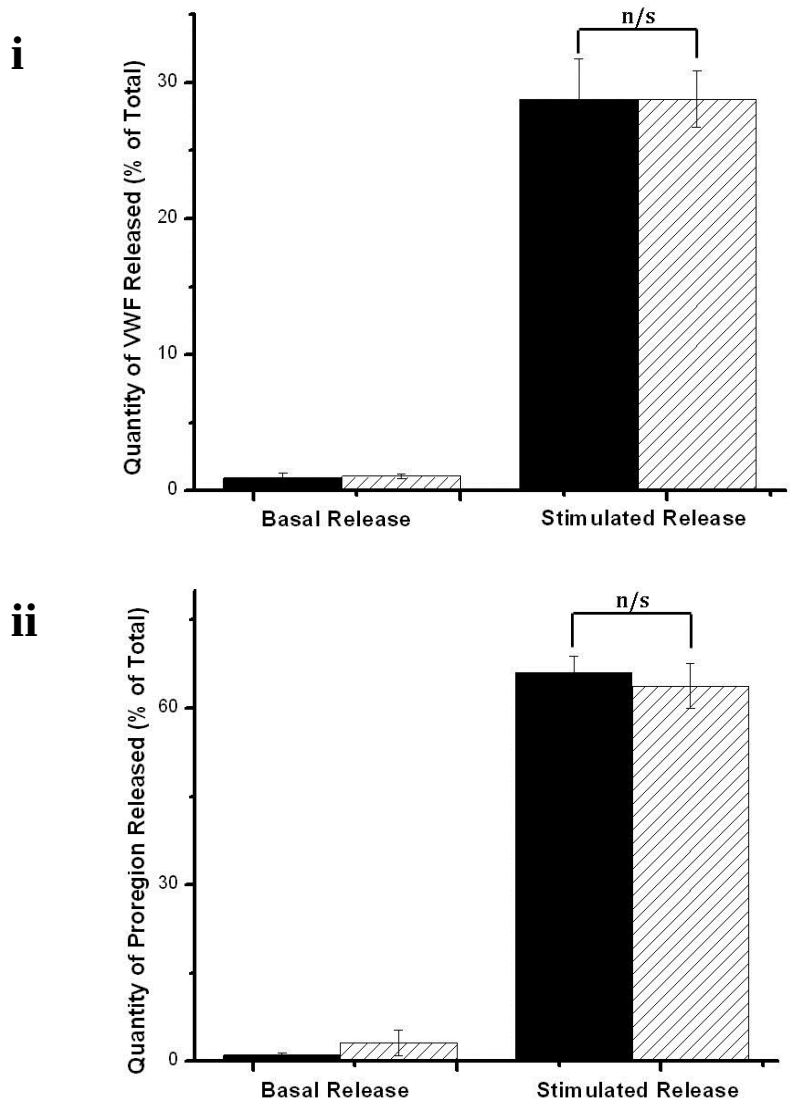

Figure 8.1. SYT I up-regulation does not affect the exocytosis of WPBs.

HUVECs were transfected with either SYTI-EGFP or YFP. Media and lysates were collected from cells after forty-eight hours and processed for VWF and proregion ELISAs. Cells incubated with a control non-stimulating solution provided the data for basal secretion. Cells incubated with 1 µM ionomycin provided the data for stimulated secretion. Panel (i) shows the quantity of VWF released as a percentage of the total quantity of VWF in the cells. Panel (ii) shows the quantity of proregion released as a percentage of the total quantity of proregion in the cells. No significant differences in the extent of WPB secretion are apparent between cells expressing SYTI-EGFP and those expressing YFP. Black bars represent YFP-transfected cells. Hatched bars represent SYTI-EGFP-transfected cells.

n/s = non-significant (p-value › 0.05)

n = 3 replicates from one vial of HUVECs; data is representative of 3 individual experiments performed on separate vials of HUVECs.

dependent secretion of synaptic vesicles from neurons, it was decided to pursue knock-down studies using SYT I siRNA.

8.2.3.1 The Optimization of the Knock-Down Protocol:

Initially, it was necessary to optimize the knock-down protocol for SYT I. Therefore, HUVECs were transfected with varying quantities of either SYT I siRNA or with non-targeting control oligos and were allowed to grow to confluency for either twenty-four or forty-eight hours. Following each time-point lysates were extracted from the cell cultures and Western blotting were performed using an α-SYT I antibody with the aim to determine the efficiency of the knock-down procedure. The results of this are shown in Figure 8.2. As can be seen, HUVECs transfected with both 200 and 400 pMol of SYT I siRNA show a strong knock-down effect forty-eight hours following transfection. By contrast, lysates extracted from HUVECs which were left for twenty-four hours following siRNA transfection showed no significant reduction in the quantity of cellular SYT I (data not shown).

The presence of any gross morphological changes to HUVECs following transfection with SYT I siRNA were examined by ICC. HUVECs were transfected with 400 pMol of either SYT I siRNA or control siRNA and grown to confluency for forty-eight hours. The cultures were then fixed and stained for VWF and LAMP1 with the intention to identify alterations to the number and structure of WPBs or to the morphology of HUVECs. The results of this are shown in Figure 8.3. As can be seen, no obvious differences are apparent between HUVECs transfected with SYT I siRNA and those transfected with either control oligos or with dH_20. Indeed, all cultures have grown to confluency and contain high number of rod-shaped WPBs, suggesting that the knock-down of SYT I does not lead to any visible defects in WPB synthesis.

8.2.3.2 SYT I Knock-Down ELISAs:

As the optimum conditions for the knock-down of SYT I in HUVECs have now been established VWF and proregion ELISAs were performed with the aim to determine if the knock-down of SYT I in HUVECs affects the exocytosis of WPBs. The results of this are shown in Figure 8.4. As can be seen, the knock-down of SYT I does not affect the quantity of either VWF or proregion secreted from HUVECs compared with cells transfected with

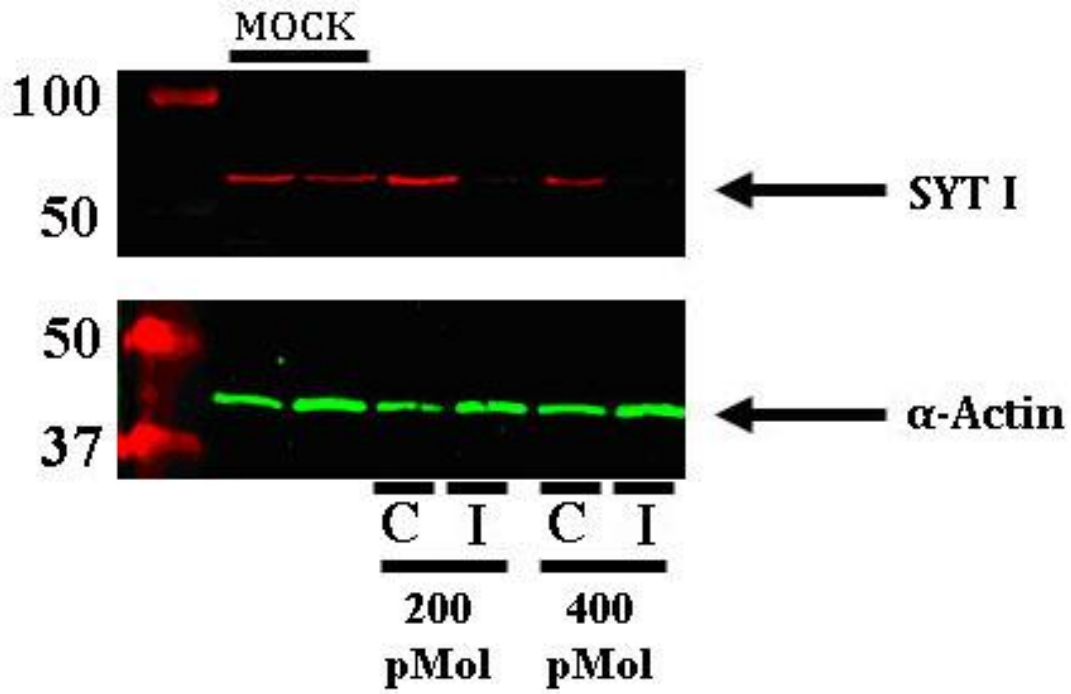

Figure 8.2. The SYT I protein is depleted in HUVECs following siRNA transfection.
Cells have been transfected with varying quantities of either SYT I siRNA (I) or control non-targeting oligos (C) as indicated and were allowed to grow to confluency for forty-eight hours. A mock transfection was also performed (4 µL dH_2O). Lysates were extracted and probed by Western blotting for SYT I (upper blot) and actin (lower blot). The sizes of the protein marker are indicated on the left (kDa). The extent of the knock-down of SYT I in SYT I-siRNA-transfected HUVECs is 83.43% (400 pMol) and 69.31% (200 pMol) of that seen in control siRNA-transfected HUVECs (normalized to the total quantity of protein as determined from the actin loading control).

control oligos, indicating that the knock-down of SYT I does not influence the secretion of WPBs from endothelial cells.

8.3 The Function of SYT III in HUVECs:

8.3.1 Background Information:

8.3.1.1 The Physical Properties of SYT III:

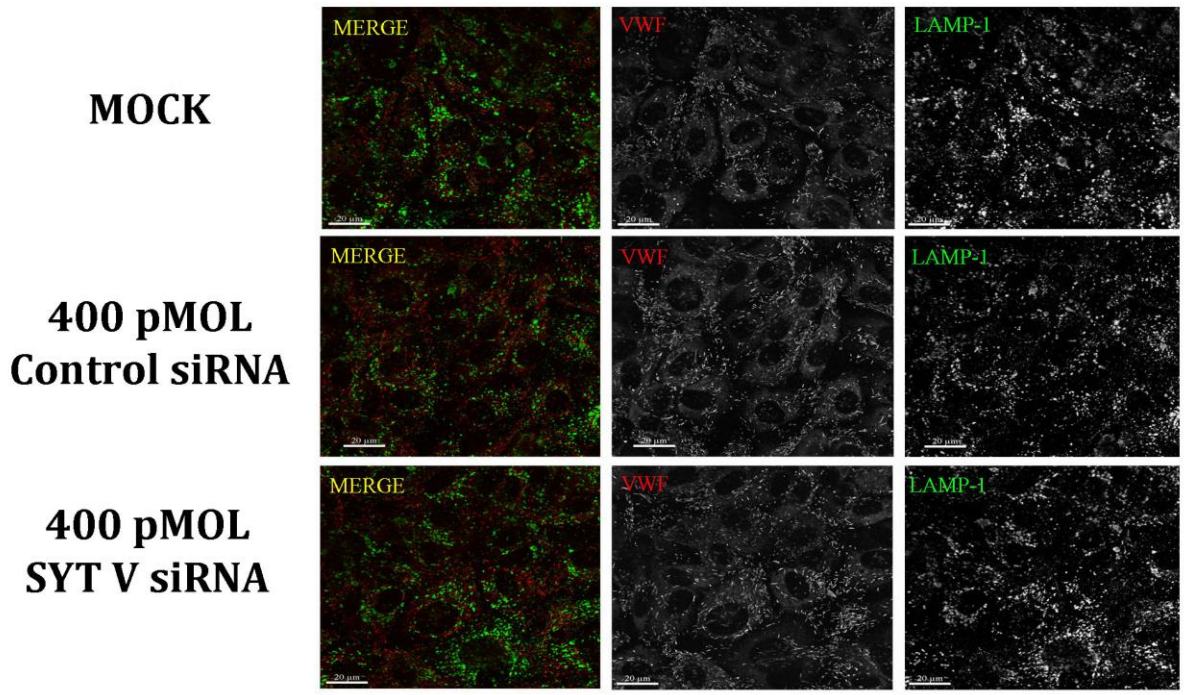

Figure 8.3. The knock-down of SYT I does not affect the morphology of either HUVECs or their WPBs.

HUVECs transfected with 400 pMol of either SYT I siRNA or with control non-targeting oligos as indicated were stained with antibodies against both VWF and LAMP1. A mock transfection was also included (4 µl of dH_20). The left-hand panels show the merged images, the middle panels show the VWF stain in the red channel, and the right-hand panels show the LAMP1 stain in the green channel. All cultures examined have grown to confluency and HUVECs appear morphologically normal. Likewise, each culture contains high numbers of large, rod-shaped WPBs.

SYT III was first identified in rat endocrine and neuronal cells and in the hormone-secreting clonal cell lines AtT-20, MIN6, GH3, PC12, RINm5F, and HIT-T15 (Mizuta *et al.* 1994). This member of the SYT family is the only isoform which can bind to negatively-charged phospholipids in an Mg^{2+}-dependent manner via a mechanism which requires the N-terminus of the C2A domain (Fukuda *et al.* 1997). Therefore SYT III may have a unique role in the regulation of exocytosis by allowing the induction of secretory events by Mg^{2+} ions.

SYT III, along with SYTs V and X, shows no significant IP_4 binding activity in either the C2A or C2B domains (Ibata *et al.* 1998). This lack of IP_4 binding is due to the combined

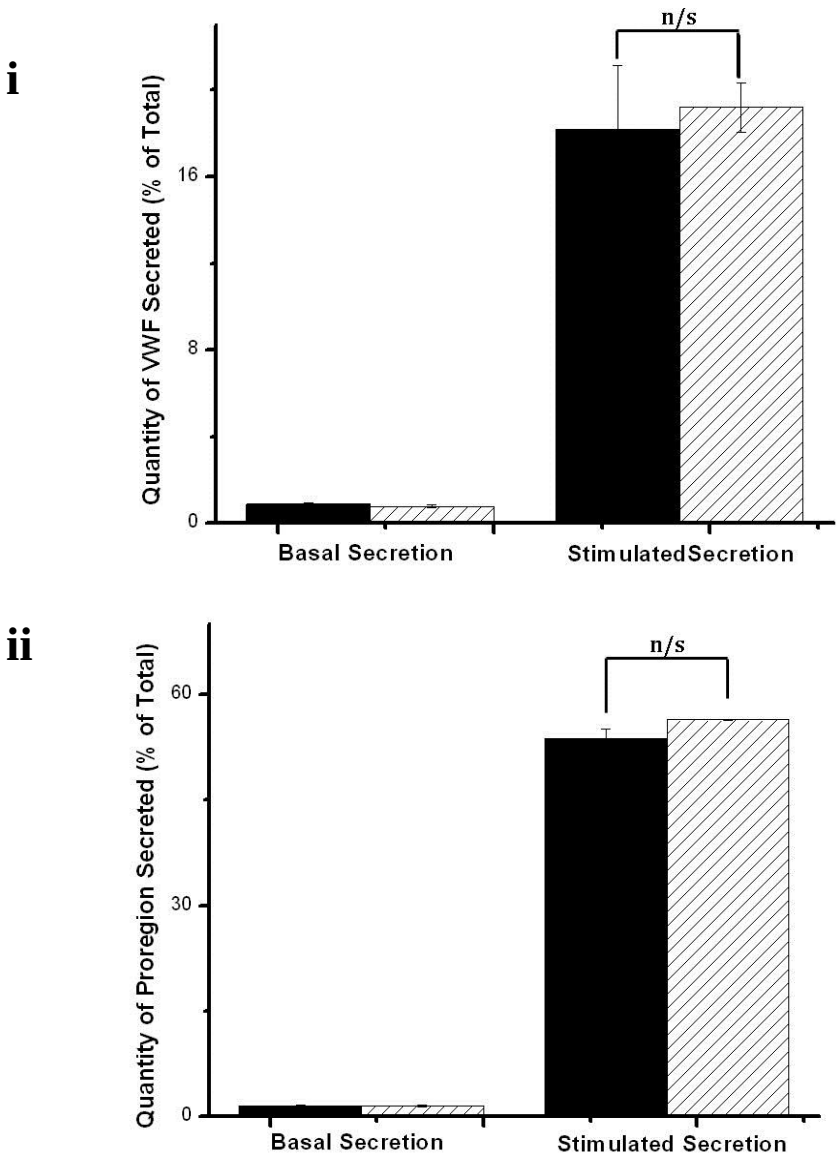

Figure 8.4. SYT I knock-down does not affect the exocytosis of WPBs.

HUVECs were transfected with either SYT I siRNA (400 pMol) or control siRNA (400 pMol). Media and lysates were collected from cells after forty-eight hours and processed for VWF and proregion ELISAs. Cells incubated with a control non-stimulating solution provided the data for basal secretion. Cells incubated with 1 µM ionomycin provided the data for stimulated secretion. Panel (i) shows the quantity of VWF released as a percentage of the total quantity of VWF in the cells. Panel (ii) shows the quantity of proregion released as a percentage of the total quantity of proregion in the cells. Black bars represent control siRNA-transfected cells. Hatched bars represent SYT I-siRNA-transfected cells.

n/s = non-significant (p-value › 0.05)

n = 3 replicates from one vial of HUVECs; data is representative of 3 individual experiments performed on separate vials of HUVECs.

effect of several residues (P505, E509, N510, E537, and D540) which are located in the C-terminal region of the SYT III protein.

8.3.1.2 The Crystal Structure of the SYT III C2 Domains:

The crystal structure of the SYT III C2AB domain has been determined both with and without bound Ca^{2+} ions. These models have shown that the two C2 domains act independently of one another, bind three Ca^{2+} ions each, have a wide range of movement in solution, and are composed of eight-stranded β-sandwiches with type I C2 topology (Sutton *et al.* 1999, Vrijic *et al.* 2010). Three conserved loops at the apex of each C2 domain compose the Ca^{2+}-binding sites. Loop 3 of the C2B Ca^{2+}-binding region is linked by disulphide bonding to another C2B domain, providing a mechanism for oligomerization (Sutton *et al.* 1999). Interestingly, it is the highly divergent linker region between the C2 domains of a SYT protein which determines the amount of flexibility the molecule has; the SYT III linker region contains a high proportion of glycine residues which impart substantial flexibility to the overall protein whereas other SYT isoforms contain proline residues and so are more restricted in their range of movement (Sutton *et al.* 1999).

Following Ca^{2+} binding, the SYT III molecule undergoes large conformational changes which result in the two C2 domains migrating to the same plane as a result of a hairpin twist in the 7-residue linker region (Vrijic *et al.* 2010). This allows their simultaneous insertion into target membranes. Additionally, a key lysine residue becomes exposed which functions to enhance interactions with anionic phospholipids in the membrane. In contrast, the endocytic motif WHXL is buried within the Ca^{2+}-bound crystal but not in the free structure.

It is thought that, in the absence of free Ca^{2+} ions, the SYT III protein is found bound to the *trans*-SNARE complex. Subsequent Ca^{2+} binding following stimulation then induces a large conformational change in SYT III which stabilizes the SYTIII:SNARE complex and allows the insertion of the SYT III moiety into the target membrane (Vrijic *et al.* 2010). This model is similar to that generated for SYT I and suggests a common mechanism of fusion pore formation within the SYT family. Additionally, the Ca^{2+}-binding loops in the SYT III crystal structure resemble the membrane-binding loops of certain viral fusion proteins such as glycoprotein E1 of the Semliki forest virus.

Based on the crystal structures which have been developed for SYT III, a general model depicting the regulation of exocytosis by SYTs has been proposed. In theory, Ca^{2+}-

binding to SYTs would allow them to insert into target membranes by neutralizing the negatively-charged amino acids found within the SYT C2 domains. Additionally, a polybasic region located in the C2 domains inserts into the negatively-charged area at the centre of the SNARE complex. It is possible that SYTs may function as inhibitors of exocytosis by binding to SNAREs in their Ca^{2+}-independent state, thereby blocking fusion pore formation. However, following calcium binding the SYTs preferentially bind to phospholipids in target membranes rather than SNARE molecules and this change in binding affinity allows fusion to proceed.

8.3.1.3 The Expression and Function of SYT III in the Nervous System:

SYT III is present throughout the rat CNS in a heterogeneous distribution (Marqueze *et al.* 1995, Butz *et al*. 1999). Its expression is strongest in the hippocampus and cerebellum and weakest in the cerebral cortex and olfactory bulb. It is also found in the spinal cord and hindbrain at moderate levels. The expression level of SYT III mRNA increases during development from E19 to adulthood in correlation with synaptogenesis (Butz *et al.* 1999). Light microscopy has demonstrated that SYT III is concentrated on the plasma membrane surrounding synapses in a similar pattern to neurexins (Butz *et al.* 1999). Interestingly, in the bovine retina SYT III shows a similar distribution to SYT I and indeed SYT III is co-expressed with SYT I in hippocampal synapses (Ullrich *et al.* 1994).

The function of SYT III in the nervous system is current unclear. In PC12 cells, SYTIII-GFP localizes to the plasma membrane and its over-expression results in defective neurite formation (Saegusa *et al.* 2002). SYT III appears to play a unique role in the regulation of synaptic vesicle exocytosis in the goldfish retina where it is found as a protein of 78 kDa (Berntson and Morgans, 2003). In mammalian retinas, SYT I and SYT II are localized to photoreceptor and biopolar cell terminals. However, in the goldfish retina SYT III is found in small domains of PKC-labelled bipolar cell terminals whereas SYTs I and II are absent from ribbon synaptic terminals of photoreceptors. Based on the observed staining pattern SYT III is not found on synaptic vesicles in bipolar cells and hence probably functions as a plasma membrane protein. SYT III is also found enriched in the rat retina in the inner and outer plexiform layers.

SYT III levels in the rat hippocampus are reduced following both a single and repeated electroconvulsive seizure (an animal model of electroconvulsive therapy) (Elfving *et al*. 2008). Electroconvulsive therapy is the treatment of choice for drug-resistant depressive

disorders but its mechanism of action is currently unclear. These results suggest that SYT III up-regulation may be involved in the development of depression.

8.3.1.4 The Expression and Function of SYT III in Non-Neuronal Cells:

SYTIII is found as an expression transcript in RBL-2H3 cells, a rat tumour cell line of mucosal mast cells (Baram *et al.* 2001). Additionally, SYT III is found in pancreatic acinar cells as an mRNA transcript and as a 63-kDa protein which co-localizes with LAMP1 in membrane fractions (Falkowski *et al.* 2011). However, SYT III does not play a role in the exocytosis of zymogen granules from acinar cells. SYT III mRNA is present in murine T-cells and the SYT III protein is found in multivesicular bodies containing the chemokine receptor CXCR4 and LAMP1 (Masztalerz *et al.* 2006). The CXCR4-regulated migration of T-cells and their extravasation to fibroblast monolayers can be inhibited by the knock-down of SYT III. It is now known that the inhibition of SYT III in T-cells impairs CXCR4 recycling and therefore leads to reduced levels of the protein on the plasma membrane.

It has now been established that SYT III is involved in mediating the recycling of proteins from the plasma membrane. Indeed, SYT III is an essential factor regulating the formation of rab11-positive perinuclear endocytic recycling compartments (Grimberg *et al*. 2002). In RBL-2H3 cells, SYT III co-localizes with markers of the early endosomes such as EEA-1, annexin II, transferrin, and syntaxin 7, and also co-localizes with the secretory granule markers histamine and serotonin. This distribution pattern was not consistent among RBL-2H3 cells suggesting that SYT III cycles between early endosomes and other organelles. When SYT III is knocked-down, internalized transferrin does not reach perinuclear endocytic recycling compartments but instead is distributed in vesicles throughout the cytosol. Additionally, Rab11 which normally traffics to recycling endosomes remains cytosolic in SYTIII-deficient cells, suggesting that SYT III regulates the *de novo* formation of recycling endosomes. It is noteworthy to consider that this study reported the existence of SYT III as an 80 kDa protein in the rat brain and as a 65 kDa protein in RBL-2H3 cells, suggesting that SYT III undergoes cell-specific post-translational modifications (Grimberg *et al*. 2002). Additionally, the Western blotting of rat brain homogenates has identified proteins representing SYT III with molecular weights of 46 and 66 kDa (Brown *et al*. 2000).

Lastly, SYT III is known to be involved in the regulation of insulin exocytosis and is found co-localized with insulin on secretory granules in rat pancreatic islets and in BtC3,

MIN6, and RINm5F cells (Mizuta *et al.* 1997, Gao *et al.* 2000). The up-regulation of the SYT III protein results in increased insulin secretion and an increase in the calcium sensitivity of secretory events (Gao *et al.* 2000). In contrast, antibodies against the SYT III protein inhibit insulin secretion from pancreatic β-cells (Mizuta *et al.* 1997, Brown *et al.* 2000). It is interesting to consider that the level of the SYT III protein is decreased in Goto-Kakizaki rat models of type 2 (non-insulin dependent) diabetes mellitus compared with control rats, suggesting that the SYT III may have a physiological role in the development or progression of diabetes (Zhang *et al.* 2002).

In conclusion, the SYT III protein is found expressed in a number of tissues with particular enrichment in certain regions of the brain. The function of SYT III in neuronal tissue is currently unclear. However, in non-neuronal tissue SYT III has an established role in the regulation of insulin secretion and interestingly appears to be crucial for the formation of recycling endosomes. Numerous studies have demonstrated that the SYT III protein is likely to undergo extensive post-translational modifications as its reported molecular weight varies considerably between cell types.

8.3.2 SYTIII-EGFP Over-Expression ELISAs:

Over-expressed SYTIII-EGFP localizes to the plasma membrane, TGN, and endosomal system in our model endothelial cells (see Chapter 4). Therefore endogenous SYT III is probably not located in a subcellular position which would allow it to regulate the exocytosis of WPBs and therefore is unlikely to be the calcium sensor responsible for governing this process. In order to test this hypothesis over-expression VWF and proregion ELISAs were performed using the SYTIII-EGFP construct. Representative assays are shown in Figure 8.5. No significant differences in the secretion of either VWF or proregion between HUVECs expressing SYTIII-EGFP and those expressing the control construct YFP are apparent, indicating that the up-regulation of SYT III does not influence the exocytosis of WPBs from HUVECs.

8.4 The Function of SYT VI in HUVECs:

8.4.1 Background Information:

8.4.1.1 The Subcellular Localization and Physical Properties of SYT VI:

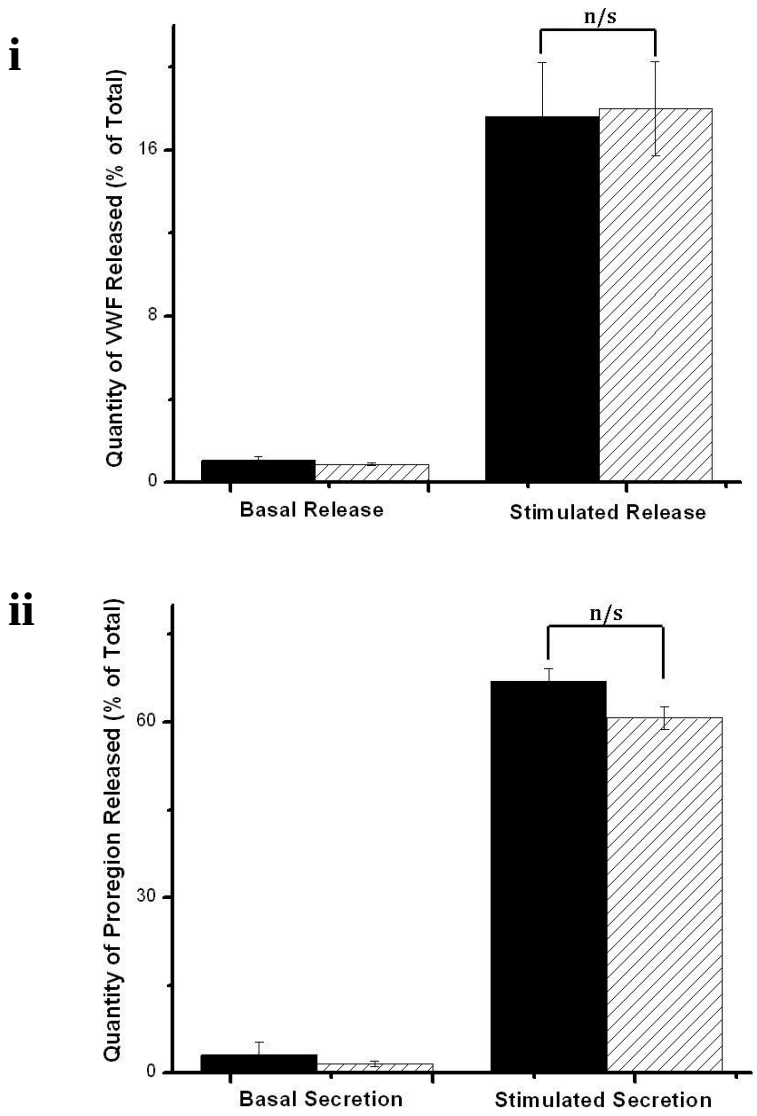

Figure 8.5. SYT III up-regulation does not affect the exocytosis of WPBs.

HUVECs were transfected with either SYTIII-EGFP or YFP. Media and lysates were collected from cells after eight hours and processed for VWF and proregion ELISAs. Cells incubated with a control non-stimulating solution provided the data for basal secretion. Cells incubated with 1 µM ionomycin provided the data for stimulated secretion. Panel (i) shows the quantity of VWF released as a percentage of the total quantity of VWF in the cells. Panel (ii) shows the quantity of proregion released as a percentage of the total quantity of proregion in the cells. No significant differences in the extent of WPB secretion are apparent between cells expressing SYTIII-EGFP and those expressing YFP. Black bars represent YFP-transfected cells. Hatched bars represent SYTIII-EGFP-transfected cells.

n/s = non-significant (p-value › 0.05)

n = 3 replicates from one vial of HUVECs; data is representative of 3 individual experiments performed on separate vials of HUVECs.

First identified in the adult mouse cerebellum in 1999, SYT VI is unique among the SYT family members in that its major isoform does not contain a transmembrane domain and therefore is not an integral membrane protein (Fukuda and Mikoshiba, 1999). Specifically, the major splice variant of SYT VI lacks the last 85 amino acids of the N-terminus which normally constitute the SYT transmembrane domain and therefore is designated SYTVIΔTM. This major isoform accounts for 85% of SYT VI transcripts in the rodent cerebellum, while three additional splice variants make up the remaining 15% (Fukuda and Mikoshiba, 1999). The two shorter isoforms are produced by alternative splicing of the transmembrane domain and ultimately encode the same protein product.

SYT VI derived from the adult mouse brain is visible on a Western blot as two closely-related bands of approximately 50 kDa (Fukuda and Mikoshiba, 1999). Following the subcellular fractionation of the mouse olfactory bulb, these two bands are seen in both the membrane and soluble fractions and can be eliminated from the membrane fraction by prior incubation with 1M NaCl buffer (Butz *et al.* 1999, Fukuda and Mikoshiba, 1999). The appearance of two distinct bands may be due to either the alternative splicing of the cytoplasmic domain of SYT VI or may be the result of post-translational modifications to the same protein product. Following its over-expression in COS-7 cells, full-length transmembrane SYT VI appears as a band of 58 kDa on Western blots (Fukuda and Mikoshiba, 1999).

The tissue distribution and subcellular localization of SYT VI are currently unclear and most likely vary depending on the isoform in question. SYT VI is most prominently expressed in the thymus (Craxton and Goedert, 1999). Additionally, SYT VI mRNA is found at low levels throughout the brain with the highest levels of expression reported in the olfactory bulb (Butz *et al.* 1999). In hippocampal neurons, over-expressed pHluorin-SYTVI is found in both axons and dendrites where it localizes to the plasma membrane and internal vesicles (Dean *et al.* 2012). In both PC12 and COS-7 cells, over-expressed SYTVIΔTM localizes primarily to the internal and plasma membranes, although a proportion of the protein is found in the cytosol. In contrast, the full-length protein is trafficked to the ER and to the Golgi (Fukuda and Mikoshiba, 1999). This observation was confirmed in a later study which reported the localization of SYTVI-GFP to the ER in PC-12 cells (Saegusa *et al* 2002). These subcellular localization studies have demonstrated that, in spite of its lack of either a transmembrane domain or N-terminal palmitoylation sites, SYT VI is able to interact with internal membranes. It is now known that this ability is the result of the final 29 amino acids of the SYT VI C-terminus, as the removal of these residues by deletion mutagenesis impairs

the membrane association of SYT VI by 60% (Fukuda and Mikoshiba, 1999). Additionally, it is likely that interactions between the C2 domains and negatively-charged phospholipids contribute to the ability of SYTVIΔTM to bind to internal membranes.

Due to its lack of a transmembrane domain, the SYT VI protein displays unique physical properties compared with other members of the SYT family. For example, SYTVIΔTM is unable to dimerize with SYTs III, V, VI, or X because it lacks the crucial N-terminal region required for dimerization (Fukuda and Mikoshiba, 1999). It is also unable to interact with full-length versions of itself or with any other cysteine-containing SYTs even in the presence of high Ca^{2+} concentrations. The only exception to this was a weak interaction formed with SYT X. Like many other members of the SYT family, the C2B domain of SYT VI does show weak IP_4 binding activity (Ibata *et al*. 1998).

8.4.1.2 SYT VI and Acrosome Exocytosis from Sperm Cells:

The majority of the work examining the subcellular localization and function of SYT VI has been performed in human sperm cells and involves the exocytosis of the acrosome. The acrosome is a single large secretory granule containing the degradative enzymes hyaluronidase and acrosin. Following the binding of receptors on the sperm plasma membrane with components of the egg's zona pellucida, the acrosome membrane fuses with the plasma membrane and releases its degradative contents into the hard shell surrounding the egg. It is now known that SYT VI is heavily involved in the regulation of this Ca^{2+}-dependent process.

The SYT VI protein is present in human sperm cells, appearing as a band of 66 kDa on Western blots, and ICC has shown that SYT VI localizes to the outer acrosomal membrane (Michaut *et al.* 2001). Both an anti-SYT VI antibody and a fusion protein containing the SYT VI C2 domains are able to inhibit acrosome exocytosis when applied to permeabilized sperm cells. However, the phosphorylation of this fusion protein by phorbyl esters abolishes its ability to inhibit exocytosis, suggesting that the phosphorylation of SYT VI plays a role in the regulation of its function. Indeed, recombinant SYT VI is phosphorylated *in vitro* following its incubation with PKC and PMA.

The signalling pathways regulating the SYTVI-induced fusion of the acrosome with the plasma membrane have been studied extensively in recent years. It is now know that each of the SYT VI C2 domains can block the exocytosis of the acrosome, as when either the C2A or C2B domain is expressed individually in spermatozoa exocytosis is inhibited (Roggero *et*

al. 2005). However, individual domains expressed in isolation have a 5-fold lower potency than both C2 domains expressed together, suggesting that the two domains play a role in the initiation of acrosome exocytosis. The ability of the C2 domains of SYT VI to block acrosome exocytosis can be inhibited by their prior phosphorylation with purified PKCβII (Roggero *et al*. 2005). Likewise, the inhibitory effect of phosphorylation is abolished by incubation with the PKC-inhibitor chelerythrine indicating that, as previously suggested (Michaut *et al.* 2001) PKC is required for the phosphorylation of SYT VI. Indeed, it is now known that endogenous SYT VI is phosphorylated in the acrosome region in unstimulated sperm cells, and an antibody against phosphorylated SYT VI is able to block acrosome exocytosis (Roggero *et al*. 2005). Interestingly, as the process of acrosome secretion proceeds the level of phosphorylated SYT VI decreases and the antibody against phosphorylated SYT VI is only inhibitory at early time-points in the acrosome reaction. In contrast, an antibody which recognizes both phosphorylated and dephosphorylated SYT VI is inhibitory throughout the secretory reaction. Therefore, in resting cells, SYT VI is phosphorylated by PKC and this appears to inhibit the fusion of the acrosome with the plasma membrane. However, following stimulation, SYT VI is dephosphorylated, allowing the exocytic reaction to proceed.

The sites of phosphorylation in the C2B domain of SYT VI have been identified by site-directed mutagenesis as Thr418 and Thr419, which are found in the fourth β-strand of the highly-conserved polybasic region (Roggero *et al*. 2005). The mutation of these two residues to glutamine abolishes the inhibitory effect of the recombinant SYT VI peptide. It is interesting to consider that the fourth β-strand of the polybasic region is a so-called 'effector region' and binds to a number of target molecules including inositol polyphosphates, PIP_2, SNAREs, and AP2. It is also an essential region for mediating oligomerization in other SYT family members. Hence, the phosphorylation state of this region would have significant implications for the overall function of the SYT VI protein. The phosphorylation site in the SYT VI C2A domain has been identified as Thr284. Although this residue is also found within a polybasic region, it is unclear what direct functional consequences its phosphorylation would have on the activity of the SYT VI protein.

It has now been established that the dephosphorylation of the SYT C2B domain during the early stages of acrosome exocytosis occurs as a result of the actions of calcineurin, a Ca^{2+}-dependent serine/threonine phosphatase, as an antibody against the α-subunit of calcineurin is able to inhibit exocytosis (Bennett *et al.* 2010). The dephosphorylation of SYT VI is vital for successful acrosome fusion, as the calcineurin inhibitor cyclosporin A inhibits

exocytosis whereas the over-expression of a catalytically-active version of calcineurin rescues this effect. This calcineurin variant also dephosphorylates the C2B domain of SYT VI in an Mn^{2+}-dependent manner in an *in vitro* model of exocytosis. The dephosphorylation of SYT VI by calcineurin must occur within a specific window of time, as shown by the observation that if sperm cells are treated with catalytically-active calcineurin before ionomycin stimulation then the exocytosis of the acrosome is inhibited. Therefore the premature dephosphorylation of SYT VI inhibits exocytosis. The addition of phosphorylated SYT VI C2B domain restores acrosome exocytosis, indicating that SYT VI plays an active role in the instigation of fusion. Indeed, phosphorylated SYT VI may prevent the premature formation of the *trans*-SNARE complex whilst the dephosphorylation of SYT VI allows the assembly of the fusion apparatus.

Lastly, it has been reported that the dephosphorylation of the SYT VI C2B domain modulates a complexin/SYT VI interaction which regulates the exocytosis of the acrosome (Roggero *et al.* 2007). Complexins bind to SNARE complexes by inserting as an antiparallel α-helix between the synaptobrevin and syntaxin helices. They can have both inhibitory and activating roles in relation to secretory events. It is thought that SYT I can displace complexins from the SNARE apparatus in a Ca^{2+} -dependent manner, allowing the exocytosis of docked granules to proceed. It is currently unclear which complexins are expressed in human sperm cells, although it is known that antibodies against complexin I and II are able to inhibit acrosome exocytosis. The addition of both the C2B domain of SYT VI and an α-complexin antibody blocks the formation of the *trans*-SNARE complex in human spermatozoa. This can be reversed by adding back complexin. However, as with dephosphorylation this effect appears to be time-dependent as the addition of complexin blocks exocytosis once the SNAREs have formed the *trans*-complex. This in-turn is relieved by the addition of the SYT VI C2B domain and Ca^{2+} ions. Therefore, complexins and SYT VI form an active complex which regulates acrosome exocytosis, and indeed it is possible that SYT VI may function to displace complexins from the fusion apparatus, allowing secretion to proceed. This ability is dependent on the dephosphorylation of SYT VI, as the addition of either phosphorylated wild-type SYT VI or a phosphomimetic variant blocks the ability of SYT VI to displace complexin.

The data discussed here has presented a model whereby SYT VI regulates the exocytosis of the acrosome from sperm cells through a balance between its phosphorylation by PKC and dephosphorylation by calcineurin (Michaut *et al.* 2001, Roggero *et al.* 2005, Roggero *et al.* 2007, Bennett *et al.* 2010). This model is summarized in Figure 8.6. Indeed,

this work has generated the clearest example of how phosphorylation can influence the function of a member of the SYT family, and it is likely that other SYTs are regulated in a similar manner.

8.4.2 SYTVI-EGFP Over-Expression ELISAs:

In order to test if the up-regulation of SYT VI affects the exocytosis of WPBs from HUVECs VWF and proregion ELISAs were performed using samples derived from SYTVI-EGFP- and YFP-transfected cells. Representative assays are shown in Figure 8.7. As can be seen, the expression of SYTVI-EGFP does not affect the secretion of either VWF or proregion from HUVECs compared with the expression of YFP. Hence SYT VI is unlikely to be involved in the regulation of WPB exocytosis from endothelial cells.

8.5 The Function of Synaptotagmin XI in HUVECs:

8.5.1 Background Information:

There is currently little known regarding the distribution and function of the 431-amino acid protein sensor SYT XI. This Ca^{2+}-independent member of the SYT family was first characterized in 1997 where it was reported to contain two cytoplasmic C2 domains as is characteristic of the SYT family. However, due to a mutation to one of the essential Ca^{2+}-coordinating aspartates in the C2A domain it is unable to bind Ca^{2+} ions (van Poser *et al.* 1997). Like SYT IV, SYT XI cannot bind phospholipids in a Ca^{2+}-dependent manner, and therefore is considered to be Ca^{2+}-independent. SYT XI is expressed at high levels in the brain and at low levels in most other tissues (van Poser *et al.* 1997). The intracellular distribution of SYT XI is currently unclear, although in transfected PC12 cells a fluorescent construct containing SYT XI cDNA was shown to localize to the Golgi network (Fukuda and Mikoshiba, 2001), and in hippocampal neurons a pH-sensitive variant of SYT XI localizes to the dendrites (Dean *et al.* 2012). A single paper has suggested its function may be as an inhibitor of fast pre-synaptic neurotransmission (Wang *et al.* 2001), although no information to support this hypothesis has been provided in recent years.

Most interest in the SYT XI gene and its protein product stems from the reported associations between human psychiatric disorders and the expression and intracellular interactions of SYT XI. Indeed, SYT XI is known to interact with parkin, a protein implicated

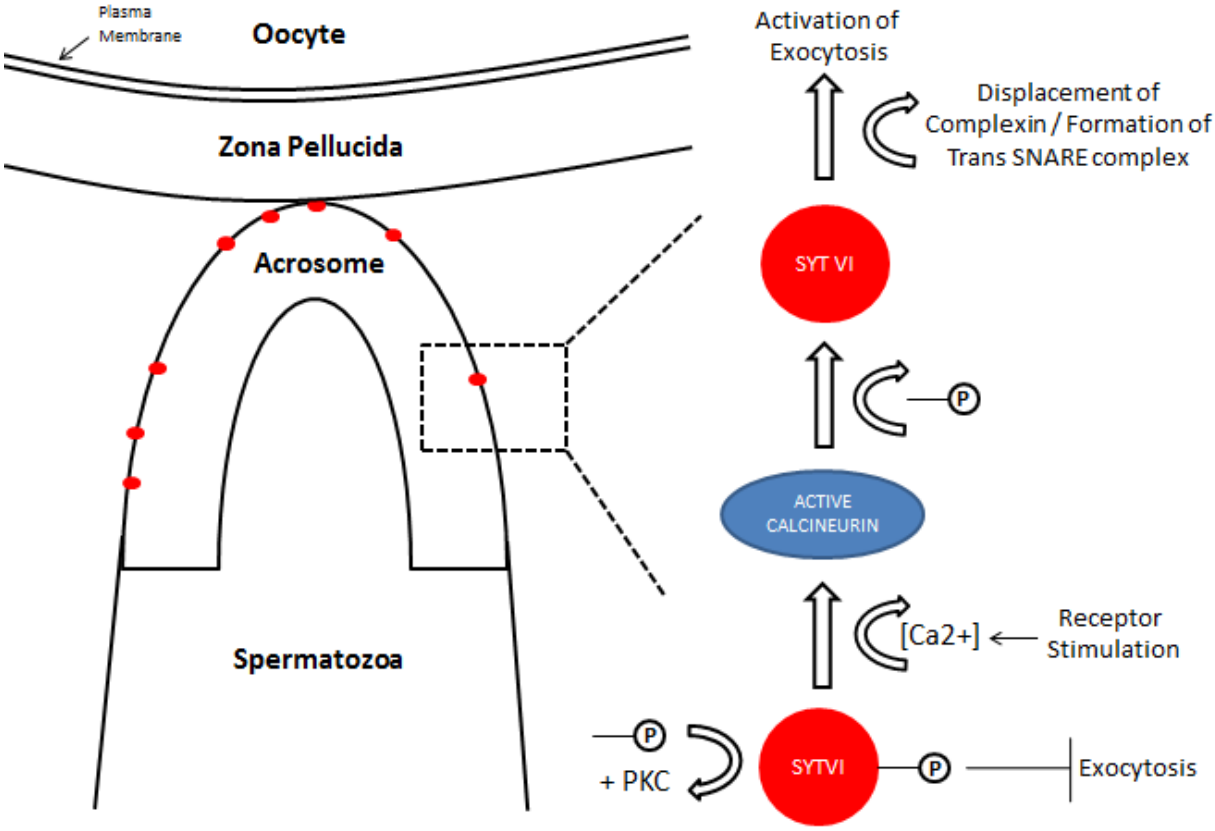

Figure 8.6. SYT VI regulates the exocytosis of the acrosome from sperm cells.

A model explaining the activity of the SYT VI protein in the regulation of acrosome exocytosis from human sperm cells is shown. In the resting cell, SYT VI is phosphorylated by PKC and acts as an inhibitor of exocytosis. However following the stimulation of the spermatozoa by contact with the zona pellucida the concentration of Ca^{2+} in the cytoplasm increases, resulting in the activation of calcineurin and the dephosphorylation of SYT VI. Dephosphorylated SYT VI is able to displace complexin from the ternary SNARE complex, allowing the formation of the *trans*-SNARE complex and the fusion of the acrosome membrane with the plasma membrane.

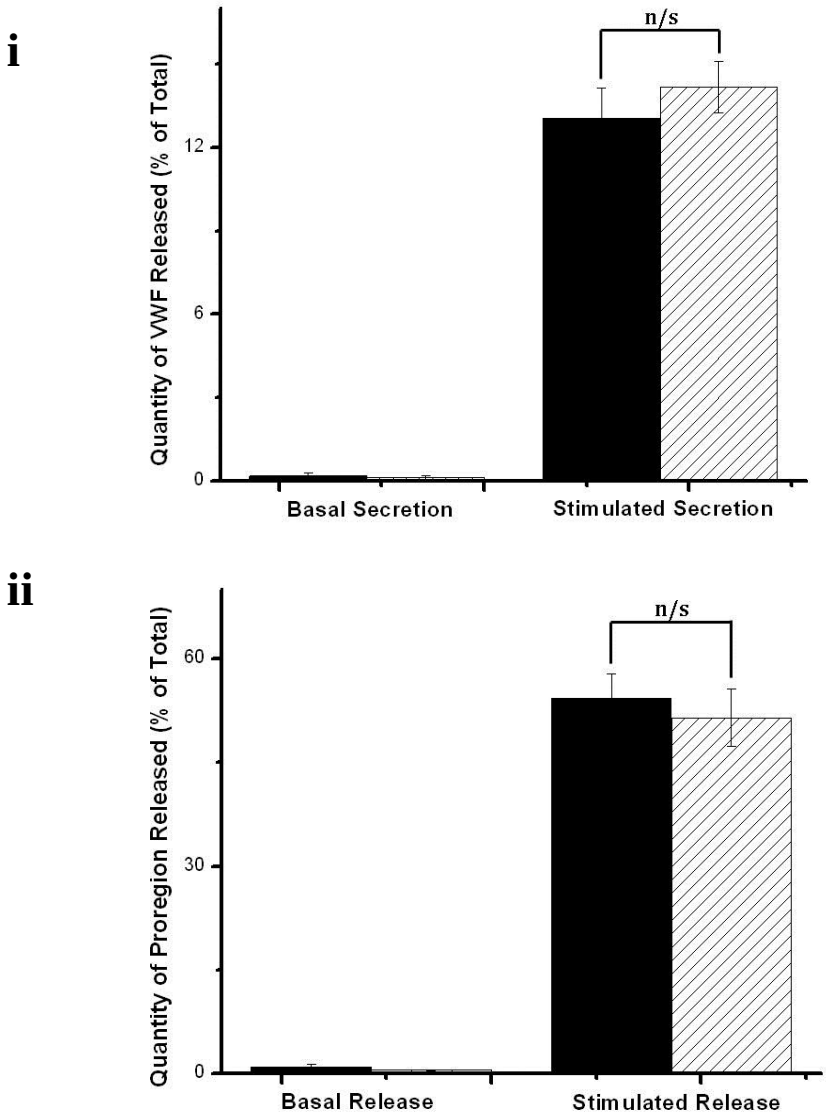

Figure 8.7. SYT VI up-regulation does not affect the exocytosis of WPBs.

HUVECs were transfected with either SYTVI-EGFP or YFP. Media and lysates were collected from cells after forty-eight hours and processed for VWF and proregion ELISAs. Cells incubated with a control non-stimulating solution provided the data for basal secretion. Cells incubated with 1 µM ionomycin provided the data for stimulated secretion. Panel (i) shows the quantity of VWF released as a percentage of the total quantity of VWF in the cells. Panel (ii) shows the quantity of proregion released as a percentage of the total quantity of proregion in the cells. No significant differences in the extent of WPB secretion are apparent between cells expressing SYTVI-EGFP and those expressing YFP. Black bars represent YFP-transfected cells. Hatched bars represent SYTVI-EGFP-transfected cells.

n/s = non-significant (p-value › 0.05)

n = 3 replicates from one vial of HUVECs; data is representative of 3 individual experiments performed on separate vials of HUVECs.

in the pathogenesis of Parkinson's disease. Parkin is a ubiquitin ligase and is involved in the targeting of misfolded proteins for destruction via the proteasome complex. Mutations in the parkin gene can lead to autosomal recessive Parkinson's disease. It has been demonstrated by co-immunoprecipitation and yeast two-hybrid analysis that parkin can bind to SYT XI via its C2A and C2B domains (Huynh *et al.* 2003). This interaction results in the ubiquitination of SYT XI, and indeed mutations in the parkin gene can lead to a reduced binding affinity for and decreased ubiquitination of SYT XI. In both PC12 cells and cells of the human substantia nigra, SYT XI and parkin were found co-localized at the nuclear membrane and perinuclear area. Interestingly, ICC of brain sections from patients suffering from sporadic Parkinson's disease showed that SYT XI is localized to Lewy bodies. It has been suggested that SYT XI may be involved in synaptic vesicle trafficking due to the link between its accumulation in Lewy bodies and the subsequent dysregulation of dopaminergic neurons in the substantia nigra (Huynh *et al.* 2003).

The human SYT XI gene is located on chromosome 1q21-22 and consists of 4 exons (Yokota *et al.* 2003). Immediately upstream of the SYT XI gene there exists a tandem repeat of a 33 base-pair sequence which has promoter-like activity (Yokota *et al*. 2003). The transfection of constructs containing different numbers of tandem repeats placed immediately upstream of the reporter gene firefly luciferase into COS-1 cells demonstrated that the promoter-like activity of this region increases in a linear fashion with the increasing number of repeats. This region upstream of the SYT XI gene has been loosely linked to familial schizophrenia, as within a sample of 60 Japanese schizophrenia patients two showed polymorphisms in this region whereas no polymorphisms were reported in a pool of 68 healthy individuals (Yokota *et al*. 2003). Recently, this work has been extended and it has been demonstrated that the overexpression of SYT XI is associated with the development of schizophrenia (Inoue *et al.* 2007). This was shown using a larger sample size of 227 Japanese schizophrenic patients versus 198 healthy controls. As previously reported, an increasing number of tandem repeats in the region upstream of the SYT XI gene leads to the increased transcription of the gene. This is most likely due to a stronger interaction with the transcription factor Sp 1. Additionally, a SNP (T/C) in the SYT XI 5' un-translated region has been identified which is now known to influence the level of transcription of SYT XI independently of the number of tandem repeats in the upstream region (Inoue *et al.* 2007). This SNP is located within the binding sequence for the transcription factor YY1, and indeed gel mobility shift assays revealed that YY1 binds to the cytosine genotype of the SNP with a

four-fold higher affinity than the thymine genotype. However, no significant association was found between this SNP and the development of schizophrenia.

Therefore, the true function of the SYT XI protein and its intracellular localization in healthy tissue are not known. However, current interest in this protein stems from its possible links with psychiatric disorders such as Parkinson's disease and schizophrenia. It is noteworthy that the closest relative of SYT XI, SYT IV, has also been associated with the development of psychiatric diseases (Ferguson *et al*. 2001).

8.5.2 SYTXI-EGFP Over-Expression ELISAs:

In order to investigate the possibility that SYT XI may be involved in the secretion of WPBs from HUVECs over-expression VWF ELISAs were performed using the SYTXI-EGFP construct. The results of a representative assay are shown in Figure 8.8. As can be seen, no significant differences are apparent between the quantity of VWF secreted from cells expressing SYTXI-EGFP compared with those expressing the control construct YFP. Therefore, at this point it would appear that SYTXI-EGFP over-expression does not affect the quantity of VWF released from HUVECs following ionomycin stimulation.

.

8.6 The Roles of SYTs I, III, VI, and XI in Human Endothelial Cells: A Discussion

8.6.1 The Role of SYT I:

SYT I is the most well-characterized member of the SYT family and has a proven fundamental role in the regulation of fast synaptic transmission in neurons. Here, I have shown that SYT I is expressed in endothelial cells as both an mRNA transcript and as a protein. Additionally, over-expressed SYTI-mCherry localizes to the plasma membrane and lysosomes in HUVECs. The fact that SYT I localizes to the plasma membrane when up-regulated in HUVECs led me to believe that this member of the SYT family is involved in mediating WPB exocytosis as it has been suggested that different members of the SYT family located on closely-positioned but opposing membranes can form oligomers which contribute to the formation of the fusion pore in a similar manner to SNARE proteins (Sujita *et al.* 2001, Sudhof 2002, Gerber and Sudhof, 2002). Therefore, endothelial SYT I may be located in an ideal subcellular position to allow it to regulate WPB fusion as a plasma membrane SYT. However, functional studies involving both over-expression and knock-down ELISAs

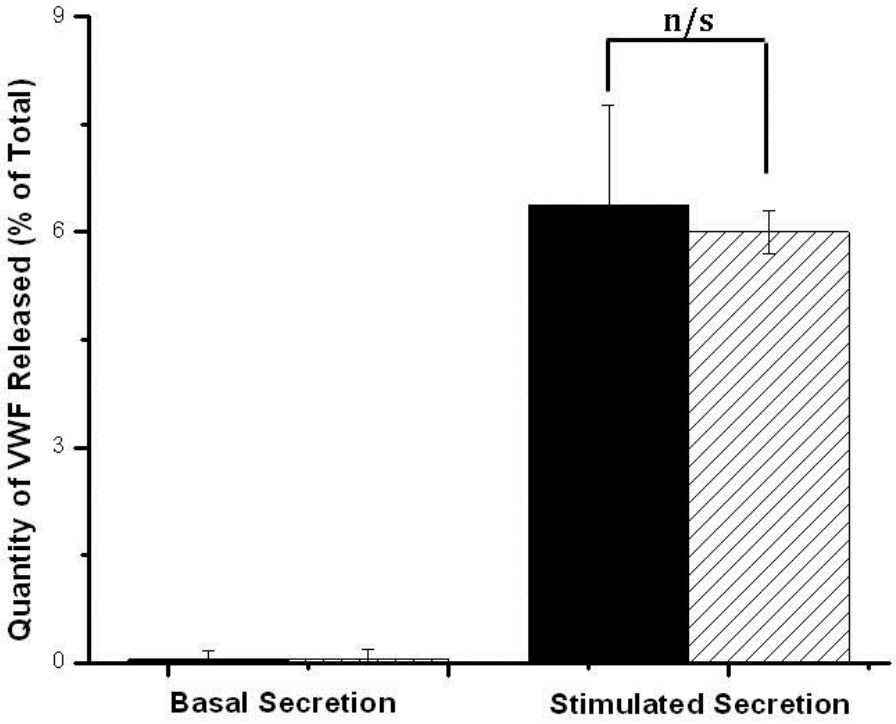

Figure 8.8. **SYT XI up-regulation does not affect the exocytosis of WPBs.**

The results of a representative experiment examining the effects of SYTXI-EGFP over-expression on VWF secretion are shown. Media and lysate were collected from cells expressing either SYTXI-EGFP or a cytoplasmic control construct (YFP) and a VWF ELISA was performed. The graph shows the quantity of VWF released as a percentage of the total quantity of VWF in the cells. Cells incubated with a control non-stimulating solution provided the data for the basal release of VWF. Cells incubated with 1 µM ionomycin provided the data for the stimulated release of VWF. Black bars represent YFP-transfected cells. Hatched bars represent SYTXI-EGFP-transfected cells.

n/s = non-significant (p-value › 0.05)

n = 3 replicates from one vial of HUVECs; data is representative of 3 individual experiments performed on separate vials of HUVECs.

suggested that SYT I plays no role in mediating the exocytosis of WPBs as no effect on the secretion of either VWF or proregion was seen following the up-regulation or inhibition of SYT I in HUVECs. This observation was not entirely surprising as SYT I is a low-affinity calcium sensor which is specialized for fast synaptic transmission. This is contrast to the relatively slow release kinetics of large dense-core vesicles such as WPBs. Additionally, SYT I is primarily expressed in neuronal cells where its role in synaptic transmission has been well

established. In contrast its role in non-neuronal secretory tissue is more unclear. With this in mind and considering the functional studies performed here I will discount this member of the SYT family as a potential candidate for the role of the calcium sensor regulating WPB release at the plasma membrane. However, definitive proof would be provided by repeating these biochemical assays using endothelial cells isolated from SYT I $^{-/-}$ embryonic mice as these reagents are widely available.

8.6.2 The Role of SYT III:

The absence of SYT III from WPBs implies that this member of the SYT family is not involved in mediating the Ca^{2+}-dependent exocytosis of these organelles. Over-expression ELISAs using the SYTIII-EGFP construct confirmed this theory as the up-regulation of SYT III does not affect the release of either VWF or proregion from stimulated HUVECs. Therefore this member of the SYT family will be discounted as a possible candidate for the role of the calcium sensor mediating WPB exocytosis. However, as mentioned (Chapter 4) the work done here suggests that SYT III may play an essential role in the formation of recycling endosomes in HUVECs. Future work could focus on testing this hypothesis with knock-down and mutagenesis studies. Specifically, it would be of interest to determine the effect of the loss of a functional SYT III protein on the distribution of rab11 and the morphology of endocytic granules in HUVECs. The generation of a SYT III $^{-/-}$ mouse would also prove indispensable for the investigation of the true function of this member of the SYT family in endothelial cells and in other cell types, particularly in neurons.

8.6.3 The Role of SYT VI:

The work presented in the previous chapters has demonstrated that SYT VI is found as both an mRNA transcript and as a protein in human endothelial cells. The subcellular localization of SYT VI in HUVECs is currently unclear as the endogenous protein is found predominately as a component of the early endosomes whereas over-expression studies using the SYTVI-EGFP construct indicated that over-expressed SYT VI localizes to the endoplasmic reticulum and plasma membrane. However, what is clear is that SYT VI is not found as a component of the WPBs and therefore is unlikely to be involved in the regulation of their Ca^{2+}-mediated fusion with the plasma membrane. This hypothesis was strengthened by the observation that the over-expression of SYTVI-EGFP in HUVECs does not affect the

secretion of either VWF or proregion from transfected cells compared with YFP-expressing control cells. Therefore, this work will conclude that SYT VI is not involved in the regulation of WPB exocytosis from HUVECs but rather plays another role in endothelial cell biology. It would be of interest to determine precisely which isoforms of SYT VI are expressed in HUVECs using variant-specific PCR in the future. Once the number and identity of the isoforms expressed in HUVECs have been established, a series of SYTVI-EGFP vectors could be generated from HUVEC cDNA. These reagents could be used to determine the true extent of the subcellular localization of the SYT VI protein(s) as it is likely that each isoform displays a unique distribution pattern. Future work to determine the role of SYT VI in HUVECs could involve knock-down or mutagenesis studies, and as a long-term project a SYTVI-KO mouse would prove insightful as to the function of this poorly-characterized SYT in many different cell types. However, this is of course beyond the scope of this project.

8.6.4 The Role of SYT XI:

SYT XI is a ubiquitously-expressed Ca^{2+}-insensitive member of the SYT family. Although the SYT XI gene has been loosely linked with the development of human psychiatric disorders the function of the SYT XI protein is currently unknown. Here, I have demonstrated that SYT XI mRNA is present in HUVECs and have attempted to determine the subcellular localization and function of this SYT isoform in our model endothelial cells.

Over-expression VWF ELISAs have demonstrated that SYT XI up-regulation in HUVECs does not affect WPB exocytosis in response to stimulation by 1 µM ionomycin. This was not entirely unexpected as due to its Golgi distribution the SYT XI protein is not in a subcellular location which would allow it to regulate the fusion of WPBs with the plasma membrane. However SYT XI may be involved in mediating the biosynthesis of WPBs at the Golgi although ICC revealed that WPBs in SYTXI-EGFP transfected cells appear morphologically normal. Therefore, SYT XI most likely plays an as-yet unidentified role in endothelial cell biology and may be involved in either the formation of subcellular vesicles or the fusion of recycling vesicles returning cargo to the TGN.

Future work attempting to determine the role of this Ca^{2+}-insensitive member of the SYT family could focus on mutagenesis or knock-down studies. I took the decision not to pursue these avenues for the purposes of this investigation. Equally, live-cell imaging using over-expressed SYTXI-EGFP would provide a definitive answer to the question as to whether or not SYT XI is involved in WPB exocytosis, as over-expression ELISAs are

always limited by the transfection efficiency of the over-expressed construct. Finally, it would be of general interest to generate a SYT XI knock-out mouse to determine if this animal shows any obvious phenotypic abnormalities, particularly a higher susceptibility to developing symptoms resembling human psychiatric disorders.

Chapter 9
Final Discussion

Over the course of my project I have attempted to determine the identity of the calcium sensor responsible for mediating the Ca^{2+}-induced exocytosis of WPBs from human endothelial cells. It is my hypothesis that this process is regulated by one or more members of the SYT family as this group of proteins has been shown to have an extensive and fundamental role in the regulation of secretory events from a vast range of cell types. In this thesis, I have provided evidence demonstrating that SYTs I, III, V, VI, VII, VIII, XI, and XVII can be found as mRNA transcripts in our model endothelial cells. I have also shown that the majority of these SYTs are found as proteins in HUVECs. Unfortunately, for the most part my attempts to determine the endogenous distribution of the endothelial-expressed SYTs by ICC were unsuccessful. Therefore I constructed a series of fluorescent fusion proteins which were over-expressed in HUVECs with the aim to determine the subcellular distribution of the SYTs in our model endothelial cells. The results of this work are summarized in full in Table 4.2. Of particular note, I detected the presence of SYTs V, VII, VIII, and XVII on WPBs and as a result of these observations the majority of the functional studies described here focused on characterizing the role of these four members of the SYT family in endothelial cells. Indeed, my principal molecule of interest was SYT VII as this highly-conserved protein has a well-established role in regulating the Ca^{2+}-mediated exocytosis of large secretory organelles from a range of cell types (Andrews and Chakrabarti, 2005). Through the use of a novel dose-response assay I was able to demonstrate that SYT VII does indeed play a role in the regulation of WPB exocytosis by mediating the calcium sensitivity of secretion. Additionally, over-expression ELISAs suggested a more unclear role for SYTs V and XVII in the regulation of VWF secretion from HUVECs which warrants further investigation. Lastly, it is noteworthy that I have demonstrated the expression and surprisingly extensive distribution of SYT XVII in endothelial cells as to my knowledge this will be the first study attempting to characterize the tissue distribution, subcellular localization, and function of this newest member of the SYT family.

As would be expected I encountered a number of challenges over the course of this project. Firstly, as documented I have been unable to determine the endogenous distribution of the SYTs in HUVECs as commercial antibodies are unable to recognize SYT protein by ICC under the conditions used in our laboratory. It is possible that members of the SYT

family are expressed in endothelial cells at a level which falls below the detection criteria of the antibodies or it may be that the particular SYT isoforms expressed in HUVECs are not recognized by the commercial antibodies, most of which have been developed using one common variant of their target protein. Another possibility is that in resting HUVECs the SYTs exist as a complex with other molecular mediators of exocytosis and are therefore inaccessible to their antibodies. It should be noted that this inability to detect endogenous SYTs by ICC is commonplace in the literature and therefore the majority of investigators opt for the over-expression of fluorescent fusion proteins to determine the distribution of the SYTs in their cells of interest. This was the path I took although it would also have been possible to personally design and manufacture variant-specific antibodies once the full sequences of the endothelial-expressed SYTs had been established. However, due to the number of proteins under investigation in this report I have been unable to attempt this in the time available. In the future it would be of particular interest to design non-commercial antibodies against SYTs V, VII, VIII, and XVII to confirm that these proteins do indeed localize endogenously to the WPBs as has been strongly suggested by the over-expression studies performed here.

A particularly time-consuming obstacle to my progress was my failure to generate SYT-EGFP fusion vectors using conventional cloning techniques dependent on enzyme-driven ligation. Despite repeated attempts to troubleshoot the cloning protocol I was consistently unable to clone SYT cDNA into parent EGFP vectors. This inhibited my progress for some time as without these reagents I was unable to determine the distribution of the endothelial-expressed SYTs. Therefore I attempted a novel ligation-independent cloning (LIC) method which by-passed the need for restriction and ligation enzymes. This method proved extremely effective and I was able to generate SYT-EGFP fusion vectors. These new tools enabled me to determine the distribution of the SYTs in HUVECs which in turn allowed the identification of strong candidates for the role of the calcium sensor regulating WPB release on which I based my functional studies. Of course, care must be taken with the interpretation of these observations as the distribution of over-expressed SYT protein may not necessarily be representative of that of the endogenous protein. However, in most cases my findings have been consistent with published studies examining the distribution of SYTs in other cell types. Additionally, this systematic screening approach involving the expression of GFP-tagged protein has proved successful for determining the distribution of Rab proteins in PC12 cells (Tsuboi and Fukuda, 2006) and HUVECs (Zografou *et al.* 2012).

An essential component of the functional studies performed here was the use of siRNA to eliminate SYT mRNA from HUVECs with the aim to determine the effects of the knock-down of individual SYTs on WPB exocytosis. However, in most cases the quantification of the knock-down effect was challenging as I was unable to use ICC to demonstrate the loss of endogenous protein in fixed cells. Instead, I relied on Western blotting which was in turn complicated by the difficulty in visualizing SYT protein by immunoblotting and by the simultaneous expression of multiple SYT variants in HUVEC lysate. It would have been possible to use real-time PCR (Q-PCR) to determine the exact extent of mRNA knock-down in HUVECs. However, this method would not provide a reliable estimate of the extent of protein knock-down as it is likely that each SYT variant has a different degree of stability in endothelial cells. In order to determine the absolute effect of the knock-down of the SYT family members on WPB exocytosis it would be essential to produce or obtain SYT $^{-/-}$ mice, as only this approach would allow the complete elimination of all variants of each SYT from endothelial cells. These reagents are available for a small number of the SYT family members and I have trialed methods for isolating and culturing endothelial cells derived from murine lung tissue. The long-term goal of this was to establish a colony of SYT VII $^{-/-}$ mice which would provide a source of SYT VII $^{-/-}$ endothelial cells for future experiments. In the immediate future it would be of interest to perform double knock-out experiments as members of the SYT family are known to function both cooperatively and redundantly to regulate secretory events (Lynch and Martin, 2007, Nishiki and Augustine, 2004). It would be of particular interest to selectively eliminate combinations of the WPB-localized SYTs to determine if this additive approach yields a greater functional effect than the single knock-outs performed here.

The majority of the functional studies described in this report relied upon the over-expression of SYT-EGFP constructs and therefore have limitations of their own. In most cases the transfection efficiency of the construct was poor with the majority of transfected HUVECs failing to express the ectopic DNA. A possible solution to this would have been to differentiate between expressing and non-expressing HUVECs through cell sorting by flow cytometry using an α-GFP antibody. However, it would be of greater importance and more efficient to perform live-cell imaging experiments using HUVECs over-expressing the SYT-EGFP constructs. This would allow the accumulation of real-time kinetic data on a single-cell level and would provide an accurate measure of the effect of the up-regulation of the SYT family members on both the rate and extent of WPB exocytosis from HUVECs. However, in order to perform these assays it was essential to create either red-fluorescent versions of my

EGFP-tagged SYT constructs or develop a red-fluorescent pH-sensitive marker of WPBs. To this aim I have attempted to create a construct consisting of the WPB-resident protein proregion coupled to the novel pH-sensitive red fluorescent proteins Fuji and pH Tomato (both a kind gift from Professor Robert E. Campbell of the University of Alberta) with the aim to use these reagents to selectively mark WPBs in transfected cells. However this has been unsuccessful thus far.

As a final point, all of the secretion assays performed here have utilized the non-physiological reagent ionomycin to induce WPB exocytosis. The mechanism of action of ionomycin in endothelial cells is currently unclear although it is known to induce a reversible biphasic increase in the cytoplasmic Ca^{2+} concentration, with the initial spike resulting from the release of Ca^{2+} ions from intracellular stores and the second, more-sustained increase resulting from the influx of Ca^{2+} across the plasma membrane in response to store depletion (Morgan and Jacob, 1994). Indeed, rather than induce uncontrolled Ca^{2+} influx across the plasma membrane ionomycin mimics the endogenous signaling pathways initiated by physiological agonists such as histamine (Morgan and Jacob, 1994). However, ionomycin does induce a stronger secretory response from HUVECs than histamine and so it is possible that it triggers the release of a reserve pool of WPBs which is not accessible to physiological agonists (Erent *et al.* 2007). It may also be the case that ionomycin exposure results in the loss of the spatial control of WPB exocytosis as a more global response to stimulation would be induced compared to that initiated by receptor-based signaling pathways. These considerations may be relevant to the work described here as the WPB-localized SYTs may specifically label distinct subpopulations of granules. For example, a cursory examination of the subcellular distribution of over-expressed SYTVIII-EGFP in HUVECs suggests that this construct might preferentially localize to rounder granules and so may influence WPB morphology, perhaps through the recruitment of other membrane proteins during granule formation at the TGN. The rigorous analysis of the distribution of over-expressed SYTs in HUVECs may identify certain WPBs which are labeled by specific SYTs, such as those which form the RRP or those which contain certain subsets of cargo proteins. Equally, more detailed investigations into the morphology of WPBs in HUVECs which have been treated with SYT siRNA may reveal subtle changes in granule size and shape. Therefore it would be of interest, firstly, to repeat the secretion assays performed here with a physiological agonist such as histamine to determine the reproducibility of the ionomycin-induced stimulation data, and secondly to perform an analysis of the spatial distribution of the SYTs in HUVECs and the specific features of the granules to which they preferentially localize.

It is my hope that this work will prove of general interest to those working in the field of regulated exocytosis and its control by the SYT family. Additionally, my observations have provided a solid foundation on which future investigations aiming to further characterize the role of the SYT family in the control of WPB exocytosis can be based. However, it is essential to consider that WPB exocytosis may well be regulated by a family of calcium sensors entirely separate to the SYTs, and other possible candidates for the role of the Ca^{2+} sensor include but are not limited to the annexins, the Doc2 proteins, MCTPs, copines, the VP115 family, and the ferlins (for reviews describing these protein families see Burgoyne and Morgan, 1998, Sudhof 2002, and Pang and Sudhof, 2010). Indeed, I have demonstrated by PCR that HUVECs express Doc2A and Doc2B (data not shown) in addition to the eight SYTs described here. However, the SYT family is the most well-characterized group of calcium sensors with a fundamental role in the regulation of Ca^{2+}-mediated exocytosis, and given the extensive expression of the SYTs in HUVECs I have limited my investigations to this collection of Ca^{2+}-binding proteins.

In conclusion, over the course of this thesis I have described my attempts to determine the identity of the Ca^{2+} sensor regulating WPB exocytosis from human endothelial cells. WPBs are specialized secretory organelles which have considerable clinical relevance, being implicated in the pathology of atherosclerosis, thrombosis, and malaria. Additionally, in recent years exciting new links between WPB exocytosis and the development of multiple sclerosis, the recruitment of stem cells, and the metastasis of cancerous cells have been proposed. With this in mind it is essential to fully understand the mechanisms of WPB exocytosis with the aim that this process may be manipulated in the future for the benefit of human health. Finally, WPBs provide an excellent general model of regulated exocytosis and therefore insights into how this process is controlled at the molecular level can be applied to other secretory systems in order to better understand this fundamental aspect of cell biology.

References

Adolfsen, B., S. Saraswati, M. Yoshihara, and J.T. Littleton. 2004. Synaptotagmins are trafficked to distinct subcellular domains including the postsynaptic compartment. *J Cell Biol*. 166:249-60.

Aird, W.C. 2007. Phenotypic heterogeneity of the endothelium: I. Structure, function, and mechanisms. *Circ Res*. 100:158-73.

Andersson, S.A., A.H. Olsson, J.L. Esguerra, E. Heimann, C. Ladenvall, A. Edlund, A. Salehi, J. Taneera, E. Degerman, L. Groop, C. Ling, and L. Eliasson. 2012. Reduced insulin secretion correlates with decreased expression of exocytotic genes in pancreatic islets from patients with type 2 diabetes. *Mol Cell Endocrinol*. 364:36-45.

Andrews, N.W., and S. Chakrabarti. 2005. There's more to life than neurotransmission: the regulation of exocytosis by synaptotagmin VII. *Trends Cell Biol*. 15:626-31.

Arantes, R.M., and N.W. Andrews. 2006. A role for synaptotagmin VII-regulated exocytosis of lysosomes in neurite outgrowth from primary sympathetic neurons. *J Neurosci*. 26:4630-7.

Arribas, M., and D.F. Cutler. 2000. Weibel-Palade body membrane proteins exhibit differential trafficking after exocytosis in endothelial cells. *Traffic*. 1:783-93.

Aslanidis, C., and P.J. de Jong. 1990. Ligation-independent cloning of PCR products (LIC-PCR). *Nucleic Acids Res*. 18:6069-74.

Bacharach, E., A. Itin, and E. Keshet. 1992. In vivo patterns of expression of urokinase and its inhibitor PAI-1 suggest a concerted role in regulating physiological angiogenesis. *Proc Natl Acad Sci U S A*. 89:10686-90.

Bachetti, T., and L. Morbidelli. 2000. Endothelial cells in culture: a model for studying vascular functions. *Pharmacol Res*. 42:9-19.

Bai, J., P. Wang, and E.R. Chapman. 2002. C2A activates a cryptic Ca(2+)-triggered membrane penetration activity within the C2B domain of synaptotagmin I. *Proc Natl Acad Sci U S A*. 99:1665-70.

Bai, J., C.T. Wang, D.A. Richards, M.B. Jackson, and E.R. Chapman. 2004. Fusion pore dynamics are regulated by synaptotagmin*t-SNARE interactions. *Neuron*. 41:929-42.

Baram, D., Y.A. Mekori, and R. Sagi-Eisenberg. 2001. Synaptotagmin regulates mast cell functions. *Immunol Rev*. 179:25-34.

Bauer, A.T., E.A. Strozyk, C. Gorzelanny, C. Westerhausen, A. Desch, M.F. Schneider, and S.W. Schneider. 2011, Cytotoxicity of silica nanoparticles through exocytosis of von Willebrand factor and necrotic cell death in primary human endothelial cells. *Biomaterials*. 32:8385-93.

Becker, S.M., L. Delamarre, I. Mellman, and N.W. Andrews. 2009. Differential role of the Ca(2+) sensor synaptotagmin VII in macrophages and dendritic cells. *Immunobiology*. 214:495-505.

Berntson, A.K., and C.W. Morgans. 2003. Distribution of the presynaptic calcium sensors, synaptotagmin I/II and synaptotagmin III, in the goldfish and rodent retinas. *J Vis*. 3:274-80.

Berridge, M.J. 2009. Inositol trisphosphate and calcium signalling mechanisms. *Biochim Biophys Acta*. 1793:933-40.

Berton, F., C. Iborra, J.A. Boudier, M.J. Seagar, and B. Marqueze. 1997. Developmental regulation of synaptotagmin I, II, III, and IV mRNAs in the rat CNS. *J Neurosci*. 17:1206-16.

Bierings, R., N. Hellen, N. Kiskin, L. Knipe, A.V. Fonseca, B. Patel, A. Meli, M. Rose, M.J. Hannah, and T. Carter. 2012. The interplay between the Rab27A effectors Slp4-a and MyRIP controls hormone-evoked Weibel-Palade body exocytosis. *Blood*. 120:2757-67.

Birch, K.A., J.S. Pober, G.B. Zavoico, A.R. Means, and B.M. Ewenstein. 1992. Calcium/calmodulin transduces thrombin-stimulated secretion: studies in intact and minimally permeabilized human umbilical vein endothelial cells. *J Cell Biol*. 118:1501-10.

Birnboim, H.C., and J. Doly. 1979. A rapid alkaline extraction procedure for screening recombinant plasmid DNA. *Nucleic Acids Res.* 7:1513-23.

Bock, J.B., H.T. Matern, A.A. Peden, and R.H. Scheller. 2001. A genomic perspective on membrane compartment organization. *Nature*. 409:839-41.

Bonfanti, R., B.C. Furie, B. Furie, and D.D. Wagner. 1989. PADGEM (GMP140) is a component of Weibel-Palade bodies of human endothelial cells. *Blood*. 73:1109-12.

Bonthron, D.T., R.I. Handin, R.J. Kaufman, L.C. Wasley, E.C. Orr, L.M. Mitsock, B. Ewenstein, J. Loscalzo, D. Ginsburg, and S.H. Orkin. 1986. Structure of pre-pro-von Willebrand factor and its expression in heterologous cells. *Nature*. 324:270-3.

Bordier, C. 1981. Phase separation of integral membrane proteins in Triton X-114 solution. *J Biol Chem*. 256:1604-7.

Brandt, D.S., M.D. Coffman, J.J. Falke, and J.D. Knight. 2012.Hydrophobic contributions to the membrane docking of synaptotagmin 7 C2A domain: mechanistic contrast between isoforms 1 and 7. *Biochemistry*. 51:7654-64.

Braun, S., and S. Jentsch. 2007. SM-protein-controlled ER-associated degradation discriminates between different SNAREs. *EMBO Rep*. 8:1176-82.

Brauneis, U., Z. Gatmaitan, and I.M. Arias. 1992. Serotonin stimulates a Ca2+ permeant nonspecific cation channel in hepatic endothelial cells. *Biochem Biophys Res Commun*. 186:1560-6.

Brose, N., K. Hofmann, Y. Hata, and T.C. Sudhof. 1995. Mammalian homologues of Caenorhabditis elegans unc-13 gene define novel family of C2-domain proteins. *J Biol Chem*. 270:25273-80.

Brown, H., B. Meister, J. Deeney, B.E. Corkey, S.N. Yang, O. Larsson, C.J. Rhodes, S. Seino, P.O. Berggren, and G. Fried. 2000. Synaptotagmin III isoform is compartmentalized in pancreatic beta-cells and has a functional role in exocytosis. *Diabetes*. 49:383-91.

Bryant, N.J., and D.E. James. 2001. Vps45p stabilizes the syntaxin homologue Tlg2p and positively regulates SNARE complex formation. *EMBO J*. 20:3380-8.

Burgoyne, R.D., and A. Morgan. 1998. Calcium sensors in regulated exocytosis. *Cell Calcium*. 24:367-76.

Burridge, K.A., and M.H. Friedman. 2010. Environment and vascular bed origin influence differences in endothelial transcriptional profiles of coronary and iliac arteries. *Am J Physiol Heart Circ Physiol*. 299:H837-46.

Butz, S., R. Fernandez-Chacon, F. Schmitz, R. Jahn, and T.C. Sudhof. 1999. The subcellular localizations of atypical synaptotagmins III and VI. Synaptotagmin III is enriched in synapses and synaptic plasma membranes but not in synaptic vesicles. *J Biol Chem*. 274:18290-6.

Cambien, B., and D.D. Wagner. 2004. A new role in hemostasis for the adhesion receptor P-selectin. *Trends Mol Med*. 10:179-86.

Carmeliet, P., L. Schoonjans, L. Kieckens, B. Ream, J. Degen, R. Bronson, R. De Vos, J.J. van den Oord, D. Collen, and R.C. Mulligan. 1994. Physiological consequences of loss of plasminogen activator gene function in mice. *Nature*. 368:419-24.

Carter, T.D., G. Zupancic, S.M. Smith, C. Wheeler-Jones, and D. Ogden. 1998. Membrane capacitance changes induced by thrombin and calcium in single endothelial cells cultured from human umbilical vein. *J Physiol*. 513 (Pt 3):845-55.

Chakrabarti, S., K.S. Kobayashi, R.A. Flavell, C.B. Marks, K. Miyake, D.R. Liston, K.T. Fowler, F.S. Gorelick, and N.W. Andrews. 2003. Impaired membrane resealing and autoimmune myositis in synaptotagmin VII-deficient mice. *J Cell Biol*. 162:543-9.

Choi, K., M. Kennedy, A. Kazarov, J.C. Papadimitriou, and G. Keller. 1998. A common precursor for hematopoietic and endothelial cells. *Development*. 125:725-32.

Choi, S.S., J.Y. Jung, D.H. Lee, J.Y. Kang, and S.H. Lee. 2012. Expression and regulation of SNAP-25 and synaptotagmin VII in developing mouse ovarian follicles via the FSH receptor. *J Mol Histol*. 44:47-54.

Cines, D.B., E.S. Pollak, C.A. Buck, J. Loscalzo, G.A. Zimmerman, R.P. McEver, J.S. Pober, T.M. Wick, B.A. Konkle, B.S. Schwartz, E.S. Barnathan, K.R. McCrae, B.A. Hug, A.M. Schmidt, and D.M. Stern. 1998. Endothelial cells in physiology and in the pathophysiology of vascular disorders. *Blood*. 91:3527-61.

Cambien, B., and D.D. Wagner. 2004. A new role in hemostasis for the adhesion receptor P-selectin. *Trends Mol Med*. 10:179-86.

Campbell, W,B., Halushka, P,V 1996 Eicosanoids and platelet-activating factor, in Hardman JG, Limbird LE, Molinoff PM, Ruddon RW, filman AG (eds): Goodman and Gilman's The Pharmacologic Basis of Therapeutics. New York, NY, McGraw-Hill, p601

Castaman, G., S.H. Giacomelli, P. Jacobi, T. Obser, U. Budde, F. Rodeghiero, S.L. Haberichter, and R. Schneppenheim. 2010. Homozygous type 2N R854W von Willebrand factor is poorly secreted and causes a severe von Willebrand disease phenotype. *J Thromb Haemost*. 8:2011-6.

Castillo Bennett, J., C.M. Roggero, F.E. Mancifesta, and L.S. Mayorga. Calcineurin-mediated dephosphorylation of synaptotagmin VI is necessary for acrosomal exocytosis. *J Biol Chem*. 285:26269-78.

Chalfie, M., Y. Tu, G. Euskirchen, W.W. Ward, and D.C. Prasher. 1994. Green fluorescent protein as a marker for gene expression. *Science*. 263:802-5.

Chapman, E.R., P.I. Hanson, S. An, and R. Jahn. 1995. Ca2+ regulates the interaction between synaptotagmin and syntaxin 1. *J Biol Chem*. 270:23667-71.

Chen, X., D.R. Tomchick, E. Kovrigin, D. Arac, M. Machius, T.C. Sudhof, and J. Rizo. 2002. Three-dimensional structure of the complexin/SNARE complex. *Neuron*. 33:397-409.

Colvin, R.A., T.K. Means, T.J. Diefenbach, L.F. Moita, R.P. Friday, S. Sever, G.S. Campanella, T. Abrazinski, L.A. Manice, C. Moita, N.W. Andrews, D. Wu, N. Hacohen, and A.D. Luster. 2010. Synaptotagmin-mediated vesicle fusion regulates cell migration. *Nat Immunol*. 11:495-502.

Cooper, P.R., N.J. Nowak, M.J. Higgins, D.M. Church, and T.B. Shows. 1998. Transcript mapping of the human chromosome 11q12-q13.1 gene-rich region identifies several newly described conserved genes. *Genomics*. 49:419-29.

Craxton, M., and M. Goedert. 1999. Alternative splicing of synaptotagmins involving transmembrane exon skipping. *FEBS Lett*. 460:417-22.

Craxton, M., A. Olsen, and M. Goedert. 1997. Human synaptotagmin V (SYT5): sequence, genomic structure, and chromosomal location. *Genomics*. 42:165-9.

Cullere, X., S.K. Shaw, L. Andersson, J. Hirahashi, F.W. Luscinskas, and T.N. Mayadas. 2005. Regulation of vascular endothelial barrier function by Epac, a cAMP-activated exchange factor for Rap GTPase. *Blood*. 105:1950-5.

Cutler, D.F. 2002. Introduction: lysosome-related organelles. *Semin Cell Dev Biol*. 13:261-2.

Czibener, C., N.M. Sherer, S.M. Becker, M. Pypaert, E. Hui, E.R. Chapman, W. Mothes, and N.W. Andrews. 2006. Ca2+ and synaptotagmin VII-dependent delivery of lysosomal membrane to nascent phagosomes. *J Cell Biol*. 174:997-1007.

Dai, X.Q., G. Plummer, M. Casimir, Y. Kang, C. Hajmrle, H.Y. Gaisano, J.E. Manning Fox, and P.E. MacDonald. 2011. SUMOylation regulates insulin exocytosis downstream of secretory granule docking in rodents and humans. *Diabetes*. 60:838-47.

Damle, N.K., and L.V. Doyle. 1987. Interleukin-2 activated human killer lymphocytes: lack of involvement of interferon in the development of IL-2-activated killer lymphocytes. *Int J Cancer*. 40:519-24.

Dasgupta, S., and R.B. Kelly. 2003. Internalization signals in synaptotagmin VII utilizing two independent pathways are masked by intramolecular inhibitions. *J Cell Sci*. 116:1327-37.

Davis, A.F., J. Bai, D. Fasshauer, M.J. Wolowick, J.L. Lewis, and E.R. Chapman. 1999. Kinetics of synaptotagmin responses to Ca2+ and assembly with the core SNARE complex onto membranes. *Neuron*. 24:363-76.

Davletov, B., J.M. Sontag, Y. Hata, A.G. Petrenko, E.M. Fykse, R. Jahn, and T.C. Sudhof. 1993. Phosphorylation of synaptotagmin I by casein kinase II. *J Biol Chem*. 268:6816-22.

Davletov, B.A., and T.C. Sudhof. 1993. A single C2 domain from synaptotagmin I is sufficient for high affinity Ca2+/phospholipid binding. *J Biol Chem*. 268:26386-90.

Dean, C., F.M. Dunning, H. Liu, E. Bomba-Warczak, H. Martens, V. Bharat, S. Ahmed, and E.R. Chapman. 2012. Axonal and dendritic synaptotagmin isoforms revealed by a pHluorin-syt functional screen. *Mol Biol Cell*. 23:1715-27.

Dejana, E. 2004. Endothelial cell-cell junctions: happy together. *Nat Rev Mol Cell Biol*. 5:261-70.

Dekker, R.J., R.A. Boon, M.G. Rondaij, A. Kragt, O.L. Volger, Y.W. Elderkamp, J.C. Meijers, J. Voorberg, H. Pannekoek, and A.J. Horrevoets. 2006. KLF2 provokes a gene expression pattern that establishes functional quiescent differentiation of the endothelium. *Blood*. 107:4354-63.

de Leeuw, H.P., P.M. Koster, J. Calafat, H. Janssen, A.J. van Zonneveld, J.A. van Mourik, and J. Voorberg. 1998. Small GTP-binding proteins in human endothelial cells. *Br J Haematol*. 103:15-9.

de Mast, Q., E. Groot, P.B. Asih, D. Syafruddin, M. Oosting, S. Sebastian, B. Ferwerda, M.G. Netea, P.G. de Groot, A.J. van der Ven, and R. Fijnheer. 2009. ADAMTS13 deficiency with elevated levels of ultra-large and active von Willebrand factor in P. falciparum and P. vivax malaria. *Am J Trop Med Hyg*. 80:492-8.

de Wit, H., A.M. Walter, I. Milosevic, A. Gulyas-Kovacs, D. Riedel, J.B. Sorensen, and M. Verhage. 2009. Synaptotagmin-1 docks secretory vesicles to syntaxin-1/SNAP-25 acceptor complexes. *Cell*. 138:935-46.

Dietrich, L.E., C. Boeddinghaus, T.J. LaGrassa, and C. Ungermann. 2003. Control of eukaryotic membrane fusion by N-terminal domains of SNARE proteins. *Biochim Biophys Acta*. 1641:111-9.

Djamiatun, K., A.J. van der Ven, P.G. de Groot, S.M. Faradz, D. Hapsari, W.M. Dolmans, S. Sebastian, R. Fijnheer, and Q. de Mast. 2012 Severe dengue is associated with consumption of von Willebrand factor and its cleaving enzyme ADAMTS-13. *PLoS Negl Trop Dis*. 6:e1628.

Dong, J.F., J.L. Moake, L. Nolasco, A. Bernardo, W. Arceneaux, C.N. Shrimpton, A.J. Schade, L.V. McIntire, K. Fujikawa, and J.A. Lopez. 2002. ADAMTS-13 rapidly cleaves newly secreted ultralarge von Willebrand factor multimers on the endothelial surface under flowing conditions. *Blood*. 100:4033-9.

Drake, T.A., J.H. Morrissey, and T.S. Edgington. 1989. Selective cellular expression of tissue factor in human tissues. Implications for disorders of hemostasis and thrombosis. *Am J Pathol*. 134:1087-97

Dulubova, I., S. Sugita, S. Hill, M. Hosaka, I. Fernandez, T.C. Sudhof, and J. Rizo. 1999. A conformational switch in syntaxin during exocytosis: role of munc18. *EMBO J*. 18:4372-82.

Dvorak, A.M., and D. Feng. 2001. The vesiculo-vacuolar organelle (VVO). A new endothelial cell permeability organelle. *J Histochem Cytochem*. 49:419-32.

Egan, K., and G.A. FitzGerald. 2006. Eicosanoids and the vascular endothelium. *Handb Exp Pharmacol*:189-211.

Elfving, B., B.E. Bonefeld, R. Rosenberg, and G. Wegener. 2008. Differential expression of synaptic vesicle proteins after repeated electroconvulsive seizures in rat frontal cortex and hippocampus. *Synapse*. 62:662-70.

Erent, M., A. Meli, N. Moisoi, V. Babich, M.J. Hannah, P. Skehel, L. Knipe, G. Zupancic, D. Ogden, and T. Carter. 2007. Rate, extent and concentration dependence of histamine-evoked Weibel-Palade body exocytosis determined from individual fusion events in human endothelial cells. *J Physiol*. 583:195-212.

Ewenstein, B.M., M.J. Warhol, R.I. Handin, and J.S. Pober. 1987. Composition of the von Willebrand factor storage organelle (Weibel-Palade body) isolated from cultured human umbilical vein endothelial cells. *J Cell Biol*. 104:1423-33.

Falcke, M., J.L. Hudson, P. Camacho, and J.D. Lechleiter. 1999. Impact of mitochondrial Ca2+ cycling on pattern formation and stability. *Biophys J*. 77:37-44.

Falkowski, M.A., D.D. Thomas, S.W. Messenger, T.F. Martin, and G.E. Groblewski. 2011. Expression, localization, and functional role for synaptotagmins in pancreatic acinar cells. *Am J Physiol Gastrointest Liver Physiol*. 301:G306-16.

Fayos, B.E., and B.W. Wattenberg. 1997. Regulated exocytosis in vascular endothelial cells can be triggered by intracellular guanine nucleotides and requires a hydrophobic, thiol-sensitive component. Studies of regulated von Willebrand factor secretion from digitonin permeabilized endothelial cells. *Endothelium*. 5:339-50.

Ferguson, G.D., L. Vician, and H.R. Herschman. 2001. Synaptotagmin IV: biochemistry, genetics, behavior, and possible links to human psychiatric disease. *Mol Neurobiol*. 23:173-85.

Fernandes, M.C., A.R. Flannery, N. Andrews, and R.A. Mortara. 2013. Extracellular amastigotes of Trypanosoma cruzi are potent inducers of phagocytosis in mammalian cells. *Cell Microbiol*. 15:977-991

Fernandez, I., D. Arac, J. Ubach, S.H. Gerber, O. Shin, Y. Gao, R.G. Anderson, T.C. Sudhof, and J. Rizo. 2001. Three-dimensional structure of the synaptotagmin 1 C2B-domain: synaptotagmin 1 as a phospholipid binding machine. *Neuron*. 32:1057-69.

Fernandez, I., J. Ubach, I. Dulubova, X. Zhang, T.C. Sudhof, and J. Rizo. 1998. Three-dimensional structure of an evolutionarily conserved N-terminal domain of syntaxin 1A. *Cell*. 94:841-9.

Fernandez, J.M., E. Neher, and B.D. Gomperts. 1984. Capacitance measurements reveal stepwise fusion events in degranulating mast cells. *Nature*. 312:453-5.

Fernandez-Chacon, R., A. Konigstorfer, S.H. Gerber, J. Garcia, M.F. Matos, C.F. Stevens, N. Brose, J. Rizo, C. Rosenmund, and T.C. Sudhof. 2001. Synaptotagmin I functions as a calcium regulator of release probability. *Nature*. 410:41-9.

Fiedler, U., M. Scharpfenecker, S. Koidl, A. Hegen, V. Grunow, J.M. Schmidt, W. Kriz, G. Thurston, and H.G. Augustin. 2004. The Tie-2 ligand angiopoietin-2 is stored in and rapidly released upon stimulation from endothelial cell Weibel-Palade bodies. *Blood*. 103:4150-6.

Flannery, A.R., C. Czibener, and N.W. Andrews. 2010. Palmitoylation-dependent association with CD63 targets the Ca2+ sensor synaptotagmin VII to lysosomes. *J Cell Biol*. 191:599-613.

Fowler, K.T., N.W. Andrews, and J.W. Huleatt. 2007. Expression and function of synaptotagmin VII in CTLs. *J Immunol*. 178:1498-504.

Frangogiannis, N.G. 2006. Targeting the inflammatory response in healing myocardial infarcts. *Curr Med Chem*. 13:1877-93.

Fu, J., A.P. Naren, X. Gao, G.U. Ahmmed, and A.B. Malik. 2005. Protease-activated receptor-1 activation of endothelial cells induces protein kinase Calpha-dependent phosphorylation of syntaxin 4 and Munc18c: role in signaling p-selectin expression. *J Biol Chem*. 280:3178-84.

Fukuda, M. 2008. Regulation of secretory vesicle traffic by Rab small GTPases. *Cell Mol Life Sci*. 65:2801-13.

Fukuda, M., E. Katayama, and K. Mikoshiba. 2002. The calcium-binding loops of the tandem C2 domains of synaptotagmin VII cooperatively mediate calcium-dependent oligomerization. *J Biol Chem*. 277:29315-20.

Fukuda, M., T. Kojima, and K. Mikoshiba. 1997. Regulation by bivalent cations of phospholipid binding to the C2A domain of synaptotagmin III. *Biochem J*. 323 (Pt 2):421-5.

Fukuda, M., and K. Mikoshiba. 1999. A novel alternatively spliced variant of synaptotagmin VI lacking a transmembrane domain. Implications for distinct functions of the two isoforms. *J Biol Chem*. 274:31428-34.

Fukuda, M., and K. Mikoshiba. 2000. Distinct self-oligomerization activities of synaptotagmin family. Unique calcium-dependent oligomerization properties of synaptotagmin VII. *J Biol Chem*. 275:28180-5

Fukuda, M., and K. Mikoshiba. 2001. Mechanism of the calcium-dependent multimerization of synaptotagmin VII mediated by its first and second C2 domains. *J Biol Chem*. 276:27670-6.

Fukuda, M., Y. Ogata, C. Saegusa, E. Kanno, and K. Mikoshiba. 2002. Alternative splicing isoforms of synaptotagmin VII in the mouse, rat and human. *Biochem J*. 365:173-80.

Fulop, T., S. Radabaugh, and C. Smith. 2005. Activity-dependent differential transmitter release in mouse adrenal chromaffin cells. *J Neurosci*. 25:7324-32.

Fuster, W., E.J. Bowie, J.C. Lewis, D.N. Fass, C.A. Owen, Jr., and A.L. Brown. 1978. Resistance to arteriosclerosis in pigs with von Willebrand's disease. Spontaneous and high cholesterol diet-induced arteriosclerosis. *J Clin Invest*. 61:722-30.

Gao, Z., J. Reavey-Cantwell, R.A. Young, P. Jegier, and B.A. Wolf. 2000. Synaptotagmin III/VII isoforms mediate Ca2+-induced insulin secretion in pancreatic islet beta -cells. *J Biol Chem*. 275:36079-85

Garland, C.J., F. Plane, B.K. Kemp, and T.M. Cocks. 1995. Endothelium-dependent hyperpolarization: a role in the control of vascular tone. *Trends Pharmacol Sci*. 16:23-30.

Gauthier, B.R., D.L. Duhamel, M. Iezzi, S. Theander, F. Saltel, M. Fukuda, B. Wehrle-Haller, and C.B. Wollheim. 2008. Synaptotagmin VII splice variants alpha, beta, and delta are expressed in pancreatic beta-cells and regulate insulin exocytosis. *FASEB J*. 22:194-206.

Geppert, M., Y. Goda, R.E. Hammer, C. Li, T.W. Rosahl, C.F. Stevens, and T.C. Sudhof. 1994. Synaptotagmin I: a major Ca2+ sensor for transmitter release at a central synapse. *Cell*. 79:717-27.

Gerasimenko, J.V., O.V. Gerasimenko, and O.H. Petersen. 2001. Membrane repair: Ca(2+)-elicited lysosomal exocytosis. *Curr Biol*. 11:R971-4.

Gerber, S.H., and T.C. Sudhof. 2002. Molecular determinants of regulated exocytosis. *Diabetes*. 51 Suppl 1:S3-11.

Gerona, R.R., E.C. Larsen, J.A. Kowalchyk, and T.F. Martin. 2000. The C terminus of SNAP25 is essential for Ca(2+)-dependent binding of synaptotagmin to SNARE complexes. *J Biol Chem*. 275:6328-36.

Gimbrone, M.A., Jr., R.S. Cotran, and J. Folkman. 1974. Human vascular endothelial cells in culture. Growth and DNA synthesis. *J Cell Biol*. 60:673-84.

Giraudo, C.G., A. Garcia-Diaz, W.S. Eng, Y. Chen, W.A. Hendrickson, T.J. Melia, and J.E. Rothman. 2009. Alternative zippering as an on-off switch for SNARE-mediated fusion. *Science*. 323:512-6.

Glavan, G. 2008. Intermittent L-DOPA treatment differentially alters synaptotagmin 4 and 7 gene expression in the striatum of hemiparkinsonian rats. *Brain Res*. 1236:216-24.

Glavan, G., and M. Zivin. 2005. Differential expression of striatal synaptotagmin mRNA isoforms in hemiparkinsonian rats. *Neuroscience*. 135:545-54.

Gomi, H., K. Mori, S. Itohara, and T. Izumi. 2007. Rab27b is expressed in a wide range of exocytic cells and involved in the delivery of secretory granules near the plasma membrane. *Mol Biol Cell*. 18:4377-86.

Gospodarowicz, D., J. Moran, D. Braun, and C. Birdwell. 1976. Clonal growth of bovine vascular endothelial cells: fibroblast growth factor as a survival agent. *Proc Natl Acad Sci U S A*. 73:4120-4.

Gratton, J.P., P. Bernatchez, and W.C. Sessa. 2004. Caveolae and caveolins in the cardiovascular system. *Circ Res*. 94:1408-17.

Grimberg, E., Z. Peng, I. Hammel, and R. Sagi-Eisenberg. 2003. Synaptotagmin III is a critical factor for the formation of the perinuclear endocytic recycling compartment and determination of secretory granules size. *J Cell Sci*. 116:145-54.

Grishanin, R.N., J.A. Kowalchyk, V.A. Klenchin, K. Ann, C.A. Earles, E.R. Chapman, R.R. Gerona, and T.F. Martin. 2004. CAPS acts at a prefusion step in dense-core vesicle exocytosis as a PIP2 binding protein. *Neuron*. 43:551-62.

Gustavsson, N., Y. Lao, A. Maximov, J.C. Chuang, E. Kostromina, J.J. Repa, C. Li, G.K. Radda, T.C. Sudhof, and W. Han. 2008. Impaired insulin secretion and glucose intolerance in synaptotagmin-7 null mutant mice. *Proc Natl Acad Sci U S A*. 105:3992-7.

Gustavsson, N., S.H. Wei, D.N. Hoang, Y. Lao, Q. Zhang, G.K. Radda, P. Rorsman, T.C. Sudhof, and W. Han. 2009. Synaptotagmin-7 is a principal Ca2+ sensor for Ca2+ -induced glucagon exocytosis in pancreas. *J Physiol*. 587:1169-78.

Hamm, A., N. Krott, I. Breibach, R. Blindt, and A.K. Bosserhoff. 2002. Efficient transfection method for primary cells. *Tissue Eng*. 8:235-45.

Han, W., J.S. Rhee, A. Maximov, Y. Lao, T. Mashimo, C. Rosenmund, and T.C. Sudhof. 2004. N-glycosylation is essential for vesicular targeting of synaptotagmin 1. *Neuron*. 41:85-99.

Han, W.Q., M. Xia, C. Zhang, F. Zhang, M. Xu, N.J. Li, and P.L. Li. 2011. SNARE-mediated rapid lysosome fusion in membrane raft clustering and dysfunction of bovine coronary arterial endothelium. *Am J Physiol Heart Circ Physiol*. 301:H2028-37.

Han, X., C.T. Wang, J. Bai, E.R. Chapman, and M.B. Jackson. 2004. Transmembrane segments of syntaxin line the fusion pore of Ca2+-triggered exocytosis. *Science*. 304:289-92.

Hannah, M.J., A.N. Hume, M. Arribas, R. Williams, L.J. Hewlett, M.C. Seabra, and D.F. Cutler. 2003. Weibel-Palade bodies recruit Rab27 by a content-driven, maturation-dependent mechanism that is independent of cell type. *J Cell Sci*. 116:3939-48.

Hannah, M.J., R. Williams, J. Kaur, L.J. Hewlett, and D.F. Cutler. 2002. Biogenesis of Weibel-Palade bodies. *Semin Cell Dev Biol*. 13:313-24.

Hansson, G.K., and P. Libby. 2006. The immune response in atherosclerosis: a double-edged sword. *Nat Rev Immunol*. 6:508-19.

Harrison-Lavoie, K.J., G. Michaux, L. Hewlett, J. Kaur, M.J. Hannah, W.W. Lui-Roberts, K.E. Norman, and D.F. Cutler. 2006. P-selectin and CD63 use different mechanisms for delivery to Weibel-Palade bodies. *Traffic*. 7:647-62.

Hata, Y., B. Davletov, A.G. Petrenko, R. Jahn, and T.C. Sudhof. 1993. Interaction of synaptotagmin with the cytoplasmic domains of neurexins. *Neuron*. 10:307-15.

Hattori, R., K.K. Hamilton, R.P. McEver, and P.J. Sims. 1989. Complement proteins C5b-9 induce secretion of high molecular weight multimers of endothelial von Willebrand factor and translocation of granule membrane protein GMP-140 to the cell surface. *J Biol Chem*. 264:9053-60.

Haucke, V., and P. De Camilli. 1999. AP-2 recruitment to synaptotagmin stimulated by tyrosine-based endocytic motifs. *Science*. 285:1268-71.

He, L., X.S. Wu, R. Mohan, and L.G. Wu. 2006. Two modes of fusion pore opening revealed by cell-attached recordings at a synapse. *Nature*. 444:102-5.

Hewlett, L., G. Zupancic, G. Mashanov, L. Knipe, D. Ogden, M.J. Hannah, and T. Carter 2011. Temperature-dependence of weibel-palade body exocytosis and cell surface dispersal of von Willebrand factor and its propolypeptide. *PLoS One*. 6:e27314.

Hibbs, R.G., G.E. Burch, and J.H. Phillips. 1958. The fine structure of the small blood vessels of normal human dermis and subcutis. *Am Heart J*. 56:662-70.

Hollestelle, M.J., C. Donkor, E.A. Mantey, S.J. Chakravorty, A. Craig, A.O. Akoto, J. O'Donnell, J.A. van Mourik, and J. Bunn. 2006. von Willebrand factor propeptide in malaria: evidence of acute endothelial cell activation. *Br J Haematol*. 133:562-9.

Hop, C., A. Guilliatt, M. Daly, H.P. de Leeuw, H.J. Brinkman, I.R. Peake, J.A. van Mourik, and H. Pannekoek. 2000. Assembly of multimeric von Willebrand factor directs sorting of P-selectin. *Arterioscler Thromb Vasc Biol*. 20:1763-8.

Howell, G.J., S.P. Herbert, J.M. Smith, S. Mittar, L.C. Ewan, M. Mohammed, A.R. Hunter, N. Simpson, A.J. Turner, I. Zachary, J.H. Walker, and S. Ponnambalam. 2004. Endothelial cell confluence regulates Weibel-Palade body formation. *Mol Membr Biol*. 21:413-21.

Huber, D., E.M. Cramer, J.E. Kaufmann, P. Meda, J.M. Masse, E.K. Kruithof, and U.M. Vischer. 2002. Tissue-type plasminogen activator (t-PA) is stored in Weibel-Palade bodies in human endothelial cells both in vitro and in vivo. *Blood*. 99:3637-45.

Hudson, A.W., and M.J. Birnbaum. 1995. Identification of a nonneuronal isoform of synaptotagmin. *Proc Natl Acad Sci U S A*. 92:5895-9.

Hui, E., J. Bai, P. Wang, M. Sugimori, R.R. Llinas, and E.R. Chapman. 2005. Three distinct kinetic groupings of the synaptotagmin family: candidate sensors for rapid and delayed exocytosis. *Proc Natl Acad Sci U S A*. 102:5210-4.

Huo, Y., A. Hafezi-Moghadam, and K. Ley. 2000. Role of vascular cell adhesion molecule-1 and fibronectin connecting segment-1 in monocyte rolling and adhesion on early atherosclerotic lesions. *Circ Res*. 87:153-9.

Hutt, D.M., J.M. Baltz, and J.K. Ngsee. 2005. Synaptotagmin VI and VIII and syntaxin 2 are essential for the mouse sperm acrosome reaction. *J Biol Chem*. 280:20197-203.

Hutt, D.M., R.A. Cardullo, J.M. Baltz, and J.K. Ngsee. 2002. Synaptotagmin VIII is localized to the mouse sperm head and may function in acrosomal exocytosis. *Biol Reprod*. 66:50-6.

Huynh, D.P., D.R. Scoles, D. Nguyen, and S.M. Pulst. 2003. The autosomal recessive juvenile Parkinson disease gene product, parkin, interacts with and ubiquitinates synaptotagmin XI. *Hum Mol Genet*. 12:2587-97.

Ibata, K., M. Fukuda, and K. Mikoshiba. 1998. Inositol 1,3,4,5-tetrakisphosphate binding activities of neuronal and non-neuronal synaptotagmins. Identification of conserved amino acid substitutions that abolish inositol 1,3,4,5-tetrakisphosphate binding to synaptotagmins III, V, and X. *J Biol Chem*. 273:12267-73.

Iezzi, M., G. Kouri, M. Fukuda, and C.B. Wollheim. 2004. Synaptotagmin V and IX isoforms control Ca2+ -dependent insulin exocytosis. *J Cell Sci*. 117:3119-27.

Inomata, M., T. Into, M. Nakashima, T. Noguchi, and K. Matsushita. 2009. IL-4 alters expression patterns of storage components of vascular endothelial cell-specific granules through STAT6- and SOCS-1-dependent mechanisms. *Mol Immunol*. 46:2080-9.

Inoue, S., A. Imamura, Y. Okazaki, H. Yokota, M. Arai, N. Hayashi, A. Furukawa, M. Itokawa, and M. Oishi. 2007. Synaptotagmin XI as a candidate gene for susceptibility to schizophrenia. *Am J Med Genet B Neuropsychiatr Genet*. 144B:332-40.

Into, T., Y. Kanno, J. Dohkan, M. Nakashima, M. Inomata, K. Shibata, C.J. Lowenstein, and K. Matsushita. 2007. Pathogen recognition by Toll-like receptor 2 activates Weibel-Palade body exocytosis in human aortic endothelial cells. *J Biol Chem*. 282:8134-41.

Jackson, M.B., and E.R. Chapman. 2008. The fusion pores of Ca2+ -triggered exocytosis. *Nat Struct Mol Biol*. 15:684-9.

Jahn, R., and D. Fasshauer. 2012. Molecular machines governing exocytosis of synaptic vesicles. *Nature*. 490:201-7.

Jahn, R., and R.H. Scheller. 2006. SNAREs--engines for membrane fusion. *Nat Rev Mol Cell Biol*. 7:631-43.

Jaiswal, J.K., S. Chakrabarti, N.W. Andrews, and S.M. Simon. 2004. Synaptotagmin VII restricts fusion pore expansion during lysosomal exocytosis. *PLoS Biol*. 2:E233.

Jopling, H.M., A.F. Odell, N.M. Hooper, I.C. Zachary, J.H. Walker, and S. Ponnambalam. 2009. Rab GTPase regulation of VEGFR2 trafficking and signaling in endothelial cells. *Arterioscler Thromb Vasc Biol*. 29:1119-24.

Jorgensen, E.M., E. Hartwieg, K. Schuske, M.L. Nonet, Y. Jin, and H.R. Horvitz. 1995. Defective recycling of synaptic vesicles in synaptotagmin mutants of Caenorhabditis elegans. *Nature*. 378:196-9.

Journet, A.M., S. Saffaripour, E.M. Cramer, D. Tenza, and D.D. Wagner. 1993. von Willebrand factor storage requires intact prosequence cleavage site. *Eur J Cell Biol*. 60:31-41.

Jutte, N.H., C.J. Knoop, P. Heijse, A.H. Balk, B. Mochtar, F.H. Claas, and W. Weimar. 1996. Human heart endothelial-cell-restricted allorecognition. *Transplantation*. 62:403-6.

Kallenberg, L.A. 2000. Calcium signalling in secretory cells. *Arch Physiol Biochem*. 108:385-90.

Kang, R., R. Swayze, M.F. Lise, K. Gerrow, A. Mullard, W.G. Honer, and A. El-Husseini. 2004. Presynaptic trafficking of synaptotagmin I is regulated by protein palmitoylation. *J Biol Chem*. 279:50524-36

Kanthou, C., O. Benzakour, G. Patel, J. Deadman, V.V. Kakkar, and F. Lupu. 1995. Thrombin receptor activating peptide (TRAP) stimulates mitogenesis, c-fos and PDGF-A gene expression in human vascular smooth muscle cells. *Thromb Haemost*. 74:1340-7.

Katz, B., and R. Miledi. 1967. Ionic requirements of synaptic transmitter release. *Nature*. 215:651.

Kishore, B.K., J.B. Wade, K. Schorr, T. Inoue, B. Mandon, and M.A. Knepper. 1998. Expression of synaptotagmin VIII in rat kidney. *Am J Physiol*. 275:F131-42.

Knipe, L., A. Meli, L. Hewlett, R. Bierings, J. Dempster, P. Skehel, M.J. Hannah, and T. Carter. 2010. A revised model for the secretion of tPA and cytokines from cultured endothelial cells. *Blood*. 116:2183-91.

Knop, M., E. Aareskjold, G. Bode, and V. Gerke. 2004. Rab3D and annexin A2 play a role in regulated secretion of vWF, but not tPA, from endothelial cells. *EMBO J*. 23:2982-92.

Kumar, S., D.C. West, and A. Ager. 1987. Heterogeneity in endothelial cells from large vessels and microvessels. *Differentiation*. 36:57-70.

Kuo, M.C., D. Patschan, S. Patschan, L. Cohen-Gould, H.C. Park, J. Ni, F. Addabbo, and M.S. Goligorsky. 2008. Ischemia-induced exocytosis of Weibel-Palade bodies mobilizes stem cells. *J Am Soc Nephrol*. 19:2321-30.

Lai, Y., J. Diao, Y. Liu, Y. Ishitsuka, Z. Su, K. Schulten, T. Ha, and Y.K. Shin. 2013. Fusion pore formation and expansion induced by Ca2+ and synaptotagmin 1. *Proc Natl Acad Sci U S A.* 110:1333-8.

Larkin, D., B. de Laat, P.V. Jenkins, J. Bunn, A.G. Craig, V. Terraube, R.J. Preston, C. Donkor, G.E. Grau, J.A. van Mourik, and J.S. O'Donnell. 2009. Severe Plasmodium falciparum malaria is associated with circulating ultra-large von Willebrand multimers and ADAMTS13 inhibition. *PLoS Pathog*. 5:e1000349.

Leveque, C., T. Hoshino, P. David, Y. Shoji-Kasai, K. Leys, A. Omori, B. Lang, O. el Far, K. Sato, N. Martin-Moutot, and et al. 1992. The synaptic vesicle protein synaptotagmin associates with calcium channels and is a putative Lambert-Eaton myasthenic syndrome antigen. *Proc Natl Acad Sci U S A*. 89:3625-9.

Levin, E.R. 1996. Endothelins. *N Engl J Med* 333::356-356

Levine, J.D., J.M. Harlan, L.A. Harker, M.L. Joseph, and R.B. Counts. 1982. Thrombin-mediated release of factor VIII antigen from human umbilical vein endothelial cells in culture. *Blood*. 60:531-4.

Leyte, A., J. Voorberg, H.B. Van Schijndel, B. Duim, H. Pannekoek, and J.A. Van Mourik. 1991. The pro-polypeptide of von Willebrand factor is required for the formation of a functional factor VIII-binding site on mature von Willebrand factor. *Biochem J*. 274 (Pt 1):257-61.

Li, C., B. Ullrich, J.Z. Zhang, R.G. Anderson, N. Brose, and T.C. Sudhof. 1995. Ca(2+)-dependent and -independent activities of neural and non-neural synaptotagmins. *Nature*. 375:594-9.

Li, Y., P. Wang, J. Xu, F. Gorelick, H. Yamazaki, N. Andrews, and G.V. Desir. 2007. Regulation of insulin secretion and GLUT4 trafficking by the calcium sensor synaptotagmin VII. *Biochem Biophys Res Commun*. 362:658-64.

Littleton, J.T., M. Stern, K. Schulze, M. Perin, and H.J. Bellen. 1993. Mutational analysis of Drosophila synaptotagmin demonstrates its essential role in Ca(2+)-activated neurotransmitter release. *Cell*. 74:1125-34.

Llinas, R., M. Sugimori, E.J. Lang, M. Morita, M. Fukuda, M. Niinobe, and K. Mikoshiba. 1994. The inositol high-polyphosphate series blocks synaptic transmission by preventing vesicular fusion: a squid giant synapse study. *Proc Natl Acad Sci U S A*. 91:12990-3.

Lodge, R., and A. Descoteaux. 2005. Modulation of phagolysosome biogenesis by the lipophosphoglycan of Leishmania. *Clin Immunol*. 114:256-65.

Lorant, D.E., K.D. Patel, T.M. McIntyre, R.P. McEver, S.M. Prescott, and G.A. Zimmerman. 1991. Coexpression of GMP-140 and PAF by endothelium stimulated by histamine or thrombin: a juxtacrine system for adhesion and activation of neutrophils. *J Cell Biol*. 115:223-34.

Lou, P.H., N. Gustavsson, Y. Wang, G.K. Radda, and W. Han. 2011. Increased lipolysis and energy expenditure in a mouse model with severely impaired glucagon secretion. *PLoS One*. 6:e26671.

Lui-Roberts, W.W., L.M. Collinson, L.J. Hewlett, G. Michaux, and D.F. Cutler. 2005. An AP-1/clathrin coat plays a novel and essential role in forming the Weibel-Palade bodies of endothelial cells. *J Cell Biol*. 170:627-36.

Lui-Roberts, W.W., F. Ferraro, T.D. Nightingale, and D.F. Cutler. 2008. Aftiphilin and gamma-synergin are required for secretagogue sensitivity of Weibel-Palade bodies in endothelial cells. *Mol Biol Cell*. 19:5072-81.

Lynch, K.L., and T.F. Martin. 2007. Synaptotagmins I and IX function redundantly in regulated exocytosis but not endocytosis in PC12 cells. *J Cell Sci*. 120:617-27.

Ma, C., W. Li, Y. Xu, and J. Rizo. 2011. Munc13 mediates the transition from the closed syntaxin-Munc18 complex to the SNARE complex. *Nat Struct Mol Biol*. 18:542-9.

Maasho, K., A. Marusina, N.M. Reynolds, J.E. Coligan, and F. Borrego. 2004. Efficient gene transfer into the human natural killer cell line, NKL, using the Amaxa nucleofection system. *J Immunol Methods*. 284:133-40.

Manickam, V., A. Tiwari, J.J. Jung, R. Bhattacharya, A. Goel, D. Mukhopadhyay, and A. Choudhury. 2011. Regulation of vascular endothelial growth factor receptor 2 trafficking and angiogenesis by Golgi localized t-SNARE syntaxin 6. *Blood*. 117:1425-35.

Mantovani, A., S. Sozzani, A. Vecchi, M. Introna, and P. Allavena. 1997. Cytokine activation of endothelial cells: new molecules for an old paradigm. *Thromb Haemost*. 78:406-14.

Marqueze, B., J.A. Boudier, M. Mizuta, N. Inagaki, S. Seino, and M. Seagar. 1995. Cellular localization of synaptotagmin I, II, and III mRNAs in the central nervous system and pituitary and adrenal glands of the rat. *J Neurosci*. 15:4906-17.

Martina, J.A., C.J. Bonangelino, R.C. Aguilar, and J.S. Bonifacino. 2001. Stonin 2: an adaptor-like protein that interacts with components of the endocytic machinery. *J Cell Biol*. 153:1111-20.

Martinez, I., S. Chakrabarti, T. Hellevik, J. Morehead, K. Fowler, and N.W. Andrews. 2000. Synaptotagmin VII regulates Ca(2+)-dependent exocytosis of lysosomes in fibroblasts. *J Cell Biol*. 148:1141-49

Masztalerz, A., I.S. Zeelenberg, Y.M. Wijnands, R. de Bruijn, A.M. Drager, H. Janssen, and E. Roos. 2007. Synaptotagmin 3 deficiency in T cells impairs recycling of the chemokine receptor CXCR4 and thereby inhibits CXCL12 chemokine-induced migration. *J Cell Sci*. 120:219-28.

Matsushita, K., C.N. Morrell, B. Cambien, S.X. Yang, M. Yamakuchi, C. Bao, M.R. Hara, R.A. Quick, W. Cao, B. O'Rourke, J.M. Lowenstein, J. Pevsner, D.D. Wagner, and C.J. Lowenstein. 2003. Nitric oxide regulates exocytosis by S-nitrosylation of N-ethylmaleimide-sensitive factor. *Cell*. 115:139-50.

Matsushita, K., C.N. Morrell, and C.J. Lowenstein. 2004. Sphingosine 1-phosphate activates Weibel-Palade body exocytosis. *Proc Natl Acad Sci U S A*. 101:11483-7.

Matthew, W.D., L. Tsavaler, and L.F. Reichardt. 1981. Identification of a synaptic vesicle-specific membrane protein with a wide distribution in neuronal and neurosecretory tissue. *J Cell Biol*. 91:257-69.

Mayadas, T.N., R.C. Johnson, H. Rayburn, R.O. Hynes, and D.D. Wagner. 1993. Leukocyte rolling and extravasation are severely compromised in P selectin-deficient mice. *Cell*. 74:541-54.

Maximov, A., Y. Lao, H. Li, X. Chen, J. Rizo, J.B. Sorensen, and T.C. Sudhof. 2008. Genetic analysis of synaptotagmin-7 function in synaptic vesicle exocytosis. *Proc Natl Acad Sci U S A*. 105:3986-91.

Maximov, A., J. Tang, X. Yang, Z.P. Pang, and T.C. Sudhof. 2009. Complexin controls the force transfer from SNARE complexes to membranes in fusion. *Science*. 323:516-21.

McEver, R.P., J.H. Beckstead, K.L. Moore, L. Marshall-Carlson, and D.F. Bainton. 1989. GMP-140, a platelet alpha-granule membrane protein, is also synthesized by vascular endothelial cells and is localized in Weibel-Palade bodies. *J Clin Invest*. 84:92-9.

McIntosh, D.P., and J.E. Schnitzer. 1999. Caveolae require intact VAMP for targeted transport in vascular endothelium. *Am J Physiol*. 277:H2222-32.

Menasche, G., E. Pastural, J. Feldmann, S. Certain, F. Ersoy, S. Dupuis, N. Wulffraat, D. Bianchi, A. Fischer, F. Le Deist, and G. de Saint Basile. 2000. Mutations in RAB27A cause Griscelli syndrome associated with haemophagocytic syndrome. *Nat Genet*. 25:173-6.

Medcalf, R.L. 2007. Fibrinolysis, inflammation, and regulation of the plasminogen activating system. *J Thromb Haemost*. 5 Suppl 1:132-42.

Metcalf, D.J., T.D. Nightingale, H.L. Zenner, W.W. Lui-Roberts, and D.F. Cutler. 2008. Formation and function of Weibel-Palade bodies. *J Cell Sci*. 121:19-27.

Methia, N., P. Andre, C.V. Denis, M. Economopoulos, and D.D. Wagner. 2001. Localized reduction of atherosclerosis in von Willebrand factor-deficient mice. *Blood*. 98:1424-8.

Michaut, M., G. De Blas, C.N. Tomes, R. Yunes, M. Fukuda, and L.S. Mayorga. 2001. Synaptotagmin VI participates in the acrosome reaction of human spermatozoa. *Dev Biol*. 235:521-9.

Michaux, G., K.B. Abbitt, L.M. Collinson, S.L. Haberichter, K.E. Norman, and D.F. Cutler. 2006. The physiological function of von Willebrand's factor depends on its tubular storage in endothelial Weibel-Palade bodies. *Dev Cell*. 10:223-32.

Michaux, G., and D.F. Cutler. 2004. How to roll an endothelial cigar: the biogenesis of Weibel-Palade bodies. *Traffic*. 5:69-78.

Michaux, G., C.E. Dyer, T.D. Nightingale, E. Gallaud, S. Nurrish, and D.F. Cutler. 2010. A role for Rab10 in von Willebrand factor release discovered by an AP-1 interactor screen in C. elegans. *J Thromb Haemost*. 9:392-401.

Misura, K.M., R.H. Scheller, and W.I. Weis. 2000. Three-dimensional structure of the neuronal-Sec1-syntaxin 1a complex. *Nature*. 404:355-62.

Mizuno, K., T. Tolmachova, D.S. Ushakov, M. Romao, M. Abrink, M.A. Ferenczi, G. Raposo, and M.C. Seabra. 2007. Rab27b regulates mast cell granule dynamics and secretion. *Traffic*. 8:883-92.

Mizuta, M., N. Inagaki, Y. Nemoto, S. Matsukura, M. Takahashi, and S. Seino. 1994. Synaptotagmin III is a novel isoform of rat synaptotagmin expressed in endocrine and neuronal cells. *J Biol Chem*. 269:11675-8.

Moncada, S., and E.A. Higgs. 2006. Nitric oxide and the vascular endothelium. *Handb Exp Pharmacol*:213-54.

Monterrat, C., F. Boal, F. Grise, A. Hemar, and J. Lang. 2006. Synaptotagmin 8 is expressed both as a calcium-insensitive soluble and membrane protein in neurons, neuroendocrine and endocrine cells. *Biochim Biophys Acta*. 1763:73-81.

Morgan, A.J., and R. Jacob. 1994. Ionomycin enhances Ca2+ influx by stimulating store-regulated cation entry and not by a direct action at the plasma membrane. *Biochem J*. 300 (Pt 3):665-72.

Morin, O., P. Patry, and L. Lafleur. 1984. Heterogeneity of endothelial cells of adult rat liver as resolved by sedimentation velocity and flow cytometry. *J Cell Physiol*. 119:327-34.

Mueller-Klieser, W. 1997. Three-dimensional cell cultures: from molecular mechanisms to clinical applications. *Am J Physiol*. 273:C1109-23.

Munafo, D.B., J.L. Johnson, B.A. Ellis, S. Rutschmann, B. Beutler, and S.D. Catz. 2007. Rab27a is a key component of the secretory machinery of azurophilic granules in granulocytes. *Biochem J*. 402:229-39.

Nayak, R.C., S. Keshava, C.T. Esmon, U.R. Pendurthi, and L.V. Rao. 2013. Rab GTPases regulate endothelial cell protein C receptor-mediated endocytosis and trafficking of factor VIIa. *PLoS One*. 8:e59304.

Nicholson, K.L., M. Munson, R.B. Miller, T.J. Filip, R. Fairman, and F.M. Hughson. 1998. Regulation of SNARE complex assembly by an N-terminal domain of the t-SNARE Sso1p. *Nat Struct Biol*. 5:793-802.

Nightingale, T.D., K. Pattni, A.N. Hume, M.C. Seabra, and D.F. Cutler. 2009. Rab27a and MyRIP regulate the amount and multimeric state of VWF released from endothelial cells. *Blood*. 113:5010-8.

Nishiki, T., and G.J. Augustine. 2004. Synaptotagmin I synchronizes transmitter release in mouse hippocampal neurons. *J Neurosci*. 24:6127-32.

Nonet, M.L., K. Grundahl, B.J. Meyer, and J.B. Rand. 1993. Synaptic function is impaired but not eliminated in C. elegans mutants lacking synaptotagmin. *Cell*. 73:1291-305.

Noubade, R., R. del Rio, B. McElvany, J.F. Zachary, J.M. Millward, D.D. Wagner, H. Offner, E.P. Blankenhorn, and C. Teuscher. 2008. von-Willebrand factor influences blood brain barrier permeability and brain inflammation in experimental allergic encephalomyelitis. *Am J Pathol*. 173:892-900.

Osborne, S.L., T.P. Wallis, J.L. Jimenez, J.J. Gorman, and F.A. Meunier. 2007. Identification of secretory granule phosphatidylinositol 4,5-bisphosphate-interacting proteins using an affinity pulldown strategy. *Mol Cell Proteomics*. 6:1158-69.

Oyler, G.A., G.A. Higgins, R.A. Hart, E. Battenberg, M. Billingsley, F.E. Bloom, and M.C. Wilson. 1989. The identification of a novel synaptosomal-associated protein, SNAP-25, differentially expressed by neuronal subpopulations. *J Cell Biol*. 109:3039-52.

Oynebraten, I., O. Bakke, P. Brandtzaeg, F.E. Johansen, and G. Haraldsen. 2004. Rapid chemokine secretion from endothelial cells originates from 2 distinct compartments. *Blood*. 104:314-20.

Ozaka, T., Y. Doi, K. Kayashima, and S. Fujimoto. 1997. Weibel-Palade bodies as a storage site of calcitonin gene-related peptide and endothelin-1 in blood vessels of the rat carotid body. *Anat Rec*. 247:388-94.

Pang, Z.P., and T.C. Sudhof. Cell biology of Ca2+-triggered exocytosis. *Curr Opin Cell Biol*. 22:496-505.

Parisotto, D., J. Malsam, A. Scheutzow, J.M. Krause, and T.H. Sollner. 2012. SNAREpin assembly by Munc18-1 requires previous vesicle docking by synaptotagmin 1. *J Biol Chem*. 287:31041-9.

Perin, M.S. 1994. The COOH terminus of synaptotagmin mediates interaction with the neurexins. *J Biol Chem*. 269:8576-81.

Perin, M.S., N. Brose, R. Jahn, and T.C. Sudhof. 1991. Domain structure of synaptotagmin (p65). *J Biol Chem*. 266:623-9.

Perin, M.S., V.A. Fried, G.A. Mignery, R. Jahn, and T.C. Sudhof. 1990. Phospholipid binding by a synaptic vesicle protein homologous to the regulatory region of protein kinase C. *Nature*. 345:260-3.

Perin, M.S., P.A. Johnston, T. Ozcelik, R. Jahn, U. Francke, and T.C. Sudhof. 1991. Structural and functional conservation of synaptotagmin (p65) in Drosophila and humans. *J Biol Chem*. 266:615-22.

Petrenko, A.G., M.S. Perin, B.A. Davletov, Y.A. Ushkaryov, M. Geppert, and T.C. Sudhof. 1991. Binding of synaptotagmin to the alpha-latrotoxin receptor implicates both in synaptic vesicle exocytosis. *Nature*. 353:65-8.

Phiri, H.T., D.J. Bridges, S.J. Glover, J.A. van Mourik, B. de Laat, B. M'Baya, T.E. Taylor, K.B. Seydel, M.E. Molyneux, E.B. Faragher, A.G. Craig, and J.E. Bunn. Elevated plasma von Willebrand factor and propeptide levels in malawian children with malaria. *PLoS One*. 6:e25626.

Pinsky, D.J., Y. Naka, H. Liao, M.C. Oz, D.D. Wagner, T.N. Mayadas, R.C. Johnson, R.O. Hynes, M. Heath, C.A. Lawson, and D.M. Stern. 1996. Hypoxia-induced exocytosis of endothelial cell Weibel-Palade bodies. A mechanism for rapid neutrophil recruitment after cardiac preservation. *J Clin Invest*. 97:493-500.

Pober, J.S. 1998. Activation and injury of endothelial cells by cytokines. *Pathol Biol (Paris)*. 46:159-63.

Pober, J.S., and W.C. Sessa. 2007. Evolving functions of endothelial cells in inflammation. *Nat Rev Immunol*. 7:803-15.

Popp, R., and H. Gogelein. 1992. A calcium and ATP sensitive nonselective cation channel in the antiluminal membrane of rat cerebral capillary endothelial cells. *Biochim Biophys Acta*. 1108:59-66.

Predescu, S.A., D.N. Predescu, K. Shimizu, I.K. Klein, and A.B. Malik. 2005. Cholesterol-dependent syntaxin-4 and SNAP-23 clustering regulates caveolar fusion with the endothelial plasma membrane. *J Biol Chem*. 280:37130-8.

Pulido, I.R., R. Jahn, and V. Gerke. 2010. VAMP3 is associated with endothelial Weibel-Palade bodies and participates in their Ca(2+)-dependent exocytosis. *Biochim Biophys Acta*. 1813:1038-44

Pulido, I.R., T.D. Nightingale, F. Darchen, M.C. Seabra, D.F. Cutler, and V. Gerke. 2011. Myosin Va acts in concert with Rab27a and MyRIP to regulate acute von-Willebrand factor release from endothelial cells. *Traffic*. 10:1371-82

Putney, J.W., Jr. 1990. Capacitative calcium entry revisited. *Cell Calcium*. 11:611-24.

Rao, S.K., C. Huynh, V. Proux-Gillardeaux, T. Galli, and N.W. Andrews. 2004. Identification of SNAREs involved in synaptotagmin VII-regulated lysosomal exocytosis. *J Biol Chem*. 279:20471-9.

Reim, K., M. Mansour, F. Varoqueaux, H.T. McMahon, T.C. Sudhof, N. Brose, and C. Rosenmund. 2001. Complexins regulate a late step in Ca2+-dependent neurotransmitter release. *Cell*. 104:71-81.

Rhee, J.S., L.Y. Li, O.H. Shin, J.C. Rah, J. Rizo, T.C. Sudhof, and C. Rosenmund. 2005. Augmenting neurotransmitter release by enhancing the apparent Ca2+ affinity of synaptotagmin 1. *Proc Natl Acad Sci U S A*. 102:18664-9.

Ribes, J.A., C.W. Francis, and D.D. Wagner. 1987. Fibrin induces release of von Willebrand factor from endothelial cells. *J Clin Invest*. 79:117-23.

Richmond, J.E., R.M. Weimer, and E.M. Jorgensen. 2001. An open form of syntaxin bypasses the requirement for UNC-13 in vesicle priming. *Nature*. 412:338-41.

Roggero, C.M., G.A. De Blas, H. Dai, C.N. Tomes, J. Rizo, and L.S. Mayorga. 2007. Complexin/synaptotagmin interplay controls acrosomal exocytosis. *J Biol Chem*. 282:26335-43.

Roggero, C.M., C.N. Tomes, G.A. De Blas, J. Castillo, M.A. Michaut, M. Fukuda, and L.S. Mayorga. 2005. Protein kinase C-mediated phosphorylation of the two polybasic regions of synaptotagmin VI regulates their function in acrosomal exocytosis. *Dev Biol*. 285:422-35.

Romani de Wit, T., H.P. de Leeuw, M.G. Rondaij, R.T. de Laaf, E. Sellink, H.J. Brinkman, J. Voorberg, and J.A. van Mourik. 2003. Von Willebrand factor targets IL-8 to Weibel-Palade bodies in an endothelial cell line. *Exp Cell Res*. 286:67-74.

Rondaij, M.G., R. Bierings, A. Kragt, J.A. van Mourik, and J. Voorberg. 2006. Dynamics and plasticity of Weibel-Palade bodies in endothelial cells. *Arterioscler Thromb Vasc Biol*. 26:1002-7.

Rosenberg, J.B., P.A. Foster, R.J. Kaufman, E.A. Vokac, M. Moussalli, P.A. Kroner, and R.R. Montgomery. 1998. Intracellular trafficking of factor VIII to von Willebrand factor storage granules. *J Clin Invest*. 101:613-24.

Rosnoblet, C., U.M. Vischer, R.D. Gerard, J.C. Irminger, P.A. Halban, and E.K. Kruithof. 1999. Storage of tissue-type plasminogen activator in Weibel-Palade bodies of human endothelial cells. *Arterioscler Thromb Vasc Biol*. 19:1796-803.

Russell, F.D., J.N. Skepper, and A.P. Davenport. 1998. Human endothelial cell storage granules: a novel intracellular site for isoforms of the endothelin-converting enzyme. *Circ Res*. 83:314-21.

Sadler, J.E. 1998. Biochemistry and genetics of von Willebrand factor. *Annu Rev Biochem*. 67:395-424.

Saegusa, C., M. Fukuda, and K. Mikoshiba. 2002. Synaptotagmin V is targeted to dense-core vesicles that undergo calcium-dependent exocytosis in PC12 cells. *J Biol Chem*. 277:24499-505.

Saegusa, C., T. Tanaka, S. Tani, S. Itohara, K. Mikoshiba, and M. Fukuda. 2006. Decreased basal mucus secretion by Slp2-a-deficient gastric surface mucous cells. *Genes Cells*. 11:623-31.

Sambrook, J and Russell, D. W. 2001 Molecular Cloning: A Laboratory Manual, Cold Spring Harbor Laboratory Press

Sassa, T., S. Harada, H. Ogawa, J.B. Rand, I.N. Maruyama, and R. Hosono. 1999. Regulation of the UNC-18-Caenorhabditis elegans syntaxin complex by UNC-13. *J Neurosci*. 19:4772-7.

Schaumburg-Lever, G., B. Gehring, and E. Kaiserling. 1994. Ultrastructural localization of factor XIIIa. *J Cutan Pathol*. 21:129-34.

Schelling, M.E., C.J. Meininger, J.R. Hawker, Jr., and H.J. Granger. 1988. Venular endothelial cells from bovine heart. *Am J Physiol*. 254:H1211-7.

Schenkel, A.R., Z. Mamdouh, X. Chen, R.M. Liebman, and W.A. Muller. 2002. CD99 plays a major role in the migration of monocytes through endothelial junctions. *Nat Immunol*. 3:143-50.

Schilling, W.P., O.A. Cabello, and L. Rajan. 1992. Depletion of the inositol 1,4,5-trisphosphate-sensitive intracellular Ca2+ store in vascular endothelial cells activates the agonist-sensitive Ca(2+)-influx pathway. *Biochem J*. 284 (Pt 2):521-30.

Schluter, T., and R. Bohnensack. 1999. Serotonin-induced secretion of von Willebrand factor from human umbilical vein endothelial cells via the cyclic AMP-signaling systems independent of increased cytoplasmic calcium concentration. *Biochem Pharmacol*. 57:1191-7.

Schnyder-Candrian, S., L. Borsig, R. Moser, and E.G. Berger. 2000. Localization of alpha 1,3-fucosyltransferase VI in Weibel-Palade bodies of human endothelial cells. *Proc Natl Acad Sci U S A*. 97:8369-74.

Schonn, J.S., A. Maximov, Y. Lao, T.C. Sudhof, and J.B. Sorensen. 2008. Synaptotagmin-1 and -7 are functionally overlapping Ca2+ sensors for exocytosis in adrenal chromaffin cells. *Proc Natl Acad Sci U S A*. 105:3998-4003.

Schorer, A.E., C.F. Moldow, and M.E. Rick. 1987. Interleukin 1 or endotoxin increases the release of von Willebrand factor from human endothelial cells. *Br J Haematol*. 67:193-7.

Segovia, M., E. Ales, M.A. Montes, I. Bonifas, I. Jemal, M. Lindau, A. Maximov, T.C. Sudhof, and G. Alvarez de Toledo. 2010. Push-and-pull regulation of the fusion pore by synaptotagmin-7. *Proc Natl Acad Sci U S A*. 107:19032-7.

Shao, X., C. Li, I. Fernandez, X. Zhang, T.C. Sudhof, and J. Rizo. 1997. Synaptotagmin-syntaxin interaction: the C2 domain as a Ca2+-dependent electrostatic switch. *Neuron*. 18:133-42.

Shen, J., D.C. Tareste, F. Paumet, J.E. Rothman, and T.J. Melia. 2007. Selective activation of cognate SNAREpins by Sec1/Munc18 proteins. *Cell*. 128:183-95.

Shiao, S.L., J.M. McNiff, and J.S. Pober. 2005. Memory T cells and their costimulators in human allograft injury. *J Immunol*. 175:4886-96.

Shuttleworth, T.J. 1997. Intracellular Ca2+ signalling in secretory cells. *J Exp Biol*. 200:303-14.

Simionescu, M., A. Gafencu, and F. Antohe. 2002. Transcytosis of plasma macromolecules in endothelial cells: a cell biological survey. *Microsc Res Tech*. 57:269-88.

Simonson, M.S., and M.J. Dunn. 1990. Cellular signaling by peptides of the endothelin gene family. *FASEB J*. 4:2989-3000.

Sollner, T.H. 2003. Regulated exocytosis and SNARE function (Review). *Mol Membr Biol*. 20:209-20.

Sollner, T., M.K. Bennett, S.W. Whiteheart, R.H. Scheller, and J.E. Rothman. 1993. A protein assembly-disassembly pathway in vitro that may correspond to sequential steps of synaptic vesicle docking, activation, and fusion. *Cell*. 75:409-18.

Sporn, L.A., P. Rubin, V.J. Marder, and D.D. Wagner. 1984. Irradiation induces release of von Willebrand protein from endothelial cells in culture. *Blood*. 64:567-70.

Streb, H., R.F. Irvine, M.J. Berridge, and I. Schulz. 1983. Release of Ca2+ from a nonmitochondrial intracellular store in pancreatic acinar cells by inositol-1,4,5-trisphosphate. *Nature*. 306:67-9.

Sudhof, T.C. 2002. Synaptotagmins: why so many? *J Biol Chem*. 277:7629-32.

Sudhof, T.C., and J.E. Rothman. 2009. Membrane fusion: grappling with SNARE and SM proteins. *Science*. 323:474-7.

Sugita, S., W. Han, S. Butz, X. Liu, R. Fernandez-Chacon, Y. Lao, and T.C. Sudhof. 2001. Synaptotagmin VII as a plasma membrane Ca(2+) sensor in exocytosis. *Neuron*. 30:459-73.

Sugita, S., O.H. Shin, W. Han, Y. Lao, and T.C. Sudhof. 2002. Synaptotagmins form a hierarchy of exocytotic Ca(2+) sensors with distinct Ca(2+) affinities. *EMBO J*. 21:270-80.
Sumpio, B.E., J.T. Riley, and A. Dardik. 2002. Cells in focus: endothelial cell. *Int J Biochem Cell Biol*. 34:1508-12.

Sutton, R.B., B.A. Davletov, A.M. Berghuis, T.C. Sudhof, and S.R. Sprang. 1995. Structure of the first C2 domain of synaptotagmin I: a novel Ca2+/phospholipid-binding fold. *Cell*. 80:929-38.

Sutton, R.B., J.A. Ernst, and A.T. Brunger. 1999. Crystal structure of the cytosolic C2A-C2B domains of synaptotagmin III. Implications for Ca(+2)-independent snare complex interaction. *J Cell Biol*. 147:589-98.

Sutton, R.B., D. Fasshauer, R. Jahn, and A.T. Brunger. 1998. Crystal structure of a SNARE complex involved in synaptic exocytosis at 2.4 A resolution. *Nature*. 395:347-53.

Taflin, C., D. Charron, D. Glotz, and N. Mooney. 2011. Immunological function of the endothelial cell within the setting of organ transplantation. *Immunol Lett*. 139:1-6.

Terraube, V., R. Pendu, D. Baruch, M.F. Gebbink, D. Meyer, P.J. Lenting, and C.V. Denis. 2006. Increased metastatic potential of tumor cells in von Willebrand factor-deficient mice. *J Thromb Haemost*. 4:519-26.

Tiwari, A., J.J. Jung, S.M. Inamdar, C.O. Brown, A. Goel, and A. Choudhury. 2011. Endothelial cell migration on fibronectin is regulated by syntaxin 6-mediated alpha5beta1 integrin recycling. *J Biol Chem*. 286:36749-61.

Tolmachova, T., M. Abrink, C.E. Futter, K.S. Authi, and M.C. Seabra. 2007. Rab27b regulates number and secretion of platelet dense granules. *Proc Natl Acad Sci U S A*. 104:5872-7.

Tran, Q.K., K. Ohashi, and H. Watanabe. 2000. Calcium signalling in endothelial cells. *Cardiovasc Res*. 48:13-22.

Tsuboi, T., and M. Fukuda. 2006. Rab3A and Rab27A cooperatively regulate the docking step of dense-core vesicle exocytosis in PC12 cells. *J Cell Sci*. 119:2196-203.

Tucker, W.C., and E.R. Chapman. 2002. Role of synaptotagmin in Ca2+-triggered exocytosis. *Biochem J*. 366:1-13.

Turner, R.R., J.H. Beckstead, R.A. Warnke, and G.S. Wood. 1987. Endothelial cell phenotypic diversity. In situ demonstration of immunologic and enzymatic heterogeneity that correlates with specific morphologic subtypes. *Am J Clin Pathol*. 87:569-75.

Ubach, J., X. Zhang, X. Shao, T.C. Sudhof, and J. Rizo. 1998. Ca2+ binding to synaptotagmin: how many Ca2+ ions bind to the tip of a C2-domain? *EMBO J*. 17:3921-30.

Utgaard, J.O., F.L. Jahnsen, A. Bakka, P. Brandtzaeg, and G. Haraldsen. 1998. Rapid secretion of prestored interleukin 8 from Weibel-Palade bodies of microvascular endothelial cells. *J Exp Med*. 188:1751-6.

van Agtmaal, E.L., R. Bierings, B.S. Dragt, T.A. Leyen, M. Fernandez-Borja, A.J. Horrevoets, and J. Voorberg. 2012. The shear stress-induced transcription factor KLF2 affects dynamics and angiopoietin-2 content of Weibel-Palade bodies. *PLoS One*. 7:e38399.

van Breevoort, D., E.L. van Agtmaal, B.S. Dragt, J.K. Gebbinck, I. Dienava-Verdoold, A. Kragt, R. Bierings, A.J. Horrevoets, K.M. Valentijn, J.C. Eikenboom, M. Fernandez-Borja, A.B. Meijer, and J. Voorberg. 2012. Proteomic screen identifies IGFBP7 as a novel component of endothelial cell-specific Weibel-Palade bodies. *J Proteome Res*. 11:2925-36.

van Hinsbergh, V.W. 2001. The endothelium: vascular control of haemostasis. *Eur J Obstet Gynecol Reprod Biol*. 95:198-201.

van Hinsbergh, V.W. 2012. Endothelium--role in regulation of coagulation and inflammation. *Semin Immunopathol*. 34:93-106.

van Nieuw Amerongen, G.P., S. van Delft, M.A. Vermeer, J.G. Collard, and V.W. van Hinsbergh. 2000. Activation of RhoA by thrombin in endothelial hyperpermeability: role of Rho kinase and protein tyrosine kinases. *Circ Res*. 87:335-40.

van Weering, J.R., R.F. Toonen, and M. Verhage. 2007. The role of Rab3a in secretory vesicle docking requires association/dissociation of guanidine phosphates and Munc18-1. *PLoS One*. 2:e616.

Valentijn, K.M., J.E. Sadler, J.A. Valentijn, J. Voorberg, and J. Eikenboom. 2011. Functional architecture of Weibel-Palade bodies. *Blood*. 117:5033-43.

Varoqueaux, F., A. Sigler, J.S. Rhee, N. Brose, C. Enk, K. Reim, and C. Rosenmund. 2002. Total arrest of spontaneous and evoked synaptic transmission but normal synaptogenesis in the absence of Munc13-mediated vesicle priming. *Proc Natl Acad Sci U S A*. 99:9037-42.

Verhage, M., A.S. Maia, J.J. Plomp, A.B. Brussaard, J.H. Heeroma, H. Vermeer, R.F. Toonen, R.E. Hammer, T.K. van den Berg, M. Missler, H.J. Geuze, and T.C. Sudhof. 2000. Synaptic assembly of the brain in the absence of neurotransmitter secretion. *Science*. 287:864-9.

Vinet, A.F., M. Fukuda, and A. Descoteaux. 2008. The exocytosis regulator synaptotagmin V controls phagocytosis in macrophages. *J Immunol*. 181:5289-95.

Vinet, A.F., M. Fukuda, S.J. Turco, and A. Descoteaux. 2009. The Leishmania donovani lipophosphoglycan excludes the vesicular proton-ATPase from phagosomes by impairing the recruitment of synaptotagmin V. *PLoS Pathog*. 5:e1000628.

Virmani, T., W. Han, X. Liu, T.C. Sudhof, and E.T. Kavalali. 2003. Synaptotagmin 7 splice variants differentially regulate synaptic vesicle recycling. *EMBO J*. 22:5347-57.

Vischer, U.M., H. Barth, and C.B. Wollheim. 2000. Regulated von Willebrand factor secretion is associated with agonist-specific patterns of cytoskeletal remodeling in cultured endothelial cells. *Arterioscler Thromb Vasc Biol*. 20:883-91.

Vischer, U.M., and D.D. Wagner. 1993. CD63 is a component of Weibel-Palade bodies of human endothelial cells. *Blood*. 82:1184-91.

Vischer, U.M., and C.B. Wollheim. 1997. Epinephrine induces von Willebrand factor release from cultured endothelial cells: involvement of cyclic AMP-dependent signalling in exocytosis. *Thromb Haemost*. 77:1182-8.

Vischer, U.M., and C.B. Wollheim. 1998. Purine nucleotides induce regulated secretion of von Willebrand factor: involvement of cytosolic Ca2+ and cyclic adenosine monophosphate-dependent signaling in endothelial exocytosis. *Blood*. 91:118-27.

Voets, T., R.F. Toonen, E.C. Brian, H. de Wit, T. Moser, J. Rettig, T.C. Sudhof, E. Neher, and M. Verhage. 2001. Munc18-1 promotes large dense-core vesicle docking. *Neuron*. 31:581-91.

von Poser, C., K. Ichtchenko, X. Shao, J. Rizo, and T.C. Sudhof. 1997. The evolutionary pressure to inactivate. A subclass of synaptotagmins with an amino acid substitution that abolishes Ca2+ binding. *J Biol Chem*. 272:14314-9.

von Poser, C., J.Z. Zhang, C. Mineo, W. Ding, Y. Ying, T.C. Sudhof, and R.G. Anderson. 2000. Synaptotagmin regulation of coated pit assembly. *J Biol Chem*. 275:30916-24.

Vrljic, M., P. Strop, J.A. Ernst, R.B. Sutton, S. Chu, and A.T. Brunger. 2012. Molecular mechanism of the synaptotagmin-SNARE interaction in Ca2+-triggered vesicle fusion. *Nat Struct Mol Biol*. 17:325-31.

Wagner, D.D., and P.S. Frenette. 2008. The vessel wall and its interactions. *Blood*. 111:5271-81.

Wagner, D.D., J.B. Olmsted, and V.J. Marder. 1982. Immunolocalization of von Willebrand protein in Weibel-Palade bodies of human endothelial cells. *J Cell Biol*. 95:355-60.

Wagner, D.D., S. Saffaripour, R. Bonfanti, J.E. Sadler, E.M. Cramer, B. Chapman, and T.N. Mayadas. 1991. Induction of specific storage organelles by von Willebrand factor propolypeptide. *Cell*. 64:403-13.

Walent, J.H., B.W. Porter, and T.F. Martin. 1992. A novel 145 kd brain cytosolic protein reconstitutes Ca(2+)-regulated secretion in permeable neuroendocrine cells. *Cell*. 70:765-75.

Walther, K., M. Krauss, M.K. Diril, S. Lemke, D. Ricotta, S. Honing, S. Kaiser, and V. Haucke. 2001. Human stoned B interacts with AP-2 and synaptotagmin and facilitates clathrin-coated vesicle uncoating. *EMBO Rep*. 2:634-40.

Wang, P., M.C. Chicka, A. Bhalla, D.A. Richards, and E.R. Chapman. 2005. Synaptotagmin VII is targeted to secretory organelles in PC12 cells, where it functions as a high-affinity calcium sensor. *Mol Cell Biol*. 25:8693-702.

Wang, Z., H. Liu, Y. Gu, and E.R. Chapman. 2011. Reconstituted synaptotagmin I mediates vesicle docking, priming, and fusion. *J Cell Biol*. 195:1159-70.

Weibel, E.R., and G.E. Palade. 1964. New Cytoplasmic Components in Arterial Endothelia. *J Cell Biol*. 23:101-12.

Wen, H., M.W. Linhoff, M.J. McGinley, G.L. Li, G.M. Corson, G. Mandel, and P. Brehm. 2010. Distinct roles for two synaptotagmin isoforms in synchronous and asynchronous transmitter release at zebrafish neuromuscular junction. *Proc Natl Acad Sci U S A*. 107:13906-11.

Whatley, R.E., Zimmerman, G.A., Prescott, S.M., McIntyre, T.M. 1996 Platelet-activating factor and platelet-activating factor and PAF-like mimetics. *Handbook lipid Res* 8:239

White, T.A., T. Johnson, N. Zarzhevsky, C. Tom, S. Delacroix, E.W. Holroyd, S.A. Maroney, R. Singh, S. Pan, W.P. Fay, J. van Deursen, A.E. Mast, G.S. Sandhu, and R.D. Simari. 2010. Endothelial-derived tissue factor pathway inhibitor regulates arterial thrombosis but is not required for development or hemostasis. *Blood*. 116:1787-94.

Whyte, J.R., and S. Munro. 2001. The Sec34/35 Golgi transport complex is related to the exocyst, defining a family of complexes involved in multiple steps of membrane traffic. *Dev Cell*. 1:527-37.

Wilson, D.B., and M.P. Wilson. 1992. Identification and subcellular localization of human rab5b, a new member of the ras-related superfamily of GTPases. *J Clin Invest*. 89:996-1005.

Wilson, S.M., R. Yip, D.A. Swing, T.N. O'Sullivan, Y. Zhang, E.K. Novak, R.T. Swank, L.B. Russell, N.G. Copeland, and N.A. Jenkins. 2000. A mutation in Rab27a causes the vesicle transport defects observed in ashen mice. *Proc Natl Acad Sci U S A*. 97:7933-8.

Wood, P.G., and J.I. Gillespie. 1998. Evidence for mitochondrial Ca(2+)-induced Ca2+ release in permeabilised endothelial cells. *Biochem Biophys Res Commun*. 246:543-8.

Woolkalis, M.J., T.M. DeMelfi, Jr., N. Blanchard, J.A. Hoxie, and L.F. Brass. 1995. Regulation of thrombin receptors on human umbilical vein endothelial cells. *J Biol Chem*. 270:9868-75.

Wu, X., K. Rao, M.B. Bowers, N.G. Copeland, N.A. Jenkins, and J.A. Hammer, 3rd. 2001. Rab27a enables myosin Va-dependent melanosome capture by recruiting the myosin to the organelle. *J Cell Sci*. 114:1091-100.

Xue, M., T.K. Craig, O.H. Shin, L. Li, C.A. Brautigam, D.R. Tomchick, T.C. Sudhof, C. Rosenmund, and J. Rizo. 2010. Structural and mutational analysis of functional differentiation between synaptotagmins-1 and -7. *PLoS One*. 5.

Yamamoto, K., and D.J. Loskutoff. 1996. Fibrin deposition in tissues from endotoxin-treated mice correlates with decreases in the expression of urokinase-type but not tissue-type plasminogen activator. *J Clin Invest*. 97:2440-51.

Yano, K., D. Gale, S. Massberg, P.K. Cheruvu, R. Monahan-Earley, E.S. Morgan, D. Haig, U.H. von Andrian, A.M. Dvorak, and W.C. Aird. 2007. Phenotypic heterogeneity is an evolutionarily conserved feature of the endothelium. *Blood*. 109:613-5.

Yokota, H., T. Tsujita, Y. Okazaki, E. Kikuya, and M. Oishi. 2003. Polymorphic 33-bp repeats with promoter-like activity in synaptotagmin 11 gene. *DNA Res*. 10:287-9.

Yoshihara, M., and J.T. Littleton. 2002. Synaptotagmin I functions as a calcium sensor to synchronize neurotransmitter release. *Neuron*. 36:897-908.

Yoshihara, M., and E.S. Montana. 2004. The synaptotagmins: calcium sensors for vesicular trafficking. *Neuroscientist*. 10:566-74.

Zannettino, A.C., C.A. Holding, P. Diamond, G.J. Atkins, P. Kostakis, A. Farrugia, J. Gamble, L.B. To, D.M. Findlay, and D.R. Haynes. 2005. Osteoprotegerin (OPG) is localized to the Weibel-Palade bodies of human vascular endothelial cells and is physically associated with von Willebrand factor. *J Cell Physiol*. 204:714-23.

Zhang, J.Z., B.A. Davletov, T.C. Sudhof, and R.G. Anderson. 1994. Synaptotagmin I is a high affinity receptor for clathrin AP-2: implications for membrane recycling. *Cell*. 78:751-60.

Zhang, W., A. Khan, C.G. Ostenson, P.O. Berggren, S. Efendic, and B. Meister. 2002. Down-regulated expression of exocytotic proteins in pancreatic islets of diabetic GK rats. *Biochem Biophys Res Commun*. 291:1038-44.

Zhang, L., D. Lou, H. Jiao, D. Zhang, X. Wang, Y. Xia, J. Zhang, and M. Xu. 2004. Cocaine-induced intracellular signaling and gene expression are oppositely regulated by the dopamine D1 and D3 receptors. *J Neurosci*. 24:3344-54.

Zhang, X., M.J. Kim-Miller, M. Fukuda, J.A. Kowalchyk, and T.F. Martin. 2002. Ca2+-dependent synaptotagmin binding to SNAP-25 is essential for Ca2+-triggered exocytosis. *Neuron*. 34:599-611.

Zhang, J., and M. Xu. 2006. Opposite regulation of cocaine-induced intracellular signaling and gene expression by dopamine D1 and D3 receptors. *Ann N Y Acad Sci*. 1074:1-12.

Zhao, H., Y. Ito, J. Chappel, N.W. Andrews, S.L. Teitelbaum, and F.P. Ross. 2008. Synaptotagmin VII regulates bone remodeling by modulating osteoclast and osteoblast secretion. *Dev Cell*. 14:914-25.

Zografou, S., D. Basagiannis, A. Papafotika, R. Shirakawa, H. Horiuchi, D. Auerbach, M. Fukuda, and S. Christoforidis. A complete Rab screening reveals novel insights in Weibel-Palade body exocytosis. *J Cell Sci*. 125:4780-90.

Zupancic, G., D. Ogden, C.J. Magnus, C. Wheeler-Jones, and T.D. Carter. 2002. Differential exocytosis from human endothelial cells evoked by high intracellular Ca(2+) concentration. *J Physiol*. 544:741-55.

Appendix 1.0: The Creation of the Dose-Response Curve of Proregion Secretion Against Ionomycin Concentration:

1.0 Designing a suitable assay:

In order to determine if the calcium sensitivity of WPB exocytosis is affected by the over-expression or knock-down of individual SYTs it was necessary to construct a dose-response curve describing the exocytosis of proregion in response to varying concentrations of agonists. For this assay I used a proregion ELISA and un-transfected HUVECs stimulated with increasing concentrations of the calcium ionophore ionomycin. Ionomycin elicits the rapid, sustained, and reliable secretion of WPBs from HUVECs, and therefore will provide the sensitivity required for these experiments.

Initially, it was necessary to determine the optimum design of this assay. I had the option of using either 6-well or 24-well plates for culturing HUVECs prior to stimulation. The Carter lab routinely uses 6-well plates for ELISA assays. However, the 6-well plates would prevent the examination of a large number of different conditions due to the limited number of available wells and hence would make the construction of a complete dose-response curve challenging. The alternative culture method, the 24-well plate, has not been used in the Carter lab before for ELISA assays and therefore I initially proceeded by determining the accuracy and reproducibility of secretion data obtained from cells cultivated on 24-well plates as opposed to 6-well plates. Hence, a low (0.05 μM), medium (1.0 μM), and high (5 μM) concentration of ionomycin was applied to confluent HUVECs grown in wells on either a 6-well or a 24-well plate. The same volume of cells was seeded into each well relative to the surface area available for growth. The results of this preliminary experiment are shown in Figure One. As can be seen, a clear dose-dependent secretory response is obvious from cells grown in both the 6- and 24-well plate. However, cells grown in the 24-well plate show greater absolute quantities of proregion secreted compared with those from the 6-well plate. Hence, due to the fact that the 24-well plate yielded higher quantities of secreted proregion and also allows considerably more conditions to be screened in a single experiment it was decided to use the 24-well plate format for all subsequent assays.

2.0 Creating the dose-response curve:

Once the technicalities of the experimental design had been established I then proceeded to construct an expanded dose-response curve using un-transfected HUVECs grown in 24-well plates. An equal volume of cell suspension was seeded into each well 48 hours prior to stimulation. Cells were stimulated with ionomycin at a concentration of 0 µM, 0.01 µM, 0.03 µM, 0.1 µM, 0.3 µM, 1 µM, 3 µM, 10 µM, or 20 µM. Following stimulation, media was collected from each well and the quantity of secreted proregion was determined by a proregion ELISA. The raw data from a representative experiment is shown in Table 1. The data is expressed as arbitrary units relative to the quantity of proregion in a known standard. To obtain a sufficient range of ionomycin concentrations the experiments were carried out over two separate 24-well plates. This experimental design was useful because in order to ensure that the same number of cells were present in each well, two conditions (0.3 µM and 1 µM) were represented on both plates. The proregion ELISA was repeated using lysates extracted from stimulated cells in these wells. The quantity of proregion contained within these cells grown on different plates but representing the same conditions was shown to be not significantly different (3.25 versus 3.03 for 0.3 µM, p-value ≥ 0.05; 2.51 versus 2.50 for 1 µM, p-value ≥ 0.05). The full dose-response curve representing the combined results of three individual experiments is shown in Figure Two. As individual endothelial cell cultures are heterogeneous and the absolute quantity of proregion secreted varied between cultures, the results have been normalized to the quantity of proregion secreted at 10 µM ionomycin. It is interesting to note that maximal secretion occurred at 3 µM, and decreased between 10 and 20 µM. It may be that higher concentrations of ionomycin lead to an excessive calcium influx into the cell resulting in apoptosis. This would explain the decreased quantity of proregion secreted at ionomycin concentrations higher than 3 µM.

Therefore, this assay has allowed me to construct a reproducible dose-response curve for proregion secretion against increasing ionomycin concentrations. It is now possible to manipulate the expression profile of the various SYTs within HUVECs to determine the effect on calcium sensitivity.

Ionomycin Concentration (µM)	Mean of Three Replicates (Arbitrary Units of Proregion Secretion)	Standard Deviation
Ethanol Control (0)	3.067	0.06565
0.01	6.86	0.06928
0.03	10.73	0.01882
0.1	14.90	0.28143
0.3	22.29	0.61789
1	32.80	1.57206
3	56.49	9.16858
10	42.79	2.3362

- **Table One,** showing the raw data obtained from a representative assay of proregion secretion versus increasing concentrations of ionomycin. Data is expressed as arbitrary units relative to the quantity of proregion in a known standard.

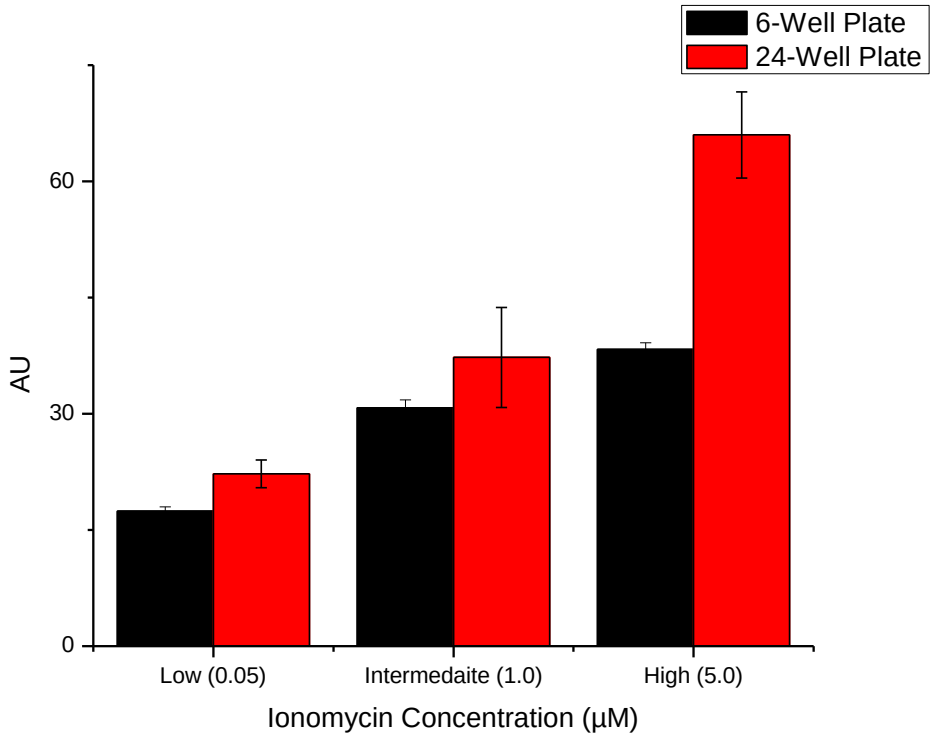

- **Figure One** showing the secretory dose-response seen following the application of varying concentrations of ionomycin to cells grown in wells on either a 6-well or 24-well plate, as indicated. The x-axis represents arbitrary units of secreted proregion compared to a known standard, as determined by the plate reader. Note the significantly higher quantity of proregion secreted from cells cultured in a 24-well plate compared with those cultured in a 6-well plate.

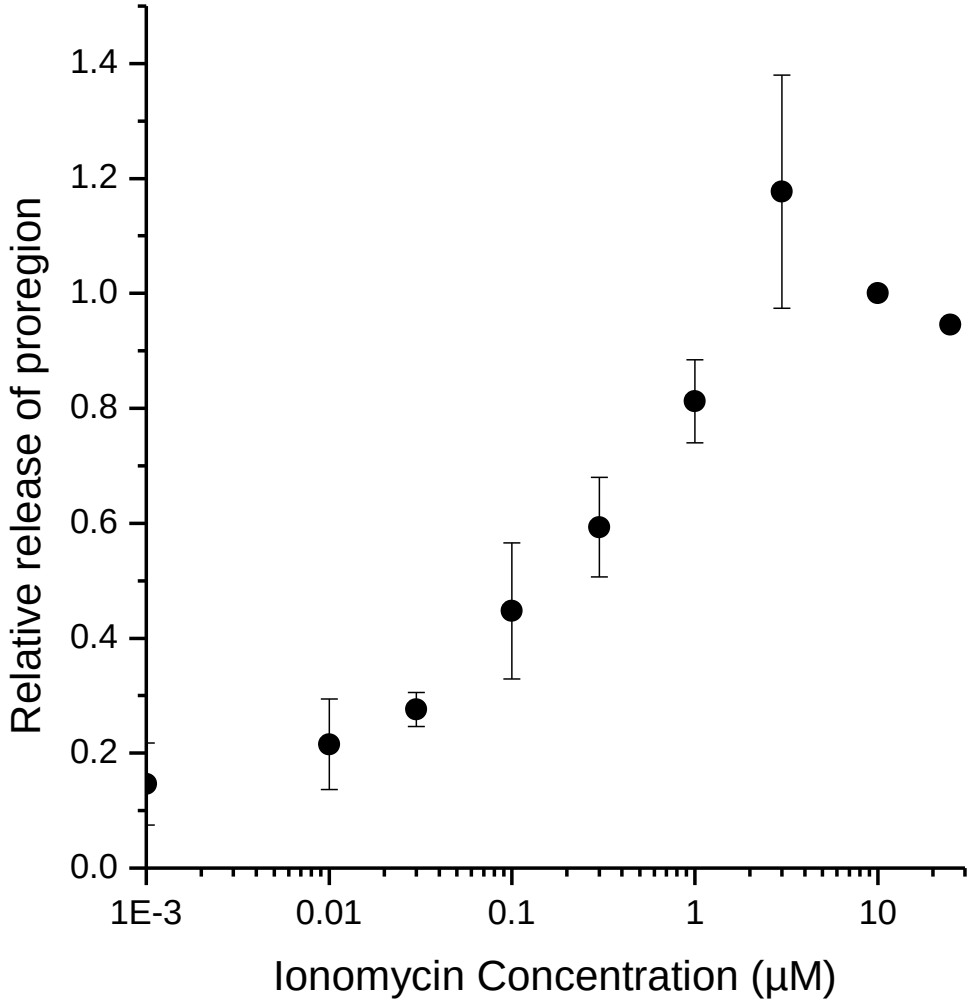

- **Figure Two**, showing the dose-response curve of proregion secretion against increasing concentrations of ionomycin. Results from three individual experiments have been normalized to the maximum secretion obtained at 10 µM. The lowest value represents the basal secretion seen when an ethanol control is used in place of ionomycin.

Appendix 2.0: The Determination of the Expression of SYT VII Isoforms in HUVECs:

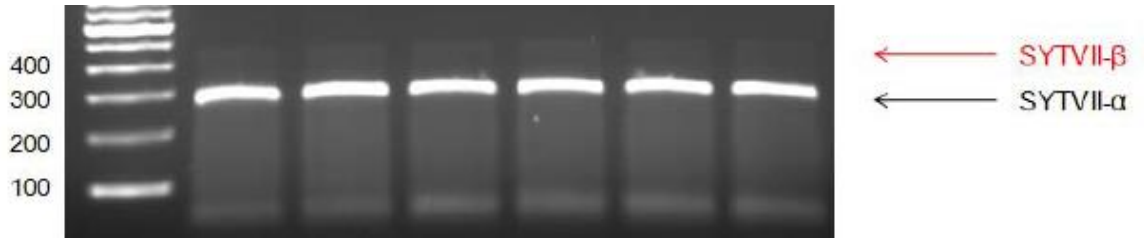

The agarose gel above shows the RT-PCR of HUVEC mRNA using primers specific for the highly-spliced spacer region of SYT VII. The major isoform of SYTVII, SYTVII-α, is visible at approximately 300 bp and the minor isoform, SYTVII-β, is present at approximately 450 bp. Although faint, this top band is typical of published work describing the SYTVII-β isoform which is expressed at much lower levels compared with SYTVII-α (Fukuda *et al.* 2002). Hence, preliminary investigations suggest that HUVECs express SYTVII-α and –β.

Appendix 3.0: Screening the α-SYT I antibody for non-specific binding, auto-fluorescence, and the bleed-through effect.

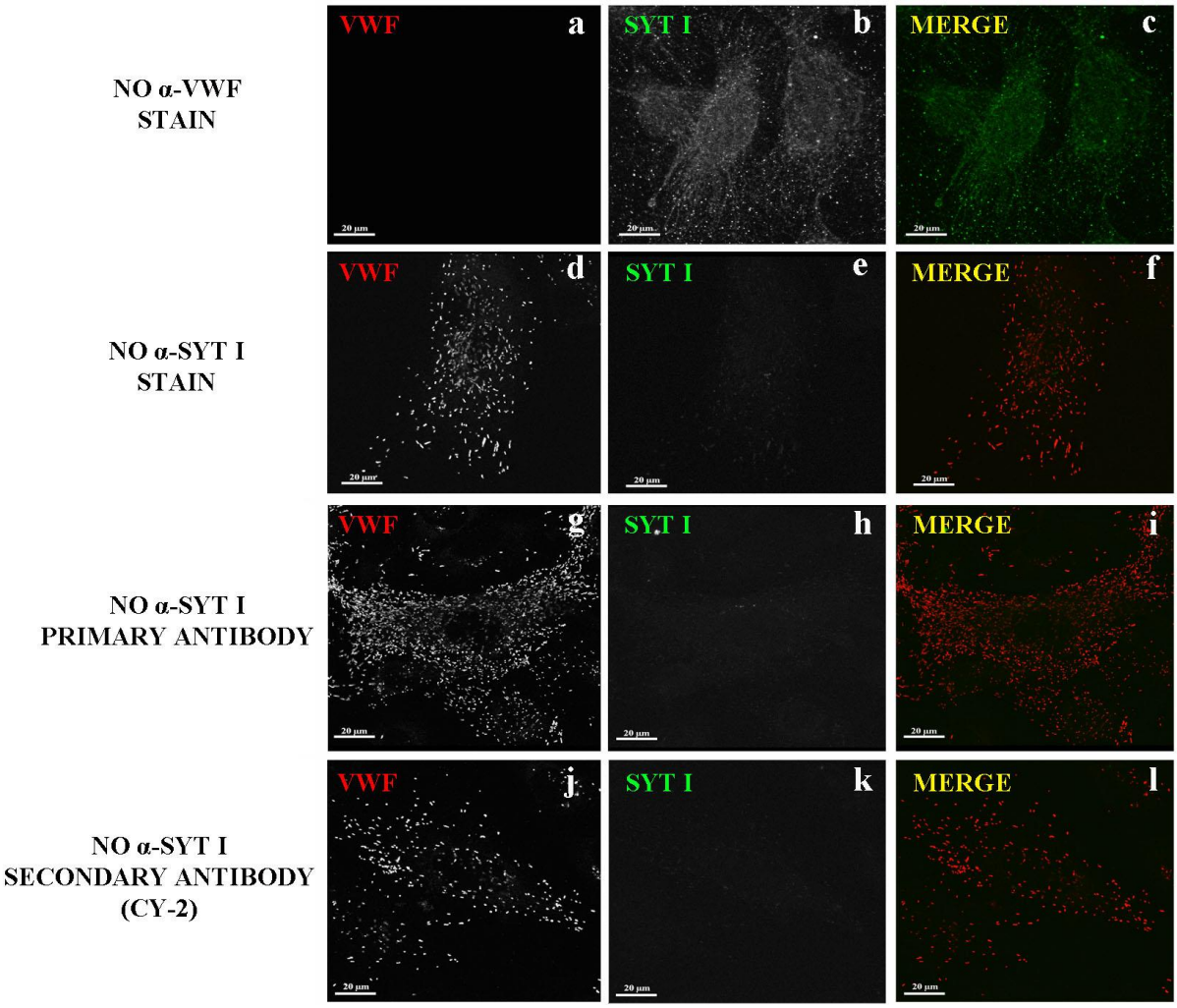

- **Figure One**, showing the results of screening the α-SYT I antibody for background fluorescence, non-specific binding, and the bleed-through effect (i.e. the leaking of signal between channels due to saturation of the image). Panels a-c show the results of omitting the VWF stain entirely. Panels d-f show the results of omitting the SYT I stain entirely. Panels g-i show the results of omitting the SYT I primary antibody. Panels j-l show the results of omitting the SYT I secondary antibody (α-mouse CY-2). Panels a, d, g, and j show the red channels. Panels b, e, h, and k show the green channels. Panels c, f, i and l show the merged channels.